2013

Integrated functional anlaysis of quorum-sensing in the rice pathogenic bacterium Burkholderia glumae

Ruoxi Chen
Louisiana State University and Agricultural and Mechanical College, cruoxi@yahoo.com

INTEGRATED FUNCTIONAL ANALYSIS OF QUORUM-SENSING IN THE RICE PATHOGENIC BACTERIUM *BURKHOLDERIA GLUMAE*

A Dissertation

Submitted to the Graduate Faculty of the
Louisiana State University and
Agriculture and Mechanical College
in partial fulfillment of the
requirements for the degree of
Doctor of Philosophy

in

The Department of Plant Pathology and Crop Physiology

by
Ruoxi Chen
B.S., Shandong Agricultural University, 2008
M.S., Louisiana State University, 2011
December 2013

I would like to dedicate this dissertation to my husband Sebastian Albu for his great love and encouragement, and to my parents Tao Chen and Yinxia Zhang for their unconditional love and support.

ACKNOWLEDGEMENTS

I want to thank all the professors, colleges, and friends who helped with my study and living life. First of all, I am very grateful to all the generous help and support from my major adviser Dr. Jong Hyun Ham. He gave me this precious opportunity to study in molecular plant pathology area, offered great advice, spent time and patience to my work. I want to thank my past committee professor Dr. Milton C. Rush, who was greatly generous to me. I want to thank my current committee professors Dr. Rodrigo A. Valverde and Gregg S. Pettis, who helped me with course and research work as well as the correction of this dissertation. I want to thank my dean's representative professor Prasanta K. Subudhi, who agreed to serve as committee member and contribute time to my defense. I want to thank Dr. Joohyun Kim, who gave me great advices for the computational work. I appreciate all the teamwork I have with my lab mates, who always share good research experience with me: Inderjit Kaur, Bishnu Shrestha, Hari Karki, Rebecca Melanson, Surendra Osti and Jingyu Peng. I also want to give my gratitude to all other faculty, staff and students in my department, from where I have been learning, influenced and growing as a beginner in plant pathology.

TABLE OF CONTENTS

ABSTRACT

Quorum sensing (QS) is a cell-to-cell communication mechanism that allows bacterial cells to collectively behave like a multicellular organism. It regulates the expression of toxoflavin, one of the major virulence factors of the rice pathogen, *Burkholderia glumae*. The QS system of *B. glumae* is mediated by the core genes, *tofI* and *tofR*. *N*-octanoyl-L-homoserine lactone, the primary QS signal molecule of *B. glumae*, is synthesized by *tofI* and binds to the cognate receptor *tofR* at the quorum point. However, *tofI* and *tofR* null mutants produce toxoflavin in certain growth conditions, indicating the presence of *tofI*- and *tofR*-independent pathways for toxoflavin production. The present study identified regulators required for the *tofI*- and *tofR*-independent pathways, including flagella transcriptional activator, diguanylate cyclase, O-antigen polymerase family protein, QsmR QS-dependent master regulator and one hypothetical protein with its encoding gene located upstream of *toxJ* (encoding toxoflavin production activator). A novel QS regulatory element, *tofM*, was identified as a positive regulator of pathogenicity and a putative modulator of *tofR* in *B. glumae.* RNA-sequencing was also performed to investigate the QS regulon and medium condition-dependent gene expression in *B. glumae.* A large collection of target genes and noncoding RNAs was detected by comparative transcriptome analysis. From a comparison of the transcriptional profile of the wild type (336gr-1) and quorum sensing mutants grown on solid and liquid media, it is postulated that an alternative global regulator is activated to compensate for the dysfunction of AHL QS on solid medium.

CHAPTER 1. GENERAL INTRODUCTION

1.1 Major pathogen of rice: *Burkholderia glumae*

Burkholderia, previously recognized as a species in the rRNA group II in the genus *Pseudomonas,* was proposed in 1992 after Burkholder who described the first species in this group (Stoyanova et al., 2007; Yabuuchi et al., 1992). Since *Burkholderia cepacia* was reported in 1950, more than 80 species have been described in the genus (Stoyanova et al., 2007). The biodiversity within this genus can be observed in different species associated with various habitats. *Burkholderia* species occupy a very broad range of ecological niches and substrates including water, soil, the phyllosphere and rhizosphere, as well as humans and other animals (Stoyanova et al., 2007). Interestingly, *Burkholderia* species can be both friend and foe of humans: *B. cepacia* is well known as a registered bioagent, while *B. vietnamiensis*, *B. phymatum*, *B. ambifaria*, and *B. phytofi* can help promote plant growth. In contrast, *B. glumae, B. gladioli, B. andropogoni, B. graminis, B. plantarii* and other species have been reported as important plant pathogens on various hosts, and *B. cepacia* complex strains, *B. pseudomallei* and *B. mallei* have been implicated as causal agents of cystic fibrosis, melioidosis and glanders diseases in humans (Chowdhury and Heinemann, 2006; Coenye and Vandamme, 2003; Gerhardson, 2002; Parke and Gurian-Sherman, 2001; Stoyanova et al., 2007). Therefore, it is not surprising that as more research into the practical, beneficial and pathogenic properties of *Burkholderia* species is conducted, scientists will continue to discover more about the physiological properties and genetic components of this important group of bacteria.

Rice is one of the most important global crops sustaining nearly half of the world's population. It is also a traditional food in the southeastern United States and

provides major economic income for many farmers. Successful cultivation of rice can reduce poverty. Thus, numerous rice pathologists are working on developing new technologies to control rice diseases and sustain high levels of rice production. Historically, the following rice diseases have shown epidemic importance: sheath blight caused by *Rhizoctonia solani*, bacterial panicle blight (BPB) caused by *B. glumae*, rice blast caused by *Magnaporthe oryzae*, rice yellow mottle virus (RYMV) disease and sheath rot disease of rice caused by *Sarocladium oryzae* (Abo et al., 2000; Ham et al., 2011; Howard and Valent, 1996; Rao and Rao Manibhushan, 1996; Zheng et al., 2013).

There are three *Burkholderia* species that are major pathogens of rice: *B. plantarii* causing seedling blight, *B. glumae* causing seedling rot and bacterial panicle blight (BPB), and *B. gladioli* causing seedling bleaching and panicle blight (Azegami et al., 1987; Eberhard, 1972; Kato et al., 1992; Maeda et al., 2006; Nandakumar et al., 2009a). Among these three species, *B. glumae* and *B. plantarii* have a close phylogenetic relationship based on analysis of the conserved region of *gyrB* and *rpoD* (Maeda et al., 2006). One of the most damaging diseases on rice, especially in the southern United States including Louisiana, Arkansas and Texas, is BPB, which can cause up to 75% yield reduction (Ham et al., 2011). This rice disease has also been reported from many rice-growing areas worldwide, including East Asia, Southeast Asia and South America (Ham et al., 2011). Another pathogen causing BPB is *B. gladioli,* but it is much less aggressive than *B. glumae* (Ham et al., 2011). Limited numbers of disease management strategies have been shown to be effective. One useful control method is the chemical oxolinic acid, but not only is this chemical not available in the U.S.A, but the incidence of resistant strains following its application is also a problem

(Ham et al., 2011). *gyrA* has been known as the quinolone resistance-determining region responsible for expressing resistance against oxolinic acid (Maeda et al., 2007; Yoshida et al., 1990). Some rice varieties were found having partial resistance to BPB, but none axis shows complete resistance (Shahjahan et al., 2000b). Some field trials have revealed the potential of avirulent *B. gladioli* strains to function as biological control agents. When co-inoculaed with *B. glumae,* these strains significantly reduced the disease rate (Ham et al., 2011; Miyagawa and Takaya, 2000).

1.2 LuxI/LuxR type QS systems

There are certain social group behaviors characteristic of bacteria at high cell density, in contrast to other asocial behaviors favored by low cell density (Ng and Bassler, 2009). To perform social group behaviors, bacterial cells communicate and coordinate through quorum sensing (QS) systems. QS bacteria continuously synthesize and secrete diffusible signals (autoinducers); when the bacterial population and signal concentration reach a certain threshold level, the intracellular cognate receptor will bind onto the autoinducer and promote expression of target genes (Ng and Bassler, 2009). With QS, bacteria can greatly benefit from social group behavior. A classic example of this occurs when certain plant pathogenic bacteria escape the attack of a plant defense system (Liu et al., 2008). The virulence factors expressed by plant pathogenic bacteria can trigger the defense reaction in plant host. However, with regulation of the timing by the QS, the detectable expression of virulence genes only occurs at ‘quorum point’, when bacterial colonies are sufficient in number to tolerate and overcome the defense function of the plant host (Liu et al., 2008; Mae et al., 2001).

A fundamental model of QS systems used by plant pathogenic bacteria is the LuxI/LuxR type QS. LuxI synthesizes the autoinducer, and LuxR is the receptor of the

autoinducer at quorum point. The autoinducer signals are *N*-acyl-homoserine lactones (AHLs), which are synthesized by LuxI-family synthases from S-adenosyl methionine and fatty acid chains carried by an acyl carrier protein (von Bodman et al., 2003). The structural difference and specificity of transduction of AHLs mostly depends on the fatty acid chains, which possess 4-18 carbons (Kumari et al., 2006; Waters and Bassler, 2005). The first described example of audoinduction was the *N*-3-(oxohexanoyl) homoserine lactone/LuxI/LuxR system in the marine bacterium *Vibrio fischeri* (Fuqua et al., 1994). The luminescence gene cluster is transcribed when the *N*-3-(oxohexanoyl) homoserine lactones accumulate to around 10 nM in the surrounding environment and bind to the receptor LuxR (Eberhard, 1972; Fuqua et al., 1994).

1.3 QS system in plant pathogenic bacteria

QS plays a critical role for the expression of a wide range of pathogenesis-related behaviors. A variety of important plant pathogens depend on the LuxI/LuxR type quorum-sensing system for the regulation of virulence factors. The crown gall pathogen *Agrobacterium tumefaciens* uses the TraI/TraR system to induce the conjugal transfer of its Ti plasmid along with an opine, which is a nutrient resource for the pathogen and acts as the co-factor (von Bodman et al., 2003). The wilt-causing pathogen *Pantoea stewartii* produces extracellular polysaccharides (EPS) and colonizes the xylem tissue of the host, effectively blocking water transport (Braun, 1982). The EsaI/EsaR system is responsible for the formation of EPS and full level of virulence (von Bodman et al., 1998). The AhlI/AhlR system in *Pseudomonas syringae* can regulate the epiphytic fitness and symptoms caused by internal tissue maceration within the host (Chen, 2011; Quinones et al., 2005).

The emerging importance of certain *Burkholderia* species has favored the rapid development of studies of QS systems within this genus. The LuxI/LuxR QS systems in *Burkholderia* are variable and complicated and the most frequently studied model is the CepI/CepR global regulator (Chen, 2011; Gotschlich et al., 2001; Leo, 2006). The CepI/CepR system was the first described QS system in the *Burkholderia* genus, for siderophore ornibactin negative regulation and extracellular protease positive regulation in *B. cepacia* (Chen, 2011; Lewenza et al., 1999). It was also found that expression of plasmid-borne *cepR-lacZ* increased two-fold in *B. cepacia* CepR mutants, which indicated that the *cepR* gene had negative self-autoregulation properties (Chen, 2011; Lewenza and Sokol, 2001). A similar expression pattern was found in *B. cenocepacia* (Chen, 2011; Lewenza and Sokol, 2001). In addition to CepI/CepR, some species also have secondary QS systems that are controlled by the CepI/CepR. For example, *B. cenocepacia* has CciI/CciR within a genomic island which also contributes to virulence (Baldwin et al., 2004; Chen, 2011; Sokol et al., 2003), and an orphan CepR2 LuxR homolog autoregulator which positively regulates the siderophore pyochelin (Chen, 2011; Malott et al., 2009). The normal function of BviI/BviR in *B. vietnamiensis* requires CepR and possibly another upstream regulator element (Leo, 2006; Malott and Sokol, 2007). Three LuxI and five LuxR homologues were identified in *B. pseudomallei,* two LuxI and four LuxR homologues were identified in *B. mallei* (Leo, 2006).

Among all the *Burkholderia* species*, B. pseudomallei* and *B. mallei* appear to possess the most complicated quorum-sensing systems*. B. mallei* has two Lux homolog pairs - BmaI1/BmaR1 and BmaI3/BmaR3, and two orphan putative LuxR regulators, BmaR4 and BmaR5, for which all of the six Lux type proteins are required for full

virulence (Chen, 2011; Duerkop et al., 2008; Duerkop et al., 2007). *B. pseudomallei* has two orphan LuxR homologs and three BpsI/BpsR pairs, and two of the characterized BpsI/BpsR groups contribute to the formation of bacterial biofilms (Chen, 2011; Duerkop et al., 2007; Song et al., 2005).

1.4 The diversity of AHL signals in *Burkholderia*

There are at least six types of identified QS signals, including *N*-acyl homoserine lactones (AHLs), produced by Gram-negative bacteria e.g. *B. glumae*; autoinducing peptides (AIPs), produced by Gram-positive bacteria e.g. *Bacillus subtilis*; and autoinducer II (AI-2), the intra and inter-species cross talk signal e.g. between *Actinobacillus actinomycetemcomitans* and *Porphyromonas gingivalis* (Chen, 2011; Eberl and Riedel, 2011; Fong et al., 2001). *Burkholderia cepacia* complex (Bcc) bacteria were also found to produce other types of autoinducer-diffusible signal factors (DSFs) for intra or inter-species communication (Boon et al., 2008b; Chen, 2011; Deng et al., 2010). *B. cenocepacia* was recently reported having *cis*-2-dodecenoic acid (BDSF), which is an analogue of DSF (*cis*-11-methyl-2-dodecenoic acid), in addition to the AHL system (Boon et al., 2008a; Deng et al., 2009). One type of QS signal can be expressed in diverse kinds of bacteria and one bacterial strain can harbor more than one type of signaling system.

The dominant QS system possessed by *Burkholderia* species is the AHL/LuxI/LuxR type system. The *luxI* genes in *Burkholderia* species synthesize various AHL signals, and the list of AHL signals used by representative *Burkholderia* species is shown in Table 1.

Table 1 The distribution of *N*-acyl homoserine lactones signals in *Burkholderia* species

AHL signals	Synthase gene	Receptor gene	*Burkholderia* species	Reference
C8-, C6-HSL	*bafI*	*bafR*	*B. ambifaria*	(Zhou et al., 2003)
C8-, C6-HSL C6-, C8-HSL	*cepI* *cciI*	*cepR* *cciR*	*B. cenocepacia*	(Lewenza et al., 1999) (Malott et al., 2005)
C8-, C6-HSL	*tofI*	*tofR*	*B. glumae*	(Kim et al., 2004b)
OHC8-HSL C8-HSL	*bmaI3* *bmaI1*	*bmaR3* *bmaR1*	*B. mallei*	(Duerkop et al., 2008) (Duerkop et al., 2007)
C8-HSL	*bmuI*	*bmuR*	*B. multivorans*	(Choudhary et al., 2013)
OHC8-HSL OC14-HSL	*xenI2* *braI*	*xenR2* *braR*	*B. phytofirmans*	(Suarez-Moreno et al., 2010)
C6-, C8-HSL	*plaI*	*plaR*	*B. plantarii*	(Solis et al., 2006)
OHC10-HSL C8-HSL OHC8-HSL	*bpsI3* *bpsI1* *bpsI2*	*bpsR3* *bpsI1* *bpsI2*	*B. pseudomallei*	(Choudhary et al., 2013; Kiratisin and Sanmee, 2008)
OHC8-HSL C8-HSL OHC8-,OHC10-HSL	*btaI3* *btaI1* *btaI2*	*btaR3* *btaR1* *btaR2*	*B. thailandensis*	(Choudhary et al., 2013)
OHC10-, OC12-HSL	*braI*	*braR*	*B. unamae*	(Suarez-Moreno et al., 2010)
C8-, C6-HSL C8-, C6-, C10, OC10-, C12-HSL	*cepI* *bviI*	*cepR* *bviR*	*B. vietnamiensis*	(Malott and Sokol, 2007)
OC6-, OC8-, OC10-, OC12-HSL OHC10-, OC12- and OC14-HSL	*xenI2* *braI*	*xenR2* *braR*	*B. xenovorans*	(Suarez-Moreno et al., 2010)

OC6-HSL: *N*-3-oxo-hexanoyl-*L*-homoserine lactone
C6-HSL: *N*-hexanoyl-*L*-homoserine lactone
C8-HSL: *N*-octanoyl-*L*-homoserine lactone
OC8-HSL: *N*-3-oxooctanoyl-*L*-homoserine lactone
OHC8-HSL: *N*-3-hydroxyoctanoyl homoserine lactone
C10-HSL: *N*-decanoyl-*L*-homoserine lactone
OHC10-HSL: *N*-3-hydroxydecanoyl homoserine lactone
OC10-HSL: *N*-3-oxodecanoyl-*L*-homoserine lactone
OC12-HSL: *N*-3-oxododecanoyl homoserine lactone
OC14-HSL: *N*-3-oxotetradecanoyl-*L*-homoserine lactone

1.5 QS system in *B. glumae*

The QS system of *B. glumae* was first reported in 2004, regulating the toxoflavin synthesis operon *toxABCDE* and transport operon *toxFGHI* (Kim et al., 2004b; Shingu and Yoneyama, 2004; Suzuki et al., 2004a). Kim et al. (2004) used biosensing and chromatography to determine the existing autoinducers in *B. glumae* and found two AHL compounds: C8-HSL and C6-HSL. After cosmid library screening using an *Agrobacterium* indicator, a corresponding clone was selected, which had the *tofI* gene encoding a 22.4 kDa LuxI homolog protein and the *tofR* gene encoding a 26.6 kDa LuxR homolog protein (Kim et al., 2004b). The C8-HSL and TofR complex can activate the toxoflavin production regulator gene *toxJ* which has the *lux* box-like sequence in the upstream of its coding region (Kim et al., 2004b). This research group also confirmed that the LysR-type activator ToxR is another toxoflavin regulator and requires toxoflavin as a co-inducer (Kim et al., 2004b). In 2009, Kim et al proved their results obtained from genetic study via demonstrating the simultaneous binding of ToxR and ToxJ to the regulatory region of the *tox* operons.

1.6 QS and other signaling systems

QS is a hierarchical mechanism with many intertwined regulators coordinating together to monitor population behaviors (Chen, 2011). QS is known as the mechanism used for cell-cell communication, which is the intercellular signaling. Plant pathogenic bacteria also possess other signaling mechanisms for the regulation of gene expression corresponding to intracellular environmental change, which are called intracellular signaling systems. It is not uncommon to find interaction between intercellular and intracellular signaling systems like cyclic dimeric guanosine monophosphate (c-di-GMP) messenger (Ham, 2013). QS can also exert transcriptional control over many other

regulators including the QS master regulator QsmR (Kim et al., 2007a). In addition to the complexity of QS circuitries, QS can be subjected to other global regulators, like AraC type regulator VqsM (Dong et al., 2005).

Some plant pathogenic bacteria like Bcc bacteria, *Xanthomonas campestris* pv. *campestris* and *Xylella fastidiosa* have DSFs as a QS autoinducer (Deng et al., 2011). In *X. campestris* pv. *campestris*, the gene *rpfF* is in charge of the formation of DSFs. and the RpfC/RpfG two-component system is responsible for their reception and transduction to target genetic traits (Ham, 2013). c-di-GMP is a second messenger that is mostly used by bacteria and rapidly regulates important cellular behaviors like biofilm formation, flagella-regulated motility, exopolysaccharide biosynthesis and cell cycles (Mills et al., 2011; Sondermann et al., 2012). c-di-GMP has multiple putative domains to sense the up-and down-regulation from different molecules; specifically, the biosynthesis of c-di-GMP is activated by diguanylate cyclase (DGC) containing a GGDEF domain, and the degradation is accomplished by phosphodieasterase (PDE) containing an EAL or HD-GYP domain (Mills et al., 2011). It was reported that QS in *X. campestris* pv. *campestris* mediated c-di-GMP signaling through RpfG to control the motility of bacterial bodies (Ryan et al., 2012). One example of QS-modulated c-di-GMP messenger controlling bacterial swarming movement was also found in *Vibrio parahaemolyticus*, a human pathogen causing gasteroenteritis.(Trimble and McCarter, 2011).

In *Burkholderia*, it has been demonstrated that QS is linked with c-di-GMP (Deng et al., 2013). In *B. cenocepacia,* $RpfF_{Bc}$ is responsible for the biosynthesis of BDSF as a QS signal; the corresponding receptor is rpfR, which contains PAS, GGDEF and EAL

motifs, and also functions as the c-di-GMP PDE. (Deng et al., 2012). The binding of BDSF can boost the degradation activity of rpfR on c-di-GMP and release of pGpG (Deng et al., 2012). The same research group again extended the inter-intra cellular regulating network of *B. cenocepacia* by studying the role of the AHL QS system in the interaction among global regulators (Deng et al., 2013; Deng et al., 2012). The BDSF can bind to the PAS domain of RpfR receptor and enhance its PDE activity, then up-regulate the production of AHL by the following interaction: the work flow of the interaction is like: BDSF $\rightarrow$ (PAS) RpfR (EAL) $\rightarrow$ c-di-GMP degradation $\rightarrow$ AHL (Deng et al., 2013; Ham, 2013).

QsmR, an IclR-type transcriptional regulator, was first described as the direct positive regulator for *flhDC* genes that are responsible for downstream flagellar biosynthesis in *B. glumae* (Kim et al., 2007a). At quorum point, the C8-HSL/TofR active complex can directly bind to the promoter of the *qsmR* gene. QsmR will then directly promote the expression of *flhDC* genes that are the activators of the flagellum genetic cascade (Kim et al., 2007a). Flagella-regulated motility was proven to be required for full virulence of *B. glumae* (Kim et al., 2007a). QsmR was found to directly up-regulate the expression of *katG* encoding catalase in *B. glumae*, which protects bacterial cells from visible light (Chun et al., 2009). *katG* mutants caused less severe disease symptoms on rice, which proved that catalase also functioned as one of the virulence factors (Chun et al., 2009). Recently, QsmR was shown to regulate the *obcAB* genes for oxalate production, which has detoxifying activity toward ammonia production in the stationary phase in *B. glumae* and *B. thailandensis* (Goo et al., 2012).

1.7 The role of QS in the reaction of bacterial cell to plant host defense system

Virulent pathogens have compatible reactions to susceptible plant hosts, whereas avirulent pathogens have incompatible reactions to resistant plants (Kachroo and Kachroo, 2007). Plants can ward off invasions by pathogens through constitutive and induced defense systems (Kachroo and Kachroo, 2007; Nahar et al., 2011). In general, the plant hormones salicylic acid (SA), jasmonic acid (JA) and ethylene (ET) induce different defense pathways in individual, synergisti or antagonistic manners (Kachroo and Kachroo, 2007). The defense systems in dicotyledonous plants have been extensively studied (Nahar et al., 2011). In general, the SA pathways acts against biotrophic pathogens and is mutually antagonistic to JA/ET defenses while JA/ET pathways act against insect and necrotrophic pathogens (Nahar et al., 2011). Some plants can sense bacterial QS signals and respond by expressing their own defense systems, which can be used as biocontrol strategies (Schuhegger et al., 2006). For example, *N*-butanoyl-L-homoserine lactone (BHL) and *N*-hexanoyl-L-homoserine lactone (C6-HSL), the QS signals used by root colonizer *Serratia liquefaciens* MG1 were determined to be the inducer of the expression of salicylic acid and systemic resistance of the hosts to *Alternaria alternata* (Schuhegger et al., 2006).

Pathogens that can successfully cause diseases must have the ability to suppress or avoid plant defense responses (Bushnell and Rowell, 1981). To infect susceptible plants, pathogens use specific strategies like Type III secretion system (T3SS), phytotoxins, small molecule suppressors and gene silencing components to overcome host defense systems (Abramovitch and Martin, 2004). The mechanisms bacterial pathogens use to suppress plant defense systems are mostly T3SS related (Abramovitch and Martin, 2004). AvrPtoB T3SS effectors in strain *P. syringae* pv. *tomato* DC3000 can suppress

programed cell death (PCD) initiated by Pto and Cf9 resistance proteins in *Nicotiana benthamiana*, which was the first report about a T3SS effector acting as the PCD suppressor (Abramovitch et al., 2003). Another T3SS effector, AvrPto in *P. syringae* pv. *tomato* DC3000 suppressed the papillae-based cell wall modification response in *Arabidopsis* (Hauck et al., 2003). *hrp* genes in *X. campestris* pv. *vesicatoria* can also suppress papillae deposition (Brown et al., 1995) and nodulation outer protein L (NopL), a T3SS effector of *Rhizobium* sp. NGR234, suppresses the expression of pathogenesis-related genes in tomato (Bartsev et al., 2004). In addition to T3SS dependent factors, phytotoxins also surpress plant defenses. Along with Type III effectors in DC3000, coronatine can enhance a coronatine insensitive 1 (COI1)-dependent pathway possibly through a JA avenue to promote disease (Abramovitch and Martin, 2004; He et al., 2004). *B. glumae* was able to utilize a T3SS to make direct contact with and cause symptoms on host plants (Kang et al., 2008), but no type III effector has been identified yet (Ham et al., 2011). Since QS is the regulator of T3SS, it is possible that QS is involved in plant defense suppression.

1.8 Transposon random mutagenesis

Transposon random mutagenesis is widely used in the functional genomic study of plant bacterial pathogens. Transposons can promote their own transposition, interrupt the normal transcription of the insertion site and encode various traits like sugar utilization, colonization, pathogenicity and antibiotic resistance (Mills, 1985). The ones possessing antibiotic resistance are usually selected to perform genetic function analysis (Mills, 1985). Prior to affordability and ease of genome sequencing of bacterial plant pathogens, transposon random mutagenesis was the favored method for genome scale analysis (Jackson, 2009). Tn5 remains one of the most common transposons

used today and there are several advantages that make Tn5 suitable for mutagenesis studies: high frequencies of transposition, random insertion, stable mutation and low rates of secondary transposition (Mills, 1985).

There are some successful examples about how plant pathologists located the virulence factor genes. In 1985, the use of transposon random mutation followed by southern blot analysis revealed the genetic locus responsible for syringotoxin production in *P.syringae* pv. *syringae* was in 10.5- and 17.8-*kb EcoR*I fragments (Morgan and Chatterjee, 1985). In 1987, *pscA* was first mentioned as the gene affecting tumor formation by *A. tumefaciens* on several host plants, through the analysis of transposon inserted mutant of *pscA* (Thomashow et al., 1987). In 1991, transposon mutagenesis resulted in the discovery of T3SS genes in *X. campestris* pv. *campestris* (Arlat et al., 1991). In 1992, transposon mutation strategy proved that exopolysaccharide (EPS) was the important virulence factor for *Erwinia amylovora* (Bellemann and Geider, 1992).

Mini-Tn*5* derivatives with individual resistance markers (e.g. mini-Tn*5*Km and miniTn5*Cm*) and reporter fusion (e.g. miniTn5*lacZ*) were engineered from Tn5 (Delorenzo et al., 1990). These mini-transposons contain *Not*I, flanked by a specific Tn5 sequence useful for genetic characterization, single marker that was easier for series of plasmid introduction and selection, and a conjugal transfer factor feasible for mutagenesis of bacterial recipients like *B. glumae* (Delorenzo et al., 1990). The advancements in the development of genomics tools resulted in significant genetic discoveries in plant pathogenic bacteria. Mini-Tn*5*Km mutagenesis followed by high-performance liquid chromatography (HPLC) and thin-layer chromatography (TLC) exposed the important virulent factor thaxtomin in *Streptomyces acidiscabies* (Healy et

al., 2000). Another example is gene discovery through mini-Tn*5*Km screening (Espinosa-Urgel et al., 2000) which has revealed a putative role in seed colonization by hemolysin in *Pseudomonas putida*. Again in 1990, the fusion of the reporter gene *gusA* to Tn5 was generated to analyze the expression of symbiotic genes of *R. meliloti* in alfalfa nodules (Sharma and Signer, 1990). The mini-Tn*5*Cm inserted *rpoS* mutants of *E. carotovora* subsp. *carotovora* showed reduced stress tolerance and ability to compete with the wild type bacteria, which implied that the RpoS factor is critical for bacterial survival in competitive and stressful environments (Andersson et al., 1999). Tn5-*gusA* was also used to detect the gene cluster that is involved in the production of albicidin (Rott et al., 1996), the essential factor for development of leaf scald symptoms in sugercane caused by *X. albilineans* (Birch, 1987; Birch and Patil, 1987). Mini-transposons fused with *gusA* reporters were subsequently generated. Several plant inducible genes in *E. carotovora* subsp. *carotovora* were selected from X-Gluc plates because the promoters of those genes expressed *β*-glucuronidase, which was encoded by mini-Tn*5gusA* (Cm) that was inserted downstream of the promoter regions, when there were plant extracts in the media; and the genes identified from this procedure included the important maceration factor gene *prtW* (Marits et al., 1999). Mini-Tn*5gusA* (Km) was constructed and utilized for genomic screening of the *hrp* regulon, which led to the discovery of nine novel virulence-implicated ORFs (Fouts et al., 2002).

1.9 Quantitative PCR (qPCR) used in bacterial functional study

qPCR is one of the most popular molecular technologies used in plant disease diagnosis, facilitating the rapid quantification of pathogens, especially those present in low populations or non-culturable individuals (Okubara et al., 2005). Certain bacterial plant diseases are difficult to control; therefore, it is important to produce pathogen-free

plant propagation materials. Detecting pathogens in symptomless plant material requires highly sensitive and accurate measurements since pathogens in the latent phase remain in very low concentrations (Lopez et al., 2003). qPCR can efficiently detect one or even more pathogens in a short time by monitoring amplicons using fluorescent dyes or complimentary probes. A multiplex reaction was designed to discriminate *Ralstonia solanacearum* strains using a probe-primer set (RS) for all known *R. solanacearum* strains and another set (B2) detecting only biovar 2A, the destructive biovar causing potato brown rot disease. The multiplex reaction utilizing the probe-primer set (RS) and one additional set targeting the potato cytochrome oxidase (COX) gene was able to accurately detect *R. solanacearum* directly from the potato tuber tissue (Weller et al., 2000). qPCR can quantify the amount of the targets by monitoring fluorescent reporters in one reaction and comparing these with the standards. Using primers corresponding to intergenic sequences of the ribosomal RNA (rRNA) operon and Taqman® specific probes, qPCR distinguished the subspecies of *Clavibacter michiganensis* and quantified the absolute amount of the existing bacterial strains which provided promising insight into the ecology of the pathogen cluster (Bach et al., 2003).

qPCR is a very sensitive and convenient tool to detect target gene expression in different conditions. Reference (housekeeping) genes such as hypoxanthine-guanine phosphoribosyltransferase (HPRT) or ubiquitin are commonly used to normalize data since they are constitutively expressed. This helps to avoid loading artifacts and miscalculating the fold-change of amplicons representing the mRNA expression (Takle et al., 2007). qPCR has also been used to confirm the selection from genome scale searching of certain genetic traits (de Souza et al., 2003; Mattinen et al., 2007). The

secretome of the potato-rotting bacterium, *Pectobacterium atrosepticum* with the presence of plant extract was characterized and expression of some of the encoding genes including *vgrG* and three homologous hemolysin-coregulated proteins genes (*hcp*) were verified by qPCR (Mattinen et al., 2007). It was determined that over-expression of one of the *vgrG* genes was the primary virulence determinant (Mattinen et al., 2007). Microarray analysis was used to compare the transcriptome of fresh bacterial cultures and bacterial cultures less adept in colonizing sweet orange and periwinkle plants and found that differentially expressed genes included the ones that were potentially pathogenicity-related (de Souza et al., 2003). qPCR was performed to validate this result, and two analyses were consistent (de Souza et al., 2003). Currently, qPCR is performed routinely to verify experiments and assess the abundance of selected transcripts in different conditions following RNA-seq analysis. For example, RNA-seq and qPCR verification were performed on the transcriptome of one rice paddy isolate of *Acinetobacter oleivorans* DR1, which used the AqsI/AqsR/AHL system as its QS regulator (Kim and Park, 2013). To determine the regulon of *aqsR*-dependent QS, comparative transcriptomics between wild type and Δ*aqsR* mutant in stationary phase was performed using RNA-seq of the mRNA of the subjects (Kim and Park, 2013). The expression profiling revealed that 111 genes were up-regulated and 242 genes were down-regulated in the wild type compared with Δ*aqsR* mutant (Kim and Park, 2013). The upregulated genes *sapA* encoding putative surface adhesion protein and AOLE_11355 encoding L-asparaginase were selected from RNA-seq analysis and confirmed by qRT PCR. This result suggested that QS in strain DR1 might control SapA mediated-biofilm and amino acid utilization (Kim and Park, 2013).

1.10 Transcriptome analysis of bacteria through RNA-seq

RNA-seq is an emerging technique that provides high-throughput information about genome-wide analysis of gene expression profiles rapidly and economically (Mutz et al., 2013). RNA-seq is one transcriptomics variant of short-read next generation sequencing (NGS) technology, of which was based on pyrosequencing (Mutz et al., 2013). Through pyrosequencing, the template sequence can be recorded by sensing the release of PPi from the corresponding nucleotides at the 3' end of the primers (Mutz et al., 2013). 454 sequencing was the first reported RNA-seq platform, followed by the currently widely-used Illumina (double stranded bridge clone) and SOLiD (bead clones) platforms (Hitzemann et al., 2013; McGettigan, 2013).

Comparative analysis of transcriptomes has been useful in targeting the genes that play roles in certain bacterial behavior. For example, in a single transcriptome analysis of the opportunistic pathogen *P. aeruginosa*, researchers simultaneously identified numerous feature determinants like genes for osmotic and starvation stress responses, biofilm, pathogenesis, alginate production and QS (Balasubramanian and Mathee, 2009). In 2003, three research groups performed transcriptomics on *P. aeruginosa* by comparing the gene expression profile of wild type and *lasI*/*rhlI* (two AHL synthase genes) deficient mutants (Balasubramanian and Mathee, 2009). What they found in common was that approximately 100 genes were expressed differently, many of them encoding toxin or extracellular enzymes. This suggested a regulatory relationship between those products and QS systems (Balasubramanian and Mathee, 2009).

Compared to eukaryotes, fewer transcriptome studies have been done with bacteria, probably due to the technical difficulties associated with specific targeting of

mRNA lacking polyA tails and differentiating them from much more abundant rRNAs (Yoder-Himes et al., 2009). Therefore, improvement on the technology of mRNA enrichment was a milestone of the RNA-seq era in bacteriology. Though RNA-seq analysis has not dominated the study of bacterial phytopathogens, there are some successful examples using this powerful technology. The total RNAs of *P. syringae* pathovar tomato DC3000 growing in ion-limited media were extracted and enriched then processed for RNA-seq by Illumina (Filiatrault et al., 2010). Through data analysis, researchers were able to improve upon the annotation and discover several interesting characteristics of the genome: 1, transcription did not always start at the start codon of the annotated open reading frame (ORF); 2, 124 genes showed expression on both sense and anti-sense strands, and the coronatine gene also belonged to this group; 3, 223 genes that were expressed in ion-limited conditions encoded known or potential virulence-related traits; 4, 106 incorrect coding regions were determined, and one new ORF had potential antisense and ferric uptake regulation activities; 5, many non-coding RNAs (ncRNAs) were found, the majority of which were housekeeping RNAs, riboswitches or 5' untranslated region regulatory elements (Filiatrault et al., 2010). Comparative transcriptomics between wild type and *hrp*-mutants was performed for *X. campestris* pv. *vesicatoria* to survey its transcriptional landscape (Schmidtke et al., 2012). The RNA-seq data analysis unveiled information including the transcription start sites' (TSSs) arrangement through the genome, which was categorized into four groups: 5' of the annotated coding DNA sequence (CD), inside of CD, antisense of CD, and the orphan TSS (Schmidtke et al., 2012). Additionally, type III secretion system (T3SS) sRNAs that were potentially involved in pathogenicity were reported (Schmidtke et al.,

2012). In particular, *sX12*, which was *hrpX* (*hrp* regulator)-dependent, was determined to accumulate in stationary phase and contribute to virulence (Schmidtke et al., 2012). RNA-seq has not been widely implemented in the study of *Burkholderia* species, but its emerging role can be anticipated. To explore the niche-adaptational transcriptional responses of *B. cenocepacia*, the transcriptome of two closely related strains AU1054 (human pathogen for cystic fibrosis, CF) and HI2424 (soil dweller) were extracted from bacterial culture grown in the conditions that mimicked their national environments (Yoder-Himes et al., 2009). The RNA-seq data unraveled very complicated information from an expression profile which can be summarized as the following: environmental cues induced a unique gene expression profile; HI2424 rather than AU1054 appeared to exhibit a more striking response when adapting to its soil habitat; CF-like condition induced gene expression for energy production, translation, and virulence factors including molecular chaperones and immunogenic proteins; soil-like condition induced gene expression for signal transduction, nitrogen acquisition, and excessive uncharacterized proteins, which indicated that there is much more to learn about the soil stimuli (Yoder-Himes et al., 2009). RNA-seq based transcriptomics was also applied to investigate the regulon of QS in *Burkholderia* spp*.* There are two QS systems in *B. cenocepacia*: CepI/CepR/AHL and $RpfF_{Bc}$/RpfR/BDSF and they both regulate multiple functions (Schmid et al., 2012). To further study the interconnection between the two QS systems, RNA-seq combined with shotgun proteomics was performed to analyze the expression profile at both the transcription and translation levels (Schmid et al., 2012). The evidence demonstrated that two systems worked in an independent manner

with an overlapping stimulon including the large surface protein BapA and metalloprotease ZmpA (Schmid et al., 2012).

1.11 The recent genomics studies on *B. glumae*

Various genetic applications including genome-wide analysis have become promising for QS study in *B. glumae,* especially its genome sequence was released in 2011 on NCBI by Hwang's group (Lim et al., 2011). The same research group performed proteomic analyses to search for the QS-regulated proteins in the genome wide range (Goo et al., 2010). With the confirmation at the transcriptional level, 49 extracellular and 13 intracellular proteins, of which large portion of secreted proteins were dependent upon T3SS, were proven to be the regulon of QS (Goo et al., 2010). Genomic screening was also performed by Kim et al. (2004) to locate the *luxI* and *luxR* genes (Chen, 2011; Kim et al., 2004b). Goo et al. (2012) performed RNA-seq again to explore how QS adjusted the transcriptional profiling of *B. glumae* at different growth stages (Goo et al., 2012).

Currently genomic screening of a number of virulence regulators by using of miniTn5*Km* is being investigated in our lab (Melanson and Ham, unpublished). We previously found various unique genomic islands in the Louisiana isolated strain 336gr-1 which were not present in the Korean strain BGR1 and *vice versa* (Francis et al., 2013). Our laboratory also attempted to generate high throughput information about QS in *B. glumae* by RNA-seq techniques(Francis, 2012). Random mutagenesis and RNA-seq were applied to genomic study of the *tofI-R* system in this project, and many novel QS-related regulators were discovered.

CHAPTER 2. GENETIC DISSECTION OF THE *TOFI-TOFR* QUORUM-SENSING AND RELATED GENES IN THE RICE PATHOGEN *BURKHOLDERIA GLUMAE*

2.1 Introduction

Burkholderia glumae, the primary causal agent of bacterial panicle blight (BPB) of rice, is one of the most important disease problems affecting rice production in the southern United States, including Louisiana, Arkansas and Texas (Ham et al., 2011). This rice disease has also been reported from many rice-growing areas around the world, including east Asia, southeast Asia and South America (Ham et al., 2011). The optimal temperature range for the growth of *B. glumae* is 38 - 40°C, but this bacterium can also grow at temperatures as high as 50°C (Nandakumar et al., 2009b). A typical characteristic of *B. glumae* is the production of the bright yellow phytotoxin, toxoflavin, which is a major virulence factor of this pathogen (Iiyama et al., 1995; Kim et al., 2004a; Nagamatsu, 2002; Suzuki et al., 2004b).

In *B. glumae*, production of major virulence factors, including toxoflavin, is dependent on the quorum-sensing (QS) system mediated by a pair of LuxI and LuxR homologs, TofI and TofR (Devescovi et al., 2007a; Kim et al., 2007b; Kim et al., 2004a). QS is a cell-to-cell communication mechanism that allows bacterial cells to collectively behave like a multicellular organism. In Gram-negative bacteria, QS systems mediated by LuxI and LuxR-family proteins are involved in a diverse range of bacterial behaviors and traits, including formation of biofilm, production of virulence factors, conjugation, and antibiosis (Fuqua et al., 2001; Miller and Bassler, 2001). The LuxI/LuxR system,

* Chapter 2 previously appeared as [Chen, R.X., Barphagha, I.K., Karki, H.S., and Ham, J.H. (2012). Dissection of quorum-sensing genes in *Burkholderia glumae* reveals non-canonical regulation and the new regulatory gene *tofM* for toxoflavin production. PLoS One *7*]. It is reprinted by permission of PLoS One.

which is considered the prototype of the QS systems of Gram-negative bacteria, was first discovered from *Vibrio fischeri*, a luminous symbiont in marine animals (Eberhard, 1972; Fuqua et al., 1994). LuxI-family proteins are synthases that produce *N*-acyl homoserine lactone (AHL)-type intercellular signal molecules; LuxR-family proteins are cognate receptors that specifically bind to the AHL molecules (Dunlap, 1999).

Two types of AHL molecules, *N*-octanoyl homoserine lactone (C8-HSL) and *N*-hexanoyl homoserine lactone (C6-HSL), are synthesized by the LuxI-family protein of *B. glumae*, TofI (Kim et al., 2004a). It is thought that the LuxR-family protein of *B. glumae*, TofR, specifically binds to C8-HSL and the resultant TofR-C8-HSL complex triggers the production of toxoflavin by activating the transcription of *toxJ*, which has a *lux* box-like *cis* element (*tof*-box) upstream of the coding sequence for the binding of the TofR-C8-HSL complex (Kim et al., 2004a). Unlike C8-HSL, functions of C6-HSL in *B. glumae* and other *Burkholderia* spp. remain unknown. ToxJ encoded by *toxJ* is required for the transcription of *toxR*; and ToxR, a LysR-type transcriptional regulator, in turn activates the expression of the *toxABCDE* and *toxFGHI* operons, which harbor gene clusters for toxoflavin biosynthesis and transport, respectively (Kim et al., 2004a). This regulatory cascade (the TofI/TofR QS system → ToxJ → ToxR → *toxABCDE* and *toxFGHI*) is considered to be the central regulatory system for the production of toxoflavin, which may allow *B. glumae* to attack host cells in accordance with its population levels at infection sites (Kim et al., 2004a). Nevertheless, the genetic functions of *tofI* and *tofR* as well as additional components of the QS system governing the expression of bacterial virulence genes in *B. glumae* are not fully understood.

In this study, a series of deletion mutants deleted in the QS genes, *tofI* and *tofR*, were successfully generated from the U.S. virulent strain, 336gr-1 (Nandakumar et al., 2009a), for the further characterization of the QS system and the related global regulatory network in *B. glumae*. Through the genetic analyses conducted in this study, previously unknown *tofI*- and/or *tofR*-independent pathways for the production of toxoflavin were revealed and a new regulatory gene required for these pathways, *tofM*, was discovered between the *tofI* and *tofR* loci.

2.2 Materials and Methods

2.2.1 Bacterial strains, plasmids, media and growth conditions

The bacterial strains and plasmids used in this study are listed in Table 2.1. All the *Escherichia coli* and *B. glumae* strains were routinely grown or maintained in LB broth or on LB agar plates (Sambrook, 2001) at 30°C or 37°C (even though the original definition of LB was corrected by Bertani as 'lysogeny broth' (Bertani, 2004), the terms, 'LB broth' and 'LB agar', are used to clearly contrast two different growth conditions tested in this study). Bacterial strains grown in liquid media were incubated in a shaking incubator at 200 rpm. LB agar plates amended with 30% sucrose were used to counter-select the recombinant mutants that lost the sucrose-sensitive gene, *sacB*, through the secondary homologous recombination. The levels of bacterial growth and toxoflavin production in liquid or solid media were determined in four different growth conditions; LB alone, LB with 1 μM C6-HSL (Sigma-Aldrich, St. Louis, MO, USA); LB with 1 μM C8-HSL (Sigma-Aldrich, St. Louis, MO, USA); and LB with both 1 μM C6-HSL and 1 μM C8-HSL. The antibiotics and their working concentrations used in this study were:

ampicillin (Amp), 100 µg/ml; kanamycin (Km), 50 µg/ml; nitrofurantoin (Nit), 100 µg/ml; gentamycin (Gm), 20 µg/ml; and tetracycline (Tc), 20 µg/ml.

Table 2.1. The bacterial strains and plasmids used in these experiments

Strain or Plasmid	Description	Reference
Escherichia coli		
DH10B	F¯ *araD139* Δ(*ara, leu*)7697 Δ*lacX74 galU galK rpsL deoR* ø80d*lacZ*ΔM15 *endA1 nupG recA1 mcrA* Δ(*mrr hsdRMS mcrBC*)	(Grant et al., 1990)
DH5α	F¯ *endA1 hsdR17* (r_k^-, m_k^+) *supE44 thi-1 λ*¯ *recA1 gyrA96 relA1 deoR* Δ(*lacZYA*-argF)-U169 ø80d*lacZ*ΔM15	(Grant et al., 1990)
S17-1λpir	*recA thi pro hsdR* [res- mod+][RP4::2-Tc::Mu-Km::Tn*7*] λ *pir* phage lysogen, Sm^r/Tp^r	(Simon et al., 1983)
Burkholderia glumae		
336gr-1	Wild type strain and the causative isolate of bacterial panicle blight of rice in Crowley, LA	This study
LSUPB145	A Δ*tofI* derivative of 336gr-1	This study
LSUPB169	A Δ*tofR* derivative of 336gr-1	This study
LSUPB139	A Δ*tofI-tofR* derivative of 336gr-1	This study
LSUPB201	A Δ*tofI*/Δ*tofR* derivative of 336gr-1	This study
LSUPB286	A Δ*tofM* derivative of 336gr-1	This study
LSUPB292	A Δ*tofR*/Δ*tofM* derivative of 336gr-1	This study
LSUPB293	A Δ*tofI*/Δ*tofM*/Δ*tofR* derivative of 336gr-1	This study
LSUPB294	A Δ*tofI*/Δ*tofM* derivative of 336gr-1	This study
Chromabacterium violaceum		
Chromabacterium violaceum CV026	A biosensor that can detect AHL molecules	(McClean et al., 1997)
Plasmid		
pSC-A-amp/kan	A blunt PCR cloning vector; f1 *ori*, pUC *ori*, *lacZ*', Km^R, Amp^R	Stratagene
pRK2013::Tn*7*	A helper plasmid; ColE1 *ori*	(Ditta et al., 1980)
pL3SAC	RK2 *ori*, Tc^R, *sacB*	(Kearney and Staskawicz, 1990)
pKKSacB	A suicide vector; R6K γ-*ori*, RP4 *oriT*, *sacB*, Km^R	This study
pKNOCK-Km	A suicide vector; R6K γ-*ori*, RP4 *oriT*, Km^R	(Alexeyev, 1999)
pKNOCK-Gm	A suicide vector; R6K γ-*ori*, RP4 *oriT*, Gm^R	(Alexeyev, 1999)
pLD55	A suicide vector; f1 *ori*, R6K *γ-ori*, RP4 *oriT*, *lacZα*, Amp^R, Tc^R	(Metcalf et al., 1996)

Table 2.1 continued

Strain or Plasmid	Description	Reference
pGP5603	A suicide vector, R6K *ori*, RP4 *mob*, *lacZ*', Km^R	(Penfold and Pemberton, 1992)
pBBR1MCS-2	A broad host range cloning vector, RK2 *ori*, *lacZα*, Km^R	(Kovach et al., 1995)
Strain or Plasmid	Description	Reference
pBBR1MCS-5	A broad host range cloning vector, RK2 *ori*, *lacZα*, Gm^R	(Kovach et al., 1995)
pSCtofIU	A clone of the 545-bp upstream flanking region of *tofI* in pSC-A-amp/kan, Amp^R, Km^R	This study
pSCtofID	A clone of the 512 *bp* downstream flanking region of *tofI* in pSC-A-amp/kan, Amp^R, Km^R	This study
pLDtofID	A subslone of pSCtofID for a downstream flanking region of *tofI* in pLD55, Amp^R, Tc^R	This study
pLDtofIUD	A subclone of pSCtofIU for an upstream flanking region of *tofI* in pLDtofID, Amp^R, Tc^R	This study
pJPtofIUD	A suclone of pLDtofIUD for an upstream and downstream flanking region of *tofI* in pGP5603, Km^R	This study
pKKSacBΔtofI	A subslone of pJPtofIUD for an upstream and downstream flanking region of *tofI* in pKKSacB, Km^R	This study
pSCtofRU	A clone of the 426-bp upstream flanking region of *tofR* in pSC-A-amp/kan, Amp^R, Km^R	This study
pSCtofRD	A clone of the 892-bp downstream flanking region of *tofR* in pSC-A-amp/kan, Amp^R, Km^R	This study
pKKtofRD	A subclone of pSCtofRD for a downstream flanking region of *tofR* in pKNOCK-Km, Km^R	This study
pKKtofRUD	A subclone of pSCtofRU for a upstream flanking region of *tofI* in pKKtofRD, Km^R	This study
pKKSacBΔtofR	A subclone of pKKtofRUD for an upstream and downstream flanking region of *tofR* in pKKSacB, Km^R	This study
pLDtofIDRD	A subclone of pSCtofRD for a downstream flanking region of *tofR* in pLDtofID, Amp^R, Tc^R	This study
pKKSacBΔtofIMR	A subclone of pLDtofIDRD carrying downstream flanking regions of *tofI* and *tofR* in pKKSacB, Km^R	This study
Cos808	The cosmid clone harbouring *tofI*, *tofM* and *tofR*, Amp^R	This study
pBBtofIMR	A subclone of Cos808 for the 3,671-bp *tofI/tofM/tofR* region in pBBR1MCS-2 at *Eco*RI and *Sac*I sites, Km^R	This study

Table 2.1 continued

Strain or Plasmid	Description	Reference
pBBtofIM	A subclone of pBBtofIMR for the 2,808-bp *tofI/tofM* region in pBBR1MCS-5 at *Bgl*II and *Sac*I sites, Gm^R	This study
PBBtofRM	A subclone of pBBtofIMR for the 1,925-bp *tofR/tofM* region in pBBR1MCS-2 at *EcoR*I and *Pvu*II sites, Km^R	This study
Strain or Plasmid	Description	Reference
pSCtofMU	A PCR clone of the 433-bp upstream flanking region of *tofM* in pSC-A-amp/kan, Ap^R, Km^R	This study
pSCtofMD	A PCR clone of the 412-bp downstream flanking region of *tofM* in pSC-A-amp/kan, Ap^R, Km^R	This study
pKKSacBtofMU	A subclone of pSCtofMU for a upstream flanking region of *tofM* in pKKSacB, Km^R	This study
pKKSacBΔtofM	A clone carrying an upstream and downstream flanking region of *tofM* in pKKSacB, Km^R	This study
pSCtofM	A clone of the 986-bp including *tofM* gene and its upstream region, Ap^R, Km^R	This study

2.2.2 Recombinant DNA Techniques

Routine DNA cloning and amplification procedures were conducted following standard methods (Sambrook, 2001). PCR products used for cloning were purified using the QuickClean 5M PCR Purification Kit (GenScript, Piscataway, NJ, USA) and cloned into pSC-A-amp/kan using the Strata Clone™ PCR cloning kit (Agilent Technologies, Santa Clara, CA, USA). Genomic DNA of the wild type and mutant strains were extracted using the GenElute™ Bacterial Genomic DNA kit (Sigma-Aldrich, St. Louis, MO, USA). Electroporation for transforming *E. coli* cells was conducted with a GenePulser unit (BioRad Laboratories, Hercules, CA, USA) at 1.5 kV with 2 µl DNA and 25 µl competent cells. Triparental mating using the helper plasmid, pRK2013::Tn*7* (Ditta et al., 1980), was used to transform *B. glumae* (Figurski and Helinski, 1979). DNA were

extracted from agarose gels using the GenElute^{TM} Gel Extraction Kit (Sigma-Aldrich, St. Louis, MO, USA). DNA sequencing was performed by the LSU School of Veterinary Medicine Gene Lab. DNA concentrations were measured using a NanoDrop DN-1000 Spectrophotometer (Thermo Scientific, Wilmington, DE, USA). The genomic library of *B. glumae* 336gr-1 was created previously in our laboratory (Karki et al., 2012a).

2.2.3 Allelic exchange of the *B. glumae* genome for targeted deletions

(*This part of the work was partially performed by Ms. Inderjit Barghaphagha*)

A DNA construct in pKKSacB for deleting a target gene(s) was first introduced into a parental *B. glumae* strain via conjugation, following a previously described method (Karki et al., 2012a). Because *B. glumae* is resistant to Nit and pKKSacB contains a Km-resistance gene, the recombinant *B. glumae* strain in which a DNA construct in pKKSacB is integrated in the genome via single homologous recombination was initially selected on LB agar medium containing Km and Nit. Subsequently, the selected strain was grown overnight at 30°C in LB broth without any antibiotics. To select the mutants with secondary homologous recombination between the integrated DNA construct and the genome, which would result in the eviction of the integrated DNA construct and consequently the deletion of the target gene(s), the overnight culture was spread on LB agar medium containing 30% sucrose to select sucrose-resistant colonies. Individual sucrose-resistant colonies of *B. glumae* were then tested for the sensitivity to Km to screen marker-less deletion mutants. Deletion of target gene(s) in each of the selected Km-sensitive and sucrose-resistant mutants was confirmed by the appropriate diagnostic PCRs. Deletions of *tofI*, *tofR*, *tofM* were confirmed using the primer sets, TofI(H)F/TofI(H)R, TofR(H)F/TofR(H)R, and orf1-CT-F/orf1-CT-R, respectively, while the deletion of the entire *tofI-tofR* region in LSUPB139 was confirmed using the primer

set, TofI(H)F/TofR(H)R. Primer sequences and PCR conditions for individual primer sets are described in Table 2.2.

Table 2.2. Primers and PCR conditions used in this study.

Primer name	Primers* (5' → 3')	Annealing and extension conditions
dtof1	ACTGGTACC TCGAACCCGACTCCG	Annealing: 60°C/30 s Extension: 72°C/1 min
dtof2	GGATCCAGCTCGGCGGCGATATGG	
dtofI3	GGATCCACATCGACGCGCAGACGC	Annealing: 62°C/30 s Extension: 72°C/1 min
dtofI4	GCACTAGTATCCGCCCGAGATCCG	
TRD3	GGATCCGCGCGAACGCGAGGTGC	Annealing: 65°C/30 s Extension: 72°C/1 min
TRD6	ACTAGTACGGCGTGACCGGCGTC	
TofR BF	AGGATCCGCTGCTCGTTTTCC	Annealing: 55°C/30 s Extension: 72°C/1 min
TofR BR	GACTAGTATCAGATTGCTGCG	
TofI(H)F	GTTCGTCAACGACGACTACG	Annealing: 53°C/30 sec Extension: 72°C/2.5 min
TofR(H)R	CATGAGCATGGAAAAGAGCA	
TofI(H)F	GTTCGTCAACGACGACTACG	Annealing: 54°C/30 s Extension: 72°C/1 min
TofI(H)R	CGGAATTACCACGAGGACAC	
orf1-CT-F	ATGGTCAACAGTCCGAACACGC	Annealing: 58°C/30 s Extension: 72°C/1 min
orf1-CT-R	TCATGGGCTGCTTAAACGCAGAAG	
TofR(H)F	AAGAATGACAGCGTGGAAGC	Annealing: 50°C/30 s Extension: 72°C/1 min
TofR(H)R	CATGAGCATGGAAAAGAGCA	
tofI-jh1	GTCTACGTATTGGGACGCGAT	Annealing: 55°C/30 s Extension: 72°C/30 s
tofI-jh2	ACAGCCGCTCGATGCTGCAGA	
UPHP- FP	GGATCCACATGCCGAAGTC	Annealing: 50°C/30 s Extension: 72°C/1 min
UPHP- RP	ACTAGTGTAGGGATGAAGCA	
DwN-FP	ACTAGTCGCTGGTCGCAC	Annealing: 50°C/30 s Extension: 72°C/1 min
DwN-RP	TCTAGAGAATTTTTCGTCTTC	

2.2.4 DNA constructs for the targeted deletions of *tofI*, *tofM*, and *tofR*

(*This part of the work was mostly performed by Ms. Inderjit Barghaphagha*)

DNA constructs for deletion mutations and deletion mutants of *B. glumae* generated in this study are listed in Table 2.1. PCR primers used to create and confirm deletion mutations are listed in Table 2.2. All deletion mutants generated in this study were obtained through double-crossover homologous recombination in the flanking regions of targeted genes (Figure 2.1).

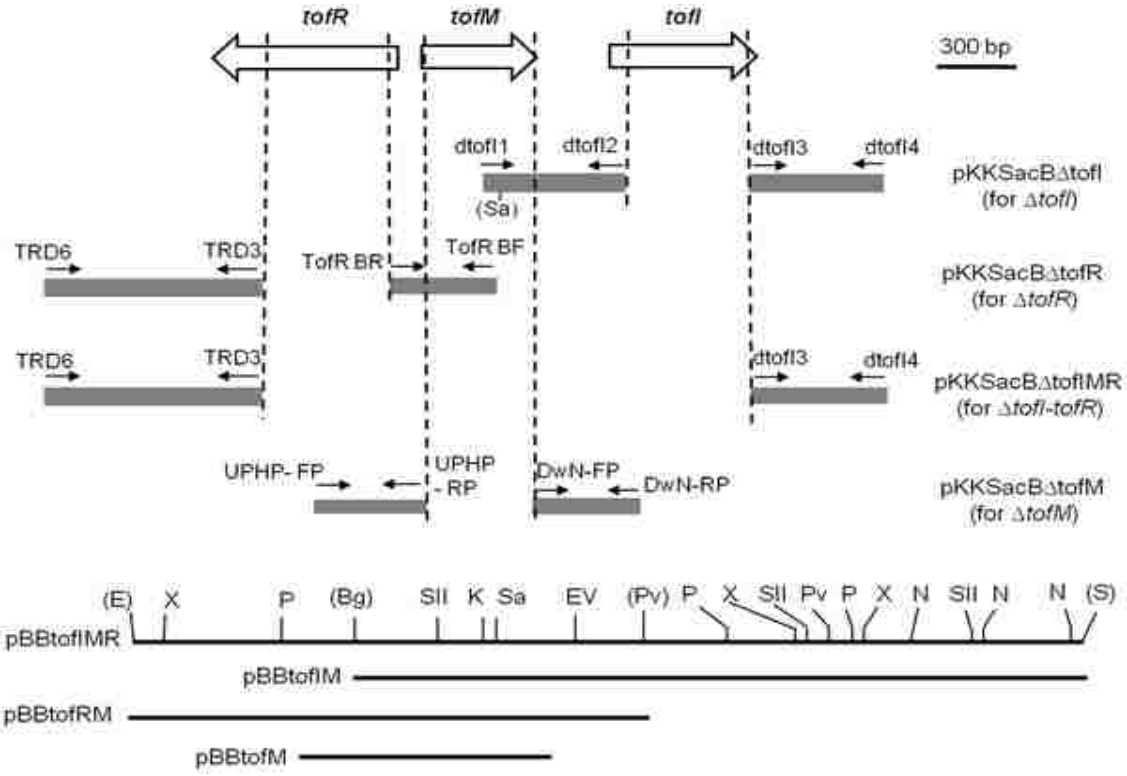

Figure 2.1. A schematic view of the *tofI*, *tofM*, and *tofR* loci and the DNA constructs used for deletion mutation and genetic complementation. The grey areas indicate the flanking regions cloned in pKKSacB for individual or combined deletions of *tofI*, *tofM*, and *tofR*. The genomic regions to be deleted with the DNA constructs in pKKSacB are indicated with vertical hatched lines, while those cloned in a broad host vector, pBBR1MCS-2 or pBBR1MCS-5, for complementation tests are indicated with horizontal solid lines. Small arrows indicate the primers (Table 2.2) used for the amplification of each flanking region. Abbreviation for restriction sites are as follows: Bg, *Bgl*II; E, *Eco*RI; EV, *Eco*RV; K, *Kpn*I; N, *Not*I; P, *Pst*I; Pv, *Pvu*II; S, *Sac*I; Sa, *Sal*I; SII, *Sac*II; X, *Xho*I. Restriction sites used for generating pBBtofIMR, pBBtofIM, and pBBtofRM are denoted with parentheses.

To construct pKKSacBΔtofI that was used to create the *tofI* deletion mutants, a 545-bp region upstream and a 512-bp region downstream of *tofI* were amplified with the primer sets, dtofI1/dtofI2 and dtofI3/dtofI4, respectively (Table 2.2). The resultant PCR products for these *tofI* flanking sequences were initially cloned into pSC-A-amp/kan to generate pSCtofIU and pSCtofID. The downstream region of *tofI* in pSCtofID was then sub-cloned into pLD55 (Metcalf et al., 1996) using *Bam*HI and *Spe*I sites to get pLDtofID. The upstream region of *tofI* in pSCtofIU was cut with *Kpn*I and *Bam*HI and was then ligated to pLDtofID, cut with the same restriction sites, to generate pLDtofIUD. Because initial attempts to generate a *tofI* deletion mutant with pLDtofIUD using the tetracycline-resistant gene in pLD55 as a counter-selection marker in the presence of fusaric acid (Metcalf et al., 1996) failed, the deletion construct cloned into pLD55 was moved to pKKSacB through the following steps: the 1.1-kb *Kpn*I/*Xba*I-cut fragment from pLDtofIUD was first ligated to pJP5603, cut with *Kpn*I and *Xba*I, to generate pJPtofIUD and increase the choice of restriction sites for the final cloning into pKKSacB; the 1.1-kb *Sal*I-cut fragment derived from the native *Sal*I site present 68 bp downstream from the 5' end of the *tofI* upstream region cloned into pJPtofIUD and the *Sal*I site in the polylinker region of the same plasmid was then ligated into pKKSacB, cut with *Sal*I, to obtain pKKSacBΔtofI.

To construct pKKSacBΔtofR that was used to create the *tofR* deletion mutants, a 426-bp region upstream and an 829-bp region downstream of *tofR* were amplified with the primer sets, TofR BF/TofR BR and TRD6/TRD3, respectively (Table 2.2). The resultant PCR products were cloned into pSC-A-amp/kan to generate pSCtofRU and pSCtofRD, respectively. The downstream region of *tofR* in pSCtofRD was removed

using the *Bam*HI site in the primer and the *Pst*I site in the polylinker region of the plasmid and subsequently ligated to pKNOCK-Km, cut with *Bam*HI and *Pst*I, to get pKKtofRD. The upstream region of *tofR* in pSCtofRU, obtained from *Spe*I and *Bam*HI digestion, was then cloned into pKKtofRD using the same restriction sites, to generate pKKtofRUD. Finally, the *Spe*I-cut 1.3-kb DNA fragment containing the recombined flanking regions of *tofR* from pKKtofRUD was cloned to pKKSacB at the *Spe*I site to obtain pKKSacBΔtofR.

To construct pKKSacBΔtofM that was used to create the *tofM* deletion mutants, a 433-bp region upstream and a 412-bp region downstream of *tofM* were amplified with the primer sets, UPHP-FP/UPHP-RP and DwN-FP/DwN-RP, respectively (Table 2.2). The amplified PCR products were initially cloned into pSC-A-amp/kan to generate pSCtofMU and pSCtofMD, respectively (Table 2.2). The upstream region of *tofM*, obtained by *Bam*HI and *Spe*I digestions of pSCtofMU, was cloned into pKKSacB at the *Bam*HI and *Spe*I sites to get pKKSacBtofMU. The downstream region of *tofM*, cut from pSCtofMD by *Spe*I and *Xba*I, was then ligated to pKKSacBtofMU, cut with *Spe*I and *Xba*I, to obtain pKKSacBΔtofM.

To construct pKKSacBΔtofIMR that was used for the deletion of the entire *tofI-tofR* region, the downstream region of *tofR* in pSCtofRD was obtained by *Kpn*I and *Bam*HI digestions and subsequently ligated into pLDtofID, cut with *Kpn*I and *Bam*HI, to get pLDtofIDRD. The 1.3-kb DNA fragment that resulted from the *Spe*I digestion of pLDtofIDRD was then ligated to the *Spe*I-cut pKKSacB to obtain the final deletion construct, pKKSacBΔtofIMR.

2.2.5 DNA constructs for the complementation of the QS mutants

(*This part of the work was partially performed by Ms. Inderjit Barghaphagha*)

A cosmid library of the *B. glumae* 336gr-1 genome was screened with the primers, tofI-jh1 and tofI-jh2, to identify the cosmid clone that contains *tofI*. The cosmid clone, pCos808, was identified to contain *tofI* as well as *tofR* and *tofM*. pBBtofIMR, which contains *tofI*, *tofM*, and *tofR*, was constructed by cloning a 3,670-bp DNA fragment containing *tofI*, *tofM*, and *tofR* from Cos809 into pBBRMCS-2 using the *Eco*RI and *Sac*I sites. pBBtofIM was generated by subcloning the 2,808-bp *tofI/tofM* region of pBBtofIMR into pBBRMCS-5 using *Bgl*II and *Sac*I sites. pBBtofRM was constructed by subcloning the 1,925-bp *tofR/tofM* region of pBBtofIMR in pBBRMCS-2 using *EcoR*I and *Pvu*II sites. For pBBtofM, a 986-bp region that includes *tofM* was amplified using the primers orf1-CT-F and orf1-CT-R (Figure 2.1 and Table 2.2). The PCR products were initially cloned into the pSC-A-amp/kan vector following the manufacturer's protocol to generate pSCtofM. Then, the *tofM* region of pSCtofM was subcloned into pBBR1MCS-5 using *Spe*I and *Hind*III sites to get pBBtofM.

For complementation, each of these constructs was introduced into the appropriate *B. glumae* strain through triparental mating (Karki et al., 2012a).

2.2.6 AHL production assays

Chromobacterium violaceum CV026, which produces the purple pigment, violacein, in the presence of AHL molecules (McClean et al., 1997), was used as a biosensor to determine the AHL production by *B. glumae*. The AHL production assay was performed following the procedure used by Kim *et al.* (2004) with some modifications. Briefly, the supernatant fraction of an overnight culture of each *B. glumae* strain grown in LB broth at 37°C obtained after centrifugation was extracted with an

equal volume of ethyl acetate, air-dried in a fume hood, and the residue dissolved in 1% volume of sterile distilled deionized water. Then, 20 µl of each culture extract were applied to the cells of *C. violaceum* CV026 immediately after they were inoculated on a LB agar plate. The production of the purple pigment by this biosensor strain was observed after 48 h incubation at 30°C.

2.2.7 Quantification of bacterial growth

To quantify bacterial growth in liquid and solid media, an equal amount of overnight culture per volume of medium was applied to liquid and solid media (~10^6 cell/ml medium). For solid medium, 12.5 µl of an overnight culture were spread on an LB agar plate containing approximately 12.5 ml of LB agar. For liquid media, 3 µl of the same overnight culture were added to 3 ml LB broth. After incubation at 37°C for 24 h, bacterial growth was determined by measuring the absorbance of the bacterial culture suspension at 600 nm (OD_{600}). Overnight cultures in LB broth were measured directly. Cultures grown on LB agar plates were resuspended in 12.5 ml of fresh LB broth and then measured for OD_{600}.

2.2.8 Quantification of toxoflavin production

Toxoflavin production by each strain of *B. glumae* was quantified following a previously established method (Kim et al., 2004a) with some modifications for cultures grown in both liquid and solid media. For bacteria grown in LB broth, toxoflavin present in the supernatant obtained from the centrifugation of 1 ml of culture was extracted with 1 ml of chloroform. Following centrifugation, the chloroform fraction was transferred to a new microtube and air-dried in a fume hood. The residue in the microtube was dissolved in 1 ml of 80% methanol. For bacteria grown on LB agar, bacterial cells were removed from the surface of the agar and the remaining agar containing the diffused

toxoflavin was cut into small pieces with a razorblade. The chopped agar was then mixed with chloroform in 1:1 (w/v) ratio for toxoflavin extraction and the chloroform fraction was filtered through filter paper and collected in a new microtube. Chloroform was evaporated and culture filtrate residue was dissolved in 80% methanol as previously described. The absorbance of each sample was measured at 393 nm to determine the relative amount of toxoflavin (Jung et al., 2011).

2.2.9 Virulence tests for *B. glumae*

(*This part of the work was partially performed by Mr. Hari Karki*)

The onion assay system that was previously used to determine the virulence of *Burkholderia cenocepacia* (Jacobs et al., 2008) and *B. glumae* (Karki et al., 2012a; Karki et al., 2012b) was adopted in this study with minor modifications. Briefly, the fleshy scales of yellow onions were cut into pieces (~2 X 4 cm) with a sterile razorblade and a 2 mm-slit was made in the center of each onion piece with a sterile micropipette tip. Two microliters of bacterial suspensions made from cultures grown on a LB agar plate, suspended in 10 mM $MgCl_2$ and adjusted to 5 X 10^7 CFU/ml, were applied to the slit on each piece of onion scale. The inoculated onion scales were incubated in a moist chamber at 30°C for 72 h. The virulence level of each *B. glumae* strain was assessed by measuring the area of maceration on each onion scale. Virulence of *B. glumae* strains in rice was tested following a previously established method (Karki et al., 2012b).

2.3 Results

2.3.1 Generation of a series of markerless deletion mutants of *tofI* and *tofR*

Mutant derivatives of *B. glumae* 336gr-1 with deleted *tofI*, *tofR*, or the entire *tofI-tofR* region, including the intergenic region, were generated using the pKKSacB system (Ham and Barphagha, *unpublished*), following the procedures described in the Materials

and Methods section (Table 2.1 and Figure 2.1). Genetic confirmation of the deletion mutants, LSUPB145 (*ΔtofI*), LSUPB169 (*ΔtofR*), and LSUPB139 (*ΔtofI-tofR*), was performed using PCR and primers corresponding to the DNA sequences flanking each deleted region (Figure 2.2 and Table 2.2). The size of the PCR products amplified from each mutant was the same as that of the PCR products amplified from the DNA construct used for the corresponding deletion mutation, and the size difference of the PCR products between the wild type and each mutant was matched to the predicted size of the deleted DNA sequence (Figure 2.2).

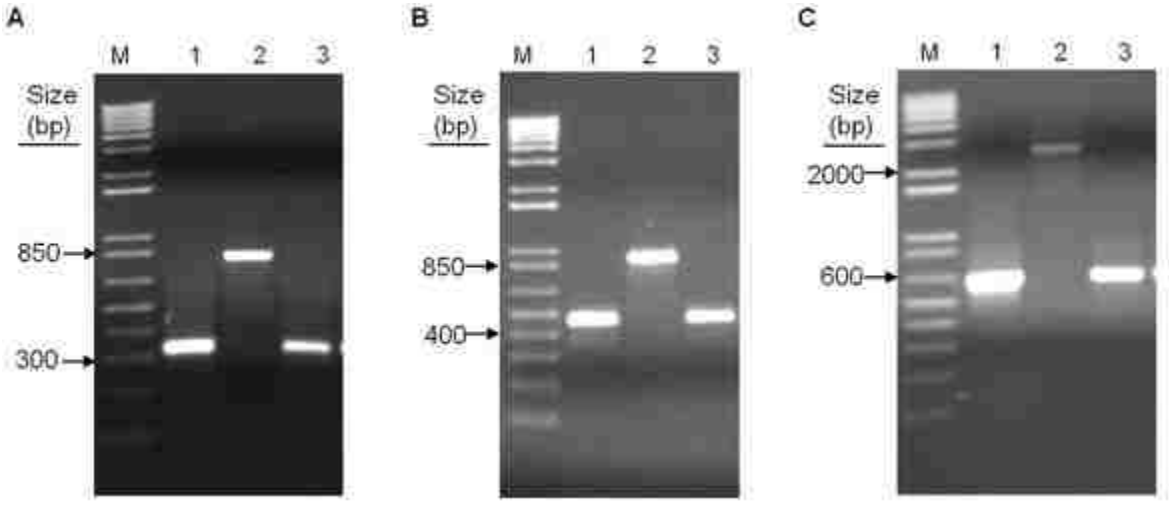

Figure 2.2. PCR products from diagnostic PCRs used to confirm deletion mutations in *Burkholderia glumae* and *N*-acyl homoserine lactone (AHL) signal production and toxoflavin production of deletion mutants. (A) PCR products amplified from primers, TofI(H)F and TofI(H)R, to confirm the *tofI* deletion in LSUPB145. Template DNA for each lane is as follows: 1, pKKSacBΔtofI; 2, genomic DNA of *B. glumae* 336gr-1; and 3, genomic DNA of *B. glumae* LSUPB145. (B) PCR products amplified with primers, TofR(H)F and TofR(H)R, to confirm the *tofR* deletion in LSUPB169. Template DNA for each lane is as follows: 1, pKKSacBΔtofR; 2, genomic DNA of *B. glumae* 336gr-1; and 3, genomic DNA of *B. glumae* LSUPB169. (C) PCR products amplified with primers, TofI(H)F and TofR(H)R, to confirm the *tofI-tofR* deletion in LSUPB139. Template DNA for each lane is as follows: 1, pKKSacBΔtofIMR; 2, genomic DNA of *B. glumae* 336gr-1; and 3, genomic DNA of *B. glumae* LSUPB139. M indicates the 1 kb Plus DNA ladder (Invitrogen, Santa Clara, CA, USA) used as a marker.

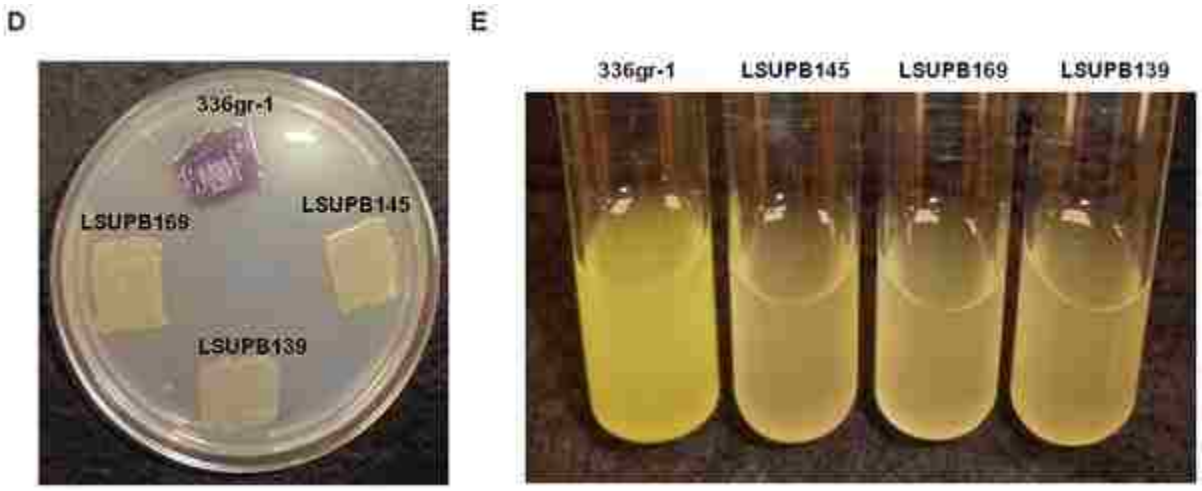

Figure 2.2. PCR products from diagnostic PCRs used to confirm deletion mutations in *Burkholderia glumae* and *N*-acyl homoserine lactone (AHL) signal production and toxoflavin production of deletion mutants. (D) Violacein production, shown as a purple pigment, by the biosensor, *Chromobacterium violaceum* CV026, in the presence of the culture extracts of the *B. glumae* strains, 336gr-1, LSUPB145, LSUPB169, and LSUPB139. Photo was taken 48 h after application of bacterial culture extracts on *C. violaceum* CV026 inoculated onto a LB agar plate. (E) Toxoflavin production, shown as a yellow pigment, in the LB broth by *B. glumae* strains, 336gr-1, LSUPB145, LSUPB169, and LSUPB139. Photo was taken after 24 h incubation at 37°C.

Mutations in *tofI* and *tofR* were also confirmed with the biosensor strain, *C. violaceum* CV026, which produces the purple pigment, violacein, in the presence of AHL compounds, including C6-HSL and C8-HSL (McClean et al., 1997). The culture extract of the wild type strain, 336gr-1, caused the production of violacein by the biosensor, while that of the deletion mutants did not (Figure 2.2D), indicating that these mutants did not produce the AHL molecules required for QS. Likewise, none of the mutants produced toxoflavin in either LB agar or LB broth (Figures 2.2E and 2.3). These results were consistent with the previous study by Kim *et al.* (2004), which showed the dependence of toxoflavin production by *B. glumae* on *tofI* and *tofR*.

2.3.2 Restoration of bacterial growth and toxoflavin production in the Δ*tofI* strain, LSUPB145, by C8-HSL

All the QS mutants produced little toxoflavin compared to the wild type in both liquid and solid media (Figure 2.3). If 1 µM C8-HSL was added to the media, the *ΔtofI* mutant, LSUPB145, regained the ability to produce toxoflavin, but the *ΔtofR* mutant, LSUPB169, and the *ΔtofI-tofR* mutant, LSUPB139, did not (Figure 2.3). Patterns of toxoflavin production by mutant strains in the presence of exogenous synthetic AHL compounds were similar in both liquid and solid media (Figure 2.3). In both growth conditions, LSUPB145 appeared to produce more toxoflavin than the wild type 336gr-1 in the presence of 1 µM C8-HSL (Figure 2.3). According to the statistical analysis using a two-sample t-test, the toxoflavin production in 336gr-1 and LSUPB145 was significantly different from each other in solid media (T value = -3.97, P value = 0.0166) but not in liquid media (T value = -1.95, P value = 0.1888).

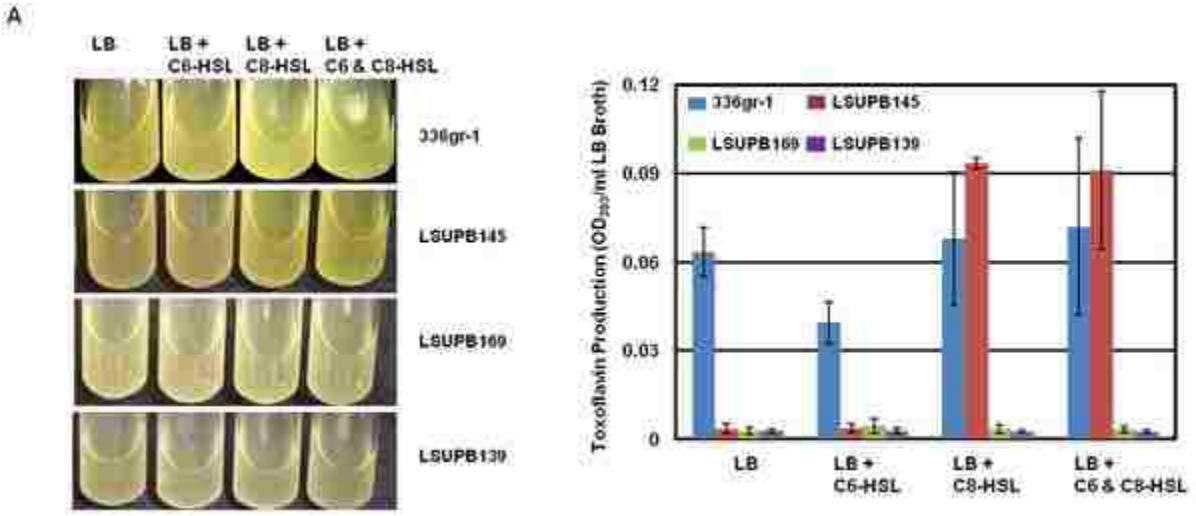

Figure 2.3. Toxoflavin production by *Burkholderia glumae* strains, 336gr-1 (wild type), LSUPB145 (*ΔtofI*), LSUPB169 (*ΔtofR*) and LSUPB139 (*ΔtofI-tofR*) in the presence or absence of 1 µM *N*-hexanoyl homoserine lactone (C6-HSL) and *N*-octanoyl homoserine lactone (C8-HSL) in LB broth (A). LB broth and LB agar were inoculated with equal amounts of bacterial cells (~10^6 CFU) per ml of media. Photos were taken and toxoflavin were quantified after 24 h incubation at 37°C. Error bars indicate the standard deviation from three replications.

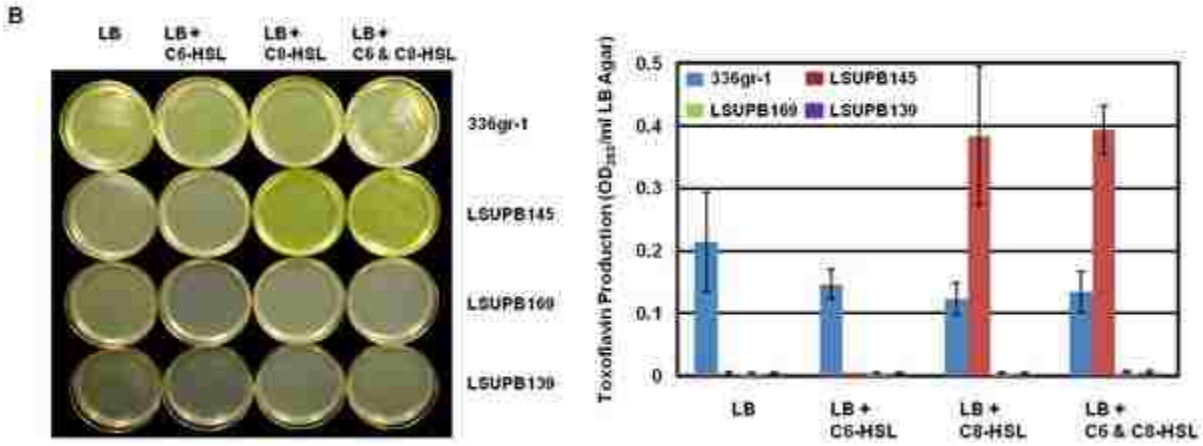

Figure 2.3. Toxoflavin production by *Burkholderia glumae* strains, 336gr-1 (wild type), LSUPB145 (*ΔtofI*), LSUPB169 (*ΔtofR*) and LSUPB139 (*ΔtofI-tofR*) in the presence or absence of 1 µM *N*-hexanoyl homoserine lactone (C6-HSL) and *N*-octanoyl homoserine lactone (C8-HSL) on LB agar (B). LB broth and LB agar were inoculated with equal amounts of bacterial cells (~10^6 CFU) per ml of media. Bacteria were spread uniformly on LB agar plates with a spreader. Photos were taken and toxoflavin were quantified after 24 h incubation at 37°C. LB agar plates were photographed after removal of bacterial culture from the medium. Error bars indicate the standard deviation from three replications.

In addition, the QS mutant strains showed reduced growth when compared to the wild type in both liquid and solid media after 24 h incubation at 37°C (Figures 2.4 and 2.5). ANOVA and post hoc LSD tests validated that the observed growth reduction of all the three QS mutants in both types of medium condition was statistically significant (not shown). The difference in bacterial growth between the wild type and the QS mutants appeared to be greater in solid media than in liquid media (Figure 2.4). Addition of C8-HSL to both liquid and solid media restored the growth of the *ΔtofI* strain, LSUPB145, to the wild type level, but did not have any effect on the growth of the other QS mutants or the wild type strain (Figures 2.4 and 2.5). C6-HSL did not affect the growth of any strain tested (Figures 2.4 and 2.5).

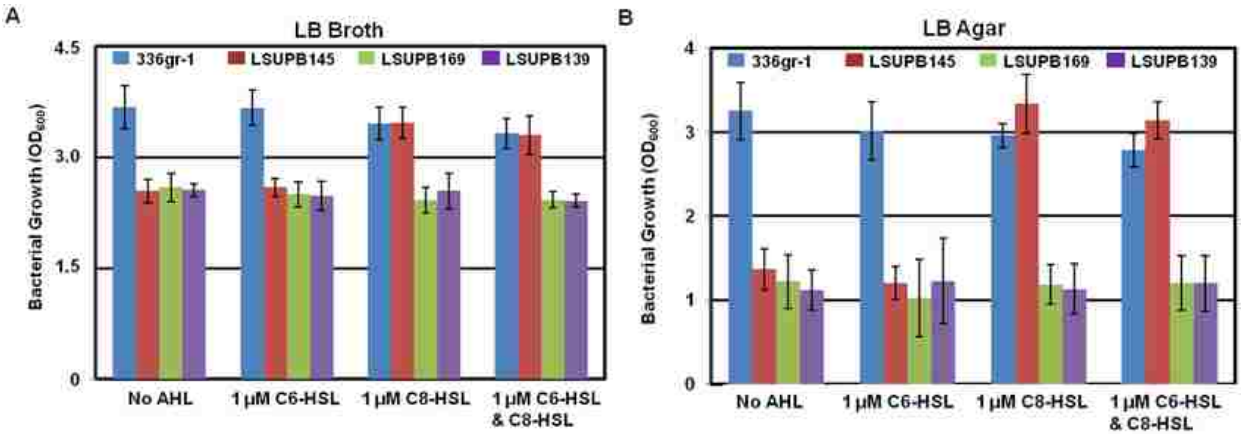

Figure 2.4. Bacterial growth of *Burkholderia glumae* strains, 336gr-1 (wild type), LSUPB145 (*ΔtofI*), LSUPB169 (*ΔtofR*) and LSUPB139 (*ΔtofI-tofR*) in the presence or absence of 1 µM *N*-hexanoyl homoserine lactone (C6-HSL) and *N*-octanoyl homoserine lactone (C8-HSL) in LB broth (A) and on LB agar (B). LB broth and LB agar were inoculated with equal amounts of bacterial cells (~10^6 CFU) per ml of media. Absorbance of each bacterial culture was measured after 24 h incubation at 37°C. Error bars indicate the standard deviation from three replications.

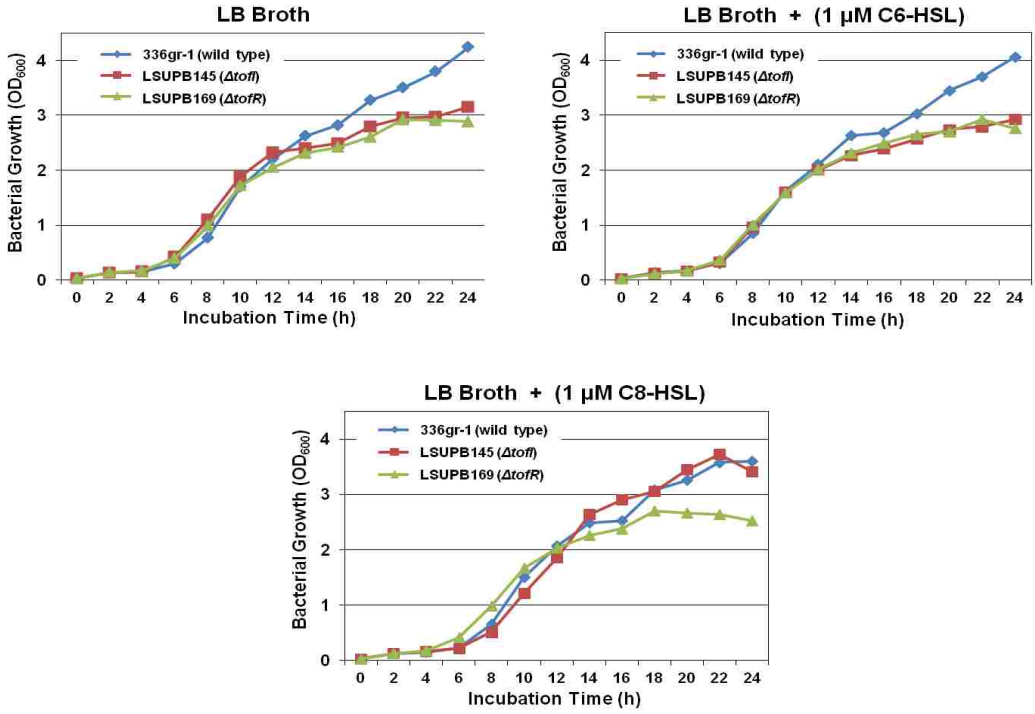

Figure 2.5. Growth curves of *B. glumae* strains, 336gr-1 (wild type), LSUPB145 (*ΔtofI*), and LSUPB169 (*ΔtofR*) grown in LB broth (top left), LB broth amended with 1 µM *N*-hexanoyl homoserine lactone (C6-HSL) (top right), and LB broth amended with or *N*-octanoyl homoserine lactone (C8-HSL) (bottom). Bacteria were grown at 37°C in a shaking incubator at ~200 rpm. Similar patterns of data were obtained from three independent experiments.

2.3.3 Toxoflavin production of Δ*tofI* and Δ*tofR* derivatives of the wild type strain, 336gr-1, at high culture density on LB agar

ΔtofI and *ΔtofR* mutants, LSUPB145 and LSUPB169, respectively, produced toxoflavin when grown on solid media after inoculation with the streaking method using an inoculation loop (Figure 2.6A). The *ΔtofI-tofR* strain, LSUPB139, on the other hand, did not produce any detectable toxoflavin in the same condition (Fig 2.6A). Even though LSUPB145 and LSUPB169 produced less amounts of toxoflavin than the wild type, 336gr-1, did in this growth condition (Figure 2.6A), their phenotypes were strikingly different from those shown in LB broth (Figure 2.3A) or LB agar inoculated with the spreading method (Figure 2.3B).

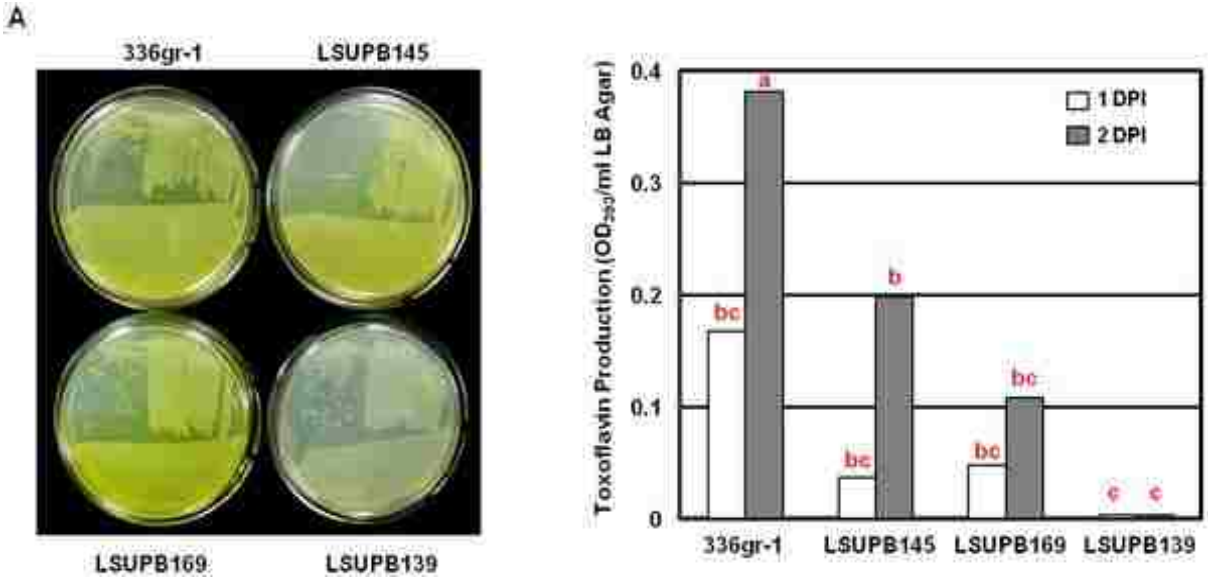

Figure 2.6. Toxoflavin production (A) and virulence phenotypes (B) by *Burkholderia glumae* strains, 336gr-1 (wild type), LSUPB145 (*ΔtofI*), LSUPB169 (*ΔtofR*) and LSUPB139 (*ΔtofI-tofR*). (A) LB agar plates inoculated with the streaking method with inoculums from fresh bacterial colonies of *B. glumae* strains. Photos were taken and quantification procedures were performed 48 h after incubation at 37°C. Columns for toxoflavin production (A) represent the mean values from three replications and five replications, respectively. The letters above columns indicate significant differences among *B. glumae* strains ($P < 0.01$). DPI: days post inoculation.

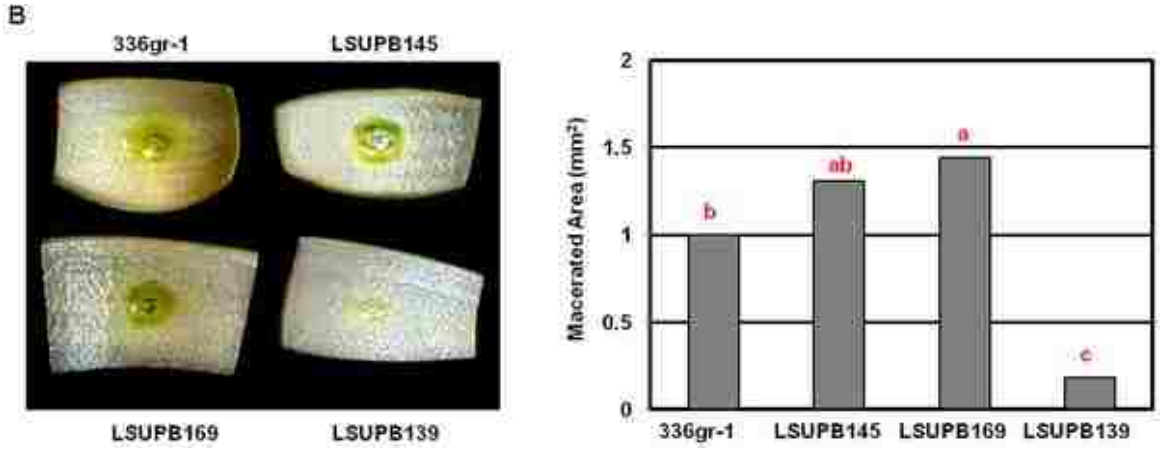

Figure 2.6. Toxoflavin production (A) and virulence phenotypes (B) by *Burkholderia glumae* strains, 336gr-1 (wild type), LSUPB145 (*ΔtofI*), LSUPB169 (*ΔtofR*) and LSUPB139 (*ΔtofI-tofR*). (B) Virulence phenotypes on onion bulb scales. Photos were taken and maceration was measured 72 h after incubation in a wet chamber at 30°C. Columns for area of maceration (B) represent the mean values from three replications and five replications, respectively. The letters above columns indicate significant differences among *B. glumae* strains ($P < 0.01$). DPI: days post inoculation.

Similar results were observed in tests with other types of solid media, including King's B agar (Schaad et al., 2001) (data not shown). In an onion assay established to indirectly determine the virulence of *B. glumae* (Karki et al., 2012b), LSUPB145 and LSUPB169, but not LSUPB139, were able to cause comparable or larger maceration symptoms on onion bulb scales in comparison with the wild type (Figure 2.6B). Inoculums prepared from the cultures in LB broth and LB agar showed similar results (data not shown).

2.3.4 Identification of a new regulatory gene, *tofM*, in the intergenic region between *tofI* and *tofR*

Based on the observation mentioned above, we speculated that toxoflavin could be produced in a *tofI*- or *tofR*-independent manner at certain growth conditions but could not be produced without both *tofI* and *tofR*. To verify this notion, a *tofI/tofR* double deletion mutant (*ΔtofI/ΔtofR*), LSUPB201, was generated through consecutive deletions of *tofI* and *tofR* and its phenotype in toxoflavin production was tested in various

conditions. Unlike the *ΔtofI-tofR* strain LSUPB139, the *ΔtofI/ΔtofR* mutant LSUPB201 still produced toxoflavin on LB agar medium when it was inoculated with the streaking method (Figures 2.7 and 2.8B). The only difference between LSUPB139 (*ΔtofI-tofR*) and LSUPB201 (*ΔtofI/*Δ*tofR*) was the presence of the intergenic region between *tofI* and *tofR* (Figure 2.1), suggesting that unknown genetic element(s) present between *tofI* and *tofR* may be responsible for the *tofI* and *tofR*-independent production of toxoflavin. According to the annotated whole genome sequence of *B. glumae* BGR1 (NCBI Reference Sequence: NC_012721.2), the coding sequences of *tofI* (locus tag: bglu_2g14490) and *tofR* (locus tag: bglu_2g14470) are 612 bp- and 720 bp-long, respectively, and are separated by a region of DNA 799 bp in length that includes a single ORF (locus tag: bglu_2g14480) that is divergently transcribed from *tofR* (Figure 1). The deduced amino acid sequence of this ORF showed 22.4% identity to that of RsaM in *Pseudomonas fuscovaginae* (Mattiuzzo et al., 2011) and was found to be highly conserved among *Burkhoderia* spp. (Table 2.3 and Figure 2.9). The DNA sequence of the *tofI-tofR* intergenic region of *B. glumae* 336gr-1 was identical to that of *B. glumae* BGR1.

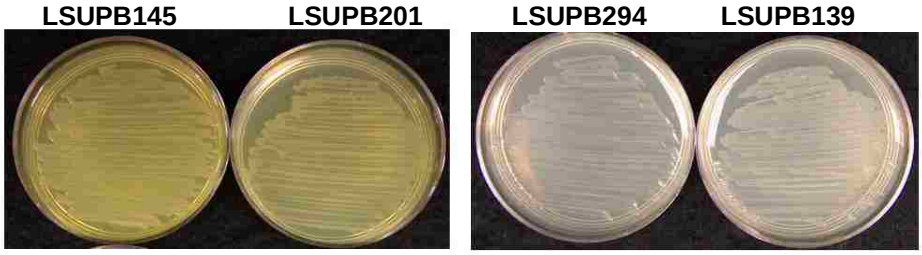

Figure 2.7. Toxoflavin production by *B. glumae* strains, LSUPB145 (*ΔtofI*), LSUPB201 (*ΔtofI/ΔtofR*), LSUPB294 (*ΔtofI/ΔtofM*) and LSUPB139 (*ΔtofI-tofR*) on LB agar plates. Bacteria were inoculated on LB agar plates with the streaking method from fresh colonies of *B. glumae* strains. Toxoflavin production is indicated by the presence of the yellow pigment in the media. Photo was taken after 24 h incubation at 37°C.

Table 2.3. TofM homologs in *Burkholderia* spp. and *Pseudomonas fuscovaginae*

Locus_tag/Gene	Protein ID (Accession #)	Organism	Identity (similarity)
bglu_2g14480	YP_002909042.1	*Burkholderia glumae* BGR1	100%
bgla_2g11060	YP_004349067.1	*B. gladioli* BSR3	80.0% (88.7%)
bgla_1p1750	YP_004362596.1	*B. gladioli* BSR3	23.7% (35.3%)
BCAM1869	YP_002234480.1	*B. cenocepacia* J2315	52.9% (59.2%)
Bcenmc03_5575	YP_001779190.1	*B. cenocepacia* MC0-3	52.2% (59.2%)
Bcen_3642	YP_623507.1	*B. cenocepacia* AU 1054	52.2% (59.2%)
Bmul_3970	YP_001583945.1	*B. multivorans* ATCC 17616	55.6% (63.4%)
Bamb_4117	YP_776004.1	*B. ambifaria* AMMD	52.9% (59.9%)
BamMC406_4582	YP_001811254.1	*B. ambifaria* MC40-6	51.6% (58.6%)
BamMC406_5824	YP_001815818.1	*B. ambifaria* MC40-6	28.0% (38.5%)
Bcep1808_5261	YP_001117675.1	*B. vietnamiensis* G4	52.2% (61.1%)
Bcep18194_B1051	YP_371809.1	*Burkholderia* sp. 383	51.6% (59.9%)
BTH_II1511	YP_439707.1	*B. thailandensis* E264	51.3% (65.8%)
BURPS668_A1294	YP_001062291.1	*B. pseudomallei* 668	50.3% (63.1%)
BPSS0886	YP_110895.1	*B. pseudomallei* K96243	49.7% (62.4%)
BWAA1346	YP_105962.1	*B. mallei* ATCC 23344	49.7% (62.4%)
rsaM	CBI67624.1/ RsaM	*Pseudomonas fuscovaginae* UPB0736	22.4% (37.2%)
BURPS1106A_A1576	YP_001075610.1	*B. pseudomallei* 1106a	32.5% (43.5%)

Table 2.3 continued

Locus_tag/Gene	Protein ID (Accession #)	Organism	Identity (similarity)
BURPS1106B_0414	ZP_04810916.1	*B. pseudomallei* 1106b	32.5% (43.5%)
BURPS668_A1657	YP_001062653.1	*B. pseudomallei* 668	32.5% (43.5%)
GBP346_B0905	EEP50658.1	*B. pseudomallei* MSHR346	32.5% (43.5%)
BPSS1179	YP_111192.1	*B. pseudomallei* K96243	28.7% (38.9%)
BURPS1710A_A0737	ZP_04955066.1	*B. pseudomallei* 1710a	17.1% (23.2%)
BURPS1710b_A0144	YP_335303.1	*B. pseudomallei* 1710b	17.1% (23.2%)
Locus_tag/Gene	Protein ID (Accession #)	Organism	Identity (similarity)
BTH_II1228	YP_439424.1	*B. thailandensis* E264	28.2% (41.2%)
Bamb_6054	YP_777932.1	*B. ambifaria* AMMD	24.2% (33.3%)
BamMC406_5825	YP_001815819.1	*B. ambifaria* MC40-6	11.5% (20.2%)

To determine the function of this ORF, deletion mutations of this ORF were made in strains with the genetic backgrounds of Δ*tofI* and Δ*tofR*, as well as the wild type background, generating LSUPB201, LSUPB292, and LSUPB286, respectively. The toxoflavin production by LSUPB286 (*ΔtofM*) was not significantly different from that by the wild type in both LB broth and LB agar conditions at 30°C (Figure 2.8A). However, this mutant produced a less amount of toxoflavin when compared to the wild type at 37°C and this tendency was more obvious when the bacteria were grown on LB agar medium (Figure 2.8A). Moreover, the same deletion in the Δ*tofI* or Δ*tofR* backgrounds resulted in an almost complete loss of the ability to produce toxoflavin, indicating that this ORF is required for the normal production of toxoflavin (Figure 2.6B). Thus, this

ORF was considered as a functional gene and named as *tofM*, after *rsaM* due to the sequence homology and similarity in genetic location between *luxI* and *luxR* homolgs (Mattiuzzo et al., 2011) (Figure 2.9).

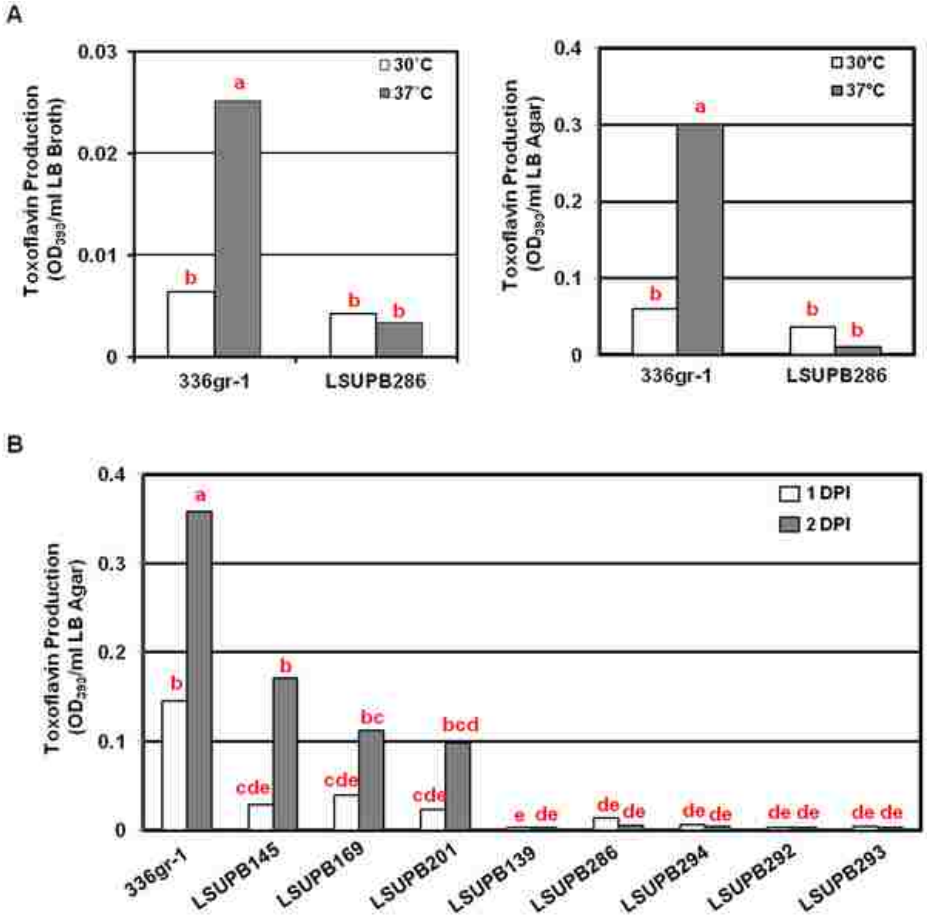

Figure 2.8. Toxoflavin production of *Burkholderia glumae tofM* deletion mutants in various genetic backgrounds. (A) Toxoflavin production by 336gr-1 (wild type) and LSUPB286 (*ΔtofM*) in LB broth (left) and on LB agar (right). Equal amounts of bacterial cells (~ 10^6 CFU/ml medium) were inoculated in both LB broth and LB agar media. For inoculation on LB agar plates, bacterial suspensions were uniformly spread with a spreader. Toxoflavin production was determined 24 h after incubation at 30°C or 37°C. (B) Toxoflavin production on LB agar plated by *B. glumae* strains, 336gr-1 (wild type), LSUPB145 (*ΔtofI*), LSUPB169 (*ΔtofR*), LSUPB201 (*ΔtofI/ΔtofR*), LSUPB139 (*ΔtofI-tofR*), LSUPB286 (*ΔtofM*), LSUPB294 (*ΔtofI/ΔtofM*), LSUPB292 (*ΔtofR/ΔtofM*) and LSUPB293 (*ΔtofI/ΔtofM/ΔtofR*). Bacteria were inoculated with the streaking method from fresh bacterial colonies. Toxoflavin production was determined 24 and 48 h after incubation at 37°C. Each column for A indicates a mean values from three replications, while that for B represents a mean value from six replications conducted in two independent experiments. The letters above columns indicate significant differences among *B. glumae* strains ($P < 0.01$).

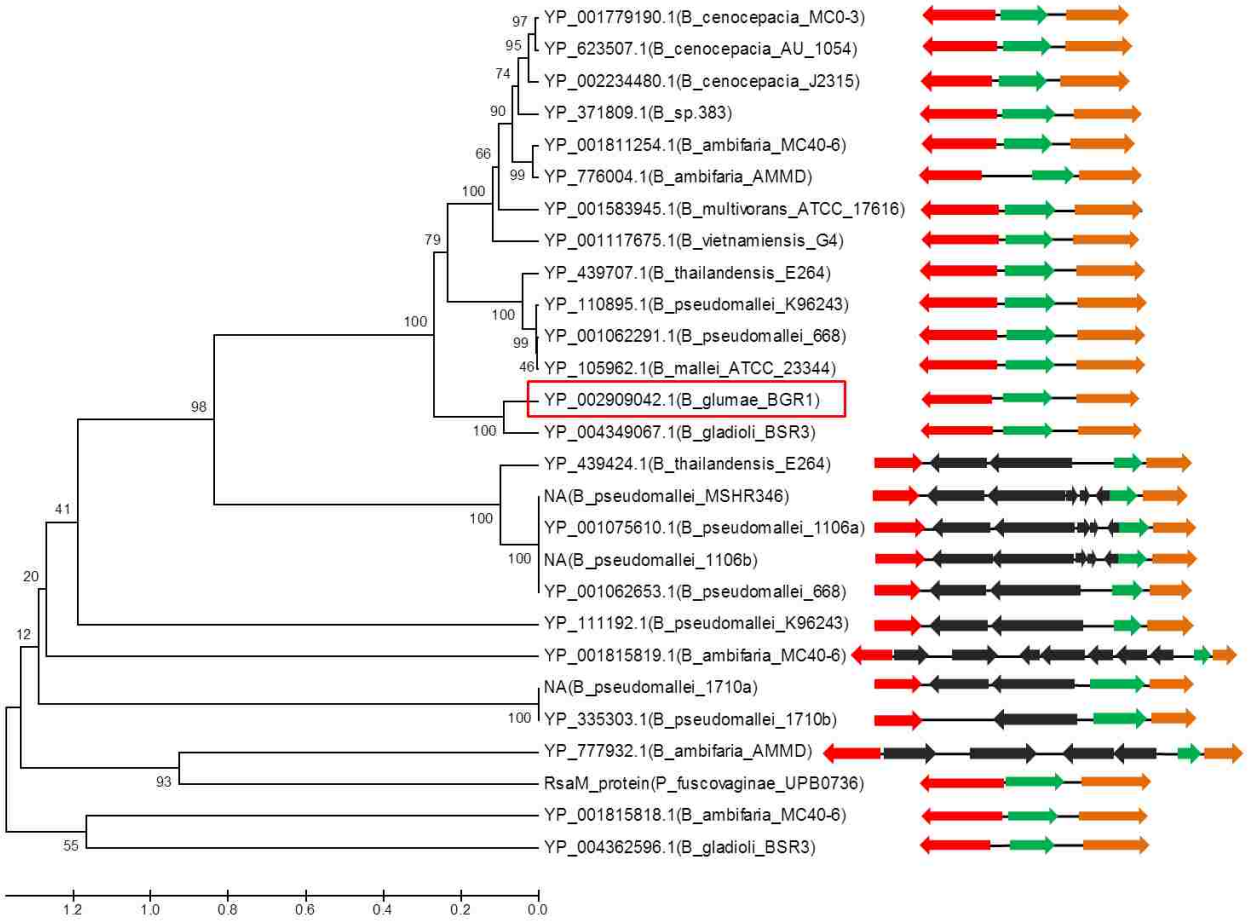

Figure 2.9. A phylogenetic tree of the RsaM homologs found from the genome sequences of *Burkholderia* spp. and the relative positions and transcriptional directions of the *rsaM* homologs. The accession number of TofM is indicated with a red box. Red, green, and orange arrows indicate the homologs of *luxR*, *rsaM*, and *luxI*, respectively. Arrow direction indicates the transcriptional direction of depicted genes; arrow size is not proportional to the size of the corresponding genes. The phylogenetic tree was conducted with MEGA5 (Tamura et al., 2011) using the UPGMA method based on the amino acid sequences of the 27 RsaM homologs including TofM. Bootstrap values from 1000 replicates were given next to the branches. The numbers indicating the evolutionary distance at the bottom of the tree represent the number of amino acid substitutions per site.

Complementation with the *tofM* clone, pBBtofM, restored toxoflavin production by the Δ*tofM* strain, LSUPB286 (Figures 2.10B, 2.10C, and 2.11). However, complementation with this *tofM* clone did not restore the production of toxoflavin on LB

agar by LSUPB294 (Δ*tofI*/Δ*tofM*), LSUPB292 (Δ*tofR*/Δ*tofM*), LSUPB293 (Δ*tofI*/Δ*tofM*/Δ*tofR*), or LSUPB139 (Δ*tofI-tofR*) (Figure 2.11). Complementation with pBBtofRM, which contains *tofR* and *tofM*, restored the toxoflavin-deficient phenotype of the Δ*tofR*/Δ*tofM* strain, LSUPB292, but did not restore the *tofI*-independent production of toxoflavin in LSUPB293 (Δ*tofI*/Δ*tofM*/Δ*tofR*) and LSUPB139 (Δ*tofI-tofR*) (Figure 2.11). Complementation with pBBtofIM, which contains *tofI* and *tofM*, did not restore the production of toxoflavin in the Δ*tofI*/Δ*tofM* mutant, LSUPB294 (Figure 2.11). Furthermore, complementation with pBBtofIMR, which contains *tofI*, *tofM* and *tofR*, restored the production of toxoflavin in LSUPB293 (Δ*tofI*/Δ*tofM*/Δ*tofR*), LSUPB139 (Δ*tofI-tofR*) and LSUPB201 (Δ*tofI/tofR*), but did not restore the production of toxoflavin in LSUPB286 (Δ*tofM*), LSUPB292 (Δ*tofR*/Δ*tofM*), or LSUPB294 (Δ*tofI*/Δ*tofM*) (Figures 2.10A and 2.11).

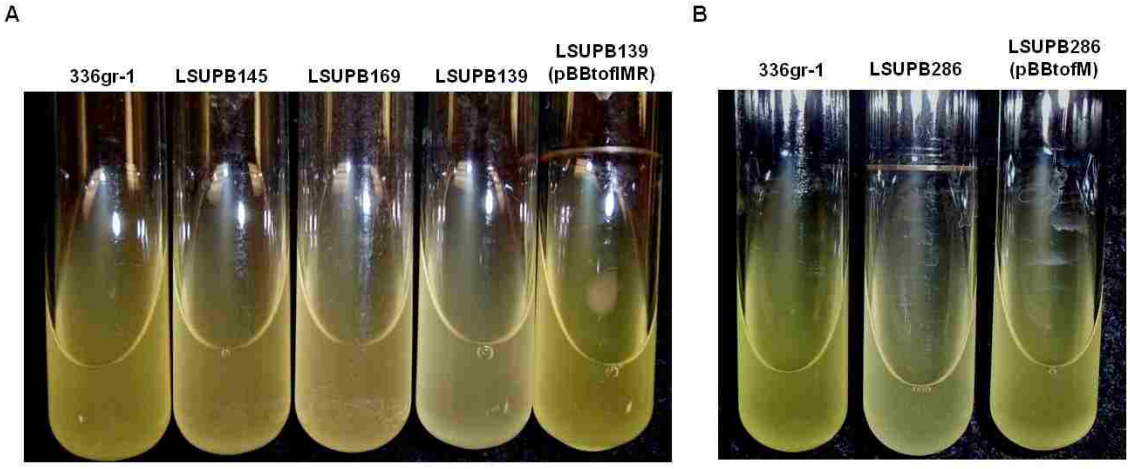

Figure 2.10. Toxoflavin production of *Burkholderia glumae* mutants and mutants complemented with functional clones of the mutated genes. (A)Toxoflavin production of 336gr-1 (wild type), LSUPB145 (*ΔtofI*), LSUPB169 (*ΔtofR*), LSUPB139 (*ΔtofI-tofR*) and LSUPB139 with pBBtofIMR. (B) Toxoflavin production of 336gr-1 (wild type), LSUPB286 (*ΔtofM*) and LSUPB286 with pBBtofM in LB broth. Photos were taken at 24 h after incubation at 37°C.

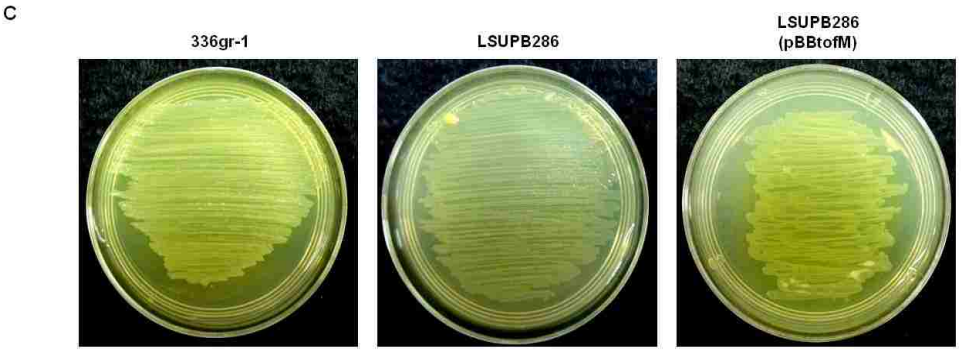

Figure 2.10. Toxoflavin production of *Burkholderia glumae* mutants and mutants complemented with functional clones of the mutated genes. (C) Toxoflavin production of 336gr-1 (wild type), LSUPB286 (*ΔtofM*) and LSUPB286 with pBBtofM in LB agar. Photos were taken at 24 h after incubation at 37°C.

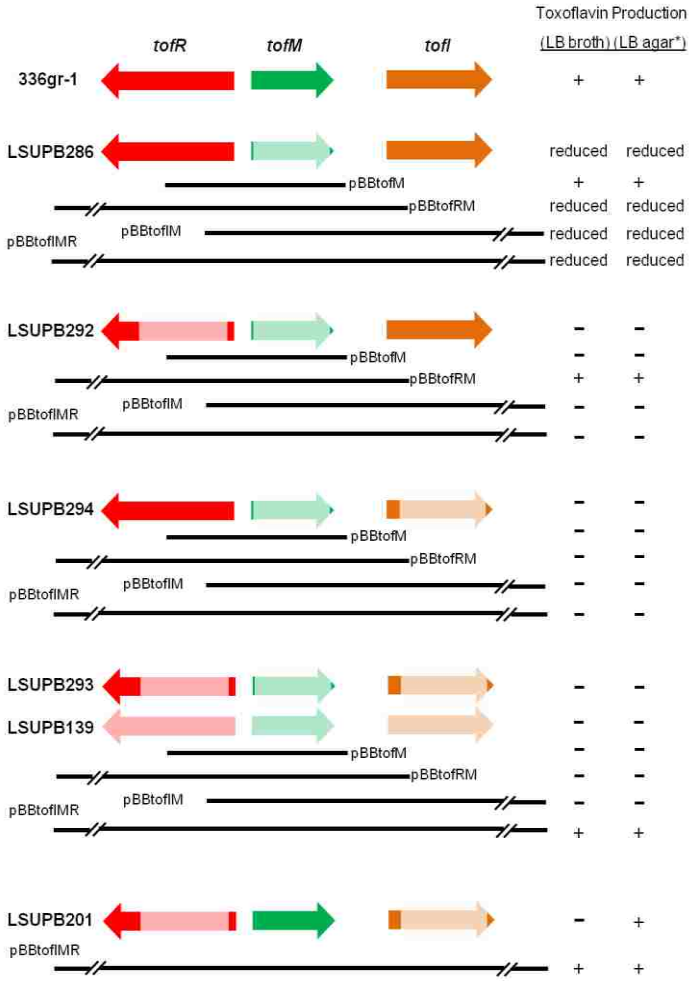

Figure 2.11. A schematic diagram summarizing the complementation tests conducted in this study. The area deleted in each gene(s) is indicated in a lighter version of the color of the gene. *Toxoflavin production by bacteria inoculated with the streaking method.

2.3.5 Virulence phenotypes of *tofI*, *tofR*, and *tofM* mutants in rice plants

In a greenhouse test, the abilities of LSUPB145 (Δ*tofI*) and LSUPB169 (Δ*tofR*) to cause symptoms in rice panicles were comparable to that of the wild type, 336gr-1 (Figure 2.12). However, the Δ*tofM* mutant LSUPB286 was significantly less virulent than the wild type and *tofI* or *tofR* mutants (Figure 2.12). In this test, LSUPB139 (Δ*tofI-tofR*) caused few visible symptoms, indicating that *tofI*, *tofR* and *tofM* are collectively required for the pathogenicity of *B. glumae* in rice (Figure 2.12).

Figure 2.7. The virulence of *Burkholderia glumae* strains in rice. The numbers indicate the disease severities caused by each strain of *B. glumae* or water. Disease severity was determined with a 0- 9 scale (0 - no symptom, 9 – more than 80% discolored panicles) at 10 days after bacterial inoculation and each number indicates a mean value from at least five replications. The superscript letters of the disease severity values indicate significant differences among *B. glumae* strains ($P < 0.01$).

2.4 Discussion

The QS system mediated by the TofI AHL synthase and the TofR AHL receptor is known to be a central regulatory element that governs the expression of the major virulence factors of *B. glumae*, including toxoflavin (Kim et al., 2007b; Kim et al., 2004a), lipase (Devescovi et al., 2007a), and flagella (Kim et al., 2007b). In this study, a series of *tofI*, *tofM* and *tofR* mutants were generated to dissect the function of each of these QS components in the production of toxoflavin in *B. glumae*. LSUPB145 (Δ*tofI*) and LSUPB169 (Δ*tofR*) produced significantly reduced amounts of toxoflavin compared with the wild type strain, 336gr-1 (Figures 2.2, 2.3, and 2.10A). In addition, the ability of LSUPB145 to produce toxoflavin was restored by the addition of 1 μM C8-HSL, but not C6-HSL (Figure 2.3). These results were consistent with previous studies with another *B. glumae* strain, BGR1, which demonstrated the dependency of toxoflavin production on the TofI/TofR QS system and C8-HSL (Kim et al., 2007b; Kim et al., 2004a). Although TofI synthesizes both C6-HSL and C8-HSL as major products (Kim et al., 2004a), the role of C6-HSL is still unknown. Notably, the *tofI* deletion mutant, LSUPB145, produced higher amounts of toxoflavin compared to the parental strain, 336gr-1, in the presence of 1 μM C8-HSL (Figure 2.3). This pattern was more obvious in LB agar than in LB broth (Figure 2.3B). This result strongly suggests that *tofI* is involved in an unknown activity that suppresses the function of C8-HSL in toxoflavin production.

Intriguingly, even though AHL signals were not produced by either the Δ*tofI* or the Δ*tofR* mutant (data not shown), both mutants were able to produce high levels of toxoflavin when inoculated with the streaking method on the LB (Figure 2.6) or KB agar media (data not shown). Further, LSUPB201, which has deletions of both *tofI* and *tofR*, also produced considerable amounts of toxoflavin on solid media (Figures 2.7 and 2.8).

The *tofI*, *tofR* and *tofI/tofR* mutants generated via different approaches, including transposon mutagenesis and homologous recombination, produced phenotypes similar to those of the Δ*tofI*, Δ*tofR*, and Δ*tofI*/Δ*tofR* strains, indicating that the observed toxoflavin production by *tofI*, *tofR*, and *tofI/tofR* mutants is not an artifact (data not shown). Additionally, significant growth defects observed with the QS mutants suggest that the TofI/TofR QS system controls the bacterial genes required for optimal bacterial growth.

We speculated that the deviated phenotypes of LSUPB145 (*ΔtofI*) and LSUPB169 (*ΔtofR*) in toxoflavin production on solid media dependent on different methods of inoculation might be due to the differences in bacterial concentration of the initial inoculum. To test this hypothesis, an overnight culture (~10^9 CFU/ml) of LSUPB145 grown in LB broth was inoculated on LB agar with the streaking method, while a concentrated bacterial suspension (~ 10^{11} CFU/ml) of the same strain was inoculated on LB agar with the spreading method. When an overnight culture (~10^9 CFU/ml) of LSUPB145 was inoculated on LB agar plates with the streaking method, the bacterial cultures frequently failed to produce toxoflavin but occasionally (with about 30% chance) produced toxoflavin (data not shown). In contrast, when a concentrated bacterial suspension (~10^{11} CFU/ml) was inoculated on LB agar plates with the spreading method, the bacterial cultures frequently produced toxoflavin but occasionally (with about 30% chance) failed to produce toxoflavin (data not shown). In both inoculation conditions, the chance to produce toxoflavin increased as the bacterial concentration of the initial inoculum was higher (data not shown). These observations suggest that both initial concentration of bacterial inoculum and method of bacterial

inoculation are critical factors for the *tofI*- or *tofR*-independent production of toxoflavin on solid media.

Based on the observed toxoflavin production by the *tofI*, *tofR* and *tofI/tofR* mutants at certain growth conditions, we speculated that *B. glumae* possesses alternative regulatory pathway(s) for the production of toxoflavin in the absence of TofI and TofR. Because the *ΔtofI-tofR* mutant, LSUPB139, did not produce toxoflavin in any growth condition tested (Figures 2.2, 2.3, 2.6, 2.7, and 2.10A), the intergenic region between *tofI* and *tofR* was thought to contain at least one regulatory gene that is responsible for toxoflavin production and independent of *tofI* and *tofR*. Indeed, a putative gene divergently transcribed from *tofR* was found to be involved in the production of toxoflavin and deletion of *tofM* in the wild type background caused a significant reduction in toxoflavin production and virulence in rice (Figures 2.8A and 2.12). Toxoflavin production of the Δ*tofM* strain, LSUPB286, was restored to wild type levels following complementation with the *tofM* clone, pBBtofM (Figures 2.10B, 2.10C, and 2.11). Nevertheless, complementation of the mutants with functional clones of the mutated genes was frequently unsuccessful (Figure 2.11), implying that the accurate balance of gene expression based on the correct genomic position and gene dosage of *tofI*, *tofM* and *tofR* is critical for the regulation of toxoflavin production by these genes. In this regard, it is noteworthy that the *ΔtofM* mutant was complemented by a *tofM* clone carrying *tofM* only (pBBtofM), but not by *tofM* clones carrying additional genes (pBBtofRM, pBBtofIM and pBBtofIMR); likewise, the *ΔtofRM* and *ΔtofIMR* mutants were complemented only by pBBtofRM and pBBtofIMR, respectively (Figure 2.11). We do not

know why the *ΔtofIM* mutant could not be complemented by any clones carrying both *tofI* and *tofM*, including pBBtofIM (Figure 2.11).

Taken together, these results indicate that *tofM* is a positive regulator for toxoflavin production. When *B. glumae* is grown in liquid media or on solid media after inoculation with the spreading method, TofM may supplement the regulatory function of the TofI/TofR QS in the production of toxoflavin. When *B. glumae* is grown on solid media after inoculation with the streaking method, however, TofM may cause the TofI/TofR QS-independent production of toxoflavin. Even though TofM is likely a key regulatory component of the *tofI*- and *tofR*-independent pathway(s) for toxoflavin production, additional regulatory components required for the production of toxoflavin in the absence of *tofI* or *tofR* have been identified and are currently being analyzed (Chen and Ham, *unpublished*).

Even though *tofM* was identified as a positive regulator for toxoflavin production in this study, its homolog, *rsaM*, was first reported as a novel negative regulator for the QS systems of another rice pathogenic bacterium, *P. fuscovaginae* (Mattiuzzo et al., 2011). Nevertheless, *rsaM* seems to exert positive functions for virulence as well because an *rsaM* mutant of *P. fuscovaginae* showed attenuated virulence in rice (Mattiuzzo et al., 2011). Both *tofM* and *rsaM* are present in the intergenic region of *luxI* and *luxR* homologs and are oriented divergently from the *luxR* homologs (Figure 2.9). Recent studies on *Pseudomonas* spp. including *P. aeruginosa*, *P. putida*, and *P. fuscovaginae* revealed that *rsaL* and *rsaM*, present in the intergenic regions of *luxI* and *luxR* homologs, act as negative regulators controlling the homeostasis of AHL levels (Venturi et al., 2011). In this study, positive function of *tofM* in virulence was observed

(Figure 2.12), however, repressive action of *tofM* on the AHL-mediated QS was somewhat ambiguous in the AHL-detection assay using the biosensor *C. violaceum* CV026 (Figure 2.13). The biosensor strain treated with the culture filtrate of the *tofM* mutant, LSUPB286, showed a stronger purple color than that treated with the culture filtrate of the wild type, 336gr-1 (Figure 2.13). However, this phenotype of LSUPB286 suggesting a negative role of *tofM* in the AHL-mediated QS could not be complemented by the *tofM* clone, pBBtofM. Quantitative analyses to precisely determine the roles of *tofM* in the expression of *tofI* and *tofR*, as well as other virulence genes, of *B. glumae* and in the production of AHL compounds are currently being conducted (Chen and Ham, *unpublished*).

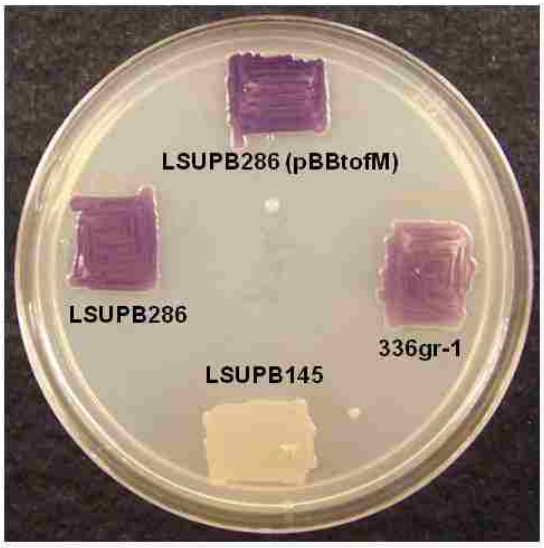

Figure 2.13. AHL production by *B. glumae* strains, 336gr-1 (wild type), LSUPB145 (*ΔtofI*), LSUPB286 (*ΔtofM*), and LSUPB286 complemented with pBBtofM. AHL production by each strain of *B. glumae* is indicated by the production of violacein by the biosensor, *Chromobacterium violaceum* CV026. Photo was taken 48 h after application of *B. glumae* culture extracts on the biosensor and incubation at 30°C.

A database search for *tofM* revealed that *tofM* homologs are conserved in many *Burkholderia* spp. (Table 2.3 and Figure 2.9), suggesting the importance of their functions for ecological fitness. *B. gladioli*, which also causes BPB of rice, possesses

two *tofM* homologs along with two sets of *luxI* and *luxR* homologs. Between the two predicted proteins encoded by the *tofM* homologs of *B. gladioli*, one shows the highest level of homology (80% amino acid sequence identity) to TofM, while the other shows only 23.7% identity (Table 2.3). It is noteworthy that, among the *tofM* homologs investigated in this study, all of the homologs with greater than 49% identity in deduced amino acid sequence to *tofM* had the same position and orientation patterns as *tofM* and *rsaM* relative to their neighboring *luxI* and *luxR* homologs (Table 2.3 and Figure 2.9). Regarding the conserved genetic locations and amino acid sequences of encoded proteins, it is very probable that the *tofM* homologs of other *Burkholderia* spp., including the select agents, *B. mallei* and *B. pseudomallei*, execute similar functions to *tofM*. Thus, elucidation of the *tofM* function in the TofI/TofR QS system of *B. glumae* would provide useful insights into the counter parts of human and animal pathogenic *Burkholderia* spp.

Conclusively, *tofI*- and *tofR*-independent production of toxoflavin in *B. glumae* was revealed for the first time in this study and *tofM* was identified as a key genetic component of this newly found pathway for toxoflavin production. *tofM* alone was also found to contribute to the full virulence of *B. glumae* 336gr-1. Further studies to determine the regulatory functions of *tofM* in the expression of *tofI* and *tofR* as well as other virulence genes of *B. glumae* would lead to a better understanding of the global regulatory system that governs the expression of virulence genes in this pathogen and, possibly, other related bacterial species.

CHAPTER 3. FUNCTIONAL GENOMIC STUDIES OF THE QUORUM-SENSING SYSTEM IN *BURKHOLDERIA GLUMAE*

3.1 Introduction

Burkholderia glumae causes bacterial panicle blight of rice and produces major virulence factors, including toxoflavin, under the control of the quorum sensing (QS) system mediated by the *luxI* homolog, *tofI*, and the *luxR* homolog, *tofR* (Chen et al., 2012). A series of markerless deletion mutants of *B. glumae* for *tofI* and *tofR* were generated for comprehensive characterization of the QS system of this pathogen (Chen et al., 2012). Consistent with the previous studies by other research groups, *ΔtofI* or *ΔtofR* strains of *B. glumae* did not produce toxoflavin in Luria-Bertani (LB) broth (Chen et al., 2012). However, these mutants produced high levels of toxoflavin when they were grown on solid media, including Luria broth (LB) agar and King's B (KB) agar (Chen et al., 2012). These results indicate the presence of previously unknown regulatory pathways for the production of toxoflavin on solid media, which are independent of *tofI* and/or *tofR* (Chen et al., 2012).

Kim et al. (2004) used biosensor and chromatography to determine the existing autoinducers in *B. glumae* and found two LuxI type compounds, *N*-octanoyl homoserine lactone (C8-HSL) and *N*-hexanoyl homoserine lactone (C6-HSL). C8-HSL is considered the functional autoinducer, while the role of C6-HSL is still not clear. Several important genetic traits determined to be regulated by C8-HSL include: the *tox* cluster that encodes toxoflavin (Kim et al., 2004b; Shingu and Yoneyama, 2004; Suzuki et al., 2004a), *lipA* encoding LipA lipase (Devescovi et al., 2007b), flagella and QsmR, as an IclR-type transcriptional regulator (Devescovi et al., 2007b), and another QsmR regulated gene *katG* that encodes protective catalase (Chun et al., 2009). The regulon

of QS listed above is important for the survival, colonization and pathogenesis of *B. glumae*, so it will be beneficial to expand the knowledge upon the regulatory network mediated by C8-HSL and find the function of C6-HSL in the QS of *B. glumae*.

Questions remain regarding the function of QS, as a global regulator for the phytopathogen *B. glumae*, and the roles that this system plays upon plant defense suppression. The type III secretion system (T3SS), which is a common plant defense suppressing mechanism, has been demonstrated as a regulon unit of QS (Kang et al., 2008). The inner-systems of *B. glumae* may have effective pathways modulated by QS to alter the cellular activity to avoid host plant resistance and cause disease. Better knowledge regarding QS can provide insights about plant disease control.

In this study, transposon random mutagenesis, a comparably economical method, was used to initiate the genome wide search of C8-HSL and C6-HSL-dependent genes, unknown regulatory pathways for the production of toxoflavin, and gene candidates reacting to the salicylic acid (SA) and jasmonic acid (JA) host defense systems.

3.2 Material and methods

3.2.1 Growth conditions of bacterial strains

The bacterial strains and plasmid constructs used in this study are listed in Table 1. Media used for routine growth of bacterial strains were LB broth or LB agar (Sambrook, 2001) with appropriate antibiotics. Liquid cultures were incubated in a shaking incubator at 200 rpm. The antibiotics and their working concentrations used in this study were: ampicillin (Amp), 100 µg/ml; kanamycin (Km), 50 µg/ml; nitrofurantoin (Nit), 100 µg/ml; and gentamycin (Gm), 20 µg/ml. The artificial AHL molecule was applied at a working concentration of 2 nM. Salicylic acid and jasmonic acid were

applied at working concentrations of 1 mM and 0.5 mM. Substrate X-glucose was applied at a working concentration of 40 mM.

Table 3.1. Bacterial strains and plasmids list

Strain or Plasmid	Description	Reference
Escherichia coli		
DH10B	F^- *araD139* Δ(*ara, leu*)7697 Δ*lacX74 galU galK rpsL deoR* ø80d*lacZ*ΔM15 *endA1 nupG recA1 mcrA* Δ(*mrr hsdRMS mcrBC*)	Grant et al. (1990)
DH5α	F^- *endA1 hsdR17* (r_k^-, m_k^+) *supE44 thi-1* λ^- *recA1 gyrA96 relA1 deoR* Δ(*lacZYA*-argF)-U169 ø80d*lacZ*ΔM15	(Grant et al., 1990)
S17-1λpir	*recA thi pro hsdR* [res- mod+][RP4::2-Tc::Mu-Km::Tn*7*] λ *pir* phage lysogen, Sm^r/Tp^r	(Simon et al., 1983)
Burkholderia glumae		
336gr-1	WT strain and the causative isolate of bacterial panicle blight of rice in Crowley, LA	This study
Strain or Plasmid	Description	Reference
LSUPB22	spontaneous mutant of 336gr-1	This study
LSUPB145	A Δ*tofI* derivative of 336gr-1	(Chen et al., 2012)
LSUPB169	A Δ*tofR* derivative of 336gr-1	(Chen et al., 2012)
LSUPB139	A Δ*tofI-tofR* derivative of 336gr-1	(Chen et al., 2012)
LSUPB286	A Δ*tofM* derivative of 336gr-1	(Chen et al., 2012)
LSUPB172	A derivative of 336gr-1 with pLG6gustoxA introduced in the bacterial cell	This study
LSUPB178	A derivative of Δ*tofI* with pLG6gustoxA introduced in the bacterial cell	This study
LSUPB324	A derivative of Δ*tofR* with pLG6gustoxA introduced in the bacterial cell	This study
LSUPB503	A Δ*tofI* derivative that is defective in *flhD* gene	This study
LSUPB273	A 336gr-1 derivative that is defective in *qsmR* gene	This study
LSUPB275	A Δ*tofI* derivative that is defective in *qsmR* gene	This study
LSUPB277	A Δ*tofR* derivative that is defective in *qsmR* gene	This study
LSUPB445	A Δ*tofR* derivative that is defective in *orf2* gene	This study
LSUPB460	A 336gr-1 derivative that is defective in *dgcB* gene	This study
LSUPB462	A Δ*tofI* derivative that is defective in *dgcB* gene	This study

Table 3.1 continued

Strain or Plasmid	Description	Reference
LSUPB464	A Δ*tofM* derivative that is defective in *dgcB* gene	This study
LSUPB472	LSUPB460 complemented by pBB-2dgcB	This study
LSUPB473	LSUPB462 complemented by pBB-2dgcB	This study
LSUPB515	A Δ*tofI* derivative that is defective in *wzyB* gene	This study
LSUPB516	A Δ*tofR* derivative that is defective in *wzyB* gene	This study
Chromabacterium violaceum		
Chromabacterium violaceum CV026	A biosensor that can detect AHL molecules	(McClean et al., 1997)
Plasmid		
pSC-A-amp/kan	A blunt PCR cloning vector; f1 *ori*, pUC *ori*, *lacZ*', Km^R, Amp^R	Stratagene
pRK2013::Tn*7*	A helper plasmid; ColE1 *ori*	(Ditta et al., 1980)
mini-Tn*5*Km	A derivative of mini-Tn*5* transposon, R6K *ori*,RP4 *oriT*, Km^R	(Delorenzo et al., 1990)
mini-Tn*5*Cm	A derivative of mini-Tn*5* transposon, R6K *ori*, RP4 *oriT*, Cm^R	(Delorenzo et al., 1990)
mini-Tn*5gus*	A derivative of mini-Tn*5* transposon containing β-glucuronidase gene, R6K *ori*,RP4 *oriT*, Km^R	(Fouts et al., 2002)
Strain or Plasmid	Description	Reference
pKNOCK-Km	A suicide vector; R6K *ori*, RP4 *oriT*, Km^R	(Alexeyev, 1999)
pKNOCK-Gm	A suicide vector; R6K *ori*, RP4 *oriT*, Gm^R	(Alexeyev, 1999)
pBBR1MCS-2	A broad host range cloning vector, RK2 *ori*, *lacZα*, Km^R	(Kovach et al., 1995)
Cos676	The cosmid clone harbouring *dcgB,* AmpR	This study
pBB2GUS	a derivative of pBBR1MCS-2 containing a promoterless *gusA*	Ham and Barphagha, unpublished
pSC-A-pToxA	A topo clone of 682 *bp* upstream promoter and partial coding region of *toxA* in pSC-A-amp/kan, Amp^R, Km^R	Ham and Barphagha, unpublished
pBB2GUS-pToxA	A subclone of pSC-A-pToxA for the promoter and partial coding region of *toxA* in pBB2GUS at *HindIII* site	Ham and Barphagha, unpublished
pKGpToxA-GUS	A subclone of pBB2GUS-pToxA for the promoter and partial coding region of *toxA* gene and *gusA* gene in pKNOCK-Gm at *Kpn*I and *Spe*I sites	Ham and Barphagha, unpublished
PSC-qsmR	A topo clone of 355 *bp* internal region of *qsmR* gene in pSC-A-amp/kan, Amp^R, Km^R	This study
PSC-flhD	A topo clone of 304 *bp* internal region of *flhD* gene in pSC-A-amp/kan, Amp^R, Km^R	This study

Table 3.1 continued

Strain or Plasmid	Description	Reference
PSC-orf2	A topo clone of 402 *bp* internal region of *luxRB* gene in pSC-A-amp/kan, Amp^R, Km^R	This study
PSC-dgcB	A topo clone of 376 *bp* topo clone of internal region of *pascB* gene in pSC-A-amp/kan, Amp^R, Km^R	This study
PSC-wzyB	A topo clone of *bp* topo clone of internal region of *oapB* gene in pSC-A-amp/kan, Amp^R, Km^R	This study
pKKmqsmR	A subclone of pSC-qsmR for the internal region of *qsmR* gene in pKNOCK-Km at *KpnI* and *SacII* sites, Km^R	This study
pKKmflhD	A subclone of pSC-flhD for the internal region of *flhD* gene in pKNOCK-Km at *EcoRI* site, Km^R	This study
pKKmorf2	A subclone of pSC-orf2B for the internal region of *luxRB* gene in pKNOCK-Km at *EcoRI* site, Km^R	This study
pKGmdgcB	A subclone of pSC-dgcB for the internal region of *dgcB* gene in pKNOCK-Km at *SpeI* and *HindIII* sites, Km^R	This study
Strain or Plasmid	Description	Reference
pKGmwzyB	A subclone of pSC-oapB for the internal region of *dgcB* gene in pKNOCK-Gm at *SpeI* and *KpnI* sites, Km^R	
pBB-2dgcB	A subclone of cosmid for the coding and promoter region of *dgcB* gene in pBBR1MCS-2 at *HindIII* and *SpeI* (or *NheI*) sites, Km^R	This study

3.2.2 Recombinant DNA techniques

General PCR cloning were conducted following standard methods (Sambrook, 2001). A Strata Clone^{TM} PCR cloning kit (Agilent Technologies, Santa Clara, CA, USA) was used for cloning PCR products into a pSC-A-amp/kan vector. The pSC-A-amp/kan vectors containing the expected size of homologous DNA inserts were sequenced at the GeneLab at the LSU School of Veterinariary Medicine or at Macrogen USA (http://www.macrogenusa.com) using M13 forward and reverse primers. A GenePulser unit (BioRad Laboratories, Hercules, CA, USA) was used to perform electroporation for

transforming *E. coli* competent cells under 1.5 kV, between 1 µl ligated DNA and 25 µl competent cells. The triparental mating technique was used for the transformation of *B. glumae* (Figurski and Helinski, 1979). Digested DNAs were extracted from the agarose gel using GenElute™ Gel extraction kits (Sigma-Aldrich, St. Louis, MO, USA). The concentrations of the purified DNA and RNA were measured using a NanoDrop DN-1000 Spectrophotometer (Thermo Scientific, Wilmington, DE, USA). All the restriction enzymes used in this study were ordered from New England Biolabs (Beverly, MA, USA). The genomic library was previously created in our laboratory (Karki et al., 2012a).

Table 3.2. The PCR programs and primers used in the mutagenesis studies.

Amplified region	Product length	Primers* (forward & reverse)	PCR programs
Promoter and partial coding region of *toxA*	682 *bp*	ToxA PF: AAGCTTTCCCTTCGCTTTTC (*Hind*III) ToxA PR: CTCGAGACCAATCATGTGGAA (*Xho*I)	Annealing at 55 °C Extension for 1 minute
Flanking region of miniTn5*gus* insertion	Variable	Y Linker Primer: CTGCTCGAATTCAAGCTTCT Tn5 primer: GGCCAGATCTGATCAAGAGA	Annealing at 58 °C Extension for 1 minute (Kwon and Ricke, 2000)
Internal region for *qsmR*	355 *bp*	QSMRIK FP: CCGCCTCGGTGCTCGAACTG QSMRIK RP: AGCGTATCCTCCAGGGCGGG	Annealing at 60 °C Extension for 1 minute
Internal region of *flhD*	304 *bp*	FlhD-1: AATGCTCGCCGAGATCAA FlhD-2: TTAGCGGAGGCTTTCGAC	Annealing at 54 °C Extension for 40 seconds
Internal region of *flhC*	462 *bp*	FlhC-1: GTGCTCGAGGTCAAGGAAATC FlhD-2: CAGCCCGCAGACGAAAC	Annealing at 54 °C Extension for 40 seconds

Table 3.2 continued

Amplified region	Product length	Primers* (forward & reverse)	PCR programs
Internal region of *orf2*	402 *bp*	OR-1: GATTCAGGCGGGCTAGTTT OR-2: CGCCGAATACGGCTACTG	Annealing at 54 °C Extension for 40 seconds
Amplified region	Product length	Primers* (forward & reverse)	PCR programs
Internal region of *dgcB*	376 *bp*	DGC-FP: CGTAGGTGTCGTTGTACTGC TTGA DGC-RP: ATCATCGTGCTGTCGACCAA GGA	Annealing at 58 °C Extension for 30 seconds
Internal region of *wyzB*	370 *bp*	Oap-1: ACTCGCACGACATCTTCATC Oap-2: GGGTTCGTGCCGTAATAGA G	Annealing at 53 °C Extension for 30 seconds
Region spanning the potential suicide vector inserted sites in *flhD*	445 *bp*	FLHD-C1: GCCACAATGACTGCAAGAAT ATAA FLHD-C2: GCAGATGATGTAGGGAGTG TTAG	Annealing at 53 °C Extension for 30 seconds
Region spanning the potential suicide vector inserted sites in *orf2*	683 *bp*	orf2-C1: GGCAGCAAATCTCCGTTTAT TC orf2-C2: GTACCGGTGCTGGATATGAT T	Annealing at 54 °C Extension for 45 seconds
Region spanning the potential suicide vector inserted sites in *qsmR*	863 *bp*	QsmR-C1: CCAGCGTGGACTTTGTCAT QsmR-C2: CAGTCTCGAGCAGCCATTC	Annealing at 52.5 °C Extension for 1 minute
Region spanning the potential suicide vector inserted sites in *dgcB*	878 *bp*	DGCB-C1: ATTGCGCATTCTGAAGGAAA C DGCB-C2: CAGCACGACACCGAACT	Annealing at 55 °C Extension for 1 minute

Table 3.2 continued

Amplified region	Product length	Primers* (forward & reverse)	PCR programs
Region spanning the potential suicide vector inserted sites in *wzyB*	818 *bp*	Oap-C1: TGCACTATCACCTCGGTCT Oap-C2: CCAGTCGTGCAGTTCCTC	Annealing at 55 °C Extension for 1 minute
Internal region of DNA gyrase subunit A (*gyrA*) gene	140 *bp*	GyrA-q1: CACGACTACATCCTCTGTT TCTC GyrA-q2: ACGTTGATCTTCTCGCCTT C	For qPCR: Annealing at 53 °C Extension for 30 seconds
Internal region of *flhC*	89 *bp*	FlhC-q1: GCTCGAGGTCAAGGAAATCA FlhC-q2: GAGACAGGTTAGTCTCGGTT TC	For qPCR: Annealing at 53 °C Extension for 30 seconds

*: The restriction sites added in the primers were highlighted.

3.2.3 Construction of pLG6gustoxA

(*This part of the work was performed by Ms. Inderjit Barghaphagha*)

To generate the *toxA* gene expression system, 562 *bp* upstream and 108 *bp* continuous coding regions of *toxA* DNA were amplified by primer set ToxA PF/ToxA PR (Table 3.2). The resultant PCR products were initially cloned into pSC-A-amp/kan, generating pSC-A-pToxA. The homologous region was then sub-cloned into pBB2GUS (Ham and Barphagha, unpublished) using *Hind*III site to obtain pBB2GUS-pToxA. The region containing the promoter of *toxA* and the promoterless *gusA* gene was cut with *Kpn*I and *Spe*I and ligated to pKNOCK-Gm to generate pLG6gustoxA.

Later, pLG6gustoxA was introduced into Δ*tofI* and Δ*tofR,* respectively, through tri-parental mating. Strains LSUPB178 (Δ*tofI*::pLG6gustoxA) and LSUPB324 (Δ*tofR*::pLG6gustoxA) selected from LB/Km/Nit media were generated for the following genomic screening.

3.2.4 Genomic screening for *tofI* or *tofR*-independent toxoflavin production factors using mini-Tn*5*Cm

To find the genes required for *tofI* or *tofR*-independent toxoflavin production, a mini-Tn*5*Cm transposon was introduced to LSUPB178 and LSUPB324. After tri-parental mating, the mutants not exhibiting blue pigment (no *β*-glucuronidase gene activities) on LB/Gm/Cm/Nir/X-gluc plates after two days' incubation at 37 °C were collected and characterized.

3.2.5 Genomic screening of C8-HSL or C6-HSL regulon using mini-Tn5*gus*

To find the genetic traits regulated by different QS signals (C8-HSL or C6-HSL), mini-Tn*5gus* was introduced to LSUPB145 (Δ*tofI*). Three different selective plates were used after tri-parental mating: LB/Gm/Km/Nit, LB/Gm/Km/Nit/C8-HSL and LB/Gm/Km/Nit/C6-HSL. The random mutants expressing different *β*-glucuronidase activities (blue pigment production) on three plates were collected and characterized.

3.2.6 Genomic screening of JA and SA reponses using mini-Tn*5gus*

To find the genes *B. glumae* used to react to jasmonic acid (JA) and salicylic acid (SA) signaling defense systems, miniTn*5gus* was introduced to LSUPB22. Three selective plates LB/Km/Nit/X-gluc, LB/Km/Nit/X-gluc/JA and LB/Km/Nit/X-gluc/SA were used to pick the random mutants that responded to JA or SA.

3.2.7 Determination of the flanking sequences of transposon insertions in selected random mutants

(*This part of the work was partially performed by Ms. Inderjit Barghaphagha*)

The flanking sequences of the inserted transposon in selected mutants from random mutagenesis were amplified (Kwon and Ricke, 2000). Genomic DNA of the WT or mutant strains was extracted using a GenElute^{TM} Bacterial Genomic DNA kit (Sigma-Aldrich, St. Louis, MO, USA). Two enzymes, *PstI* and *NlaIII*, were used to perform

restriction digestion of 4 mg genomic DNAs. Regular phenol extraction and ethanol precipitation were used to purify the fragmented DNA samples. Ligation was performed between the cut DNAs and Y shaped linker. Y Linker Primer CTGCTCGAATTCAAGCTTCT (specific to Y linker sequence) and Tn5 primer GGCCAGATCTGATCAAGAGA (specific to transposon) were used to amplify the DNA sequences flanking where the transposon inserted.

3.2.8 Site-directed mutagenesis

(*This part of the work was partially performed by Ms. Inderjit Barghaphagha*)

Briefly, the internal DNA sequence of interesting genes selected from genomic screening were amplified using the primers indicated in Table 3.2 and cloned into pKNOCK-Km or pKNOCK-Gm suicide vectors. The vectors with homologous DNA were later introduced to *B. glumae* strains by tri-parental mating. Specifically, the cloning procedure is described as follows. PCR products 355 *bp* of *qsmR*, 304 *bp* of *flhD*, 402 *bp* of *orf2*, 376 *bp* of *dgcB* and 370 *bp* of *wzyB* were topo-cloned into PSC-A-amp/kan to generate PSC-qsmR, PSC-flhD, PSC-orf2, PSC-dgcB and PSC-wzyB constructs. *KpnI* and *SacII* were used to transfer the *qsmR* region in PSC-qsmR to pKNOCK-Km to generate construct pKKmqsmR. *EcoR*I site was used to move the *flhD* and *orf2* regions in PSC-flhD and PSC-orf2 to pKNOCK-Km vector and generate constructs pKKmflhD and pKKmorf2, respectively. *SpeI* and *HindIII* were used to subclone the *dgcB* region from pSC-dgcB to pKNOCK-Gm to generate pKGmdgcB. *SpeI* and *KpnI* were used to subclone the *wzyB* region from pSC-wzyB to pKNOCK-Gm to generate pKGmwzyB.

3.2.9 Confirmation of the site-directed mutants

PCR was used to confirm if the entry vectors were integrated in the chromosome at the target locus. The primers designed from the flaking sequences of the mutated

genes were utilized to determine if the genomic DNAs of site-directed mutants had different amplicons with their parental strains. Primer pairs FLHD-C1/FLHD-C2, orf2-C1/orf2-C2, QsmR-C1/QsmR-C2, DGCB-C1/DGCB-C2, and Oap-C1/Oap-C2 were used to amplify the *flhD*, *orf2*, *qsmR*, *dgcB* and *wzyB* deficient mutants and their corresponding parental strains. The PCR products were visualized by electrophoresis.

3.2.10 DNA constructs for the complementation of *dgcB* defective mutants

(*This part of the work was mostly performed by Ms. Inderjit Barghaphagha*)

To generate the construct that can express *dgcB* gene back in the *dgcB* defective derivatives, Cos676, a cosmid clone from the cosmid library of the *B. glumae* 336gr-1 genome, was determined to contain *dgcB* through the screening of the cosmid clones in the cosmid library using the primers, DGC-FP and DGC-RP (Table 3.2). The 5815-*bp* target DNA fragment that contained *dgcB* and its promoter region was digested from the cosmid at *HindIII* and *NheI* sites. Vector pBBR1MCS-2 was digested at *HindIII* and *SpeI* (compatible with *NheI*) sites. The target homologous fragment was then ligated to pBBR1MCS-2 to generate the construct pBB-2dgcB for the complementation of *dgcB* defective mutants.

3.2.11 Quantification of toxoflavin production of the site-specific mutants

To prepare the inoculum for toxoflavin assay, overnight bacterial cultures were adjusted to OD_{600}=100 (10^{11} cfu). One loopful of the inoculum was taken and streaked on a LB agar plate. After 24 h incubation at 37°C, the bacterial culture was scraped off the surface of the LB agar. 5 g agar was then cut into small pieces with a razor blade. The chopped agar pieces were mixed with 5 ml chloroform and left to sit at room temperature for 30 minutes. The chloroform fraction was then transferred to a new tube and air-dried under a fume hood. The remaining materials in the dried tube were

dissolved in 1 ml of 80% methanol. The OD values of 10 X dilutions of the toxoflavin solution were measured at 393 nm to determine the quantity of toxoflavin (Jung et al., 2011).

3.2.12 Alternative virulence assay

The onion assay for specific mutants was same to the onion virulence assay in Chapter 2.

3.2.13 Extraction of mRNAs of LSUPB460 (336gr-1::pKGm*dgcB*) and reverse transcriptase PCR

To determine the regulatory role of *dgcB* in motility and EPS formation, the total mRNAs were extracted from LSUPB460. The protocol was slightly modified from the protocol published in the thesis of Francis (Francis, 2012). The one ml overnight culture was washed down twice by and resuspended in equal volumes of LB broth. 10 µl of the resuspension were inoculated in 10 ml LB broth and incubated at 37 ºC. 1 ml bacterial culture with OD_{600}=1.0 then was then pelleted and placed in liquid nitrogen for 5-10 seconds. The frozen RNA pellet was resuspended in equal volume of TRIzol® Reagent (Invitrogen), and incubated for 5 minutes at room temperature. 200 µl chloroform was added to the mixture which was later vortexed vigorously for 15 seconds and allowed to sit at room temperature for 3 minutes. The interphases were separated by centrifugation at 13.2 X 1000 rpm for 15 minutes at 4 ºC with a microcentrifuge. The top aqueous layer was transferred to a fresh tube, mixed with 500 µl chloroform then centrifuged for 5 minutes at full speed at 4 ºC. The aqueous layer was mixed with 500 µl isopropanol, incubated at room temperature for 5 minutes and then centrifuged 10 minutes at full speed at 4 ºC. The supernatant was carefully removed and the RNA pellet was washed with 75% ethanol. After the pellet was dried, it was resuspended in 22 µl RNase free

water. Two replicates from the extraction experiment were combined together for the following RNA purification and enrichment.

DNA-free™ DNase Treatment and Removal Reagents (Life Technologies, Grand Island, NY, USA) were used to remove residual DNA. 5 µl 10X DNase I Buffer and 1 µl DNase I were added to the RNA sample. The mixture was briefly centrifuged and incubated at 37 ºC for 20 minutes. Five microliter of the inactivation reagent was added to the mixture. After 2 minutes incubation at room temperature, the resuspension was spun down at max speed and 44 µl supernatant was taken and saved from each reaction. Removal of DNA was verified by PCR using rDNA spacer regions primers BglumaeFwd and BglumaeRv (Takeuchi et al., 1997).

ProtoScript® First Strand cDNA Synthesis Kit (New England Biolabs, Ipswich, MA, USA) was used to perform reverse transcriptase PCR on 500 ng RNAs. The generated cDNAs was used as template for quantitive (qPCR).

3.2.14 qPCR

To determine the regulatory role of QS and *dgcB* genes on different bacterial features like flagellar expression, toxoflavin production, and polysaccharide transportation, qPCR was used to compare the expression conditions of *tofI, toxA,* and *flhC* in different mutation backgrounds.

Primer pairs GyrA-q1/GyrA-q2, ToxA-q-1/ToxA-q-2 and FlhC-q1/FlhC-q2 (Table 2) corresponding to genes *gyrA, tofI, toxA* and *flhC* were designed with the software on the Integrated DNA Technologies (IDT) website (http://www.idtdna.com/Primerquest/Home/Index). Eight microliters of template cDNAs and 1 µl 5 nM primers were mixed with 2X Power SYBR^{R} Green PCR Master Mix (Life Technologies, Grand Island, NY, USA) to perform qPCR on IQ^{TM}5 Multicolor Real-Time

PCR Detection System (Bio-Rad Laboratories, Hercules, CA, USA), and the data were monitored by iQ™5 Optical System Software (Bio-Rad Laboratories, Hercules, CA, USA). Each reaction had three technical replicates. To optimize the primers and ensure the target gene was correctly amplified, a gradient PCR and melt curve analysis was performed first. The PCR cycles were followed by melting curve analysis from 50 °C to 95 °C to verify the specificity of the primers.

The expression ratios of *fliA, flhC* and *ragA* in different genetic backgrounds were estimated through Normalized Expression (ΔΔ CT) setting in the iQ^{TM}5 software, while the housekeeping gene *gyrA* was used as reference gene. Normalization method was chosen to calculate the expression fold change of target genes; the formula is target gene's expression = fold change in target gene/fold change of the reference gene, i.e. $\text{Normalized Expression (gene } X) = \frac{\text{Relative quantity (gene } X)}{\text{Relative quantity } (gyrA)}$.

3.3 Results

3.3.1 *gus* gene expressed in Δ*tofI*::pLGgustoxA and Δ*tofR*::pLGgustoxA

A promoterless *gusA* gene was ligated with a *toxA* promoter subcloned to a suicide vector, and new vector pKGpToxA-GUS was generated. After introduction of this vector to 336gr-1, the reporter system proved able to express *β*-glucuronidase and catalyze substrate X-gluc to produce blue color on LB/Gm/Nit/X-gluc selective plates. Later, pLG6gustoxA was introduced to LSUPB145 and LSUPB169 to generate LSUPB178 (Δ*tofI*::pLG6gustoxA) and LSUPB324 (Δ*tofR*::pLG6gustoxA), which were used as the template for transposon genomic screening for toxoflavin regulator and C8-HSL regulon.

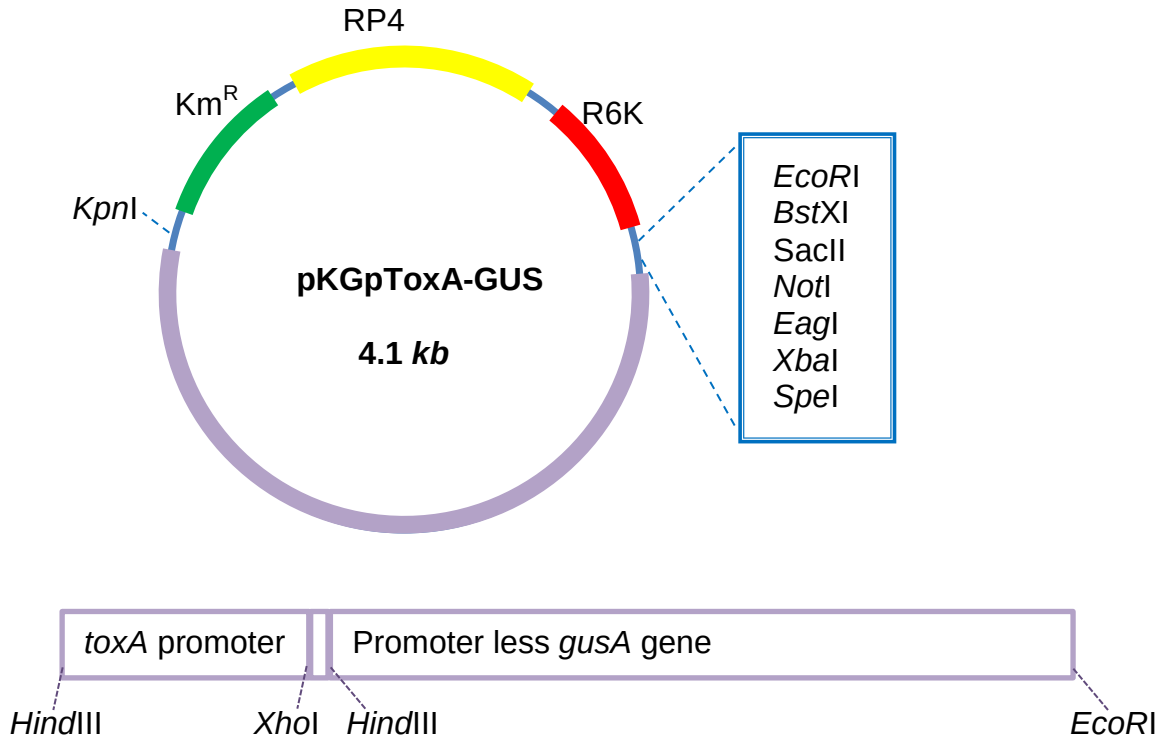

Figure 3.1. Construction of the newly generated vector pKGpToxA-GUS vector. The *toxA* promoter and promoter less *gusA* gene was inserted into the pKNOCK-Gm vector at *Kpn*I and *Spe*I sites. pKGpToxA-GUS has Km^R gene, RP4 and R6K origins, which give this vector Km resistance, conjugative and suicide properties.

3.3.2 15 of 4400 mini-Tn*5*Cm inserted Δ*tofI* derivatives were sequenced for the identification of the disrupted gene

As expected, LSUPB178 (Δ*tofI*::pLG6gustoxA) expressed blue pigment in the X-gluc supplemented media. After mini-Tn*5*Cm initiated random mutagenesis, the resultant colonies that did not exhibit blue color were picked from selective plates LB/Gm/Cm/Nir/X-gluc. The chosen mutants were considered as those that contained transposon inserted in the genetic components of the *tofI*-independent toxoflavin production pathway. Meaningful results were obtained with 15 mutant strains (Table 3.3) from the sequencing of regions flanking the transposon insertion sites. Later, all of the 15 mutants were observed to be toxoflavin-deficient when grown on LB agar at 37 °C (data not shown).

Mini-Tn*5*Cm was found to hit two genes *toxR* and *toxA* that were already known to be required for toxoflavin production (Kim et al., 2004b), which provides one evidence to confirm the validity of the experiment. The focused functional characterization of genes that encode the flagellar transcriptional activator FlhD (gene name *flhD*), a diaguanylate cyclase (assigned gene name *dgcB*), and an O-antigen polymerase family protein (assigned gene name *wzyB*) were approached by targeted mutagenesis (Figure 3.2).

Table 3.3. List of *tofI*-independent genes contributing to *tofI*-independent toxoflavin production

Name of random mutants	Relation with *toxA* gene	Locus of inserted genes (identities from BLAST)	Function of disrupted genes
LSUPB186	Positive regulator	bglu_1g10100 (24/24 100%)	Succinylornithine transaminase
LSUPB187	Positive regulator	Around 333 *bp* to 5' of bglu_2g10840 (134/134 100%)	putative LysM domain-containing protein
LSUPB182	Positive regulator	bglu_1g02180 (379/379 100%)	Diguanylate cyclase
LSUPB183	Positive regulator	Around 129 *bp* to 5' of bglu_1g01780 (930/930 100%)	Flagellar transcriptional activator FlhD
LSUPB184	Positive regulator	26 *bp* to 5' of bglu_2g07160 (215/217 99%)	Catechol 1,2-dioxygenase
LSUPB185	Positive regulator	bglu_1g00380 (208/210 99%)	General secretory pathway protein D
LSUPB188	Positive regulator	Around 48 *bp* to the 5' of bglu_2g22000 (168/168 100%)	Hypothetical protein

Table 3.3 continued

Name of random mutants	Relation with *toxA* gene	Locus of inserted genes (identities from BLAST)	Function of disrupted genes
LSUPB189	Positive regulator	bglu_1g07800 (128/129 99%)	Hypothetical protein
LSUPB192	Positive regulator	bglu_2g06390 (532/534 99%)	LysR family transcriptional regulator (*toxR*)
LSUPB193	Positive regulator	Around 207 *bp* to the 5' of bglu_2g06400 (654/700 93%)	putative ubiquinone/menaquinone biosynthesis methyltransferase (*toxA*)
LSUPB194	Positive regulator	bglu_2g18120 (278/281 99%)	Amylo-alpha-1,6-glucosidase family protein
LSUPB209	Positive regulator	bglu_1g33070 (132/132 100%)	Flagellar hook-associated protein FlgK
LSUPB210	Positive regulator	(235/238 99%)	rRNA-23S ribosomal RNA
LSUPB211	Positive regulator	bglu_1g29900 (116/116 100%)	O-antigen polymerase family protein
LSUPB212	Positive regulator	bglu_1g00440 (262/262 100%)	Glutamate--cysteine ligase
LSUPB213	Positive regulator	bglu_1g05190 (112/112 100%)	Short chain dehydrogenase

Figure 2. The organization of the genetic location of *flhD* (A), *dgcB* (B), and *wzyB* (C) as well as their neighborhood genes. The horizontal arrows indicate the genes and their transcriptional direction; the vertical arrow indicates the insertion location of transposon. The figure is not proportional to the actual size of the genes.
A: The locus and product of gene *flhD* (locus bglu_1g01780) and its downstream genes are (from left to right): bglu_1g01780: transcriptional activator FlhD; bglu_1g01790: transcriptional activator FlhC; bglu_1g01800: flagellar motor protein MotA; bglu_1g01810: flagellar motor protein MotB; bglu_1g01820: chemotaxis two-component response regulator CheY1; bglu_1g01830: chemotaxis protein CheA; bglu_1g01840: chemotaxis protein CheW; bglu_1g01850: methyl-accepting chemotaxis protein; bglu_1g01860: CheR-type MCP methyltransferase; bglu_1g01870: chemoreceptor glutamine deamidase CheD; bglu_1g01880: chemotaxis-specific methylesterase; bglu_1g01890: chemotaxis protein CheY; bglu_1g01900: chemotaxis regulator CheZ.
B. The locus and product of *dgcB* (bglu_1g02180) and its neighborhood genes are (from left to the right): bglu_1g02250: lipoprotein; bglu_1g02240: OmpW family outer membrane protein; bglu_1g02230: lysine exporter protein LysE/YggA; bglu_1g02220: 2-hydroxy-3-oxopropionate reductase; bglu_1g02210: oxalate/formate antiporter; bglu_1g02200: major facilitator superfamily oxalate/formate antiporter; bglu_1g02190: hypothetical protein; bglu_1g02180: diguanylate cyclase; bglu_1g02170: cytochrome c family protein; bglu_1g02160: transporter; bglu_1g02150: phosphoheptose isomerase; bglu_1g02140: hypothetical protein; bglu_1g02130: Uroporphyrin-III C/tetrapyrrole(Corrin/Porphyrin) methyltransferase; bglu_1g02120: lipoprotein A family protein; bglu_1g02110: beta-lactamase-like protein.
C. The locus and product of *wzyB* (bglu_1g2890) and its neighborhood genes are (from left to the right) bglu_1g29970: recombinase A; bglu_1g29960: recombination regulator RecX; bglu_1g29950: hypothetical protein; bglu_1g29940: uccinyl-CoA synthetase subunit beta; bglu_1g29930: succinyl-CoA synthetase subunit alpha; bglu_1g29920: integral membrane protein TerC; bglu_1g29910: type IV fimbrial pilin protein; bglu_1g2900: O-antigen polymerase family protein; bglu_1g2890: TonB domain-containing protein; bglu_1g29880: porin; bglu_1g29870: molybdenum cofactor biosynthesis protein MoaC; bglu_1g29860: M48 family peptidase; bglu_1g29850: hypothetical protein.

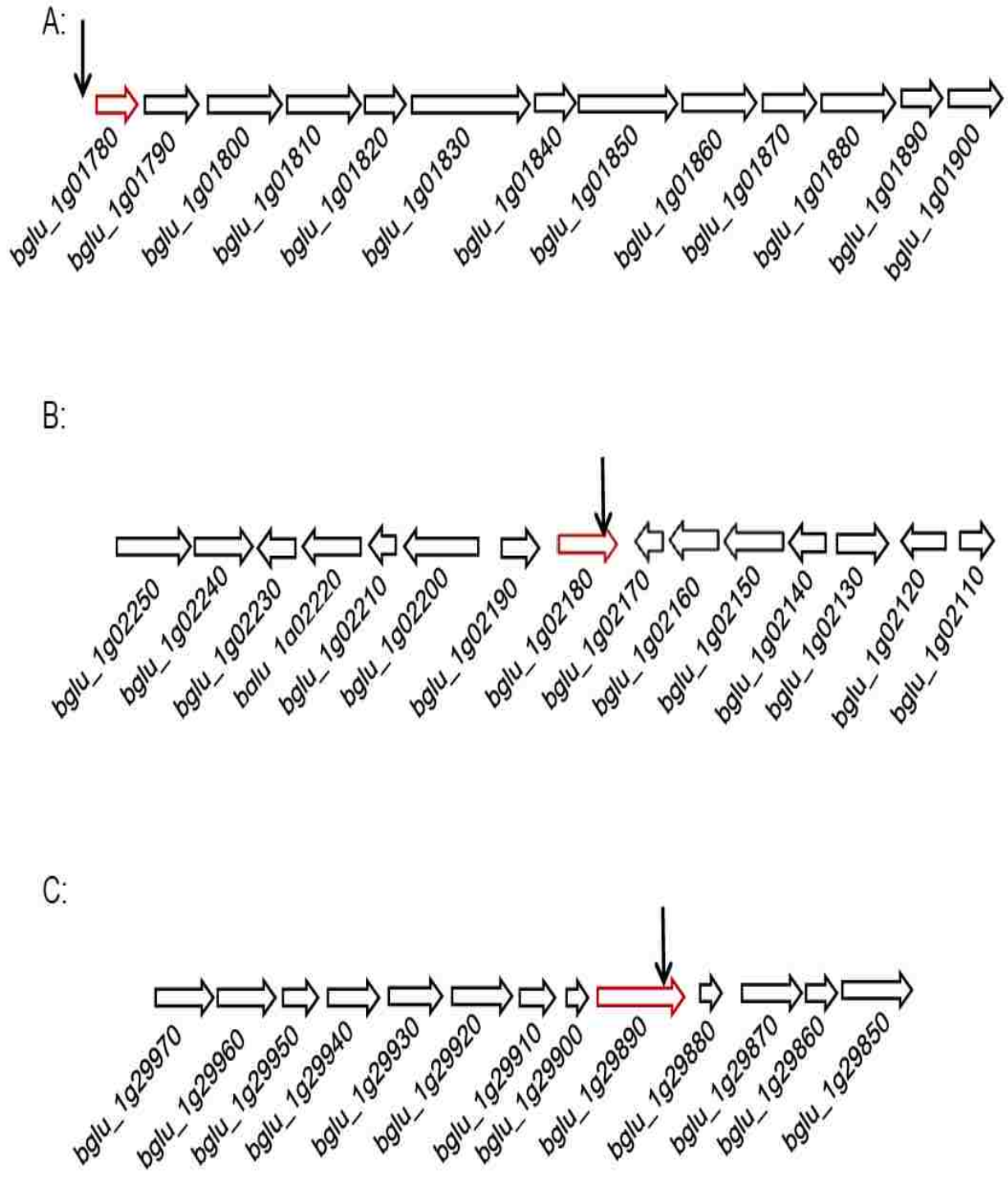
A:
bglu_1g01780
bglu_1g01790
bglu_1g01800
bglu_1g01810
bglu_1g01820
bglu_1g01830
bglu_1g01840
bglu_1g01850
bglu_1g01860
bglu_1g01870
bglu_1g01880
bglu_1g01890
bglu_1g01900
B:
bglu_1g02250
bglu_1g02240
bglu_1g02230
balu_1a02220
bglu_1g02210
bglu_1g02200
bglu_1g02190
bglu_1g02180
bglu_1g02170
bglu_1g02160
bglu_1g02150
bglu_1g02140
bglu_1g02130
bglu_1g02120
bglu_1g02110
C:
bglu_1g29970
bglu_1g29960
bglu_1g29950
bglu_1g29940
bglu_1g29930
bglu_1g29920
bglu_1g29910
bglu_1g29900
bglu_1g29890
bglu_1g29880
bglu_1g29870
bglu_1g29860
bglu_1g29850

3.3.3 Three of 4400 mini-Tn*5*Cm inserted Δ*tofR* derivatives were sequenced for the identification of the disrupted gene

Similar to LSUPB178, LSUPB324 (Δ*tofR*::pLG6gustoxA) expressed blue pigment in the X-gluc supplemented media. After the random mutagenesis initiated by transposon mini-Tn*5*Cm, the resultant colonies that did not exhibit blue color were picked from selection plates LB/Gm/Cm/Nir/X-gluc. Meaningful results were obtained with three mutant strains (Table 3.4) from the sequencing of flanking regions of the transposon insertion sites. As expected, loss of toxoflavin was observed in all of the three mutants when grown on LB agar at 37 °C (data not shown). The focused experiments were performed on gene *qsmR* and the gene (designed name *orf2*) that was located upstream of *toxJ* by specific mutagenesis. The genetic arrangement was diagramed in Figure 3.3.

Table 3.4. List of *tofR*-independent genes contributing to *tofR*-independent toxoflavin production

Name of random mutants	Relation with *toxA* gene	Locus of inserted genes (identities from blasting)	Function of disrupted genes
LSUPB190	Positive regulator	bglu_1g10250 (105/121 87%)	IclR family regulatory protein (*qsmR*) gene
LSUPB191	Positive regulator	bglu_2g06320 (160/160 100%)	Hypothetical protein in the upstream of orphan LuxR family transcriptional regulator (ToxJ)
LSUPB195	Positive regulator	bglu_2g22590 (355/356 99%)	Putative PAS/PAC sensor protein

A.

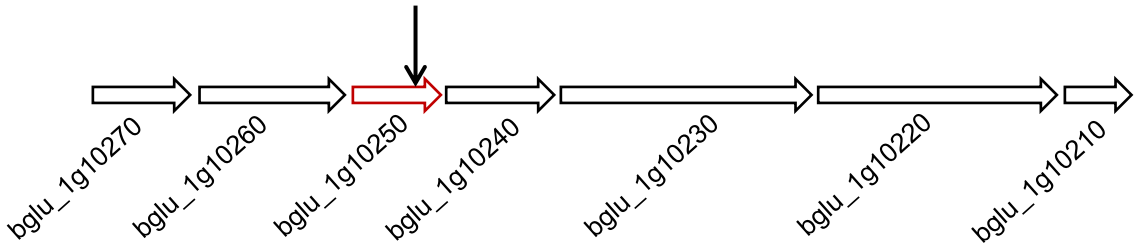

B.

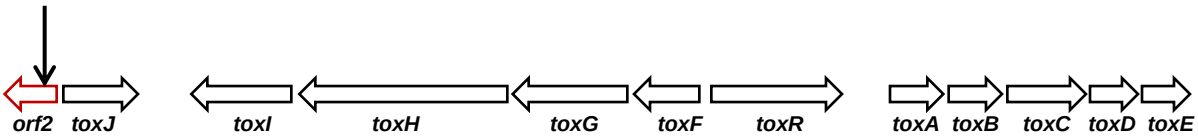

Figure 3.3. The organization of the genetic location of *qsmR* (A) and *orf2* (B) as well as their neighborhood genes. The horizontal arrows indicate the genes and their transcriptional direction; the vertical arrow indicates the insertion location of transposon. The figure is not proportional to the actual size of the genes.
A. The locus and encoding proteins of *qsmR* (locus bglu_1g10250) and its neighborhood genes are (from left to the right): bglu_1g10270: Rh-like protein/ammonium transporter; bglu_1g10260: phosphatase-like protein; bglu_1g10250: IclR family regulatory protein; bglu_1g10240: RND family efflux transporter MFP subunit; bglu_1g10230: AcrB/AcrD/AcrF family protein; bglu_1g10220 bglu_1g10210: multidrug resistance protein MdtC.
B. The locus and encoding proteins of *orf2* (locus bglu_2g06320) and its neighborhood genes are (from left to the right): bglu_2g06320: hypothetical protein; bglu_2g06320: ToxJ; bglu_2g06310: ToxI; bglu_2g06300: ToxH; bglu_2g06290: ToxG; bglu_2g06280: ToxF; bglu_2g06270: ToxR; bglu_2g06260: ToxA; bglu_2g06250: ToxB; bglu_2g06240: ToxC; bglu_2g06230: ToxD; bglu_2g06220: ToxE. The assigned names of genes were labeled underneath the horiaontal arrows.

3.3.4 Disrupted mutants of selected potential toxoflavin regulatory genes were generated and their production of toxoflavin appeared reduced

To confirm the regulatory roles of *flhD*, *dgcB,* and *wzyB* in *tofI*-independent toxoflavin production, the internal regions of *flhD*, *dgcB*, *wzyB* were amplified and cloned to pKNOCK suicide vectors, generating corresponding mutants LSUPB503, LSUPB462 and LSUPB515. The same strategy was applied to confirm the toxoflavin

regulatory roles of *qsmR* and *orf2*, which is the locus at 5' of *toxJ*. The corresponding mutants LSUPB277 and LSUPB445 were generated. The integration of entry vectors was confirmed by PCR, which utilized primers that were outside of the potential integration area in different mutants of the target genes (Figure 3.4). The PCR products of expected sizes were amplified from parental strains (LSUPB154 and LSUPB169) but not from the interesting mutants. This result suggested the integration of a suicide vector between the two primers' binding sites.

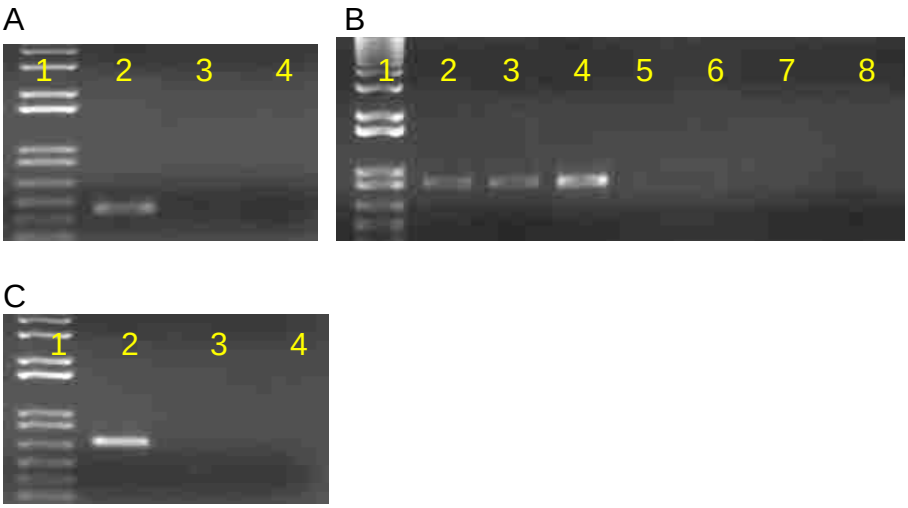

Figure 3.4. PCR confirmation of disruptive mutation of genes *flhD* (A), *qsmR* (B), and *orf2* (C).
A. PCR product bands with expected size 445 *bp* amplified and shown on the agarose gel. Lane 1, 1 kb Plus DNA ladder; lane 2, PCR products from LSUPB145 genome; Lane 2: no PCR products amplified from LSUPB503 genome; Lane 4: reagent mixture without template.
B. PCR product bands with expected size 863 *bp* amplified and shown on the agarose gel. Lane 1, 1 kb Plus DNA ladder; lane 2, 3, 4 PCR products from 336gr-1, LSUPB145 and LSUPB169 genomes; Lane 5, 6, 7: no PCR products amplified from LSUPB273, LSUPB275 and LSUPB277 genomes; Lane 4: reagent mixture without template.
C. PCR product bands with expected size 683 *bp* amplified and shown on the agarose gel. Lane 1, 1 kb Plus DNA ladder; lane 2, PCR products from LSUPB145 genome; Lane 2: no PCR products amplified from LSUPB445 genome; Lane 4: reagent mixture without template.

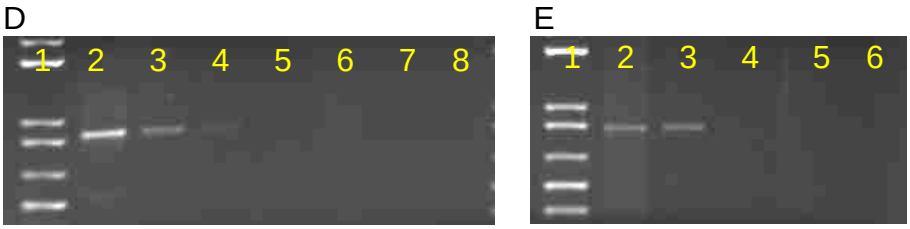

Figure 3.4. PCR confirmation of disruptive mutation of genes *dgcB* (D) and *wzyB* (E). D. PCR product bands with expected size 878 *bp* amplified and shown on the agarose gel. Lane 1, 1 kb Plus DNA ladder; lane 2, 3, 4 PCR products from 336gr-1, LSUPB145 and LSUPB286 genomes; Lane 5, 6, 7: no PCR products amplified from LSUPB460, LSUPB462 and LSUPB464 genomes; Lane 4: reagent mixture without template. E. PCR product bands with expected size 818 *bp* amplified and shown on the agarose gel. Lane 1, 1 kb Plus DNA ladder; lane 2 and 3, PCR products from LSUPB145 and LSUPB169 genomes; Lane 4 and 5: no PCR products amplified from LSUPB515 and LSUPB516 genomes; Lane 6: reagent mixture without template.

The mutants' phenotypes were then compared to previously generated QS mutants, especially LSUPB154 (Δ*tofI*) and LSUPB169 (Δ*tofR*) (Figure 3.5). Mutation of *dgcB* and *wzyB* in LSUPB145 background caused loss of toxoflavin (Figure 3.5F,G), which was observed from the bacterial culture incubated at 37 °C for one day, whereas LSUPB145 still produced a substantial amount of toxoflavin (Figure 3.5B). Loss of toxoflavin production was not observed in the *flhD* mutant in LSUPB145 background after one day incubation, but toxoflavin degradation was observed on the second day (Figure 3.5E). This result still proves the participation of *flhD* in toxoflavin production. Mutation of *qsmR* and *orf2* in LSUPB169 background caused loss of toxoflavin compared to the parental strain (Figure 3.5H, I and C), which confirmed the regulatory roles of *qsmR* and *orf2* in *tofR*-independent toxoflavin production. Furthermore, the loss of toxoflavin production of the mutants generated by targeted mutation verified the reliability of the random mutagenesis.

Figure 3.5. Confirmaiton of the deduction of regulatory roles of interesting genes from random mutagenesis by observation of toxoflavin production of the corresponding disruptive mutants. 336gr-1 (A), LSUPB145 (Δ*tofI*) (B), LSUPB169 (Δ*tofR*) (C), LSUPB286 (Δ*tofM*) (D), LSUPB503 (Δ*tofI*::*flhD*) (E), LSUPB462 (Δ*tofI*::*dgcB*) (F), LSUPB515 (Δ*tofI*::*wzyB*) (G), LSUPB277 (Δ*tofR*::*qsmR*) (H), LSUPB445 (Δ*tofR*::*orf2*) (I) were streaked on LB agar media and incubated at 37 °C for 48 h. The pictures were taken at 24 h after and 48 h after inoculation. Toxoflavin can diffuse to the surrounding area in the agar, which was easy to observe and compare. In general, the deficient mutants of interesting genes produced reduced the amount of toxoflavin at either 24 h or 48 h after inoculation.

A.

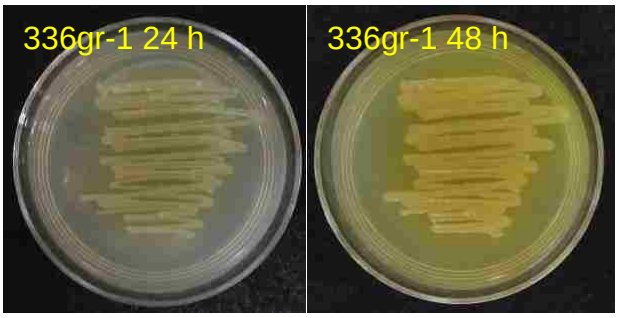
336gr-1 24 h
336gr-1 48 h

B.

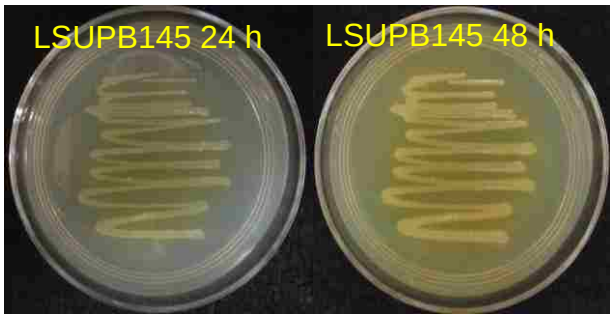
LSUPB145 24 h
LSUPB145 48 h

C.

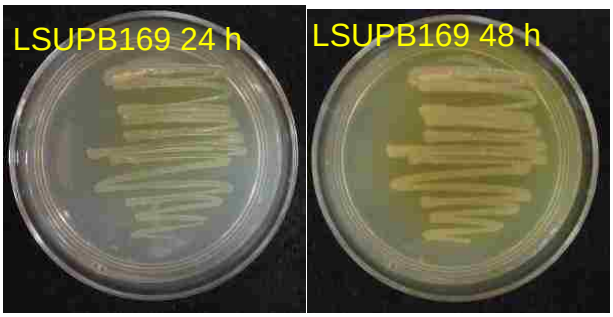
LSUPB169 24 h
LSUPB169 48 h

D.


LSUPB286 24 h
LSUPB286 48 h

E.


LSUPB503 24 h
LSUPB503 48 h

F.


LSUPB462 24 h
LSUPB462 48 h

G.

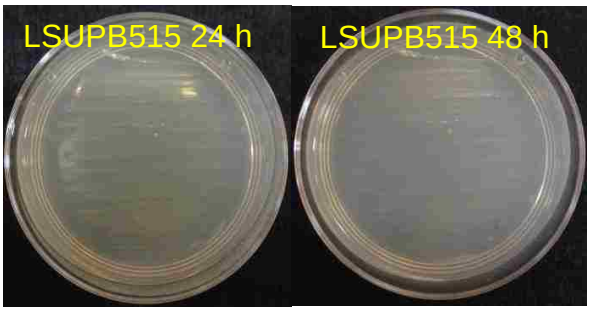
LSUPB515 24 h
LSUPB515 48 h

H.

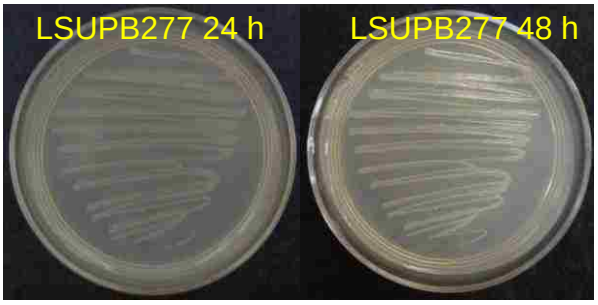
LSUPB277 24 h
LSUPB277 48 h

I.

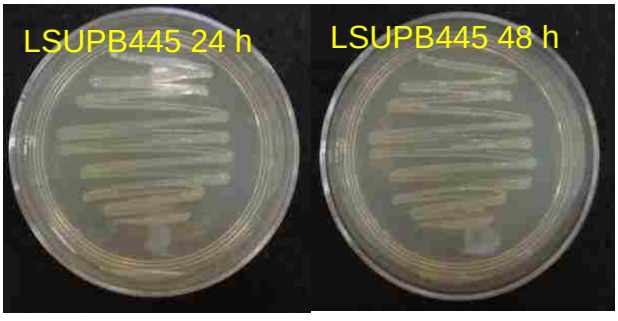
LSUPB445 24 h
LSUPB445 48 h

3.3.5 Overexpression of *dgcB* can promote toxoflavin production and possibly QS genes

The specific mutants selected genes were observed to exhibit significant reduction of toxoflavin production. The phenotypes of LSUPB462 (LSUPB145 derivative with pKGmdgcB inserted in *dgcB* gene) and LSUPB182 (LSUPB145 derivative with a transposon inserted in *dgcB* gene) are toxoflavin-deficient on solid media (Figure 3.5F) in common. This result showed the importance of diguanylate cyclase in the *tofI*-independent pathway for toxoflavin production. However, it also would be interesting to know if *dgcB* is critical for toxoflavin production when the QS system is intact. Therefore, LSUPB460 (336gr-1 derivative with transposon inserted in *dgcB* gene) was generated (Figure 3.6A), and the bacterial culture on LB agar appeared to produce less toxoflavin compared to 336gr-1. This result indicated that *dgcB* contributed, but was not essential for toxoflavin production when the QS system was intact. It was also observed that LSUPB460 had a creamy surface compared to the WT strain (Figure 3.6A). The dysfunction of *dgcB* might have triggered another physiological change like polysaccharide production. To explore the relationship between *dgcB* and the other QS elements *tofR* and *tofM*, pKGmdgcB was introduced into LSUPB169 and LSUPB286. LSUPB464, which was the *dgcB* mutant in LSUPB286 background, lost toxoflavin production ability on the LB agar (Figure 3.6B). This result again implied the requirement of *dgcB* for toxoflavin production when the QS system was not intact. The generation of *dgcB* mutant in LSUPB169 background also caused toxoflavin loss (data not shown). The toxoflavin production of the series of *dgcB* mutants was quantified (Figure 3.6C), and they were consistent with the previous observation.

A.

B.

C.

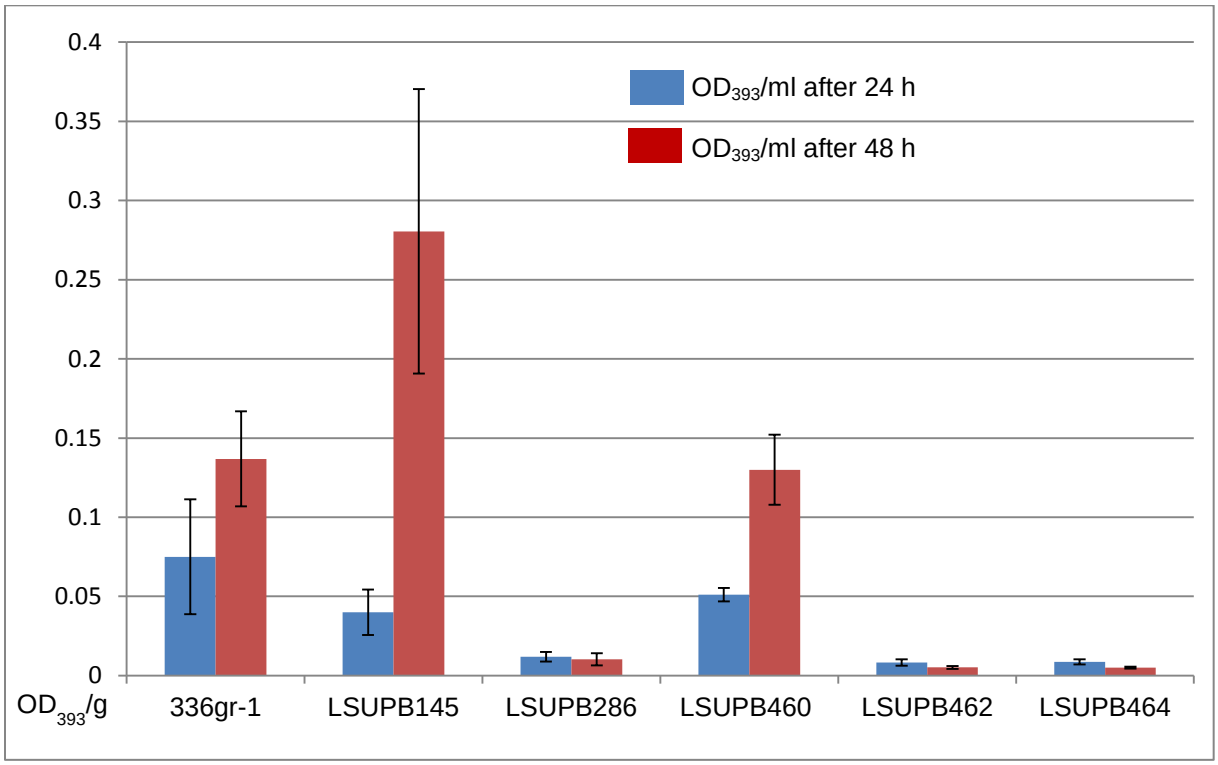

Figure 3.6. The toxoflavin production of *dgcB* mutants LSUPB460 (WT::pKGmdgcB) and LSUPB464 (Δ*tofM*::pKGmdgcB) on LB agar after 24 h and 48 h of incubation at 37 °C compared to parental strains LSUPB145 (Δ*tofI*) and LSUPB286 (Δ*tofM*). A. toxoflavin production of LSUPB460 on LB agar media. Pictures were taken at 24 h and 48 h. B. toxoflavin production of LSUPB464 on LB agar media; C. quantification of toxoflavin of series of *dgcB* mutants comparing to their template strains. The toxoflavin was extracted from three disruptive mutants LSUPB460 (336gr-1::pKGmdgcB), LSUPB362 (Δ*tofI*::pKGmdgcB) and LSUPB462 (Δ*tofM*::pKGmdgcB) and their mother strains WT strains 336gr-1, Δ*tofI* and Δ*tofM* grown on the LB agar after 24 h and 48 h. The OD_{393} values of the toxoflavin resuspension from each strain were measured, and the OD_{393}/ml were displayed in the column. X axis: the names of the strains where the toxoflavin was extracted from; Y axis: OD_{393} values of toxoflavin from 1 gram of LB agar.

To explore the relationship between QS and DgcB, qPCR was performed to determine the regulatory effect dgcB had on the *tofI* gene. The templates were cDNAs corresponding to the transcriptome of WT 336gr-1, LSUPB460 and LSUPB472 (complemented strain of LSUPB460 by pBB-2dgcB). As expected, the mutation of *dgcB* caused reduced transcription of the *toxA* gene, and the addition of the *dgcB* expression construct in the bacterial cell recovered the expression of *toxA* gene (Figure 3.7). Even though there was no significant difference between *tofI* transcription level in WT and the *dgcB* mutant, the overexpression of *dgcB* caused a substantial increase in the *tofI* expression level. This result suggested the positive regulatory role of *dgcB* toward QS.

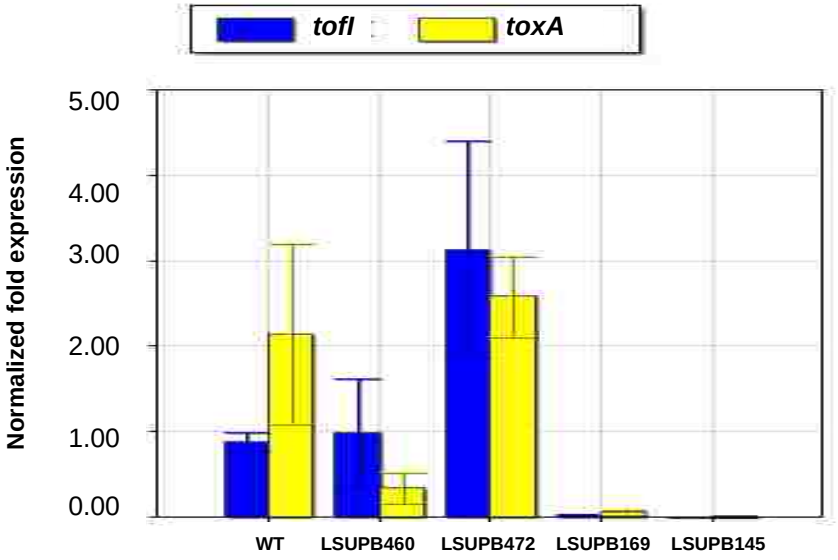

Figure 3.7. The normalized expression of *tofI* and *toxA* in WT, LSUPB460 (WT::pKGmdgcB), LSUPB472 (W::pKGmdgcB::pBB-2dgcB) (complemented strain of LSUPB460), LSUPB169 (Δ*tofR*) and LSUPB145 (Δ*tofI*) strains. The expression of housekeeping gene *gyrA* in all the mentioned strains was set as baseline to perform the normalization. WT 336gr-1 and LSUPB460, LSUPB472, LSUPB169 and LSUPB145 were incubated in LB broth until culture OD_{600}=1. The total RNAs from the bacterial culture were extracted, purified and reversely transcripted to cDNAs, which were used as the templates for qPCR. The horizontal axis represents every condition from which cDNAs generated; the vertical bar represents the normalized expression level of each gene. Blue bar indicates expression fold of *tofI*, and yellow bar indicates expression fold of *toxA.*

3.3.6 *flhD* can protect toxoflavin from early degradation, and *flhC* was possibly regulated by *dgcB*

Compared to LSUPB145, its *flhD* mutant was observed to degrade toxoflavin after 2 days' incubation at 37 °C (Figure 3.5E). The quantification data confirmed the observation (Figure 3.8). *flhC* was another insertion site for mini-Tn*5*Cm in the LSUPB145 derivative random mutants that did not express *toxA*. The specific mutation of *flhC* also caused loss of toxoflavin (data not shown). It was not surprising that the regulatory functions of *flhD* and *flhC* coincided with each other. Later, qPCR was performed to explore the relationship between *flhC* and *dgcB.* The result showed that the addition of the *dgcB* expression construct accelerated the transcription level of both *tofI* and *flhC*, which suggested that *dgcB* might be the upstream regulator for QS (Figure 3.9).

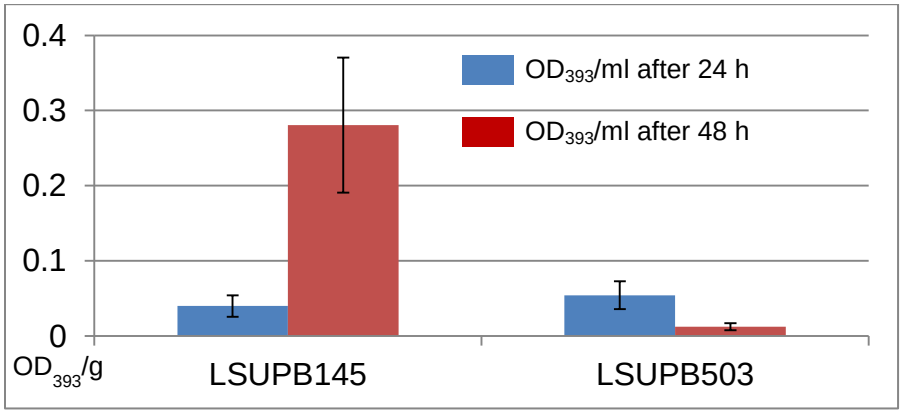

Figure 3.8. Quantification of toxoflavin produced by LSUPB503 (Δ*tofI*::pKKmflhD) compared to its mother strain LSUPB145 (Δ*tofI*) after 24 and 48 h incubation on LB agar at 37 °C. The OD_{393} values of the toxoflavin resuspension from each strain were measured, and the OD_{393}/ml was displayed. X axis: the names of the strains where the toxoflavin was extracted from; Y axis: OD_{393} values of toxoflavin from 1 gram of LB agar.

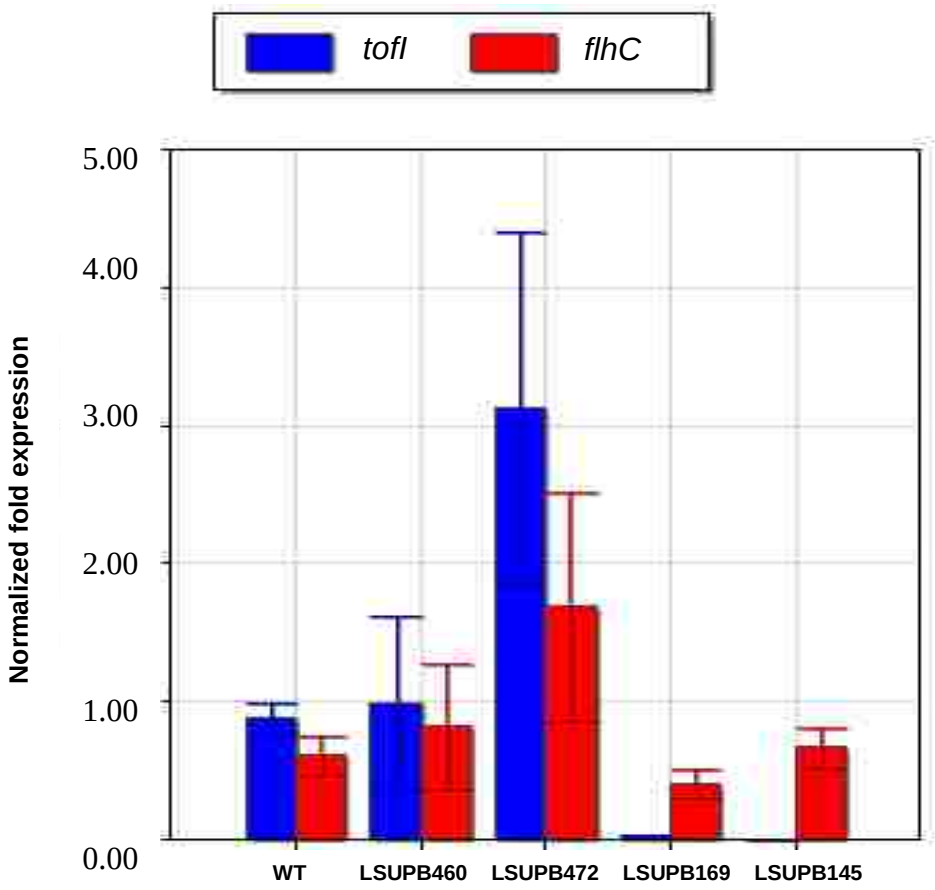

Figure 3.9. The normalized expression of *tofI* and *flhC* in WT, LSUPB460 (WT::pKGmdgcB), LSUPB472 (W::pKGmdgcB::pBB-2dgcB) (complemented strain of LSUPB460), LSUPB169 (Δ*tofR*) and LSUPB145 (Δ*tofI*) strains. The expression of housekeeping gene *gyrA* in all the mentioned strains was set as baseline to perform the normalization. WT 336gr-1 and LSUPB460, LSUPB472, LSUPB169 and LSUPB145 were incubated in LB broth until culture OD_{600}=1. Total RNAs from the bacterial culture were extracted, purified and reversely transcripted to cDNAs, which were used as the templates for qPCR. The X axis represents every condition that cDNAs were generated from; the vertical bars represent the normalized expression level of each gene. Blue bar = expression fold of *tofI*, and yellow bar = expression fold of *flhC.*

3.3.7 Disruption of *wzyB* caused slow growth of bacterial culture

LSUPB515, the *wzyB* disruptive mutant in LSUPB145 background grew very slowly on LB agar (Figure 3.5G) as well as in LB broth (Figure 3.10B), and toxoflavin production was completely lost. Because of the lack of abundant growth of the bacterial culture in LB, it was difficult to prepare inoculum for a toxoflavin quantification experiment for LSUPB515. The *wzyB* disruptive mutant in LSUPB169 background,

LSUPB516, was generated and also lost most of the toxoflavin production on LB agar (Figure 3.10A) and in broth (Figure 3.10B), and the quantification results matched the observation (Figure 3.10C).

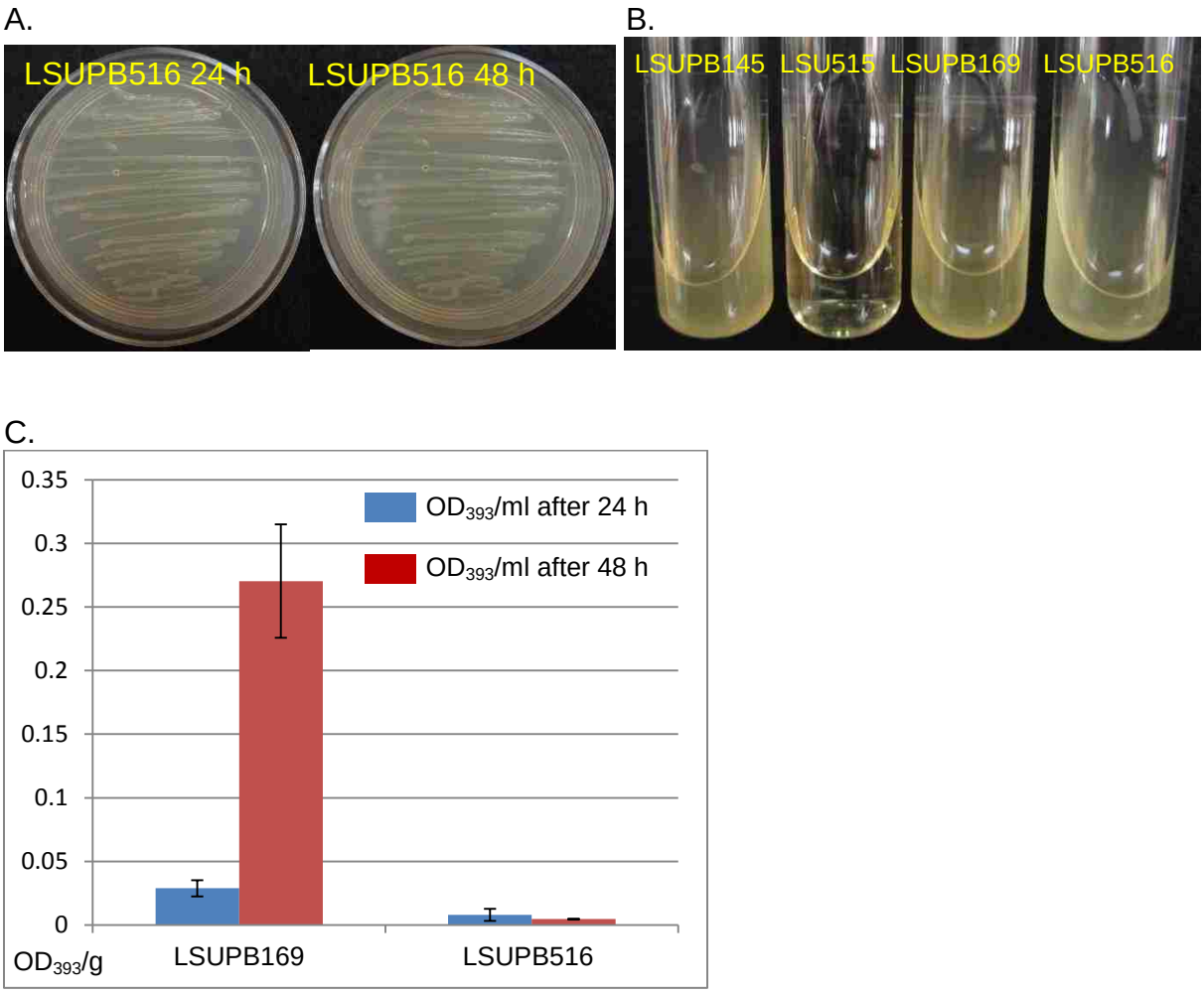

Figure 3.10. Toxoflavin growth and quantification of *wzyB* mutants. A. LSUPB516 (Δ*tofR*::pKGmwzyB) grew normally on LB agar, but did not express toxoflavin. Pictures were taken at 24 h and 48 h. B. The LB broth growth condition of LSUPB515 (Δ*tofI*::pKGmwzyB) and LSUPB516 compared to their mother strain, LSUPB145 (Δ*tofI*) and LSUPB169 (Δ*tofR*). C. quantification of toxoflavin production of *wzyB* mutant LSUPB516 compared to the template strains LSUPB169 after 24 h and 48 h incubation on LB agar at 37 °C. The OD_{393} values of the toxoflavin resuspension from each strain were measured, and the OD_{393}/ml values are displayed in the bars. X axis: the names of the strains from which the toxoflavin was extracted; Y axis: OD_{393} values of toxoflavin from 1 gram of LB agar.

3.3.8 *orf2* is important for *tofR*-independent toxoflavin production

orf2 mutant LSUPB445 did not produce observable toxoflavin, and the PCR result confirmed the reliability of the mutation. From quantification data, it was clear that the toxoflavin production from days 1 and 2 were all close to zero compared to the template strain, which meant that *orf2* is important in maintaining toxoflavin production in LSUPBB169 (Figure 3.11). This result proved that *orf2* was responsible for toxoflavin production without a functional *tofR* gene.

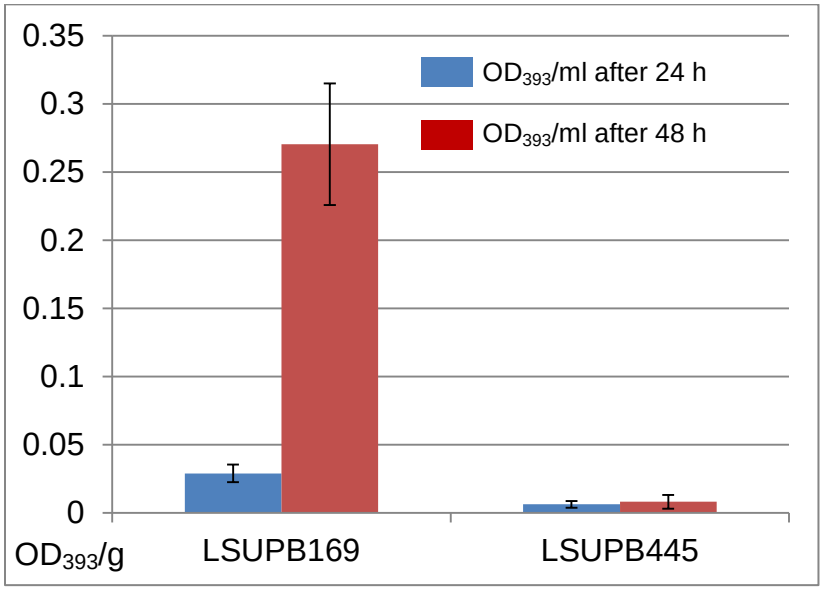

Figure 3.11. Quantification of toxoflavin production of *orf2* mutant LSUPB445 (Δ*tofR*::pKGmorf2) compared to the template strains LSUPB169 (Δ*tofR*) after 24 h and 48 h incubation on LB agar at 37 °C. The OD_{393} values of the toxoflavin resuspension from each strain were measured and the OD_{393}/ml values are displayed in the bars. X axis: names of the strains from which the toxoflavin was extracted; Y axis: OD_{393} values of toxoflavin from 1 gram of LB agar.

3.3.9 qsmR was required for toxoflavin production

LSUPB277, *qsmR* mutated in LSUPB169 background, had the same toxoflavin loss phenotype as the random mutant LSUPB190, which confirmed the important role of *qsmR* in *tofR*-independent toxoflavin production. To determine how *qsmR* was related

to toxoflavin production when the QS system is intact or in absence of the *tofI* gene, LSUPB273 (WT::pKGmdgcB) and LSUPB275 (Δ*tofI*::pKGmdgcB) were generated, and both mutants produced no observable toxoflavin (Figure 3.12A). The toxoflavin of LSUPB273, LSUPB275 and LSUPB277 was extracted and quantified, and the quantification results were consistent with the observations (Figure 3.12B). This result indicated the necessity of *qsmR* for toxoflavin production, in general.

A.

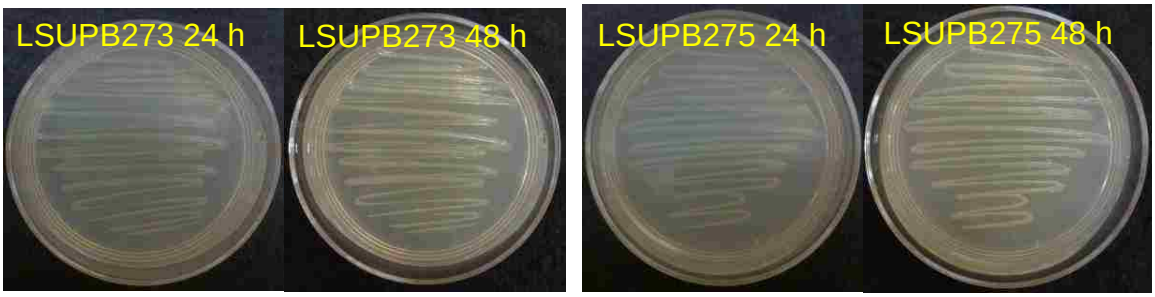

B.

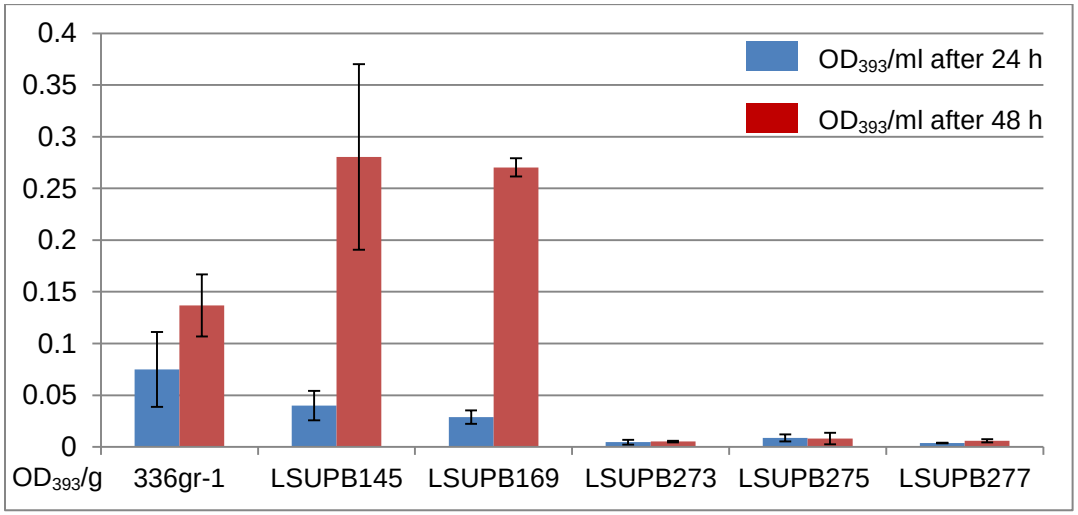

Figure 3.12. Toxoflavin production of *qsmR* mutants. A. the bacterial cultures of LSUPB515 and LSUPB516 grown on LB agar. Pictures were taken at 24 h and 48 h. B. toxoflavin produced by LSUPB273 (WT::pKKmqsmR), LSUPB275 (Δ*tofI*::qsmR) and LSUPB277 (Δ*tofR*::qsmR) compared to their mother strains WT, LSUPB145 (Δ*tofI*) and LSUPB169 (Δ*tofR*) after 24 h and 48 h incubation on LB agars at 37 °C. The OD_{393} values of the toxoflavin resuspension from each strain were measured and the OD_{393}/ml values are displayed in the column. X axis: names of the strains from which toxoflavin was extracted; Y axis: OD_{393} values of toxoflavin from 1 ml of LB agar.

3.3.10 Onion maceration caused by mutants

The virulence levels of 336gr-1 (WT), LSUPB145 (Δ*tofI*), LSUPB169 (Δ*tofR*), LSUPB286 (Δ*tofM*), LSUPB503 (Δ*tofI*::pKKmflhD), LSUPB445 (Δ*tofR*::pKKmorf1), LSUPB273 (WT::pKKmqsmR), LSUPB275 (Δ*tofI*::pKKmqsmR), LSUPB277 (Δ*tofR*::pKKmqsmR), LSUPB460 (WT::pKGmdgcB), LSUPB462 (Δ*tofI*::pKGmdgcB), LSUPB464 (Δ*tofM*::pKGmdgcB), and LSUPB516 (Δ*tofR*::pKGmwzyB) were estimated by onion scale assay to give an estimate of the virulence reaction on rice. The maceration areas from replicates were measured. None of the mutations made the *B. glumae* were completely avirulent, but exhibited reduced virulence compared to their parental strains (Figure 3.13). There was not a very strong correlation between toxoflavin production and size of the maceration area. For example, the toxoflavin production of LSUPB273, LSUPB275, LSUPB277, LSUPB462, LSUPB464, LSUPB516 was nearly abolished on the LB agar, but these isolates were still virulent on onion, which suggested the function of other virulence factors.

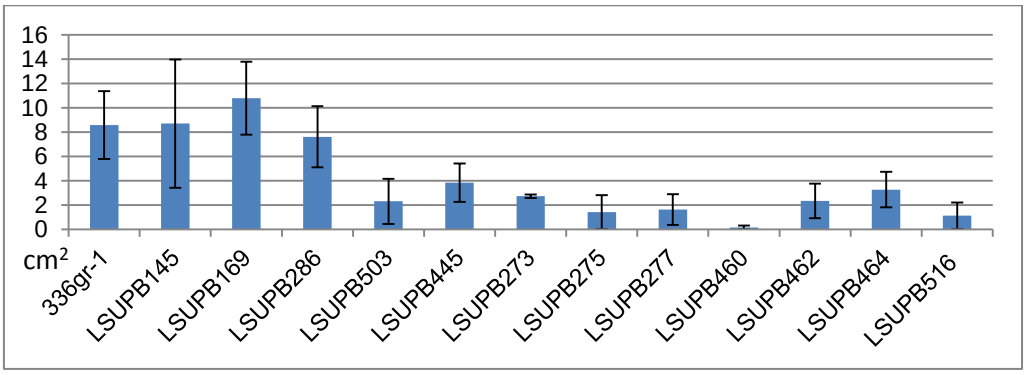

Figure 3.12. Onion virulence assay for all of the specific mutants. The maceration diameters on onion pieces were measured (a and b refer to the length of two diameters) and used to calculate the area using the formula $Area = \pi ab$. The mean of area size caused by an individual strain is displayed in each bar. The Y axis = size of maceration area in cm^2, and the X axis = the strain that caused the maceration on onion.

3.3.11 Eight out of 6000 mini-Tn*5gus* inserted Δ*tofI* derivatives were sequenced at the disrupted gene

After the introduction of mini-Tn*5gus* to the genome of LSUPB145, colonies were picked from three different X-gluc supplemented media. The aim was to find the genes regulated by C6-HSL and C8-HSL. From rounds of selection, there were very few colonies that responded to C6-HSL. Almost all the colonies with differential *gusA* gene expression on selective media shared a pattern of being only positive or negative in the presence of C8-HSL. The flanking regions of the transposon insertion site in those colonies were sequenced, and the ones that had meaningful results are shown in Table 3.5.

Table 3.5. List of genes that responded to C8-HSL.

Name of random mutants	Relation of inserted genes with C8-HSL	Locus of inserted gene (identities from BLAST)	Functions of the disrupted gene
LSUPB159	Down regulated by C8-HSL	Around 1543 *bp* to 5' of bglu_1g07720	tRNA (guanine-N(7)-)-methyltransferase
LSUPB162	Up regulated by C8-HSL	bglu_1g30220 668/745(90%)	Transglycosylase
LSUPB160	Up regulated by C8-HSL	bglu_2g05900 731/731(100%)	Ferredoxin
LSUPB163	Up regulated by C8-HSL	bglu_1g07550 (555/574 97%)	Urease, alpha subunit
LSUPB196	Down regulated by C8-HSL	bglu_2g05820 (476/476 100%)	Transcriptional regulator, AraC family
LSUPB197	Up regulated by C8-HSL	bglu_2g05850 (1136/1156 98%)	FAD/FMN-binding oxidoreductase
LSUPB198	Up regulated by C8-HSL	bglu_2g18720 (696/696 100%)	Hypothetical protein
LSUPB199	Up regulated by C8-HSL	bglu_2g07310 (383/389 98%)	Putative DEAD/DEAH box helicase

3.3.12 Nine out of 8000 mini-Tn*5gus* inserted 336gr-1 derivative were sequenced at the disrupted genes

To find the genetic components that reacted to jasmonic acid (JA) and salicylic acid (SA), the transposon mini-Tn*5gus* was introduced to the genome of 336gr-1 then the colonies were placed on three X-gluc supplemented plates including no extra, JA or SA. The mutant colonies that had differential expression of the *gusA* in the selection plates were selected and characterized (Table 3.6).

Table 3.6. List of genetic components that reacted to jasmonic acid (JA) or salicylic acid (SA)

Name of random mutants	Response to SA and JA	Locus of inserted genes	Function of inserted genes (identities)
LSUPB481	Only down regulated by SA	bglu_2g15980 (71/71 100%)	Rhodanese domain-containing protein/ Dienelactone hydrolase family protein
LSUPB482	Constitutive in all three conditions	bglu_2g02560 (93/93 100%)	type VI secretion system Vgr family protein
LSUPB483	Only down regulated by SA	bglu_2g05130 (42/42 100%)	Transcriptional regulator, winged helix family
LSUPB484	Only down regulated by SA	bglu_2g07640 (532/533 99%)	Glycine/D-amino acid oxidase
LSUPB485	Only down regulated by SA	bglu_2g12060 (304/304 100%)	protocatechuate 3,4-dioxygenase subunit beta
LSUPB486	Only up regulated by JA	bglu_1g12700 (203/203 100%)	PII uridylyl-transferase
LSUPB487	Only down regulated by SA	bglu_2g08600 (108/111 97%)	Outer membrane porin
LSUPB488	Only up regulated by SA	bglu_2g00640 (59/59 100%)	3-carboxy-cis,cis-muconate cycloisomerase
LSUPB489	Only down regulated by SA	Around 457 *bp* to 5' of bglu_1g11840 (87/90 97%)	Hypothetical protein 206 bp

3.4 Discussion

3.4.1 Genome-wide screening by random transposon mutagensis revealed novel regulators of toxoflavin in *B. glumae*

The *toxA* promoter and *gusA* transcriptional fusion was introduced to Δ*tofI* and Δ*tofR* mutants to search for the genes that could affect the expression of *toxA* or the toxoflavin biosynthesis operon. Mini-Tn*5*Cm successfully performed the random mutagenesis since the distribution of inserted genes was random. It was discovered that 15 *tofI*-independent and 3 *tofR*-independent potential regulators of toxoflavin were present in *B. glumae.* From that collection, the presence of *toxA* and *toxR* verified the reliability of this experiment. Even though there were several interesting candidates that deserved further investigation, primary genetic and phenotypic confirmation was only established for *flhD* encoding flagella transcriptional activator FlhD, *dgcB* encoding diguanylate cyclase, *wzyB* encoding O-antigen polymerase family protein and *qsmR.* From the confirmation of the partial or complete loss of toxoflavin production caused by targeted mutation, the regulatory roles of *flhD*, *dgcB*, *wzyB* and *qsmR* for the toxoflavin production were demonstrated in this study.

3.4.2 New roles of *flhD* and *flhC* in *B. glumae* as the toxoflavin production modulator

LSUPB145 still has functional flagella (Chen, 2011). The mutation of *flhD* and *flhC* caused phenotypic changes relative to the template strain LSUPB145. The mutant Δ*tofI*::pKKmflhC lost toxoflavin (data not shown due to the lack of genetic confirmation of the specific mutation), and LSUPB503 (Δ*tofI*::pKKmflhD) started to lose toxoflavin after 2 days incubation. These results implied that *flhD* and *flhC* might play important roles to support the toxoflavin production in the absence of the *tofI* gene. Another function of *flhD* may be to prevent early toxoflavin degradation. Besides *flhC* and *flhD*,

there were two other motility related proteins that were screened during the genomic study: the flagellar hook-associated protein, FlgK, and the reported motility regulator, QsmR. It appeared that motility played an important part in supplementing the loss of AHL synthase to ensure the formal QS regulon toxoflavin genes are expressed normally. This may be because free movement of bacterial cells in the population can provide another kind of signal of infection-ready mode, which is analogous to QS, allowing expression of virulence factors when the bacterial population is vigorous enough to overcome plant defense systems (Liu et al., 2008), and this motility-related signaling can up-regulate expression of a virulence factor like toxoflavin, as well.

flhD was characterized as the flagellar transcriptional activator, which was controlled by QS in *B. glumae* (Kim et al., 2007a). It was reported that *flhD* deficient mutants still produced toxoflavin but lost pathogenicity (Kim et al., 2007a). Considering the infection procedure of *B. glumae* on rice, the bacteria can live epiphytically on leaves and sheaths until the host and environment favor the infection on the panicle (Yuan, 2004), which indicates the importance of motility for successful colonization and infection at the desirable site for the pathogen. In that case, the *flhD* mutant in our study was expected to lose virulence on rice. However, the virulence assay on an alternative onion host revealed that LSUPB503 still contained partial virulence, which could be explained by the difference in inoculation methods. Kim et al., (2007) dipped rice plants in a bacterial resuspension, whereas the LSUPB503 resuspension was inoculated into the small incision on the onion skin. The latter brought more intimate contact between pathogen and host, and skipped the motility step.

The flagellum, as a single organelle, has been well recognized as a pathogenicity factor of bacteria, due to its role in versatile activities including motility, biofilm formation and virulence factor secretion similar to T3SS (Duan et al., 2013). Chemotaxis, one type of flagellum-related movement, is one of the signal transduction paradigms (Staudinger, 2007). Besides what is mentioned above, there are few records about flagellar involvment in signaling pathways for other virulence factors.

3.4.3 Overexpression of *dgcB* accelerates the expression of *tofI, toxA* and *flhC* genes

The *dgcB* gene was selected from the collection of *tofI*-independent toxoflavin regulators. The specific mutation of *dgcB* in LSUPB145 (Δ*tofI*) and LSUPB286 (Δ*tofM*) background resulted in loss of toxoflavin production, and the addition of the *dgcB* expression construct pBB-2dgcB complemented this phenotype. From qPCR, it was shown that the normal transcription of *toxA* depended on the *dgcB* gene. Based on this evidence, the conclusion can be drawn that protein diguanylate cyclase (DGC), which is the synthase of c-di-GMP, is one putative regulator of toxoflavin production. The results also showed that the mutation of *dgcB* abolished the toxoflavin production for LSUPB145 and LSUPB286, but not for 336gr-1, which implied a relation between *dgcB* and QS on toxoflavin gene regulation. The function of *dgcB* might coodinate or interefere with *tofI* and *tofM.* From the qPCR, overexpression of *dgcB* increased the transcriptional level of *tofI* which suggested that putative protein DgcB might have positively regulated *tofI* gene and was an upstream regulator of QS.

qPCR also showed that the introduction of pBB-2dgcB increased the expression of *flhC*. This result indicated that DgcB positively regulated flagellum expression, possibly through QS since the *tofI* gene followed a similar pattern. It is known that a low

concentration of c-di-GMP signals is always associated with the expression of flagella motility (Jenal and Malone, 2006).The second messenger c-di-GMP is regulated by two enzymes DGC carrying GGDEF domain and specific phosphodiesterases (PDEs) carrying EAL or HD-GYP domains. In general, overproduction of GGDEF domain proteins favors the formation of biofilm, synthesis of exopolysaccharides (EPS), and inhabits flagella-regulated motility (Hengge, 2009). In our study, DGC might positively regulate the motility of *B. glumae,* which is unusual compared to the information gathered so far.

Temperature is very critical for the control of flagella formation. QS effectively regulates the expression of flagella genes in *B. glumae* BGR1 at 28 °C but not at 37 °C (Kim et al., 2007a). The control of flagellar synthesis is also temperature-sensitive in some other bacterial species. For example, in the major food-borne pathogen *Campylobacter jejuni*, the expression of flagellin gene (*flaA*) was influenced by FlaM-FliA complex, which was dependent on temperature. At 42 °C, more FliA proteins dissociate from the complex and activate the σ^{28} promoter of genes like *flaA*, which result in longer flagella and reduced motility (Wosten et al., 2010). In another animal pathogen, *Listeria monocytogenes*, the transcription of flagella motility is repressed at 37 °C compared to lower temperatures, due to the degradation of protein thermometer GmaR, which acts as an anti-repressor for the flagellar genes (Kamp and Higgins, 2011). In our study, the temperature used to incubate the bacteria was only 37 °C. It is necessary to investigate the regulatory relationship between DGC and *flhDC* in temperatures lower than 30 °C to accurately describe the flagella regulation cascade.

The expression of the *flhDC* cluster in *Salmonella enterica* was down-regulated at poor media due to the modulation of YdiV factor, which has EAL domain (Wada et al., 2011). The YdiV protein can bind to and deactivate $FlhD_4C_2$ complex to prevent the promotion of the downstream flagella genes (Wada et al., 2011). Even with the EAL domain, the YdiV protein does not have catalytic activities to c-di-GMP, which is also the case for another YdiV flagella inhibitor protein (has weakly sequence similarity to typical EAL domain) in *Escherichia coli* (Li et al., 2012). Apparently, it is common for EAL or DGC proteins to not perform c-di-GMP turnover function, therefore, whether *dgcB* encoding protein participates in c-di-GMP or not needs more translational level studies.

So far, *B. cenocepacia* has been the only species that was reported owning functional c-di-GMP, which positively regulated the expression of EPS and biofilm (Fazli et al., 2013; Fazli et al., 2011). This published result is in conflict with what was observed from LSUPB460 (336gr-1::pKGmdgcB), which seemed to produce more EPS in the plate (Figure 3.6A). At least it is safe to say that DGC might interfere with the normal production of EPS.

3.4.4 *wzyB* might play an important role in alternative intercellular signaling for toxoflavin production in LSUPB145 (Δ*tofI*) on LB agar

Through genomic screening and mutagenetic confirmation, *wzyB* has become another putative *tofI*-independent toxoflavin production regulator. LSUPB515 (Δ*tofI*::pKGmwzyB) grew slowly and produced no observable toxoflavin; LSUPB516 also lost most of the toxoflavin compared to their template strain LSUPB169. Therefore, *wzyB* not only contributed to *tofI*- and *tofR*-independent toxoflavin production, but also played an important role in normal bacterial growth.

O-antigen is one of the three major components (the other two are lipid A and a core oligosaccharide) lipopolysaccharides (LPS) in outer membrane of negative bacteria; and is very structurally diverse and highly immunogenic (Raetz and Whitfield, 2002; Stone et al., 2012). Study of O-antigen and its synthesis pathway can provide important antibiotic targets for potential clinical use. The O-antigen polymerase family protein (encoded by *wzy* homolog) is responsible for polymerizing the O-antigen units to O-antigen chain (Daniels et al., 1998; Wang and Quinn, 2010). It is well known that LPS is a common virulence determiner (Ellis and Kuehn, 2010; Thomsen et al., 2003). As an important synthesis enzyme for O-antigen and LPS, O-antigen polymerase should be important for maintaining the virulence of pathogenic bacteria, but little research has focused on the study of *wzy* homolog. There are not many study of *wzy* homologs in bacterial phytopathogens, but recently, it was reported that non-polar mutation of the *wzy* gene in *Salmonella enterica* serovar *Typhimurium* caused attenuated virulence in mice (Kong et al., 2011).

Additionally, the relationship between motility genes, especially *flhDC* and LPS synthetic genes might deserve more investigation. There have been reports about how the subunits and enzymes involved in assembling LPS influence the motility function of bacteria. The mutation of the O-antigen gene in *Salmonella enterica* serovar Typhimurium resulted in defective bacterial swarming, and it was also suggested that the role of O-antigen was to improve the wettability of the bacterial colony (Toguchi et al., 2000). The mutation of *wzxE* gene, which was responsible for transporting O-antigen units across the inner membrane to the LPS assembling site (Wang and Quinn, 2010), caused *E. coli* to lose both swimming and swarming motility (Girgis et al., 2007).

The mutation of *waaL*, one O-antigen ligase gene, in *Vibrio fischeri* resulted in loss of motility ability and inability to survive in the co-colony assay with the wild type (Post et al., 2012). The mutation of *waaL* also blocked the expression of *flhDC* genes and aborted the swarming motility of human pathogen *Proteus mirabilis* in soft agar (Morgenstein et al., 2010), but overexpression of *flhDC* genes in *trans* overcame this defect (Morgenstein et al., 2010). Therefore, there is a possibility that *wzyB* gene interacts with the QS-regulated motility system in *B. glumae.*

3.4.5 The discovery of the *orf2* gene may add more complexity to the ToxR regulating pathway

The gene (with assigned name *orf2*) that is located in upstream of *toxJ,* the QS-dependent toxoflavin regulator, was found to be responsible for *tofR*-independent toxoflavin production. The arrangement of *orf2* (bglu_2g06320) and neighbourhood genes was indicated in Figure 3.3B. *orf2* encodes 144 residues (15.5 kilodaltonsin) long uncharacterized protein. The disruptive mutation of *orf2* in the *tofR* background resulted in the loss toxoflaivn production, which further emphasized the importance of *orf2* as one potential toxoflavin regulator.

It was previously reported that genes involved in the biosynthesis of toxoflavin in *B. glumae* were clustered together following the transcriptional direction as

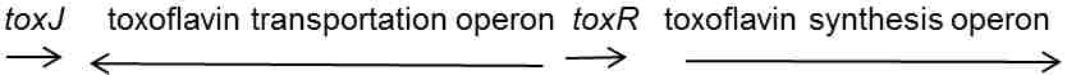

(Suzuki et al., 2004a). In general, the QS dependent genes have one 20 *bp lux* box like sequence in the 5' region (Callahan and Dunlap, 2000). There is one *lux* box like sequence between *toxJ* and *orf2* genes, and it was proven that TofR and C8-HSL complex can bind on that site and activate the expression of *toxJ* (Kim et al., 2004b). There was no

conserved domain and gene ontology term found in the database search of the *orf2* sequence. However, the fact that the binding site of the QS regulator is close to the *orf2* gene can provide some insight and reference to the future study about extension of QS regulons.

3.4.6 QsmR is a putative regulator for toxoflavin production

qsmR mutants in 336gr-1, LSUPB145 and LSUPB169 background lost toxoflavin production. Therefore, it was shown that *qsmR* can be another potential regulator for toxoflavin. QsmR was first recognized as *flhDC* flagella genes' regulator, which was activated by C8-HSL and TofR complex (Kim et al., 2007a). The disruption of *qsmR* resulted in loss of motility and pathogenicity on rice, but not toxoflavin (Kim et al., 2007a). From our study, the *qsmR* mutant did not produce observable toxoflavin on LB agar and still retained partial virulence on onion, which differed with Kim's result about the function of *qsmR* in the BGR1 strain. The mutation of *qsmR* in BGR1 caused a decrease in toxoflavin production compared to the wild type in liquid media 16 h after inoculation, but no such change on LB agar (Kim et al., 2007a). It appears that QsmR showed tighter regulation on toxoflavin production in 336gr-1 than in BGR1. Overall, QsmR is important for virulence expression of *B. glumae,* and another virulence factors regulated by QsmR catalase encoded by *katG* (Chun et al., 2009).

QsmR, as a newly discovered transcriptional activator in *Burkholderia*, has begun to attract more attention. From a proteomics search, a type II secretion system encoded by *gsp* genes was found to be regulated by QS, and QsmR was shown to be their activator through a transcriptional level study (Chun et al., 2009). In a study about how QS systems help representative *Burkholderia* species survive stationary phases, the sub-QS regulator QsmR was determined to be critical for activating the production of

oxalate and maintaining normal pH levels of (Goo et al., 2012). Without functional QsmR, there was a survival defect in *B. glumae* and *B. thailandensis* populations, which correlated with the high pH and lack of oxalate (Goo et al., 2012). Later, it was proved that QsmR directly activated the promoter of oxalate genes *obcA-B*, which protected *Burkholderia* species against base toxicity (Goo et al., 2012).

3.4.7 Several interesting genes regulated by C8-HSL can be good candidates for future study

To expand our knowledge of the regulon of C8-HSL and C6-HSL, a genome-wide search through random mutagenesis was performed. The genes that were up- or down-regulated by C8-HSL were recorded, though no gene was found corresponding to C6-HSL. The confirmation experiments for the collection have not been done yet, but the candidates still provided some insights for the future characterization work.

There are genes from the collection that brought some interesting speculation regarding the QS network. The following is some simple description about interesting candidates.

A transposon was inserted around 1543 bp to 5' of bglu_1g07720 encoding tRNA (guanine-N(7)-)-methyltransferase (locus bglu_1g07720). There was no binding domain found in the area around the transposon insertion site. It was not certain if the transposon disrupted the gene or the binding site of an unknown activator or represser, but it is still possible that tRNA (guanine-N(7)-)-methyltransferase mediated by C8-HSL is positively regulated by C8-HSL. This encoded protein has S-adenosylmethionine-dependent methyltransferase activity (NCBI). According to the definition in gene ontology, this enzyme can catalyze substrates S-adenosyl-L-methionine (SAM) and tRNA to S-adenosyl-L-homocysteine (SAH) and tRNA containing N7-methylguanin. In

general, SAM and fatty acid chains carried by acyl carrier proteins are the substrates for LuxI synthase for generating AHL signals (von Bodman et al., 2003). One experiment has been done for *Pseudomonas aeruginosa* to see if RhlI can synthesize AHL from SAH instead of SAM, and the result was negative (Parsek et al., 1999). *Salmonella enterica* serovar Typhimurium produces autoinducer 2 (AI-2) instead of AHL as the signal for QS (Beeston and Surette, 2002). It was reported that SAH was the substrate for *pfs*-dependent AI-2 synthesis, and high concentrations of SAH inhibit the SAM dependent methyltransferase reactions (Beeston and Surette, 2002). Therefore, it is possible that C8-HSL in *B. glumae* overpowers the expression AI-2 pathway in certain conditions, and AI-2 might have some cooperation with the *tofI-R* system.

Ferredoxin (locus bglu_2g05900) was selected because of up-regulation by C8-HSL. It was reported in *Erwinia carotovora* subsp. *carotovora*, that gene *ferE* encoding a ferredoxin-like protein was mediated by QS, and this gene also contributed to QS-dependent oxidative stress tolerance (Sjoblom et al., 2008). Therefore, there is a chance that the ferredoxin encoding gene in *B. glumae* is an important addition to the QS regulon.

The gene encoding AraC family transcriptional regulator (bglu_2g05820) was selected as the down-regulated gene by QS. There have been a number of studies focusing on the relationship between QS and AraC proteins. AraC family regulators were first mentioned as positive regulators of L-arabinose catabolism in *Escherichia coli* (Greenbla.J and Schleif, 1971). With the presence of arabinose, the dimer protein activates the expression of the catabolic operon of arabinose *araBAD*; with the absence of arabinose, AraC suppresses the expression of *araBAD* (Gallegos et al., 1997). AraC

type regulators also are involved in the expression of virulence factors in plant pathogens, e.g. the hypersensitive response gene *hrpB* in *B. solanacearum and the hrpB* gene in *Xanthomonas campestris* and *X. oryzae* (Gallegos et al., 1997). The opportunistic human and plant pathogen *P. aeruginosa* utilizes VqsM, a AraC type regulator, to modulate the AHL QS system and pathogenicity (Dong et al., 2005). The *vqsM* mutant exhibited diminished AHL production and virulence, and VqsR, another downstream regulator of VqsM, was able to more or less rescue the above phenotypes. This result implied VqsM is the upregulator for the AHL system through VqsR (Dong et al., 2005). A *luxR* homolog *cepR2* was found existing in *B. cenocepacia* without the adjacent *luxI* type gene, and this orphan CepR2 protein was determined to negatively regulate an AraC-family regulatory protein encoded by a neighboring gene of *cepR2* (Malott et al., 2009). Considering the extent to which AraC was involved in virulence expression of pathogenic bacteria, the study of this global regulator will need to be investigated in the future.

3.4.8 JA and SA screening generate some preliminary information

Nine mutants were collected and sequenced from JA- or SA-containing plates. It should be mentioned that reactions of those nine mutants in the plates were not very consistent. This might be because the target genes were sensitive to the micro-environment in the petri-dish. Therefore, confirmation of the gene function is required before drawing further conclusions. Assuming that the selection result is reliable, this collection might contribute to future knowledge of bacteria-plant interaction and eventually provide valuable information about antibiotic design.

CHAPTER 4. TRANSCRIPTIONAL STUDY OF THE LUX-TYPE QUORUM SENSING SYSTEM IN *BURKHOLDERIA GLUMAE*

4.1 Introduction

tofM located in middle of *tofI* and *tofR* genes was recently determined to be an important regulatory factor in *B. glumae* and is critical for the *tofI*/*tofR*-independent toxoflavin production (Chen et al., 2012). Additionally, *tofM* contributes to the full virulence of *B. glumae*, and is conserved throughout *Burkholderia species* (Chen et al., 2012). TofM shares sequence homology and genetic arrangement similarity with RsaM, which is one quorum sensing (QS) modulator in *Pseudomonas fuscovaginae*, which negatively regulates *luxI* type gene *pfsI* (Chen et al., 2012; Mattiuzzo et al., 2011). Therefore, it is interesting to determine if *tofM* has similar regulatory role with *rsaM* in the QS hierarchical mechanism in *B. glumae.* It is important to understand if the *tofI-tofR* system can self-modulate. To elucidate the relations between *tofM* and other QS genes, qunantitative PCR (qPCR) was perform the transcriptional level study of target genes.

To further investigate the regulon of QS in 336gr-1, the transcriptomes of WT and LSUPB139 (Δ*tofI-R*) were extracted at expected quorum point, which was when the toxoflavin started to produce. Then comparative transcriptome analysis was performed to find the differently expressed genes, which were also the potential QS regulon. Although the same RNA-seq data set was previously analyzed (Francis, 2012), different and improved computational tools were used in this study. RNA-seq data of WT and QS mutants of another *B. glumae* strain BGR1 were also simply analyzed to provide reference information. Some general characteristics of *B. glumae* genome were also described in this chapter.

4.2 Materials and methods

4.2.1 Growth conditions of bacterial strains

All of the *B. glumae* strains (table 1) were grown or maintained in LB broth or on LB agar plates (Sambrook, 2001). Bacterial strains grown in liquid medium conditions were placed in a shaking incubator set at 200 rpm at 37 °C.

Table 4.1. List of *B. glumae* derivatives used or generated in this study

Burkholderia glumae Strain	Description	Reference
336gr-1	A wild type strain isolated from a bacterial panicle blight symptom in Crowley, LA	(Nandakumar et al., 2009a)
LSUPB145	A Δ*tofI* derivative of 336gr-1	(Chen et al., 2012)
LSUPB169	A Δ*tofR* derivative of 336gr-1	(Chen et al., 2012)
LSUPB139	A Δ*tofI-R* derivative of 336gr-1	(Chen et al., 2012)
LSUPB286	A Δ*tofM* derivative of 336gr-1	(Chen et al., 2012)

4.2.2 Extraction of mRNAs and reverse transcriptase PCR

To determine the influence of *tofM* on the expression of *tofR*, total RNAs were extracted from *B. glumae* strains 336gr-1, LSUPB145 (Δ*tofI*), LSUPB169 (Δ*tofR*), LSUPB286 (Δ*tofM*) and LSUPB139 (Δ*tofI-tofR*) grown in LB broth. The procedure of extraction and purification was the same as the description in 2.2.12 in Chapter 2. Additionally, the total RNAs in 336gr-1, LSUPB145 (Δ*tofI*), and LSUPBLSUPB139 (Δ*tofI-tofR*) were extracted from solid media. To prepare bacterial culture grown on solid LB media, 50 µl overnight cultures of 336gr-1, LSUPB145, and LSUPB139 were dropped in middle of LB agar and incubated at 37 °C for 9 h. Each strain had two replicates. Spot cultures of each strain were then scraped off the media surface and transferred to the bottom of micro-centrifuge tubes. The tubes containing bacterial

cultures were dipped in liquid nitrogen for 15 seconds. TRIzol® Reagent (Life Technologies, Grand Island, NY, USA) was then applied to extract RNAs, and the procedure was the same as the extraction of RNAs from bacterial cultures grown in LB broth. Reverse transcriptase PCR was then performed to generate cDNAs for qPCR.

4.2.3 qPCR

To illustrate the regulatory cascade of *tofI*, *tofR* and *tofM*, the expression conditions of *tofI, tofR* and *toxA* in different genetic background were compared by qPCR. Primer pairs GyrA-q1/GyrA-q2, TofI-q-1/TofI-q-2, TofR-q-1/TofR-q-2, and ToxA-q-1/ToxA-q-2 (Table 2) corresponding to genes *gyrA, tofI, tofR* and *toxA* were designed with the software provided by the IDT website (http://www.idtdna.com/Primerquest/Home/Index). The annealing temperature was 53 °C and extension time was 30 seconds. The same method from Chapter 3 3.2.15 was used to perform qPCR and gene expression analysis.

Table 4.2. The qPCR programs and primers used in transcriptional study.

Amplified region	Product length	Primers* (forward & reverse)
Internal region of DNA gyrase subunit A (*gyrA*) gene	140 *bp*	GyrA-q1: CACGACTACATCCTCTGTTTCTC GyrA-q2: ACGTTGATCTTCTCGCCTTC
Internal region of *toxA*	111 *bp*	ToxA-q-1: TTCGGGCGTGAAATCTATCG ToxA-q-2: GAGCGGATCGCCGTATTT
Internal region of *tofI*	87 *bp*	TofI-q-1: GCTGGGTTCGTACCGTTATC TofI-q-2: TACTGATCGCGCTCGAATTT
Internal region of *tofR*	99 *bp*	TofR-q-1: CCATAGCAGCAGTACTCGAAG TofR-q-2: TGCCTACCACCAGTTCAATAC

4.2.4 Sample preparation for RNA-seq

The procedure was previously described (Francis, 2012), and it can be summarized as the following:

A volume of one ml overnight broth culture of *Burkholderia glumae* virulent strain 336gr-1 and avirulent strain LSUPB139 (Δ*tofI-R*) (Chen et al, 2012) was washed down twice and resuspended in LB broth. A volume of 15 µl of the suspension was inoculated in 15 ml LB and incubated in 37 ºC. A volume of one ml bacterial culture was harvested following the method described in 3.2.14 from Chapter 3. After the DNA elimination step as described in 3.2.14, there was no PCR product tested from 13 µg RNA sample of 336gr-1 and 11 µg RNA sample of LSUPB139 as well as the serial dilution of each RNA sample.

Agilent RNA 6000 pico kit (Agilent Technologies, Santa Clara, CA, USA) was used for quality checking of the RNA samples after DNA elimination. A NanoDrop DN-1000 Spectrophotometer (Thermo Scientific, Wilmington, DE, USA) was used to measure the 260/280 ratio (the ratio values of all the RNA samples were higher than 2.0) and concentration of RNA samples.

RNA samples were treated with a MEGAclear™ Kit (Life Technologies, Grand Island, NY, USA) to eliminate the divalent cations left in the sample solution as well as the short oligonucleotides and protein molecules. 5.9 µg RNA from 336gr-1 and 6.0 µg RNA from LSUPB139 were harvested from the treatment.

The RNA samples were then treated with a MICROBExpress™ Bacterial mRNA Enrichment Kit (Life Technologies, Grand Island, NY, USA) for the removal of rRNA. 2.4 µg enriched mRNAs from 336gr-1 and 2.2 µg mRNA from LSUPB139 were recovered using this treatment.

600 ng rRNA-cleaned total RNA was treated with RNase III (Life Technologies, Grand Island, NY, USA) to reduce the fragmentation variability. RiboMinus™

Concentration Module (Life Technologies, Grand Island, NY, USA) was used to further eliminate the rRNA. RNA-Seq Library Construction Kit (Life Technologies, Grand Island, NY, USA) was used for the transcriptome RNA library construction. The protocol was modified as follows: after purification, cDNA was first amplified by PCR, then DNA products at 170 ~250 *bp* on the 1% agarose gel from electrophoresis were excised and extracted using GenElute™ Gel Extraction Kit (Sigma-Aldrich, St. Louis, MO, USA).

4.2.5 Next generation sequencing and data analysis

A volume of 20 µl DNA sample (~6 ng/µl) from 336gr-1 and a volume of 20 µl DNA sample (~6 ng/µl) from LSUPB139 (Δ*tofI-R*) were sent to Virginia Bioinformatics Institue Core Lab. Illumina GAIIx was used to perform single-end sequencing for 50 cycles. 1.6 GB and 953.9 MB of sequence reads were generated from 336gr-1 and LSUPB139 DNA template respectively. Rockhopper (McClure et al., 2013) and DNASTAR software (DNASTAR, Inc. Madison, WI, USA) were used to analyze the RNA-seq data. The transcriptional profiles of amplicons (chromosome 1, chromosome 2, plasmid 1, plasmid 2, plasmid 3 and plasmid 4) of *B. glumae* genome were estimated. Using Rockhopper, the differently expressed genes with q value (the adjusted p value) less than 0.01 between WT and LSUPB139 were collected. The genes with expression log fold change higher than 2 between WT and LSUPB139 were also collected using DNASTAR. The prediction of operon, novel genes and 5' translated regions (UTRs) of *B. glumae* was performed based on intergenic distance and correlation of gene expression using Rockhopper based RNA-seq data of BGR1 derivatives (McClure et al., 2013).

4.3 Results

4.3.1 *tofM* is the putative positive regulator for *tofR*

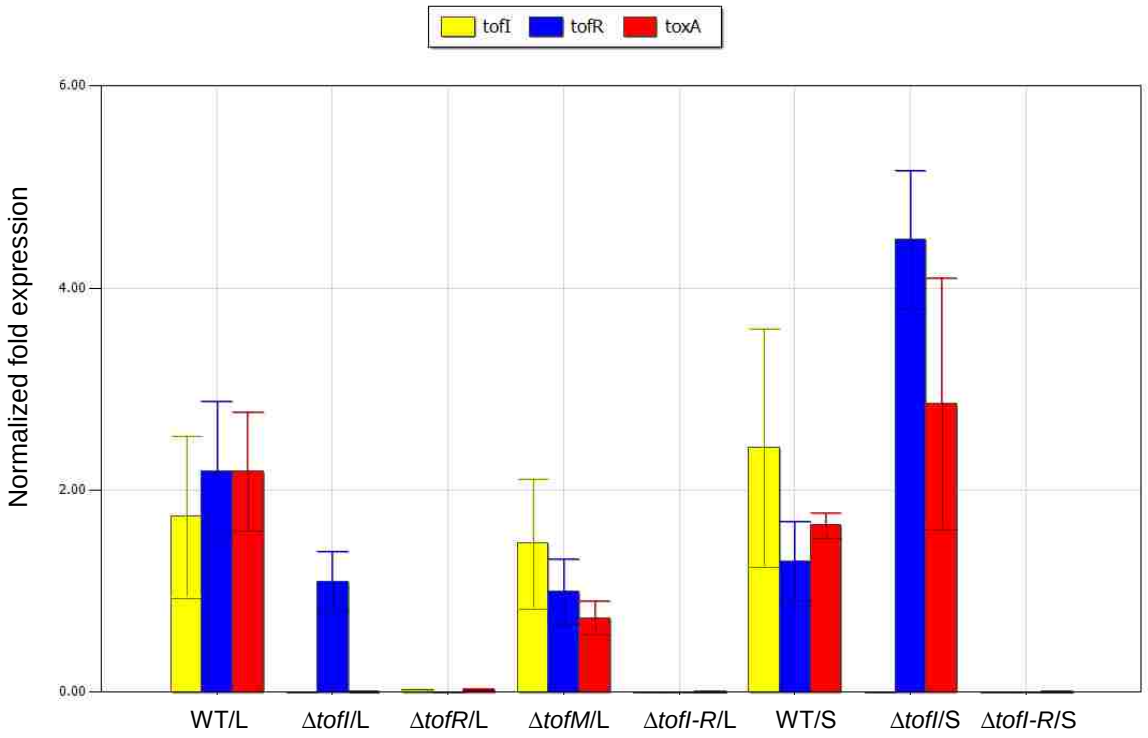

Figure 4.1. The normalized expression of *tofI*, *tofR* and *toxA* in different mutant and media (S= solid medium; L= liquid medium) combinations. The expression of housekeeping gene *gyrA* in all the mentioned backgrounds was set as the baseline to perform the normalization. WT 336gr-1 and deletion mutants LSUPB145 (Δ*tofI*), LSUPB169 (Δ*tofR*), LSUPB286 (Δ*tofM*)and LSUPB139 (Δ*tofI-R*) were incubated in LB broth until culture OD_{600}=1. The total RNAs from each bacterial culture were extracted, purified and reverse transcribed to cDNAs, which were used as the template for q-RT PCR. To investigate the different media types brought to the transcriptional profiles of different strains, the total RNAs of WT, LSUPB145, LSUPB139 grown on LB agar were also obtained with same protocol. The horizontal axis represents every condition that cDNAs were generated from; the vertical bar represents the normalized expression level of each gene. The error bar represents the standard error. The yellow bar indicates expression fold of *tofI,* the blue bar indicates expression fold of *tofR,* and the red bar indicates the expression fold of *toxA.*

The *toxA* gene barely expressed in LSUPB145 (Δ*tofI*) and LSUPB169 (Δ*tofR*), and reduced expression levels were observed in LSUPB286 (Δ*tofM*) (Figure 4.1). None

of the genes expressed in LSUPB139 (Δ*tofI-R*) in both liquid and solid conditions (Figure 4.1). Deletion of *tofR* aborted the expression of *tofI,* but not vice versa (Figure 4.1). It was obvious that liquid and solid media induced different transcription profiles, for example, the expression of *tofR* and *toxA* genes was accelerated in Δ*tofI* background on LB agar, which also matched the observation of culture morphology (Figure 4.1). One important finding in this experiment was that the expression of *tofR* was significantly reduced in the *tofM* deletion background (Figure 4.1).

4.3.2 Comparative transcriptomics of 336gr-1 and QS mutants

To explore the QS regulatory network genome-wide, the transcriptome of 336gr-1 and LSUPB134 (Δ*tofI-R*) were extracted and RNA-sequencing was conducted to investigate the regulons of the *tofI-R* QS system. DNASTAR and Rockhopper were both used to perform sequence assembly and evaluate the quality of the sequencing data and it was found that the median coverage of the total reads towards the genome sequences were less than 40% (Table 4.3), which was not high enough to generate accurate conclusions. Meanwhile, another RNA-seq project done for *B. glumae* BGR1 strain was made available to the public on Gene Expression Omnibus, NCBI (Goo et al., 2012). RNA samples obtained from bacterial cultures of strains BGR1, BGS2 (BGR1 *tofI*::Ω) and BGS9 (BGR1 *qsmR*::Ω) were incubated at LB broth for 6 h (exponential phase) and 10 h (stationary phase) (Goo et al., 2012). Rockhopper tested those data and reported much higher coverage (Table 4.3). Therefore, this set of data was used as a comparison for the data generated from 336gr-1 in our laboratory.

Table 4.3. Alignment rate of RNA-seq reads to the genome sequence.

Coverage reported from the sequencing of different transcriptome	Chromosome 1	Chromosome 2	Plasmid 1	Plasmid 2	Plasmid 3	Plasmid 4
Template coverage for 336gr-1	73.4%	62.5%	26.4%	48.5%	47.7%	18.5%
Median coverage for 336gr-1	39.2%	29.8%	10.6%	3.8%	3.9%	8.0%
Template coverage for BGR1	97.0%	95.5%	99.6%	99.3%	95.5%	95.3%
Median coverage for BGR1	178.2%	99.8%	68.6%	72.8%	41.6%	94.5%

* The data were generated by DNASTAR. 336gr-1 and BGR1 are the virulent isolates of *B. glumae* from the U.S. and Korea respectively. Template coverage means the percentage of the reference sequence that has at least one sequence covered with alignment. Median coverage means the median depth of coverage across the entire reference sequence.

4.3.3 The differently expressed genes were widely distributed in the genome

Rockhopper and DNASTAR were both used to identify the transcriptomic change in the different conditions. Rockhopper recorded the significantly differential expression (q value < 0.01) through the transcription profile (Appendix 1), and the amount of genes that changed expression levels through the experimental conditions (Table 4.4). Negative binomial distribution was used to model the RNA-seq data, and q value was reported as the false rate in the statistic test (McClure et al., 2013).173 genes including the predicted noncoding RNAs showed significantly differential expression (q<0.01) (q value is the adjusted p value) between 336gr-1 (wild type) and LSUPB139 (Δ*tofI-R* mutant). The 173 genes were comprised of 42 *tofI-R* down-regulated genes and 131 *tofI-R* up-regulated genes. Among the entire potential regulon of QS, more genes were

up-regulated. The total numbers of differently expressed genes in 336gr-1 and BGR1 data were similar. *tofI, tofR* and *tofM* shut down their expression in LSUPB134, and the expression of toxoflavin genes decreased to near zero in LSUPB134. This result revealed the reliability of RNA-seq data. The homologs of ferredoxin and AraC family protein genes selected from random mutagenesis as the potential regulon of C8-HSL were also found differently expressed in 336gr-1 and LSUPB134.

Counting the genes that had log fold changes higher than 2, there were more candidates that fit the criteria (Table 4.5). To estimate and visualize the amount of genes that were up- or down-regulated at least 2-fold in different pairs of condition, DNASTAR was used to generate a scatter plot (Figure 4.2). From the observation of the scatter plots, it can be said that most of the selected genes in 336gr-1 tended to be expressed higher than in LSUPB139 (Figure 4.2A).The transcriptome profile changed in BGR1 as growth time increased (Figure 4.2B). Disruption of *tofI* caused increase or reduction in expression of a large amount of genes at 6 h and 10 h (Figure 4.2C,D).

Table 4.4. The number of differently expressed coding genes (q value<0.01) in different amplicons of *B. glumae*

Transcriptome	Chromosome 1	Chromosome 2	Plasmid 1	Plasmid 2	Plasmid 3	Plasmid 4
336gr-1 vs LSUPB134	52	45	8	16	2	2
BGR1 vs BGS2 vs BGS9	65	64	7	3	2	2

* The data were generated by Rockhopper. 336gr-1 and BGR1 are the virulent isolates of *B. glumae* from the U.S. and Korea respectively. LSUPB134 (Δ*tofI-R*), BGS2 (BGR1 *tofI*::Ω) and BGS9 (BGR1 *qsmR*::Ω) are the mutant strains.

Table 4.5. The number of differently expressed genes in *B. glumae* with 2-fold change or greater (reduced or increased) in pairwise value comparisons through the genetic or growth conditions

comparison of strains/growth conditions	Number of genes with fold change >2	Number of genes with fold change > 4	Number of genes with fold change >8
336gr-1 vs LSUPB134	1428	585	387
BGR1 6h growth vs BGR1 10h growth	2915	1067	405
BGS2 6h growth vs BGS2 10h growth	2198	614	207
BGS9 6h growth vs BGS9 10h growth	1991	498	190
BGR1 6h growth vs BGS2 6h growth	1263	325	146
BGR1 6h growth vs BGS9 6h growth	867	207	92
BGR1 10h growth vs BGS2 10h growth	2389	712	274
BGR1 10h growth vs BGS9 10h growth	2076	507	209

* The data were generated by DNASTAR. Strains BGR1, BGS2 (BGR1 *tofI*::Ω) and BGS9 (BGR1 *qsmR*::Ω). 336gr-1 and BGR1 are the virulent isolates of *B. glumae* from the U.S. and Korea respectively. LSUPB134 (Δ*tofI-R*), BGS2 (BGR1 *tofI*::Ω) and BGS9 (BGR1 *qsmR*::Ω) are the mutant strains.

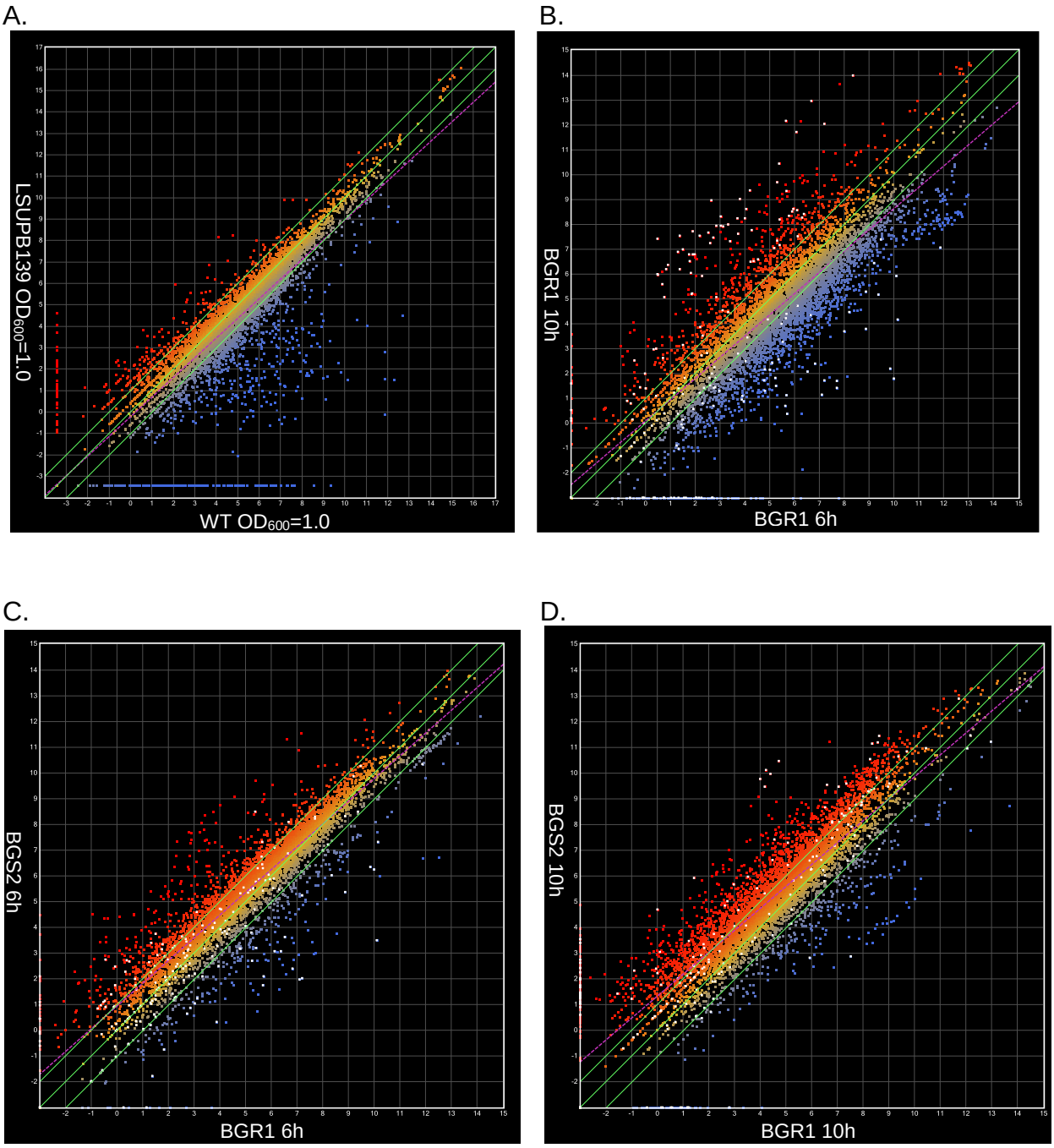

Figure 4.2. Scatter plot of the genes with expression levels changed more than 2-fold (log_2) between pairwise conditions. A, X axis: 336gr-1 transcriptome extracted at culture OD_{600}=1.0, Y axis: LSUPB134 transcriptome extracted at culture OD_{600}=1.0. B. X axis: BGR1 transcriptome extracted from culture grown for 6 h, Y axis: LSUPB134 transcriptome extracted from culture grown for 10 h. C. X axis: BGS2 transcriptome extracted from culture grown for 6 h, Y axis: BGS2 transcriptome extracted from culture grown for 10 h. D. X axis: BGS9 transcriptome extracted from culture grown for 6 h, Y axis: BGS9 transcriptome extracted from culture grown for 10 h.

4.3.4 Hierarchical clustering-heat map was generated

The genes with decreased or increased expression values of more than 8-fold between LSUPB134 and 336gr-1 were clustered and displayed in the form of a heat map (Appendices 2 and 3). Gene (bglu_2g05850) encoding FAD/FMN-binding oxidoreductase was found up-regulated by QS, which was the same result obtained from random mutagenesis in Chapter 3. The gene (bglu_1g07570) encoding urease subunit gamma was found up-regulated by QS. The gene (bglu_1g07550) encoding urease alpha subunit was found up-regulated by QS through random mutagenesis. Thus, it is possible that urease synthesis genes are regulons of QS. Some interesting genes were found from up-regulaton groups like un-characterized LuxR type regulator genes, the 3-hydroxydecanoyl-acyl carrier protein (ACP) dehydratase gene, the thioesterase superfamily protein gene and *mazE/mazF, usp* genes (Appendix 2). ABC transporter and AraC type regulators genes were found both in up-regulon and down-regulon groups (Appendices 2 and 3).

Heat map revealed two clustered gene groups that might contribute to unknown signaling pathway in 336gr-1. The gene (bglu_1g16760) encoding thioesterase superfamily protein and gene encoding 3-hydroxydecanoyl-ACP (bglu_1g16770) dehydratase were clustered together (Figure 4.3A). Those two genes possibly express in same signaling pathway. Multiple *reb* genes (bglu_2g16660, bglu_2g16670, bglu_2g1670 and bglu_2g16700) were clustered close together (Figure 4.3B). These four genes possibly express in same signaling pathway.

A.

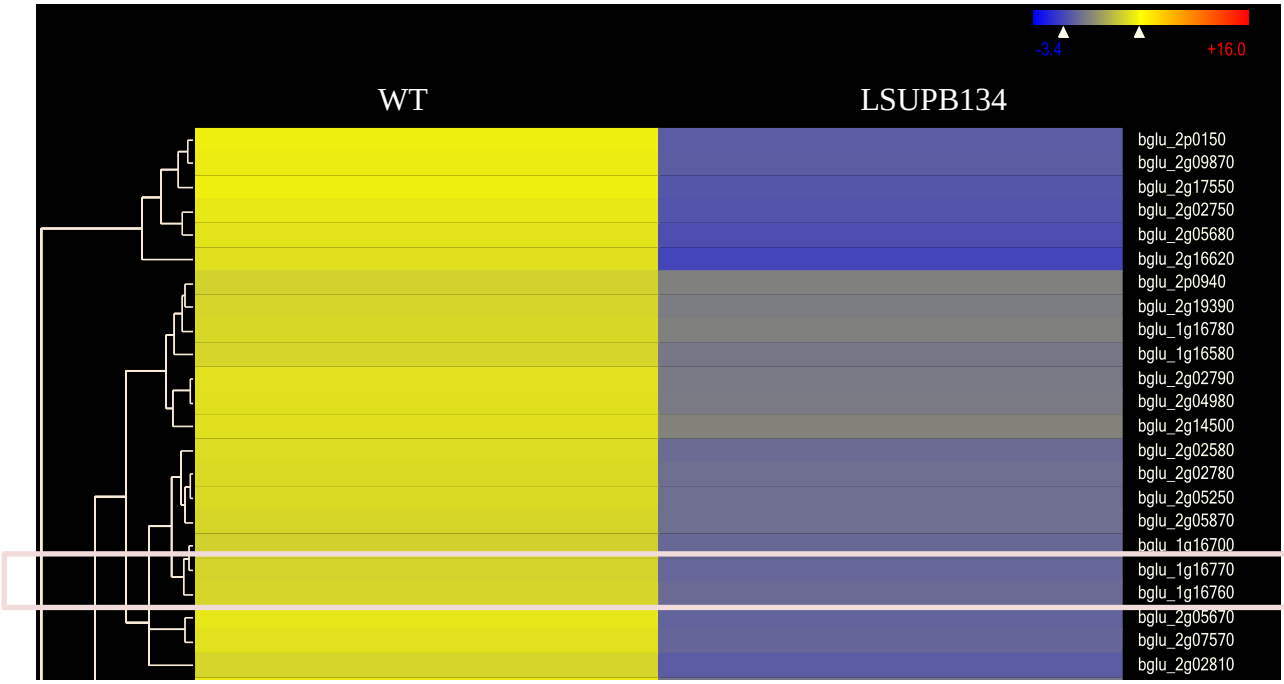

B.

Figure 4.3. Heat Maps generated by ArrayStar to display the level of gene expression by extension of the color. On the color scale, red represented high expression, yellow represented intermediate expression and blue represented low expression of genes. Each row represented an individual gene that was up-regulated by QS. Genes were clustered according to the similarity. The left column represented the transcriptome in 336gr-1, and the right column represented the transcriptome in LSUPB134. A. Acyl carrier protein (ACP) hydratase and thioesterase super family protein genes were clustered next to each other (in the pink rectangle) B. Multiple *reb* genes and *tofR* gene were clustered close together on the heat map (in the pink rectangle).

4.3.5 Most of the genes in *B. glumae* exist in operons

It is very common for bacterial genes to stay in polycistronic arrangement, but the current annotation in genome sequence databases does not indicate the boundaries of the bacterial operons. Operon prediction of *B. glumae* was performed using RNA-seq data of BGR1 derivatives. The result was shown in Table 4.6, which demonstrated that more than 50% genes were located and expressed in operons in two *B. glumae* strains.

Table 4.6A. Summary of predicted operon distribution throughout the *B. glumae* genome based on sequencing information generated from 336gr-1 derivatives.

B. glumae replicons	Chromosome 1	Chromosome 2	Plasmid 1	Plasmid 2	Plasmid 3	Plasmid 4
Number of predicted operons	642	349	27	20	21	22
Number of genes transcribed in putative operons	1923	1049	61	60	62	75
Total gene number	3495	2289	145	121	142	114

Table 4.6B. Summary of predicted operon distribution throughout the *B. glumae* genome based on sequencing information generated from BGR1 derivatives.

B. glumae replicons	Chromosome 1	Chromosome 2	Plasmid 1	Plasmid 2	Plasmid 3	Plasmid 4
Number of predicted operons	647	351	27	20	22	21
Number of genes transcribed in putative operons	1960	1072	62	62	68	77
Total gene number	3495	2289	145	121	142	114

4.3.6 Substantial amount of intergenic RNAs and antisense RNAs were found in the *B. glumae* genome

Another use of transcriptome analysis is to uncover novel RNAs, such as intergenic RNAs and antisense RNAs, which perform regulatory functions for some important traits of bacteria. Table 4.5 summarizes the entire putative novel RNAs in both 336gr-1 and BGR1, which is a useful addition to the genome database. Fifty-three of these show significantly differential expression in 336gr-1 and LSUPB134. Additionally, more non-coding novel RNAs were predicted in 336gr-1 than BGR1, especially on chromosomes 1 and 2 (Table 4.7). On the other hand, BGR1 had more noncoding RNAs on plasmids (Table 4.7).

Table 4.7. Summary of predicted non-coding RNAs throughout the *B. glumae* genome based on sequencing information generated from 336gr-1 and BGR1 derivatives.

B. glumae replicons	Chro_1	Chro_2	Pla_1	Pla_2	Pla_3	Pla_4
Number of noncoding RNAs from 336gr-1 derivative transcriptome	576 (not antisense) 245 (antisense)	315 (not antisense) 96 (antisense)	22 (not antisense) 4 (antisense)	10 (not antisense) 3 (antisense)	12 (not antisense) 2 (antisense)	2 (not antisense) 2 (antisense)
Number of noncoding RNAs from BGR1 derivative transcriptome	48 (not antisense) 325 (antisense)	2 (not antisense) 66 (antisense)	123 (not antisense) 94 (antisense)	57 (not antisense) 177 (antisense)	102 (not antisense) 97 (antisense)	46 (not antisense) 77 (antisense)

4.3.7 Many 5’ UTRs were observed in the *B. glumae* genome

Rockhopper was used to predict the UTRs (lengths varied from 1 *bp* to hundreds *bp*) based on the transcriptome from both 336gr-1 and BGR1 derivatives. After computing and estimating the continuous transcript reads of the 5’ of coding regions through the genomes, more than 1000 5’ UTRs were predicted from 336gr-1 and

around 500 5’ UTRs were predicted from BGR1 (Table 4.8). And, many potentially QS dependent genes were found having 5’ UTRs, which was a hint of regulatory element candidates.

Table 4.8. The organization of 5’ UTRs through genomes of 336gr-1 and BGR1

B. glumae replicons	Chro_1	Chro_2	Pla_1	Pla_2	Pla_3	Pla_4
Number of 5’ UTRs predicted from 336gr-1 derivative transcriptome	955	211	2	2	4	2
Number of 5’ UTRs predicted from BGR1 derivative transcriptome	291	75	37	23	27	32

4.3.8 Regulons of QsmR and TofI overlapped

To determine the hierarchy relations between global regulators QsmR and TofI and their regulon, Venn diagrams were generated to represent how much each regulator was involved in transcriptomic changes.

In Figure 4.4, circles A and B represent all the genes that showed differential expression higher than 2-fold between BGR1 and BGS2 at 6 h. 614 genes from the intersection of circle A and B possibly have included the candidates for co-regulon of QsmR and TofI at the exponential phase. It is also possible that QsmR regulator functioned in the downstream of QS for those regulaton. Circle C and D represent all the genes that show differential expression higher than 2-fold between BGR1 and BGS2 at 10 h. 1582 genes from the intersection of circle C and D possibly represent the candidate genes co-regulated by QsmR and TofI at stationary phase. It was obvious that the regulon of both QS and QsmR increased expression at stationary phase comparing to exponential phase. QS still regulated more genes than QsmR, but both of

them should have performed important roles in growth phase adjusting. Additionally, intersection AB is bigger than extra area in circle B, which indicated how most of QsmR's regulon is dependent on QS at exponential phase. This is also the case for stationary phase.

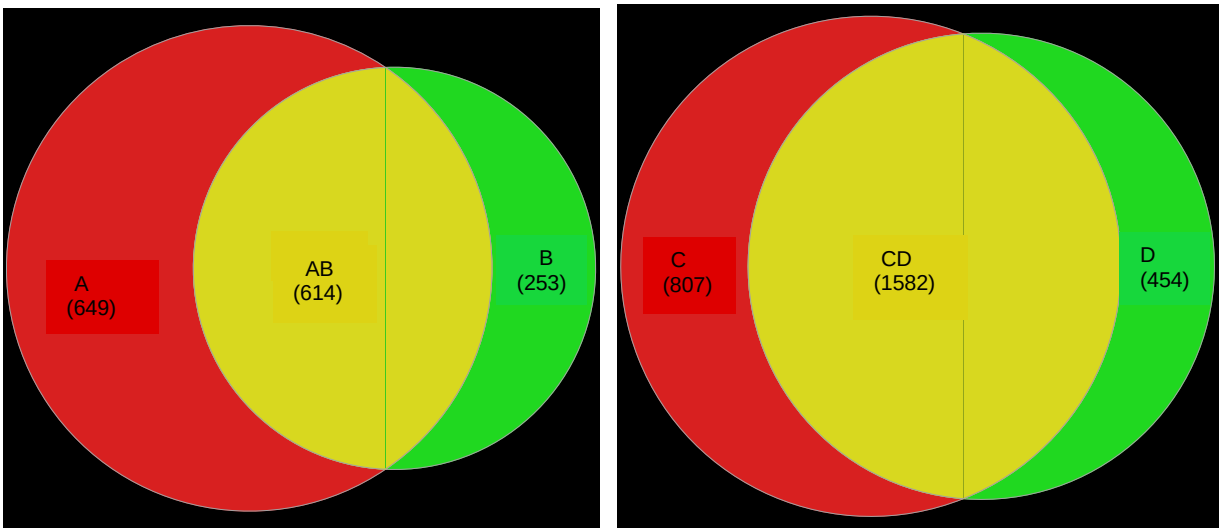

Figure 4.4. Venn diagrams generated by ArrayStar displaying the differently expressed genes (fold change >=2) in individual paired conditions, which are represented by capital letters. The numbers inside parentheses are the amount of genes that were differently expressed in individual pair of conditions. A. Genes with expression fold change higher than 2 between BGR1 6h and BGS2 at 6 h. B. Genes with expression fold change higher than 2 between BGR1 6h and BGS9 at 6 h. C. Genes with expression fold change higher than 2 between BGR1 at 1 0h and BGS2 10h. D. Genes with expression fold change higher than 2 between BGR1 at 10 h and BGS9 at 10 h.

4.4 Discussion

4.4.1 More evidence was found to prove the QS modulator properties of TofM

qPCR was performed with high reliability, and revealed some hierarchical regulation among QS and its regulon. The expression of *tofI* was abolished after the deletion of *tofR*, which agreed with the *tofI*/*tofR* relationship determined in BGR1 (Kim et al., 2004b). To discover the relationship between *tofM* and other QS genes, the

transcriptome of LSUPB286 (Δ*tofM*) was extracted and compared to 336gr-1. The expression of *tofI* and *tofR* was evaluated in both conditions.

Previously, it was reported that *tofM* acted as positive regulator for toxoflavin production and was responsible for *tofI/tofR* independent toxoflavin production (Chen et al., 2012). TofM was conserved among *Burkholderia* and shared 22.4% identity to RsaM, the QS modulator in *Pseudomonas fuscovaginae* (Chen et al., 2012). Though RsaM functions as a the negative regulator for AHL synthase genes of the two QS systems, *pfvI/pfvR* and *pfsI/pfsR* possessed by *P. fuscovaginae* (Mattiuzzo et al., 2011), TofM here was found to up-regulate the expression of *tofR,* the AHL cognate receptor gene. One factor TofM and RsaM had in common was they were required for full virulence expression; the mutation of *tofM* or *rsaM* caused attenuated disease symptoms (Mattiuzzo et al., 2011)

It was observed previously that the *tofI* deletion mutant LSUPB145 produced toxoflavin on solid agar but not liquid media. To investigate the reason for this phenomenon, the transcriptome of 336gr-1, LSUPB145 and LSUPB139 grown in both LB broth and LB agar were extracted, and the expression of *tofI*, *tofR* and *toxA* was measured. Interestingly, *tofR* and *toxA* genes were highly expressed in LSUPB145 (Δ*tofI*) on solid media, which was not the case in liquid media. Therefore, the high expression of *tofR* gene on solid media possibly is one of the factors for the production of toxoflavin on solid media.

4.4.2 Substantial changes were brought to the transcriptional profile due to the deletion of *toI-R* system

Transcriptome analysis was performed on the 336gr-1 and its *⊿tofI-R* derivative LSUPB134 to determine the differently expressed genes, which were the potential QS

regulon. Two criteria were used to select the target genes – statistics test (q value) and fold change. The RNA-seq data of BGR1, BGS2 and BGS9 were also simply analyzed to provide reference information.

From the statistical analysis, 173 genes (42 negatively regulated and 131 positively regulated) were determined potentially regulated by QS in 336gr-1. This is an important addition to the known regulon of QS in *B. glumae.* Based on the fold change, 25% of genomic genes expression changed more than 2-fold, 10% changed more than 4-fold, 8% changed more than 8-fold. The same was observed in the statistic test data, as more genes were up-regulated (data not shown). Therefore, up-regulation appeared to be a more prevalent regulatory role for *tofI-R* in 336gr-1.

4.4.3 Statistics test selected multiple potential QS-dependent signaling components in 336gr-1

Rockhopper used one new algorithm to normalize read counts for each sample by dividing the raw reads copy by the upper quartile gene expression level (McClure et al., 2013). The genes that showed significantly differential expression values ($q<0.01$) were selected by Rockhopper. Among all 173 genes, some were previously described as QS-dependent genes or published as important regulators. The expression levels of *tofI, tofR* and *tofM* were 288 RPKM (reads per kilo base per million mapped sequence reads), 58 RPKM and 114 RPKM in 336gr-1, and they all dropped to zero in LSUPB134. The expression levels of toxoflavin transportation and synthesis operons were hundreds to thousands of RPKM high, and close to zero at LSUPB134. Those results proved the RNA-seq data were reliable.

Compared to random mutagenesis, RNA-seq transcriptome analysis provides QS regulon information more efficiently. There is some overlapping of the data generated

from those two strategies. S-adenosyl-L-homocysteine (SAH) hydrolase (bglu_1g01990), which catalyzes the hydrolysis of SAH (Winzer et al., 2002), showed 1613 RPKM expression in 336gr-1 and 438 RPKM expression in LSUPB134. SAH was also the substrate of tRNA (guanine-N7-)-methyltransferase (bglu_1g07720), which can catalyze the formation of SAH and was previously found to be negatively mediated by C8-HSL in Chapter 3 (Aschhoff et al., 1976; Winzer et al., 2002). It was thought that C8-HSL QS might have repressed the AI-2 (the QS signal that uses SAH for its synthesis) system, and here, the differential expression analysis showed that SAH was possibly down-regulated by QS. Therefore, it is possible that there is some hierarchal relation between two QS systems in *B. glumae.* Another ferredoxin gene (locus bglu_1g16670) showed 100 RPKM expression in 336gr-1 and zero expression in LSUPB134. The upregulation pattern of this gene by QS from RNA-seq is similar to the ferredoxin gene (locus bglu_2g05900) found from random mutagenesis. Therefore, ferredoxin can be another candidate that depends on QS for its production. The third coincidence between the results from two strategies was the finding of the AraC family transcriptional regulator. Again, the loci of encoding genes are different. The one from random mutagenesis data was bglu_2g05820, and the two from RNA-seq data were bglu_1p0370 and bglu_2p0700. The regulation pattern for the former was down-regulation, and for the latter was up-regulation. Even with the difference, this potential regulon still deserves more confirmation and characterization. The last gene that was picked by two genomic methods was diguanylate cyclase gene. The one that showed *tofI*-independent toxoflavin regulator property had locus bglu_1g02180, and the one that

was supposedly up-regulated by QS had locus bglu_1g22970. Future study could focus on confirming which gene was closely regulated by QS in *B. glumae.*

There are many interesting findings from this gene group. The histone-like nucleoid structuring protein (H-NS) (locus bglu_1g01760) was down-regulated from 1298 RPKM to 198 RPKM after deletion of QS in 336gr-1. H-NS has been generally determined as one emerging transcriptional repressor, which can negatively regulate many bacterial physiological traits by binding on the AT-rich region of the promoter regions (Brescia et al., 2004; Silva et al., 2008; Wang et al., 2012). For example, the expression of RpoS sigma factor in *E. coli* was negatively regulated by H-NS; and EPS and biofilm formation in *Vibrio cholera* were repressed by H-NS, which was also QS dependent (Brescia et al., 2004; Svenningsen et al., 2008; Wang et al., 2012). Occasionally, H-NS was found to be a positive regulator for some genetic traits, like the RpoS factor in *E. coli* (Silva et al., 2008). So far, there has been no report about how the H-NS regulator functions in *Burkholderia.* Thus, the study of QS dependent global regulator H-NS would be useful.

Two cold shock-like protein genes and one heat shock protein gene were found differentially expressed in 336gr-1 and LSUPB134. Cold/heat shock proteins are known as the stress, especially low/high temperature responsor. The gene (bglu_1g04140) encoding cold shock-like protein CspD showed 138 RPKM in 336gr-1 and 1733 RPKM in LSUPB134, which indicated that it was down-regulated by QS. Csp family proteins mainly respond to temperature downshift, but CspD protein is stimulated at stationary phase and inhibits DNA replication in *E. coli*; the overprodcuction can be lethal to the bacterial cells (Yamanaka et al., 2001). The gene (bglu_1g08360) encoding cold-shock DNA-binding domain-containing protein showed 4413 RPKM in 336gr-1 and 580 RPKM

in LSUPB134, which meant it was up-regulated by QS. The gene encoding heat shock protein Hsp20 showed 816 RPKM and 130 RPKM expression in 336gr-1 and LSUPB134 respectively, which indicated the gene was up-regulated by QS. Hsp20 proteins were found in plants including rice, nine Hsp genes were found up-regulated at heat shock condition in rice (Ouyang et al., 2009). This report just unveiled the relationship between cold/heat shock stress-stimulated genes and QS, and more findings are expected in this area.

Four ATP-binding cassette (ABC) transporter genes (bglu_1g18030, bglu_1g18040, bglu_1g18050 and bglu_1g18060) were found up-regulated after the deletion of *tofI-R,* which suggested that those genes were down-regulated by QS in 336gr-1. Coincidently, genes with loci bglu_1g18010, bglu_1g18020, bglu_1g18030, bglu_1g18040 and bglu_1g18050 were also predicted as transcribed in a polycistronic manner. The ABC transporter has been known as an autoinducer sensor and secretion channel of QS systems in Gram-positive bacteria (Dirix et al., 2004; Knutsen et al., 2004; Kotake et al., 2008). ABC transporter genes are also regulated by QS in a few Gram negative bacteria. Recently, ABC transporter genes were identified as the overlapped regulon of AHL and BDSF QS in *B. cenocepacia* (Knutsen et al., 2004). Since the ABC transporter is critical for many important bacterial activities including nutrient uptake, colonization and toxicity (Davidson and Chen, 2004), the study about this group of genes could be very influential.

The genes encoding (bglu_2g00530) cyclic adenosine monophosphate (cAMP) receptor protein (CRP)/fumarate and nitrate reduction regulatory protein (FNR) family transcriptional regulator showed 54 RPKM expression in 336gr-1 and 258 RPKM in

LSUPB134, which suggested that the gene is down-regulated by QS in *B. glumae.* The DNA binding site of CRP regulator can be activated by cAMP to bind on the promoter of certain genes; the F-S binding motif of FNR can sense the density of oxygen and activate the FNR regulator to promote the expression of regulon (Matsui et al., 2013). There is a large collection of genes in bacteria determined as the regulon of CRP/FNR family regulator; and they are generally involved in the environmental accommodation process (Matsui et al., 2013). Some research groups have investigated the relationship between QS and CRP regulator. Vfr protein, a homolog of CRP in *E. coli,* was reported as a QS controller by binding the consensus sequence in promoter region of *lasR* gene in *P. aeruginosa* (Albus et al., 1997). CRP was proven to be the upregulator of the *hapR* gene encoding the cholera autoinducer 1 (CAI-1) receptor and is important for the survival of this pathogenic bacterium *Vibrio cholerae* in its host (Liang et al., 2007). Few publications have described the possible relationship between CRP/FNR regulator and *tofI-R* QS system in *B. glumae.* Therefore, further characterization about bglu_2g00530 can be valuable.

4.4.4 An additional potential QS regulon was discovered from fold change selection in 336gr-1

Previously, it was discussed that 173 genes were significantly ($q<0.01$) expressed between 336gr-1 and LSUPB134. q value is a better criterion to determine the differential expression values from RNA-seq data when there are enough replicates. Since the RNA sample was short of biological replicates, fold change should also be considered to identify the genes differently expressed among the genetic conditions. Therefore, genes with changed expression levels higher than 8-fold between 336gr-1 and LSUPB134 were hierarchically clustered and displayed in heat maps. 344 QS up-

regulated genes and 43 down-regulated genes were shown in Appendix 2 and 3, respectively. There is a large portion of overlapping between the gene collections that were built based on two criteria, but there are also some other genes that were picked based on expression fold change.

Two UspA domain containing genes (bglu_2g20370 and bglu_2g20280) were found up-regulated by QS. A gene with locus bglu_2g20280 was renamed usp9 from one recent publication, and gene with locus bglu_2g20370 was renamed usp10 (Kim et al., 2012). The expression of those two genes were influenced by QsmR and QS in *B. glumae* (Kim et al., 2012). Our finding agreed with this recent report. Universal stress proteins (*usp)* were first described in *E. coli* as the starvation and toxic agents responsive elements (Nystrom and Neidhardt, 1992). Two different temperature stress genes *usp1* and *usp2* were described in *B. glumae* as protective genes for the heat shock, and without them the mutants died 1 hour after heat shock; additionally, *usp1* was up-regulated in cold shock (Kim et al., 2012). Usp1 and Usp2 all contained a conserved UspA domain (Kim et al., 2012). No specific study on the function or mechanism of Usp9 and Usp10 has been done to date.

Two orphan LuxR type regulators, bglu_1g16610 and bglu_1g17030, were up-regulated by QS. It is not unusual to see bacteria possess orphan LuxR proteins, which do not pair with cognate AHL synthase. Orphan LuxR proteins have diverse functions including binding to endogenous or foreign AHLs, regulating virulence factors, nutrition uptake and antibiotic production (Subramoni and Venturi, 2009). In *Burkholderia,* there are a few reports about orphan LuxR type proteins. In *B. cenocepacia,* one orphan LuxR regulator, Cep2, was negatively regulated by another QS system CciI/R (Malott et

al., 2009). Cep2 also regulated the expression the siderophore pyochelin (Malott et al., 2005). Orphan LuxR homolog BpsR5 in *B. pseudomallei* showed partial regulation to bpsR1 (Choudhary et al., 2013). Orphan LuxR proteins BmaR4 and BmaR5 in *B. mallei* were not characterized (Choudhary et al., 2013). Our result showed that *B. glumae* might also own functional orphan LuxR type to maximize the efficiency of AHL and QS network.

The gene (bglu_1p0470) encoding MazF and the gene (bglu_1p0480) encoding MazE were found up-regulated by QS. MazF/MazE is one type of toxin-antitoxin module used by bacteria to perform programed cell death (PCD) (Engelberg-Kulka et al., 2006). MazF is the stable toxin, and MazE is the labile antitoxin that can inhibit the lethal function of MazF (Engelberg-Kulka et al., 2006). In *E. coli,* the action of *mazF/mazE* can be triggered by several stressful conditions (Engelberg-Kulka et al., 2006). QS factor EDF can directly enhance the endoribonucleolytic activity of MazF and overpower the inhibitory effect of MazE over MazF (Belitsky et al., 2011). Unlike the chromosomal *mazF/mazE* gene pair in *E. coli*, *mazF/mazE* in *B. glumae* is located on plasmid 1. However, many other bacteria also have extrachromosomal toxin-antitoxin modules, which will cause PCD due to loss of plasmids (Engelberg-Kulka et al., 2006). *mazF/mazE* in *B. glumae* might also have this property.

AraC regulator and ABC transporter genes were observed from both up- and down-regulated group. There is not an obvious genomic location preference for the regulation mode among all those genes, but shows the complexity of QS in *B. glumae.*

4.4.5 Hierarchical clustering-heat maps uncovered potential QS regulated pathways: BDSF analog signaling and R-body formation

Heat maps were generated to display the genes that might have shared the same regulation pathway. The genes with similar expression patterns were clustered close together, which was indicative of the possibility that they were regulated by the same upstream regulators (Severin et al., 2010).

The gene (bglu_1g16760) encoding thioesterase superfamily protein and gene (bglu_1g16770) having 3-hydroxydecanoyl-acyl carrier protein (ACP) dehydratase domains were clustered together (Figure 4.4B). Therefore, there was a possibility that two enzymes were involved in the same signaling pathway controlled by QS. Bcam0581 was recently discovered as the synthase for QS signal cis-2-dodecenoic acid (BDSF) in *B. cenocepacia* (Bi et al., 2012). This enzyme, which was renamed $RpfF_{Bc}$, is the homologue of crotonase family protein, but uniquely it performed bi-function 3-hydroxydodecanoyl-ACP dehydratase and thioesterase activities to generate BDSF from fatty acid synthetic intermediate (Bi et al., 2012; Schmid et al., 2012). From the operon prediction, thioeasterase and 3-hydroxydecanoyl ACP dehydratase genes were potentially transcribed in a polycistronic manner. It is possible that thioeasterase and 3-hydroxydecanoyl ACP dehydratase are co-translated to synthesize BDSF analog (with two fewer carbons than BDSF) the in *B. glumae*. As it was previously described, AI-2 also possibly exists in *B. glumae.* Therefore, the QS systems in 336gr-1 might utilize three types of signals; AHL, AI-2 and BDSF analog.

Four *reb* genes (*rebB* bglu_2g16660, *rebA* bglu_2g16670, *rebB* bglu_2g16710 and *rebB* bglu_2g16700) were clustered together (Figure 4.4B). (Raymann et al., 2013). RebB and RebA are required to form R-bodies, which are produced by obligate

bacterial endo-symbionts of *Paramecium* (Raymann et al., 2013). The R-bodies containing bacteria can turn their host to “killers” against other sensitive *Paramecium* strains, and this phenotype is possibly regulated by QS (Raymann et al., 2013). Reb homologs are distributed in many plant pathogens including *B. glumae* and *B. gladioli*, but their functions are not characterized (Raymann et al., 2013). It is possible that R-bodies also perform some QS-dependent functions in 336gr-1 to interact with the plant hosts.

4.4.6 Non-coding RNAs possibly play important roles in 336gr-1 as novel regulatory elements

5’ UTRs in bacteria usually have length less than 30 bp, and those with long length possibly function as regulatory fragments (Sorek and Cossart, 2010). More than 1,000 5’ UTRs were determined from transcriptome analysis of 336gr-1 by Rockhopper comparing to 500 5’ UTRs in BGR1, which revealed more complexity in the 336gr-1 transcriptome. The study of 5’ UTRs suggests they may also contribute to signaling in 336gr-1.

From the significantly expressed gene collection (q value < 0.01) between 336gr-1 and LSUPB134, there was one 75 *bp* long 5’ UTR continuous to the transcription region of H-NS (locus bglu_1g01760), which implied the existing of a regulator binding motif (no binding motif was found from current protein domain database yet).There were two 5’ UTRs found in front of bglu_1g04140 (cold shock-like protein CspD gene) and bglu_1g08360 (cold-shock DNA-binding domain-containing protein gene) with length more than 100 *bp* (Appendix 1). Those 5’ UTRs maybe involved in the post-transcriptional regulation, which was also dependent on QS in 336gr-1. The 5’ UTR of differently expressed genes are also good candidates of riboswitches. Riboswitches are

the 5’ UTR binding region for regulatory molecule on mRNA and are normally 100-200 bp in length (Kazanov et al., 2007; Sorek and Cossart, 2010). Their structures change due to the binding and inhibit the transcription of the downstream gene (Sorek and Cossart, 2010). So far, none of the 5’ UTRs of the differently expressed genes was found with high similarity to the published riboswitch sequence.

Noncoding RNAs (ncRNAs) are located in the intergenic region and many of them have regulatory functions; in bacteria, they are usually denoted as small RNAs (sRNAs) (Tjaden et al., 2006). From all of the identified ncRNAs, regulatory ncRNAs seemed to be most abundant (Tjaden et al., 2006). As one special case of ncRNAs, antisense RNAs (asRNAs) mentioned here are denoted to the cis-antisense RNAs that are complementary to part of the coding region mRNA (Georg and Hess, 2011). The importance of regulatory ncRNAs and their corresponding research are quickly emerging. In *Burkholderia,* a number of sRNAs in human pathogen *B. cenocepacia* have been characterized. For example, global regulator MtvR and *hfp* negative regulator *h2cR* in *B. cenocepacia* (Ramos et al., 2012; Ramos et al., 2013). But reports of sRNA in other *Burkholderia* species are rare. Around 1300 ncRNAs including 300 asRNAs were predicted through the transcriptome analysis of 336gr-1 and LSUPB134. This result was generated by software, and manual selection is required for their confirmation and future study. A similar amount of ncRNAs including 900 antisense RNAs were found from BGR1. The distributions of the ncRNAs among amplicons in 336gr-1 and BGR1 were also different; 336gr-1 had more on two chromosomes whereas BGR1 had more on the plasmids. The vast difference in transcriptome and regulation profile between two *B. glumae* strains was again presented. It was previously

published that at least 11.6% of its DNA sequence was unique to 336gr-1 genome compared to BGR1 (Francis et al., 2013). This is part of the reason for the immense difference between the transcriptome of those two strains. 53 ncRNAs including 18 asRNAs were found differently expressed in two genetic backgrounds, which is a sign of the correlation between QS and small RNA regulation in *B. glumae.* Two ncRNAs were found complementary with the *tofM* gene, and their expression was shut down at QS deletion background (Figure 4.6). This finding showed the possibility that those two ncRNAs acted as the antisense regulatory RNAs of *tofM*, or they were transcribed from novel genes.

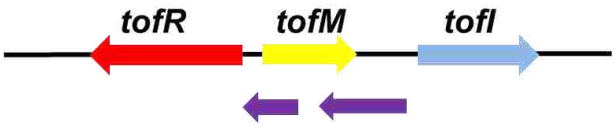

Figure 4.6. The location of antisense RNAs to *tofM* gene. Two asRNAs were found transcribed in the opposite direction with *tofM* on negative strain, and their transcripts overlap the coding region of *tofM.*

4.4.7 QS, QsmR and growth phase influence the transcriptional profile of *B. glumae*

Around 25% of genes changed their expression more than 2-fold between 336gr-1 and LSUPB134. Twenty-two and 41% of the genes changed expression more than 2-fold between BGR1 and BGS2 at 6 h and 10 h, respectively. Therefore, QS is clearly one global regulator of the *B. glumae* genome. It is reasonable that more *tofI*-dependent genes were found at 10 than 6 h because 6 and10 h were considered as before and after onset of QS (Goo et al., 2012). Before and after the onset of QS, BGR1, BGS2 and BGS9 all have 2000-3000 genes that changed expression level more than 2-fold, which again proved the dynamic property of bacterial transcriptome. Fifteen and 36% of the genes changed expression more than 2-fold between BGR1 and BGS9 at 6 and 10

h, respectively. With these data, it is also fair to claim that QsmR is a global regulator in *B. glume.*

The scatter plot was also generated to visualize the extent of the change in transcriptional profiles among different conditions. It showed a large portion of dots (representing genes) scattered from diagonal lines through all the pairwise comparisons. Moreover, just by observation from the scatter plot, it is also obvious that QS is positive regulator for most of its regulon in 336gr-1 (Figure 4.4A).

CHAPTER 5. TRANSCRIPTOME ANALYSIS OF QUORUM SENSING REGULATION IN *BURKHOLDERIA GLUMAE* DIFFERENT MEDIUM CONDITIONS BY TRANSCRIPTOME ANALYSIS

5.1 Introduction

Previously, LSUPB145 (Δ*tofI* mutant) was observed to exhibit different morphology in Luria-Bertani (LB) broth and LB agar (Chen et al., 2012). The streaked cultures on solid media produced toxoflavin, whereas the cultures grown in liquid media did not (Chen et al., 2012). Another experiment was done to demonstrate this difference. The same overnight culture of LSUPB145 was used as an inoculum for LB broth and LB agar media. At the estimated quorum point, the liquid cultures did not produce toxoflavin, but the spot cultures on LB agar produced similar levels of toxoflavin compared to the wild type strain 336gr-1. From this result, we suspected that *B. glumae* expressed very different gene profiles growing in different media conditions.

It is common for bacteria to change their transcriptomes in different environments to increase adaptability and quorum sensing (QS) often plays an important role in the environmental adaption process (Moreno-Paz et al., 2010; Wagner et al., 2004; Wang et al., 2013). Recently, it was reported that QS is required for the stationary phase adaption of *B. glumae* strain BGR1 (Kim et al., 2012). However, *B. glumae* gene expression in different medium conditions is still not known. In this Chapter, the comparative transcriptome analysis was performed to determine the effect of the medium condition on the transcriptional profile of *B. gluame*. The difference of the transcriptional profiles of the wild type and QS mutant strains of *B. glumae* strain 336gr-1 in both liquid- and solid-medium conditions was determined. This can provide reference information regarding the role of QS in bacterial adaption of *Burkholderia* species in natural environments.

5.2 Materials and Methods

5.2.1 RNA-sequencing sample preparation

Total RNAs from two biological replicates of 336gr-1, LSUPB145 (Δ*tofI*) and LSUPB139 (Δ*tofI-R*) grown in LB broth and LB agar were harvested as described in 4.2.4 in Chapter 4. Later, residual DNAs from all of the 12 samples were removed by DNA-free™ DNase Treatment and Removal Reagents (Life Technologies, Grand Island, NY, USA). The removal effect was confirmed by PCR, and no DNA was detected.

5.2.2 Next generation sequencing and data analysis

More than 3 µg RNAs from each of the 12 samples were shipped to Genomics Core Facility of the Johns Hopkins University (Baltimore, MD, USA) for cDNA library preparation and RNA-seq. Briefly, Ribo-Zero™ Magnetic reagents kit (Illumina, San Diego, California, USA) was used to remove 16S, 23S and 5S rRNAs from 1 µg of each RNA sample. rRNAs-depleted samples were then purified by Agencourt Ampure XP reagent (Beckman Coulter, Beverly, Massachusetts, USA). Purified samples were then subjected to RNA-seq libraries synthesis using the ScriptSeq™ Complete Kit (Bacteria) (Illumina, San Diego, California, USA). The final purification for generated libraries was done using Agencourt Ampure XP reagent (Beckman Coulter, Beverly, Massachusetts, USA). DNA 1000 kit and Agilent High Sensitivity DNA Kit (Agilent Technologies, Santa Clara, CA, USA) was used to evaluate the quality of RNA-seq libraries on a BioAnalyzer (Agilent Technologies, Santa Clara, CA, USA).

Illumina paired-end RNA-seq was performed with the qualified libraries. The length of the reads was100 *bp,* and the insert size was 200~300 *bp.* DNASTAR software (DNASTAR, Inc. Madison, WI, USA) was used to analyze the RNA-seq data.

5.3 Results

5.3.1 High coverage RNA-seq data were generated

To explore the QS regulatory network under different media conditions, the transcriptomes of 336gr-1, LSUPB145 and LSUPB139 were extracted and RNA-seq was performed. The assembly showed reasonably high coverage of the reads over the reference genome sequence (chromosome 1 and 2, plasmid 1, 2, 3 and 4) of *B. glumae* strain BGR1 (Table 5.1). The template coverage showed most of the reads aligned to the reference genome. Median coverage was multiple times higher than the reference sequence, which indicated the reliability of the transcriptome data.

Table 5.1. Alignment rate of RNA-seq reads to the genome sequence.

Coverage	Chromosome 1	Chromosome 2	Plasmid 1	Plasmid 2	Plasmid 3	Plasmid 4
Template coverage	87.0%	98.0%	77.0%	82.0%	53.0%	43.0%
Median coverage	1623.0%	700.2%	1023.99%	546.3%	787.8%	454.0%

* The data were generated by DNASTAR.

5.3.2 Media condition affected the QS-dependent transcriptional profile

The number of genes that changed expression rate more than 2, 4 and 8-fold between liquid and solid media conditions is reported in Table 5.2. Media condition caused 17.4% ~ 24.0% genomic genes of all three sampled strains changing expression higher than two folds. To visualize the difference between conditional transcriptomes, the DNASTAR was used to generate the results shown in Figure 5.1. From the scatter plots, it can be said that the all three strains 336gr-1, LSUPB145 and LSUPB139 tended to express higher on the solid-medium condition than in the liquid-medium condition (Figure 5.1ABC). Compared to the other two strains, LSUPB145 showed highest number of differently expressed genes between solid- and liquid-

medium conditions (Figure 5.1B), while the wild type 336gr-1 showed lowest level of change (Figure 5.1A).

Table 5.2. Number of differently expressed genes in *B. glumae* wild type, 336gr-1, and two mutants, LSUPB145 (*⊿tofI*) and LSUPB139 (*⊿tofI-R*), transcriptomes between solid- and liquid-medium conditions.

Medium comparison of different strains	The number of genes with fold change>2	The number of genes with fold change>4	The number of genes with fold change>8
Liquid 336gr-1 x solid 336gr-1	1006	276	90
Liquid LSUPB145 x solid LSUPB145	1384	478	241
Liquid LSUPB139 x solid LSUPB139	1044	330	129

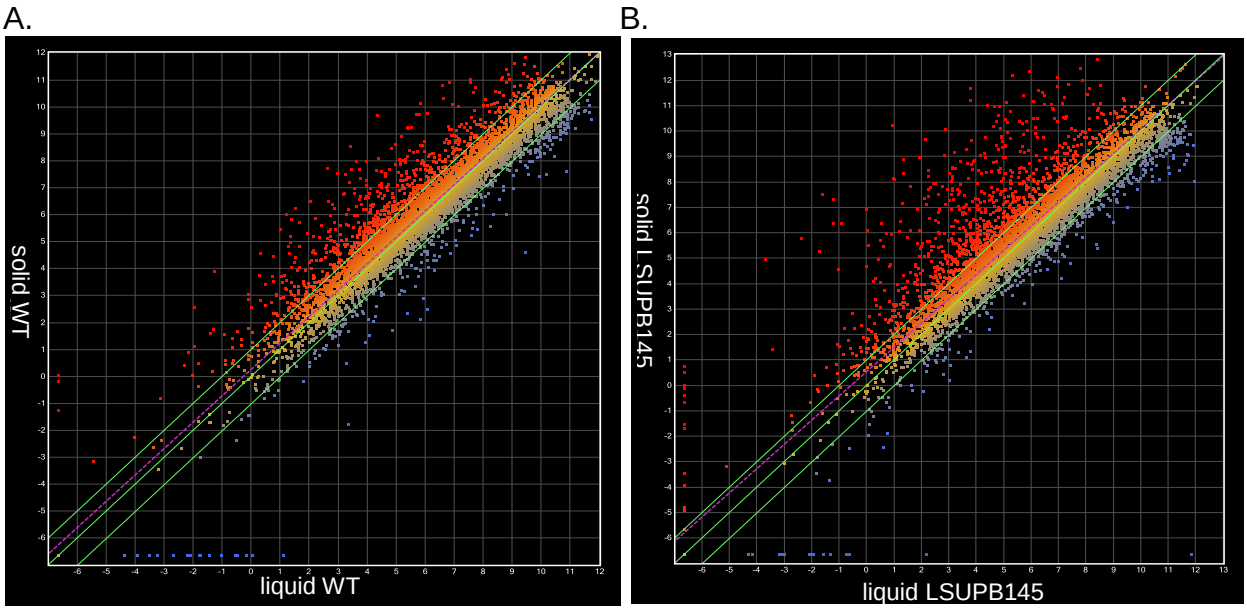

Figure 5.1. Scatter plots of the genes with expression levels changed more than 2-fold (log_2) between pairwise conditions. A, X axis: 336gr-1 (wild type) transcriptome extracted from liquid culture at OD_{600}=1.0, Y axis: 336gr-1 transcriptome extracted from culture grown on LB agar surface 9 h after spotting from overnight culture. B. X axis: LSUPB145 (*⊿tofI*) transcriptome extracted from liquid culture at OD_{600}=1.0, Y axis: LSUPB145 transcriptome extracted from culture grown on LB agar surface 9 h after spotting from overnight culture.

C.

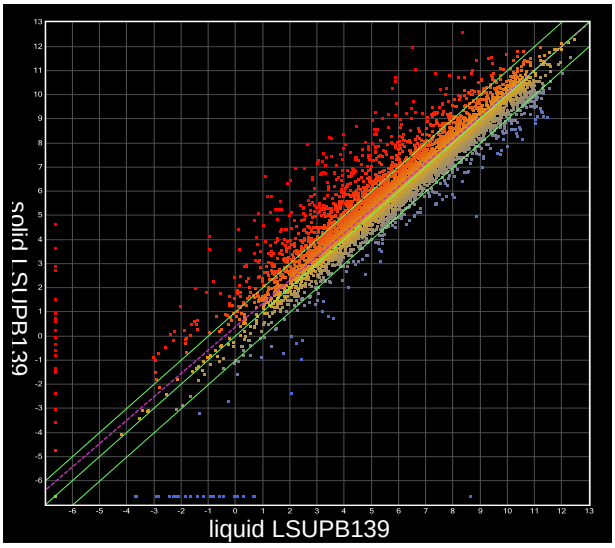

Figure 5.1. Scatter plots of the genes with expression levels changed more than 2-fold (log_2) between pairwise conditions. C. X axis: LSUPB139 (*ΔtofI-R*) transcriptome extracted from liquid culture at OD_{600}=1.0, Y axis: LSUPB139 transcriptome extracted from culture grown on LB agar surface 9 h after spotting from overnight culture.

5.3.3 Deletion of *tofI-R* caused more change in the transcriptome than deletion of *tofI*

Overall, *tofI-R* affected more genes in the *B. glumae* transcriptome than *tofI* and this difference is bigger on solid media (Table 5.3). Deletion of *tofI* in *B. glumae* on solid media caused less than half of genes expressed differentially on solid media than in liquid media. Scatter plots were generated to visualize the difference between transcriptome of the wild type and its QS mutant derivatives (Figure 5.2). In liquid media, the deletion of *tofI* or *tofI-R* mostly caused down-regulation (Figure 5.2AB). On solid media, the deletion of *tofI-R* generally caused down-regulation, while the deletion of *tofI* showed much less expression changes (Figure 5.2CD).

Table 5.3. Number of differently expressed genes among *B. glumae* wild type, 336gr-1, and two mutants, LSUPB145 (*Δtofl*) and LSUPB139 (*Δtofl-R*), transcriptomes in solid or liquid medium conditions.

Strain comparison in different medium conditions	The number of genes with fold change>2	The number of genes with fold change>4	The number of genes with fold change>8
liquid 336gr-1 x liquid LSUPB145	518	187	88
liquid 336gr-1 x liquid LSUPB139	584	284	195
solid 336gr-1 x solid LSUPB145	228	44	26
solid 336gr-1 x solid LSUPB139	651	299	205

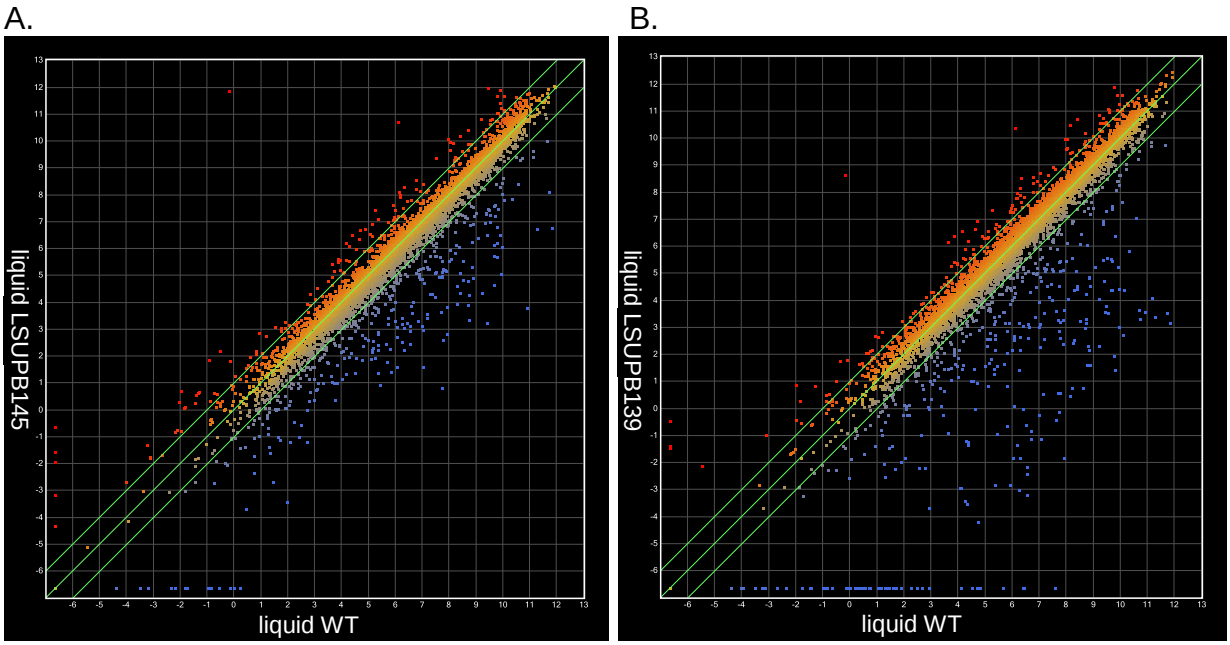

Figure 5.2. Scatter plot of the genes with expression levels changed more than 2-fold (log_2) between pairwise conditions. A, X axis: 336gr-1 (WT) transcriptome extracted from liquid culture at OD_{600}=1.0, Y axis: LSUPB145 (*Δtofl*) transcriptome extracted from liquid culture at OD_{600}=1.0. B, X axis: 336gr-1 transcriptome extracted from liquid culture at OD_{600}=1.0, Y axis: LSUPB139 (*Δtofl-R*) transcriptome extracted from liquid culture at OD_{600}=1.0.

C.

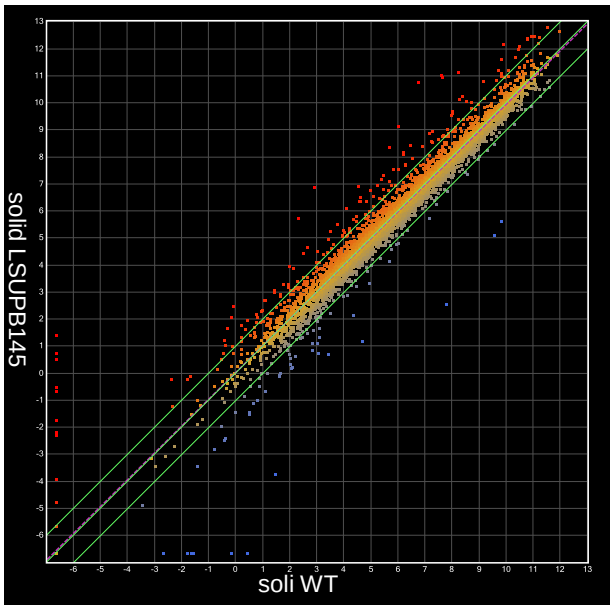

D.

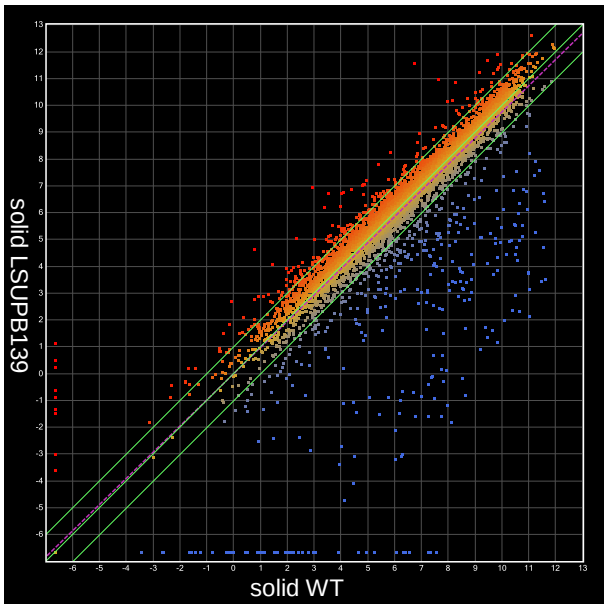

Figure 5.2. Scatter plot of the genes with expression levels changed more than 2-fold (log_2) between pairwise conditions. C, X axis: 336gr-1 transcriptome extracted from the solid culture grown on LB agar surface 9 h after spotting from overnight culture, Y axis: LSUPB145 transcriptome extracted from the solid culture grown on LB agar surface 9 h after spotting from overnight culture. D, X axis: 336gr-1 transcriptome extracted from the solid culture grown on LB agar surface 9 h after spotting from overnight culture, Y axis: LSUPB139 transcriptome extracted from the solid culture grown on LB agar surface 9 h after spotting from overnight culture.

5.3.4 The distributions of *tofI* and *tofI-R* regulon were compared

To compare the distribution of *tofI* and *tofI-R* regulons in bacterial cultures grown in liquid and solid media, Venn diagrams were generated. The number of genes in the potential regulons of *tofI* or *tofI-R* and co-regulons are represented by the size of colored circle and the intersection region, respectively (Figure 5.3). From the observation of the overlapped circles, more genes are influenced by *tofI* in liquid media than on solid media (Figure 5.3A). For the *tofI-R* regulon, the media condition did not induce a change as large as for the *tofI* regulon (Figure 5.3B). For the potential QS regulon, the amount of the *tofI*-independent genes were less than the amount *tofI*-

dependent genes in liquid media, but more than the amount of *tofI*-dependent genes on solid media (Figure 5.3C,D).

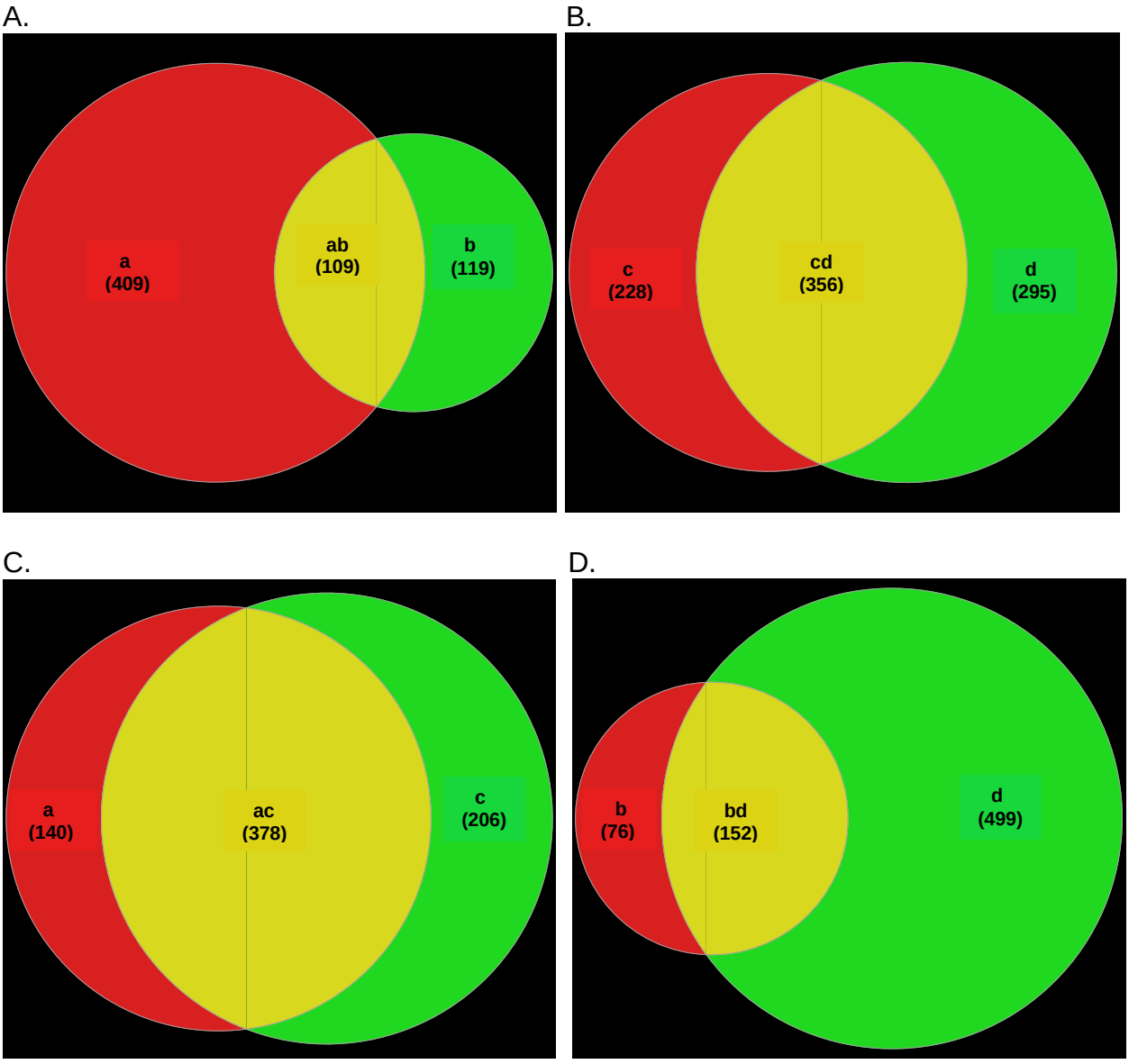

Figure 5.3. Venn diagram generated by ArrayStar displaying the differently expressed genes (fold change >=2) in individual paired conditions. The numbers inside parentheses are the genes that were differently expressed in conditions represented by a, b, c and d. a: 336gr-1 (wild type) and mutant LSUPB145 (Δ*tofI*) in LB broth. b: 336gr-1 and mutant LSUPB145 on LB agar. c: 336gr-1 and mutant LSUPB139 (Δ*tofI-R*) in LB broth. d: WT and mutant LSUPB139 on LB agar. A, Interaction of gene collections for pairs a and b. B, Interactions of gene collections for pairs c and d. C, Interactions of gene collections for pairs a and c. D, Interactions of gene for pairs b and d.

5.3.5 Differences between transcriptomes of liquid and solid cultures of *B. glumae* strains, especially LSUPB145, were detected

To determine the reason causing the phenotypic difference of LSUPB145 between liquid and solid culture conditions, the differently expressed genes were collected. A total of 1,383 genes were found with expression fold change higher than 2 between liquid and solid LSUPB145 culture, while 241 genes were found with expression fold change higher than 8. Using the selected 241 genes, hierarchical clustering-heat maps were generated (Figure 5.4). Heat maps with gene annotation are shown in Appendix 4. Figure 5.4 shows that the selected genes generally having similar expression patterns in the wild type between solid and liquid culture conditions according to the clustering results (according to the gene expression similarity through experimental conditions) shown in heat maps.

However, the selected genes displayed very different expression between in solid and liquid cultures of LSUPB145. Liquid LSUPB145 culture showed a more similar expression profile to LSUPB139, while solid LSUPB145 culture showed a more similar expression profile to 336gr-1. This gene selection includes homologs of ferredoxin, ABC transporter component, UspA domain containing protein, FAD/FMN-binding oxidoreductase, AraC regulator, RebAB proteins, thioesterase, (3R)-hydroxymyristoyl-ACP dehydratase and LuxR type autoinducer-binding regulator, which were described in Chapters 3 and 4. Additionally, MarR and TetR family regulator genes were selected as differently expressed genes.

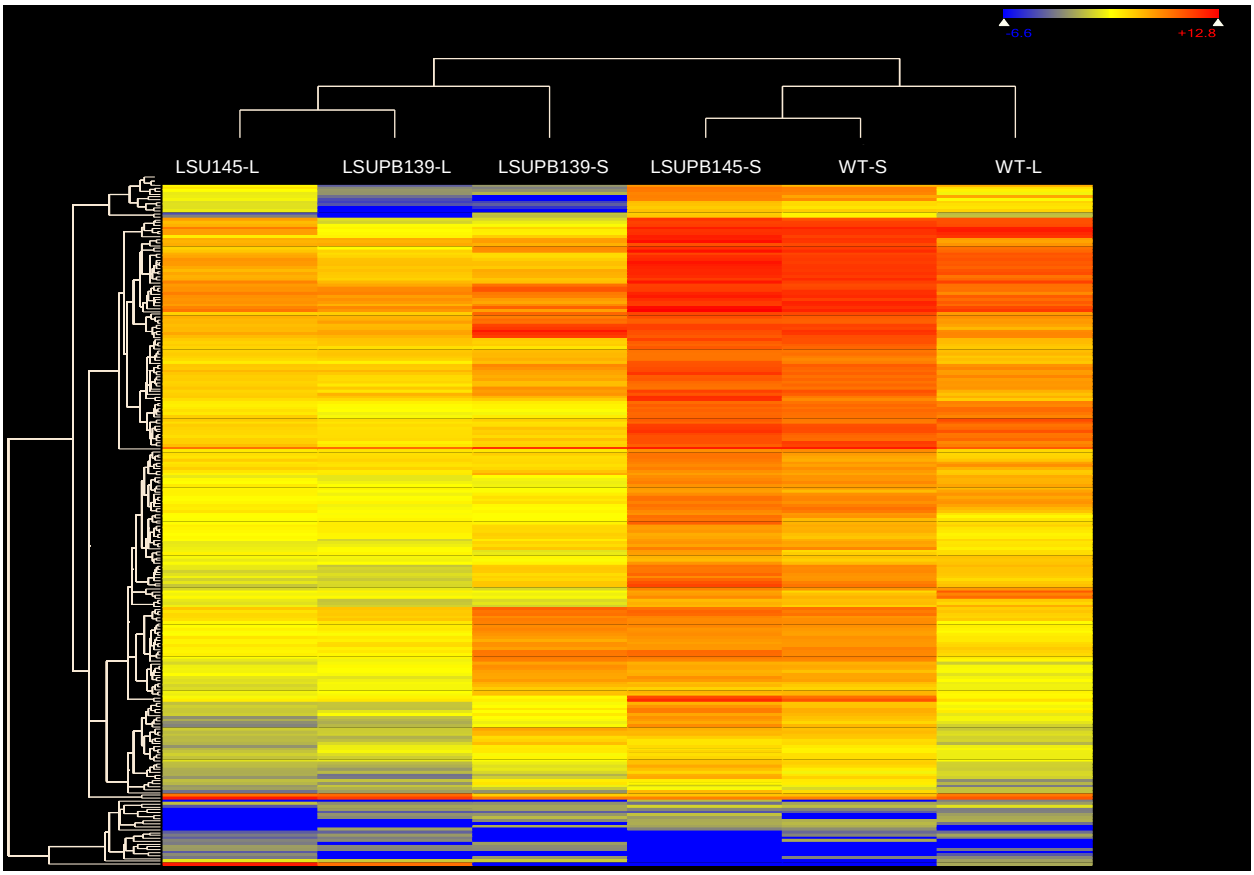

Figure 5.4. Heat Maps were generated by ArrayStar to display the level of gene expression as indicated by color. On the color scale, red represents high expression, yellow represents intermediate expression and blue represents low expression of genes. Each row represents an individual gene that was differently regulated (expression fold change higher than 8) in LSUPB145 between solid and liquid bacterial culture. The different columns represent the transcriptome in bacterial cultures (WT, LSUPB139 and LSUPB145) in different medium conditions. –L = culture from liquid medium, and -S = culture from solid medium. Genes and transcriptomes were clustered according to their expression similarity.

5.4 Discussion

5.4.1 Reliable RNA-seq data were generated

Good coverage values were reported after assembly. Template coverage is close to 100%, and median coverage is between 4.5~16 times of the reference sequence. The difference between 336gr-1 and BGR1 genomes was the main reason that the template coverage was less than 100% (Francis et al., 2013). It also revealed that a

bigger sequence difference between 336gr-1 and BGR1 reference occurs in the sequences of plasmids. Two biological replicates of each sample were performed using paired-end sequencing, which allows primers to run through the genome approximately four times for each sample. Therefore it is reasonable that the median coverage of this new set of RNA-seq data is much higher than the one for the RNA-seq data set mentioned in Chapter 4 (no biological replicates).

5.4.2 Solid and liquid media growth stimulated different transcriptional profiles

A large portion (17.4-24.0%) of the transcriptomes of 336gr-1, LSUPB145 and LSUPB139 changed between solid and liquid medium conditions. The criterion for selecting differently expressed genes was fold-change. The number of genes having fold-change higher than 2, 4 and 8 was reported. Among the three strains, LSUPB145 showed the most striking change by possessing the most number of differently expressed genes in > 2, 4, 8 fold-change levels. This result agreed with previously described morphology of LSUPB145 (Chen et al., 2012). Among the three tested samples, LSUPB145 was the only one showing an obvious phenotypic difference (toxoflavin production) between solid and liquid media. Among three strains, 336gr-1 showed the smallest number of differently expressed genes in all three fold-change levels. This result implied the general “cushion” function of QS on the transcriptome of *B. glumae* when it was switched between different growth conditions. From the scatter plot observations, all three strains 336gr-1, LSUPB145 and LSUPB139 tended to express higher on solid media. This indicated that the solid-medium condition tends to stimulate the up-regulation of genes in general.

5.4.3 The *tofI*-independent regulation was more prominent on solid media than in liquid media

The fact that deletion of *tofI-R* caused more transcriptional change than deletion of *tofI* indicated the existence of a regulon that is dependent on the *tofR, tofM* and/or other elements in the *tofI-R* region. Compared to liquid media, the transcriptome showed bigger *tofI*-independent regulon on solid media. This means solid medium is a more intriguing condition for *tofI*-independent expression. There was a much smaller difference between the transcriptome of 336gr-1 and LSUPB145 on solid media than in liquid media. This transcriptomic change showed positive correlation with the phenotypic change between 336gr-1 and LSUPB145 under different media conditions. From the observation of scattering plots, the differently expressed genes tended to show higher expression in the wild type than in the QS mutants, which indicated that *tofI* and *tofI-R* mostly performed a positive regulatory role for the genomic genes.

5.4.4 The large size of the *tofI*-independent QS regulon on solid media is detected by transcriptome analysis

Previously, it was reported that the deletion of the *tofI-R* region caused complete loss of toxoflavin, but the deletion of *tofI* did not cause loss of toxoflavin on LB agar (Chen et al., 2012). We concluded that there was some *tofI*-independent toxoflavin production existing in *B. glumae,* and this alternative pathway also required minimum QS genetic elements to function (Chen, 2011). A Venn diagram was used to visualize the distribution of the *tofI*-independent QS regulon. A total of 499 genes that were potentially regulated by QS but independent of *tofI* were found. However, the specific gene group responsible for the previously mentioned alternative pathway is not clear. More genes were influenced by *tofI* in liquid media than on solid media, which matched the observation about LSUPB145 showing similar phenotype with 336gr-1 on solid

media. The media condition did not bring about as striking a change to the transcriptome of LSUPB139 as to LSUPB145, which corresponded to LSUPB139 failing to produce toxoflavin under both media conditions.

5.4.5 QS-dependent genes were found to be responsible for transcriptome adaptation to medium condition change

Expression of approximately 24% of genomic genes increased more than 2-fold between solid and liquid culture of LSUPB145. Therefore, media condition is a major factor for transcriptomic change. The genes that showed more than 8 fold-changes in expression were selected to generate heat maps for further analysis (Appendix 4). This selection is considered as the *tofI*-independent QS regulon, which also played a role in the phenotypic difference between in solid and liquid cultures of LSUPB145. From the heat map, the selected genes showed very different expression patterns between solid and liquid cultures of LSUPB145. The transcriptomes displaying similar expression profiles were clustered together: transcriptomes of liquid LSUPB145, liquid LSUPB139, solid LSUPB139 cultures were clustered close together; transcriptomes of solid LSUPB145, liquid 336gr-1 and solid 336gr-1 were clustered close together. This distribution is in harmony with the observed phenotypes, especially toxoflavin production of each culture. Therefore it is possible that some genes in this collection are responsible for bacterial phenotypic changes in given different medium conditions.

Some genes or their homologs are mentioned in Chapters 3 and 4 as QS-dependent candidates. Gene (bglu_2g05850) encoding FAD/FMN-binding oxidoreductase was found to be differentially expressed between solid and liquid cultures LSUPB145. This gene was also detected by random mutagenesis (Chapter 3) and comparative transcriptome analysis (Chapter 4) of the QS up-regulated gene. UspA

domain containing protein (bglu_2g20360) was found to be differentially expressed between solid and liquid cultures of LSUPB145. This gene was renamed *usp6* and upregulated by QS in *B. glumae* (Kim et al., 2012). The other two homologs *usp9* and *usp10* were also detected as up-regulated genes by QS. AraC (bglu_2g16610) family transcriptional regulator was found differently expressed in LSUPB145 solid and liquid culture. Other AraC family transcriptional regulators were detected as the QS-dependent regulon by transcriptome analysis and random mutagenesis. *rebB* (bglu_2g16660 and bglu_2g16700) and *rebA* bglu_2g16670 were found to be up-regulated in LSUPB145 solid culture, and they were also found to share a very similar expression pattern with *tofR* from clustering-heat map analysis of QS up-regulated genes in Chapter 4. The gene (bglu_1g16760) encoding thioesterase superfamily protein and a gene encoding (3R)-hydroxymyristoyl-ACP (ACP) dehydratase were close on Hierarchical clustering-heat map analysis (Appendix 4). Those two genes were also clustered together on the clustering-heat map of the QS dependent genes. Two orphan LuxR type regulators (bglu_1g16610) and (bglu_1g17030) were selected as QS up-regulated features. The same genes with the addition of one orphan *luxR* (bglu_1g23190) were expressed higher in solid cultures of LSUPB145. Overall, there is an overlap between the gene collections of QS-dependent and LSUPB145 media condition-dependent. This implies that the solid media condition can compensate for the loss of *tofI* function and promote QS-dependent gene expression. Therefore, it is possible that another global regulator controls a range of genes as big as AHL QS. Given that increased expression of ACP (ACP) dehydratase and thioesterase activity genes as well as S-adenosyl-L-homocysteine (SAH) hydrolase and cyclic adenosine

monophosphate (cAMP) receptor protein (CRP), cis-2-dodecenoic acid (BDSF) analog and AI-2 QS are good candidates to be the alternative regulatory mechanism.

To estimate the possibility of having an active BDSF analog and AI-2 pathway in *B. glumae, a* search of homologs of published BDSF and AI-2 related protein was performed. In addition to ACP dehydratase and thioeasterase activity encoding genes, a protein sequence blast search (NCBI) revealed 2 homologs YP_002911224 and YP_002910351 in *B. glumae* respectively showing 37 and 27% identity to $RpfF_{Bc,}$ an enoyl CoA hydratase responsible for synthesis of BDSF in *B. cenocepacia* (Schmid et al., 2012). Their encoding genes showed 1.4 and 1.2-fold increases of expression, respectively in LSUPB145 solid culture compared to liquid culture. The protein blast also revealed four homologs, YP_002909073, YP_002912466, YP_002910896 and YP_002909734, in *B. glumae* having 30-40% identity to RpfR, the BDSF receptor protein in *B. cenocepacia* (Deng et al., 2012). The corresponding encoding genes showed 1.5, 1.5, 1.1 and 2.1-fold increases of expression, respectively in LSUPB145 solid culture than in liquid culture. Two proteins with comparably low query coverage, YP_002910913 and YP_002908679, were found to share 43% (13/37) and 29% (18/63) identity to LuxS, the terminal synthase of AI-2 in *E. coli* (Barrios et al., 2006). The encoding genes showed 1.1 and 2.4-fold increases in LSUPB145 solid culture compared to liquid culture. A protein blast also revealed that homolog YP_002911766 shares 26% identity to MqsR, the receptor of AI-2 controlling motility and biofilm formation in *E. coli* (Barrios et al., 2006). The corresponding gene showed a 1.2-fold increase of expression in solid culture compared to liquid culture of LSUPB145.

The results from transcriptional analysis and homolog comparison are not strong enough to make deductions about how AHL, BDSF analog and AI-2 interact in *B. glumae*, but these clearly show that further exploratory studies of additional QS or cell-to-cell signaling systems are worth pursuing.

CHAPTER 6. CONCLUSIONS AND PROSPECTS FOR FUTURE RESEARCH

The quorum sensing (QS) monitoring system is the regulator for the major virulence factors of *Burkholderia glumae*, which is the causal agent of bacterial panicle blight on rice. The QS system is mediated by *lux* type *tofI* and *tofR* genes. *tofI* encodes an enzyme synthesizing the autoinducer C8-HSL, and *tofR* encodes the cognate receptor of C8-HSL TofR. At threshold bacterial populations, the C8-HSL/TofR complex is formed and promotes the expression of target genes to adapt to different environment cues. To elucidate the individual functions of QS elements, a series of deletion mutants were generated through allelic exchange. It was observed that LSUPB201 (Δ*tofI*/Δ*tofR* derivative of 336gr-1) still produced a substantial amount of toxoflavin on LB agar. Further study revealed that *tofM* was located in the middle of the *tofI* and *tofR* genes and was responsible for *tofI*/*tofR* independent toxoflavin production. Toxoflavin quantification and a virulence assay demonstrated that TofM is the positive regulator of pathogenicity in *B. glumae.* TofM shared 22.4% identity with the QS modulator RsaM, which negatively regulates the expression of two AHL synthase genes in *P. fuscovaginae*. Transcriptional analysis revealed that *tofM* had a positive correlation with *toxA* and *tofR.* Therefore, TofM possibly functions as a positive modulator of QS in *B. glumae,* which is different from RsaM.

LSUPB145 (Δ*tofI*) and LSUPB169 (Δ*tofR)* produced toxoflavin on LB agar, which was different from the previous publication (Kim et al., 2004b). To investigate the genes responsible for *tofI*- and *tofR*-independent toxoflavin production, random mutagenesis was performed on two strains, LSUPB178 (Δ*tofI*::pLG6gustoxA) and LSUPB324 (Δ*tofR*::pLG6gustoxA). The random mutants failing to express the *toxA* promoter fused *gusA* gene in the X-gluc supplemented media were characterized. After the sequencing

of transposon inserted region, 15 and 3 genes were found for *tofI*- and *tofR*-independent toxoflavin regulators collection, respectively. After specific mutation and toxoflavin quantification, *flhD* encoding flagellar transcriptional activator FlhD, *dgcB* encoding diaguanylate cyclase, and *wzyB* encoding O-antigen polymerase family protein were determined to be regulatory determinants for *tofI*-independent toxoflavin production. Additionally, FlhD might prevent early degradation of toxoflavin, while WzyB might be important for bacterial growth and DgcB may affect bacterial motility and EPS production. *qsmR* and *orf2* located upstream of *toxJ,* were determined to be *tofR*-independent toxoflavin production regulatory elements.

RNA-seq was applied to the transcriptome of 336gr-1 and LSUPB134 to search for the unknown QS regulon. The RNA-seq data from another *B. glumae* strain BGR1 were used as a reference. Substantial changes occurred in the transcriptional profile of 336gr-1 genome; more than a 2-fold increase in expression was observed for a quarter of the genomic genes. QS generally functions as positive regulator. SAH, Ferredoxin, diguanylate cyclase, H-NS, urease subunit, Usp homologs, orphan LuxR type regulators, MazE/F were found to be up-regulated by QS. CRP/FNR family transcriptional regulator was down-regulated by QS. AraC regulator and ABC transporter genes were found in both up- and down-regulated gene groups. Hierarchical clustering revealed two possible regulation pathways for DSF-dependent QS signaling and R body formation. Around 1000 5’ UTRs were found in the genome of 336gr-1. A 75 *bp* 5’ UTR was found for a gene encoding H-NS, and more than 100 *bp* 5’ UTRs were found for two cold shock related genes. 53 ncRNAs including 18 asRNAs were found differently expressed

through the transcriptome analysis of 336gr-1 and LSUPB134. Two asRNAs were found to be complementary to the *tofM* gene.

To investigate the change in transcriptional profiles of 336gr-1 derivatives (especially, LSUPB145) between solid and liquid cultures, RNA-seq was again performed. The transcriptomes of bacterial cultures of LSUPB145 grown on solid and in liquid media were compared. The differentially expressed genes were selected. Strikingly, many genes from this selection were also previously identified as potential QS-dependent genes. These genes encode proteins including ferredoxin, ABC transporter component, UspA domain containing protein, FAD/FMN-binding oxidoreductase, AraC regulator, RebAB proteins, thioesterase super family protein, (3R)-hydroxymyristoyl-ACP dehydratase and LuxR type autoinducer-binding regulator. Therefore, it is possible that some other alternative regulator can perform similar global regulatory functions as AHL QS in *B. glumae*.

The majority of this project was accomplished by analyses at transcriptional level. To confirm the roles different QS related regulators play in the entire regulatory network of *B. glumae*, protein level studies need to be designed. The interaction between TofM and TofR can be characterized by protein affinity analysis. The functions of *luxIR* intergenic genes are not understood very well for most phytopathogenic bacteria, so the future studies of TofM will provide useful reference information.

Random mutagenesis and RNA-seq selected many potential regulators. The specific mutation provided preliminarily evidence regarding several toxoflavin regulators that compensate in the absence of *tofI* or *tofR*. Complementation tests need to be done in order to confirm their roles in toxoflavin production. Mechanisms of important

regulators should be approached by different post-translational tests in the future to build upon the knowledge of the entire signaling system in *B. glumae.* For the QS dependent gene candidates selected from RNA-seq, more genetic and protein level work will need to be done before any conclusions can be drawn about their true function and targets. So far, the transcriptome analysis results in this dissertation provide some potential direction in future research areas.

CITED LITERATURE

Abo, M.E., Alegbejo, M.D., Sy, A.A., and Misari, S.M. (2000). An overview of the mode of transmission, host plants and methods of detection of rice yellow mottle virus. Journal of Sustainable Agriculture *17*, 19-36.

Abramovitch, R.B., Kim, Y.J., Chen, S.R., Dickman, M.B., and Martin, G.B. (2003). *Pseudomonas* type III effector AvrPtoB induces plant disease susceptibility by inhibition of host programmed cell death. Embo Journal *22*, 60-69.

Abramovitch, R.B., and Martin, G.B. (2004). Strategies used by bacterial pathogens to suppress plant defenses. Current Opinion in Plant Biology *7*, 356-364.

Albus, A.M., Pesci, E.C., RunyenJanecky, L.J., West, S.E.H., and Iglewski, B.H. (1997). Vfr controls quorum sensing in *Pseudomonas aeruginosa*. J Bacteriol *179*, 3928-3935.

Alexeyev, M.F. (1999). The pKNOCK series of broad-host-range mobilizable suicide vectors for gene knockout and targeted DNA insertion into the chromosome of Gram-negative bacteria. Biotechniques *26*, 824-826,828.

Andersson, R.A., Koiv, V., Norman-Setterblad, C., and Pirhonen, M. (1999). Role of RpoS in virulence and stress tolerance of the plant pathogen *Erwinia carotovora* subsp *carotovora*. Microbiology-Uk *145*, 3547-3556.

Arlat, M., Gough, C.L., Barber, C.E., Boucher, C., and Daniels, M.J. (1991). *Xanthomonas campestris* contains a cluster of hrp genes related to the larger hrp cluster of *Pseudomonas solanacearum*. Mol Plant-Microbe Interact *4*, 593-601.

Aschhoff, H.J., Elten, H., Arnold, H.H., Mahal, G., Kersten, W., and Kersten, H. (1976). 7-methylguanine specific transfer-RNA-methyltransferase from *Escherichia coli*. Nucleic Acids Research *3*, 3109-3122.

Azegami, K., Nishiyama, K., Watanabe, Y., Kadota, I., Ohuchi, A., and Fukazawa, C. (1987). *Pseudomonas plantarii* sp. nov., the causal agent of rice seedling blight. Int J Syst Bacteriol *37*, 144-152.

Bach, H.J., Jessen, I., Schloter, M., and Munch, J.C. (2003). A TaqMan-PCR protocol for quantification and differentiation of the phytopathogenic *Clavibacter michiganensis* subspecies. Journal of Microbiological Methods *52*, 85-91.

Balasubramanian, D., and Mathee, K. (2009). Comparative transcriptome analyses of *Pseudomonas aeruginosa*. Human genomics *3*.

Baldwin, A., Sokol, P.A., Parkhill, J., and Mahenthiralingam, E. (2004). The *Burkholderia cepacia* epidemic strain marker is part of a novel genomic island encoding both virulence and metabolism-associated genes in *Burkholderia cenocepacia*. Infect Immun *72*, 1537-1547.

Barrios, A.F.G., Zuo, R.J., Hashimoto, Y., Yang, L., Bentley, W.E., and Wood, T.K. (2006). Autoinducer 2 controls biofilm formation in *Escherichia coli* through a novel motility quorum-sensing regulator (MqsR, B3022). J Bacteriol *188*, 305-316.

Bartsev, A.V., Deakin, W.J., Boukli, N.M., McAlvin, C.B., Stacey, G., Malnoe, P., Broughton, W.J., and Staehelin, C. (2004). NopL, an effector protein of *Rhizobium* sp NGR234, thwarts activation of plant defense reactions. Plant Physiology *134*, 871-879.

Beeston, A.L., and Surette, M.G. (2002). pfs-dependent regulation of autoinducer 2 production in *Salmonella enterica* serovar Typhimurium. J Bacteriol *184*, 3450-3456.

Belitsky, M., Avshalom, H., Erental, A., Yelin, I., Kumar, S., London, N., Sperber, M., Schueler-Furman, O., and Engelberg-Kulka, H. (2011). The *Escherichia coli* extracellular death factor EDF induces the endoribonucleolytic activities of the toxins MazF and ChpBK. Mol Cell *41*, 625-635.

Bellemann, P., and Geider, K. (1992). Localization of transposon insertions in pathogenicity mutants of *Erwinia amylovora* and their biochemical-characterization. Journal of General Microbiology *138*, 931-940.

Bertani, G. (2004). Lysogeny at mid-twentieth century: P1, P2, and other experimental systems. J Bacteriol *186*, 595-600.

Bi, H.K., Christensen, Q.H., Feng, Y.J., Wang, H.H., and Cronan, J.E. (2012). The *Burkholderia cenocepacia* BDSF quorum sensing fatty acid is synthesized by a bifunctional crotonase homologue having both dehydratase and thioesterase activities. Molecular microbiology *83*, 840-855.

Birch, R.G. (1987). Correlation between albicidin production and chlorosis induction by xanthomonas-albilineans, the sugarcane leaf scald pathogen. Physiol Mol Plant Pathol *30*, 199-206.

Birch, R.G., and Patil, S.S. (1987). Evidence that an albicidin-like phytotoxin induces chlorosis in sugarcane leaf scald disease by blocking plastid DNA-replication. Physiol Mol Plant Pathol *30*, 207-214.

Boon, C., Deng, Y., Wang, L.-H., He, Y., Xu, J.-L., Fan, Y., Pan, S.Q., and Zhang, L.-H. (2008a). A novel DSF-like signal from *Burkholderia cenocepacia* interferes with *Candida albicans* morphological transition. Isme J *2*, 27-36.

Boon, C., Deng, Y.Y., Wang, L.H., He, Y.W., Xu, J.L., Fan, Y., Pan, S.Q., and Zhang, L.H. (2008b). A novel DSF-like signal from *Burkholderia cenocepacia* interferes with *Candida albicans* morphological transition. Isme J *2*, 27-36.

Braun, E.J. (1982). Ultrastructural investigation of resistant and susceptible maize inbreds infected with *Erwinia stewartii*. Phytopathology *72*, 159-166.

Brescia, C.C., Kaw, M.K., and Sledjeski, D.D. (2004). The DNA binding protein H-NS binds to and alters the stability of RNA in vitro and in vivo. Journal of Molecular Biology *339*, 505-514.

Brown, I., Mansfield, J., and Bonas, U. (1995). Hrp genes in *Xanthomonas campestris* pv *vesicatoria* determine ability to suppress papilla deposition in pepper mesophyll cells. Mol Plant-Microbe Interact *8*, 825-836.

Bushnell, W.R., and Rowell, J.B. (1981). Suppressors of defense reactions - a model for roles in specificity. Phytopathology *71*, 1012-1014.

Callahan, S.M., and Dunlap, P.V. (2000). LuxR- and acyl-homoserine-lactone-controlled non-lux genes define a quorum-sensing regulon in *Vibrio fischeri*. J Bacteriol *182*, 2811-2822.

Chen, R.X. (2011). A molecular genetic study on the TofI/TofR quorum-sensing system of *Burkholderia glumae*: the major pathogen that causes bacterial panicle blight of Rice. In Plant Pathology & Crop Physiology (LSU ETD: Louisiana State University).

Chen, R.X., Barphagha, I.K., Karki, H.S., and Ham, J.H. (2012). Dissection of quorum-sensing genes in *Burkholderia glumae* reveals non-canonical regulation and the new regulatory gene *tofM* for toxoflavin production. PLoS One *7*.

Choudhary, K.S., Hudaiberdiev, S., Gelencser, Z., Goncalves Coutinho, B., Venturi, V., and Pongor, S. (2013). The organization of the quorum sensing *luxI/R* family genes in *Burkholderia*. International journal of molecular sciences *14*, 13727-13747.

Chowdhury, P.R., and Heinemann, J.A. (2006). The general secrotory pathway of *Burkholderia gladioli* pv. *agaricicola* BG164R is necessary for for cavity disease in white button mushrooms. Appl Environ Microbiol *72*, 3558-3565.

Chun, H., Choi, O., Goo, E., Kim, N., Kim, H., Kang, Y., Kim, J., Moon, J.S., and Hwang, I. (2009). The quorum sensing-dependent gene *kat*G of *Burkholderia glumae* is Important for protection from visible light. J Bacteriol *191*, 4152-4157.

Coenye, T., and Vandamme, P. (2003). Diversity and significance of *Burkholderia* species occupying diverse ecological niches. Environ Microbiol *5*, 719-729.

Daniels, C., Vindurampulle, C., and Morona, R. (1998). Overexpression and topology of the *Shigella flexneri* O-antigen polymerase (Rfc/Wzy). Molecular microbiology *28*, 1211-1222.

Davidson, A.L., and Chen, J. (2004). ATP-binding cassette transporters in bacteria. Annual Review of Biochemistry *73*, 241-268.

de Souza, A.A., Takita, M.A., Coletta, H.D., Caldana, C., Goldman, G.H., Yanai, G.M., Muto, N.H., de Oliveira, R.C., Nunes, L.R., and Machado, M.A. (2003). Analysis of gene

expression in two growth states of *Xylella fastidiosa* and its relationship with pathogenicity. Mol Plant-Microbe Interact *16*, 867-875.

Delorenzo, V., Herrero, M., Jakubzik, U., and Timmis, K.N. (1990). Mini-Tn*5* transposon derivatives for insertion mutagenesis, promoter probing, and chromosomal insertion of cloned DNA in gram-negative eubacteria. J Bacteriol *172*, 6568-6572.

Deng, Y., Boon, C., Eberl, L., and Zhang, L.-H. (2009). Differential modulation of *Burkholderia cenocepacia* virulence and energy metabolism by the quorum-sensing signal BDSF and its synthase. J Bacteriol *191*, 7270-7278.

Deng, Y., Lim, A., Wang, J., Zhou, T., Chen, S., Lee, J., Dong, Y.-H., and Zhang, L.-H. (2013). Cis-2-dodecenoic acid quorum sensing system modulates N-acyl homoserine lactone production through RpfR and cyclic di-GMP turnover in *Burkholderia cenocepacia*. Bmc Microbiology *13*.

Deng, Y., Wu, J.e., Tao, F., and Zhang, L.-H. (2011). Listening to a new language: DSF-based quorum sensing in Gram-negative bacteria. Chemical Reviews *111*, 160-173.

Deng, Y.Y., Schmid, N., Wang, C., Wang, J.H., Pessi, G., Wu, D.H., Lee, J., Aguilar, C., Ahrens, C.H., Chang, C.Q.*, et al.* (2012). Cis-2-dodecenoic acid receptor RpfR links quorum-sensing signal perception with regulation of virulence through cyclic dimeric guanosine monophosphate turnover. Proc Natl Acad Sci U S A *109*, 15479-15484.

Deng, Y.Y., Wu, J.E., Eberl, L., and Zhang, L.H. (2010). Structural and functional characterization of diffusible signal factor family quorum-sensing signals produced by members of the *Burkholderia cepacia* complex. Appl Environ Microbiol *76*, 4675-4683.

Devescovi, G., Bigirimana, J., Degrassi, G., Cabrio, L., LiPuma, J.J., Kim, J., Hwang, I., and Venturi, V. (2007a). Involvement of a quorum-sensing-regulated lipase secreted by a clinical isolate of Burkholderia glumae in severe disease symptoms in rice. Applied and environmental microbiology *73*, 4950-4958.

Devescovi, G., Bigirimana, J., Degrassi, G., Cabrio, L., LiPuma, J.J., Kim, J., Hwang, I., and Venturi, V. (2007b). Involvement of a quorum-sensing-regulated lipase secreted by a clinical isolate of *Burkholderia glumae* in severe disease symptoms in rice. Appl Environ Microbiol *73*, 4950-4958.

Dirix, G., Monsieurs, P., Dombrecht, B., Daniels, R., Marchal, K., Vanderleyden, J., and Michiels, J. (2004). Peptide signal molecules and bacteriocins in Gram-negative bacteria: a genome-wide in silico screening for peptides containing a double-glycine leader sequence and their cognate transporters. Peptides *25*, 1425-1440.

Ditta, G., Stanfield, S., Corbin, D., and Helinski, D.R. (1980). Broad host range DNA cloning system for Gram-negative bacteria: construction of a gene bank of *Rhizobium meliloti*. Proc Natl Acad Sci U S A *77*, 7347-7351.

Dong, Y.H., Zhang, X.F., Xu, J.L., Tan, A.T., and Zhang, L.H. (2005). VqsM, a novel AraC-type global regulator of quorum-sensing signalling and virulence in *Pseudomonas aeruginosa*. Molecular microbiology *58*, 552-564.

Duan, Q., Zhou, M., Zhu, L., and Zhu, G. (2013). Flagella and bacterial pathogenicity. Journal of Basic Microbiology *53*, 1-8.

Duerkop, B.A., Herman, J.P., Ulrich, R.L., Churchill, M.E.A., and Greenberg, E.P. (2008). The *Burkholderia mallei* BmaR3-BmaI3 quorum-sensing system produces and responds to N-3-hydroxy-octanoyl homoserine lactone. J Bacteriol *190*, 5137-5141.

Duerkop, B.A., Ulrich, R.L., and Greenberg, E.P. (2007). Octanoyl-homoserine lactone is the cognate signal for *Burkholderia mallei* BmaR1-BmaI1 quorum sensing. J Bacteriol *189*, 5034-5040.

Dunlap, P.V. (1999). Quorum regulation of luminescence in *Vibrio fischeri*. Journal of molecular microbiology and biotechnology *1*, 5-12.

Eberhard, A. (1972). Inhibition and activation of bacterial luciferase synthesis. J Bacteriol *109*, 1101-1105.

Eberl, L., and Riedel, K. (2011). Mining quorum sensing regulated proteins - role of bacterial cell-to-cell communication in global gene regulation as assessed by proteomics. Proteomics *11*, 3070-3085.

Ellis, T.N., and Kuehn, M.J. (2010). Virulence and immunomodulatory roles of bacterial outer membrane vesicles. Microbiology and Molecular Biology Reviews *74*, 81-+.

Engelberg-Kulka, H., Amitai, S., Kolodkin-Gal, I., and Hazan, R. (2006). Bacterial programmed cell death and multicellular behavior in bacteria. Plos Genetics *2*, 1518-1526.

Espinosa-Urgel, M., Salido, A., and Ramos, J.L. (2000). Genetic analysis of functions involved in adhesion of *Pseudomonas putida* to seeds. J Bacteriol *182*, 2363-2369.

Fazli, M., McCarthy, Y., Givskov, M., Ryan, R.P., and Tolker-Nielsen, T. (2013). The exopolysaccharide gene cluster Bcam1330-Bcam1341 is involved in *Burkholderia cenocepacia* biofilm formation, and its expression is regulated by c-di-GMP and Bcam1349. MicrobiologyOpen *2*, 105-122.

Fazli, M., O'Connell, A., Nilsson, M., Niehaus, K., Dow, J.M., Givskov, M., Ryan, R.P., and Tolker-Nielsen, T. (2011). The CRP/FNR family protein Bcam1349 is a c-di-GMP effector that regulates biofilm formation in the respiratory pathogen *Burkholderia cenocepacia*. Molecular microbiology *82*, 327-341.

Figurski, D.H., and Helinski, D.R. (1979). Replication of an origin-containing derivative of plasmid RK2 dependent on a plasmid function provided in *trans*. Proc Natl Acad Sci U S A *76*, 1648-1652.

Filiatrault, M.J., Stodghill, P.V., Bronstein, P.A., Moll, S., Lindeberg, M., Grills, G., Schweitzer, P., Wang, W., Schroth, G.P., Luo, S.*, et al.* (2010). Transcriptome analysis of *Pseudomonas syringae* identifies new genes, noncoding RNAs, and antisense Activity. J Bacteriol *192*, 2359-2372.

Fong, K.P., Chung, W.S.O., Lamont, R.J., and Demuth, D.R. (2001). Intra- and interspecies regulation of gene expression by *Actinobacillus actinomycetemcomitans* LuxS. Infect Immun *69*, 7625-7634.

Fouts, D.E., Abramovitch, R.B., Alfano, J.R., Baldo, A.M., Buell, C.R., Cartinhour, S., Chatterjee, A.K., D'Ascenzo, M., Gwinn, M.L., Lazarowitz, S.G.*, et al.* (2002). Genomewide identification of *Pseudomonas syringae* pv. *tomato* DC3000 promoters controlled by the HrpL alternative sigma factor. Proc Natl Acad Sci U S A *99*, 2275-2280.

Francis, F. (2012). Comparative genomics, transcriptome analysis and characterization of selected regulatory genes of *Burkholderia glumae*. In Plabt pathology and crop physiology (LSU ETD: Louisiana State University), pp. 95.

Francis, F., Kim, J., Ramaraj, T., Farmer, A., Rush, M.C., and Ham, J.H. (2013). Comparative genomic analysis of two *Burkholderia glumae* strains from different geographic origins reveals a high degree of plasticity in genome structure associated with genomic islands. Molecular Genetics and Genomics *288*, 195-203.

Fuqua, C., Parsek, M.R., and Greenberg, E.P. (2001). Regulation of gene expression by cell-to-cell communication: acyl-homoserine lactone quorum sensing. Annual review of genetics *35*, 439-468.

Fuqua, W.C., Winans, S.C., and Greenberg, E.P. (1994). Quorum sensing in bacteria: the LuxR-LuxI family of cell density-responsive transcriptional regulators. J Bacteriol *176*, 269-275.

Gallegos, M.T., Schleif, R., Bairoch, A., Hofmann, K., and Ramos, J.L. (1997). AraC/XylS family of transcriptional regulators. Microbiology and Molecular Biology Reviews *61*, 393-&.

Georg, J., and Hess, W.R. (2011). cis-antisense RNA, another level of gene regulation in bacteria. Microbiology and Molecular Biology Reviews *75*, 286-+.

Gerhardson, B. (2002). Biological substitutes for pesticides. Trends Biotechnol *20*, 338-343.

Girgis, H.S., Liu, Y.C., Ryu, W.S., and Tavazoie, S. (2007). A comprehensive genetic characterization of bacterial motility. Plos Genetics *3*, 1644-1660.

Goo, E., Kang, Y., Kim, H., and Hwang, I. (2010). Proteomic analysis of quorum sensing-dependent proteins in *Burkholderia glumae*. J Proteome Res *9*, 3184-3199.

Goo, E., Majerczyk, C.D., An, J.H., Chandler, J.R., Seo, Y.-S., Ham, H., Lim, J.Y., Kim, H., Lee, B., Jang, M.S.*, et al.* (2012). Bacterial quorum sensing, cooperativity, and anticipation of stationary-phase stress. Proc Natl Acad Sci U S A *109*, 19775-19780.

Gotschlich, A., Huber, B., Geisenberger, O., Togl, A., Steidle, A., Riedel, K., Hill, P., Tummler, B., Vandamme, P., Middleton, B.*, et al.* (2001). Synthesis of multiple N-acylhomoserine lactones is wide-spread among the members of the *Burkholderia cepacia* complex. Syst Appl Microbiol *24*, 1-14.

Grant, S.G., Jessee, J., Bloom, F.R., and Hanahan, D. (1990). Differential plasmid rescue from transgenic mouse DNAs into *Escherichia coli* methylation-restriction mutants. Proc Natl Acad Sci U S A *87*, 4645-4649.

Greenbla.J, and Schleif, R. (1971). Arabinose C-protein - regulation of arabinose operon in-vitro. Nature-New Biology *233*, 166-&.

Ham, J.H. (2013). Intercellular and intracellular signalling systems that globally control the expression of virulence genes in plant pathogenic bacteria. Mol Plant Pathol *14*, 308-322.

Ham, J.H., Melanson, R.A., and Rush, M.C. (2011). *Burkholderia glumae*: next major pathogen of rice? Mol Plant Pathol *12*, 329-339.

Hauck, P., Thilmony, R., and He, S.Y. (2003). A *Pseudomonas syringae* type III effector suppresses cell wall-based extracellular defense in susceptible Arabidopsis plants. Proc Natl Acad Sci U S A *100*, 8577-8582.

He, P., Chintamanani, S., Chen, Z.Y., Zhu, L.H., Kunkel, B.N., Alfano, J.R., Tang, X.Y., and Zhou, J.M. (2004). Activation of a COI1-dependent pathway in Arabidopsis by *Pseudomonas syringae* type III effectors and coronatine. Plant Journal *37*, 589-602.

Healy, F.G., Wach, M., Krasnoff, S.B., Gibson, D.M., and Loria, R. (2000). The *txtAB* genes of the plant pathogen *Streptomyces acidiscabies* encode a peptide synthetase required for phytotoxin thaxtomin A production and pathogenicity. Molecular microbiology *38*, 794-804.

Hengge, R. (2009). Principles of c-di-GMP signalling in bacteria. Nat Rev Microbiol *7*, 263-273.

Hitzemann, R., Bottomly, D., Darakjian, P., Walter, N., Iancu, O., Searles, R., Wilmot, B., and McWeeney, S. (2013). Genes, behavior and next-generation RNA sequencing. Genes Brain and Behavior *12*, 1-12.

Howard, R.J., and Valent, B. (1996). Breaking and entering: host penetration by the fungal rice blast pathogen *Magnaporthe grisea*. Annu Rev Microbiol *50*, 491-512.

Iiyama, K., Furuya, N., Takanami, Y., and Matsuyama, N. (1995). A role of phytotoxin in virulence of Pseudomonas glumae. Ann Phytopathol Soc Jpn *61*, 470-476.

Jackson, R.W. (2009). Plant pathogenic bacteria: genomics and molecular biology (Norfolk, UK: Caister Academic Press).

Jacobs, J.L., Fasi, A.C., Ramette, A., Smith, J.J., Hammerschmidt, R., and Sundin, G.W. (2008). Identification and onion pathogenicity of Burkholderia cepacia complex isolates from the onion rhizosphere and onion field soil. Applied and environmental microbiology *74*, 3121-3129.

Jenal, U., and Malone, J. (2006). Mechanisms of cyclic-di-GMP signaling in bacteria. In Annu Rev Genet, pp. 385-407.

Jung, W.S., Lee, J., Kim, M.I., Ma, J., Nagamatsu, T., Goo, E., Kim, H., Hwang, I., Han, J., and Rhee, S. (2011). Structural and functional analysis of phytotoxin toxoflavin-degrading enzyme. PloS one *6*, e22443.

Kachroo, A., and Kachroo, P. (2007). Salicylic acid-, jasmonic acid- and ethylene-mediated regulation of plant defense signaling. Genetic engineering *28*.

Kamp, H.D., and Higgins, D.E. (2011). A protein thermometer controls temperature-dependent transcription of flagellar motility genes in Listeria monocytogenes. PLoS Pathog *7*.

Kang, Y., Kim, J., Kim, S., Kim, H., Lim, J.Y., Kim, M., Kwak, J., Moon, J.S., and Hwang, I. (2008). Proteomic analysis of the proteins regulated by HrpB from the plant pathogenic bacterium *Burkholderia glumae*. Proteomics *8*, 106-121.

Karki, H.S., Barphagha, I.K., and Ham, J.H. (2012a). A conserved two-component regulatory system, PidS/PidR, globally regulates pigmentation and virulence-related phenotypes of *Burkholderia glumae*. Mol Plant Pathol.

Karki, H.S., Shrestha, B.K., Han, J.W., Groth, D.E., Barphagha, I.K., Rush, M.C., Melanson, R.A., Kim, B.S., and Ham, J.H. (2012b). Diversities in virulence, antifungal activity, pigmentation and DNA fingerprint among strains of *Burkholderia glumae*. PLoS One *7*.

Kato, T., Tanaka, T., and Fujita, Y. (1992). Studies on bacterial seedling blight of rice. 1. Classification of bacteria, obtained from diseased seedling of rice in Yamagata prefecture. Bull Yamagata Agric Exp Stn *26*, 103-109.

Kazanov, M.D., Vitreschak, A.G., and Gelfand, M.S. (2007). Abundance and functional diversity of riboswitches in microbial communities. Bmc Genomics *8*.

Kearney, B., and Staskawicz, B.J. (1990). Characterization of IS476 and its role in bacterial spot disease of tomato and pepper. J Bacteriol *172*, 143-148.

Kim, H., Goo, E., Kang, Y., Kim, J., and Hwang, I. (2012). Regulation of universal stress protein genes by quorum sensing and RpoS in *Burkholderia glumae*. J Bacteriol *194*, 982-992.

Kim, J., Kang, Y., Choi, O., Jeong, Y., Jeong, J.E., Lim, J.Y., Kim, M., Moon, J.S., Suga, H., and Hwang, I. (2007a). Regulation of polar flagellum genes is mediated by quorum sensing and FlhDC in *Burkholderia glumae*. Mol Microbiol *64*, 165-179.

Kim, J., Kang, Y., Choi, O., Jeong, Y., Jeong, J.E., Lim, J.Y., Kim, M., Moon, J.S., Suga, H., and Hwang, I. (2007b). Regulation of polar flagellum genes is mediated by quorum sensing and FlhDC in Burkholderia glumae. Molecular microbiology *64*, 165-179.

Kim, J., Kim, J.G., Kang, Y., Jang, J.Y., Jog, G.J., Lim, J.Y., Kim, S., Suga, H., Nagamatsu, T., and Hwang, I. (2004a). Quorum sensing and the LysR-type transcriptional activator ToxR regulate toxoflavin biosynthesis and transport in Burkholderia glumae. Molecular microbiology *54*, 921-934.

Kim, J., Kim, J.G., Kang, Y., Jang, J.Y., Jog, G.J., Lim, J.Y., Kim, S., Suga, H., Nagamatsu, T., and Hwang, I. (2004b). Quorum sensing and the LysR-type transcriptional activator ToxR regulate toxoflavin biosynthesis and transport in *Burkholderia glumae*. Mol Microbiol *54*, 921-934.

Kim, J., and Park, W. (2013). Identification and characterization of genes regulated by AqsR, a LuxR-type regulator in *Acinetobacter oleivorans* DR1. Applied Microbiology and Biotechnology *97*, 6967-6978.

Kiratisin, P., and Sanmee, S. (2008). Roles and interactions of *Burkholderia pseudomallei* BpsIR quorum-sensing system determinants. J Bacteriol *190*, 7291-7297.

Knutsen, E., Ween, O., and Havarstein, L.S. (2004). Two separate quorum-sensing systems upregulate transcription of the same ABC transporter in *Streptococcus pneumoniae*. J Bacteriol *186*, 3078-3085.

Kong, Q.K., Yang, J.S., Liu, Q., Alamuri, P., Roland, K.L., and Curtiss, R. (2011). Effect of deletion of genes involved in lipopolysaccharide core and O-antigen synthesis on virulence and immunogenicity of *Salmonella enterica* serovar Typhimurium. Infect Immun *79*, 4227-4239.

Kotake, Y., Ishii, S., Yano, T., Katsuoka, Y., and Hayashi, H. (2008). Substrate recognition mechanism of the peptidase domain of the quorum-sensing-signal-producing ABC transporter ComA from *Streptococcus*. Biochemistry *47*, 2531-2538.

Kovach, M.E., Elzer, P.H., Hill, D.S., Robertson, G.T., Farris, M.A., Roop, R.M., 2nd, and Peterson, K.M. (1995). Four new derivatives of the broad-host-range cloning vector pBBR1MCS, carrying different antibiotic-resistance cassettes. Gene *166*, 175-176.

Kumari, A., Pasini, P., Deo, S.K., Flomenhoft, D., Shashidhar, H., and Daunert, S. (2006). Biosensing systems for the detection of bacterial quorum signaling molecules. Analytical Chemistry *78*, 7603-7609.

Kwon, Y.M., and Ricke, S.C. (2000). Efficient amplification of multiple transposon-flanking sequences. Journal of Microbiological Methods *41*, 195-199.

Leo, E. (2006). Quorum sensing in the genus *Burkholderia*. Int J Med Microbiol *296*, 103-110.

Lewenza, S., Conway, B., Greenberg, E.P., and Sokol, P.A. (1999). Quorum sensing in *Burkholderia cepacia*: Identification of the LuxRI homologs CepRI. J Bacteriol *181*, 748-756.

Lewenza, S., and Sokol, P.A. (2001). Regulation of ornibactin biosynthesis and N-acyl-L-homoserine lactone production by CepR in *Burkholderia cepacia*. J Bacteriol *183*, 2212-2218.

Li, B.Q., Li, N., Wang, F., Guo, L.M., Huang, Y., Liu, X.H., Wei, T.D., Zhu, D.Y., Liu, C.L., Pan, H.F.*, et al.* (2012). Structural insight of a concentration-dependent mechanism by which YdiV inhibits *Escherichia coli* flagellum biogenesis and motility. Nucleic Acids Research *40*, 11073-11085.

Liang, W., Pascual-Montano, A., Silva, A.J., and Benitez, J.A. (2007). The cyclic AMP receptor protein modulates quorum sensing, motility and multiple genes that affect intestinal colonization in *Vibrio cholerae*. Microbiology-(UK) *153*, 2964-2975.

Lim, J., Lee, T.H., Nahm, B.H., Choi, Y.D., Kim, M., and Hwang, I. (2011). Complete genome sequence of *Burkholderia glumae* BGR1. J Bacteriol *191*, 3758-3759.

Liu, H., Coulthurst, S.J., Pritchard, L., Hedley, P.E., Ravensdale, M., Humphris, S., Burr, T., Takle, G., Brurberg, M.B., Birch, P.R.J.*, et al.* (2008). Quorum sensing coordinates brute force and stealth modes of infection in the plant pathogen *Pectobacterium atrosepticum*. PLoS Pathog *4*.

Lopez, M.M., Bertolini, E., Olmos, A., Caruso, P., Gorris, M.T., Llop, P., Penyalver, R., and Cambra, M. (2003). Innovative tools for detection of plant pathogenic viruses and bacteria. International Microbiology *6*, 233-243.

Mae, A., Montesano, M., Koiv, V., and Palva, E.T. (2001). Transgenic plants producing the bacterial pheromone N-acyl-homoserine lactone exhibit enhanced resistance to the bacterial phytopathogen *Erwinia carotovora*. Mol Plant-Microbe Interact *14*, 1035-1042.

Maeda, Y., Kiba, A., Ohnishi, K., and Hikichi, Y. (2007). Amino acid substitutions in GyrA of *Burkholderia glumae* are implicated in not only oxolinic acid resistance but also fitness on rice plants. Appl Environ Microbiol *73*, 1114-1119.

Maeda, Y., Shinohara, H., Kiba, A., Ohnishi, K., Furuya, N., Kawamura, Y., Ezaki, T., Vandamme, P., Tsushima, S., and Hikichi, Y. (2006). Phylogenetic study and multiplex PCR-based detection of *Burkholderia plantarii*, *Burkholderia glumae* and *Burkholderia gladioli* using *gyrB* and *rpoD* sequences. International Journal of Systematic and Evolutionary Microbiology *56*, 1031-1038.

Malott, R.J., Baldwin, A., Mahenthiralingam, E., and Sokol, P.A. (2005). Characterization of the cciIR quorum-sensing system in *Burkholderia cenocepacia*. Infect Immun *73*, 4982-4992.

Malott, R.J., O'Grady, E.P., Toller, J., Inhulsen, S., Eberl, L., and Sokol, P.A. (2009). A *Burkholderia cenocepacia* orphan LuxR homolog is involved in quorum-sensing regulation. J Bacteriol *191*, 2447-2460.

Malott, R.J., and Sokol, P.A. (2007). Expression of the bviIR and cepIR quorum-sensing systems of *Burkholderia vietnamiensis*. J Bacteriol *189*, 3006-3016.

Marits, R., Koiv, V., Laasik, E., and Mae, A. (1999). Isolation of an extracellular protease gene of *Erwinia carotovora* subsp *carotovora* strain SCC3193 by transposon mutagenesis and the role of protease in phytopathogenicity. Microbiology-Uk *145*, 1959-1966.

Matsui, M., Tomita, M., and Kanai, A. (2013). Comprehensive computational analysis of bacterial CRP/FNR superfamily and its target motifs reveals stepwise evolution of transcriptional networks. Genome Biology and Evolution *5*, 267-282.

Mattinen, L., Nissinen, R., Riipi, T., Kalkkinen, N., and Pirhonen, M. (2007). Host-extract induced changes in the secretome of the plant pathogenic bacterium Pectobacterium atrosepticum. Proteomics *7*, 3527-3537.

Mattiuzzo, M., Bertani, I., Ferluga, S., Cabrio, L., Bigirimana, J., Guarnaccia, C., Pongor, S., Maraite, H., and Venturi, V. (2011). The plant pathogen *Pseudomonas fuscovaginae* contains two conserved quorum sensing systems involved in virulence and negatively regulated by RsaL and the novel regulator RsaM. Environ Microbiol *13*, 145-162.

McClean, K.H., Winson, M.K., Fish, L., Taylor, A., Chhabra, S.R., Camara, M., Daykin, M., Lamb, J.H., Swift, S., Bycroft, B.W.*, et al.* (1997). Quorum sensing and Chromobacterium violaceum: exploitation of violacein production and inhibition for the detection of N-acylhomoserine lactones. Microbiology *143 (Pt 12)*, 3703-3711.

McClure, R., Balasubramanian, D., Sun, Y., Bobrovskyy, M., Sumby, P., Genco, C.A., Vanderpool, C.K., and Tjaden, B. (2013). Computational analysis of bacterial RNA-Seq data. Nucleic Acids Research.

McGettigan, P.A. (2013). Transcriptomics in the RNA-seq era. Current Opinion in Chemical Biology *17*, 4-11.

Metcalf, W.W., Jiang, W., Daniels, L.L., Kim, S.K., Haldimann, A., and Wanner, B.L. (1996). Conditionally replicative and conjugative plasmids carrying *lacZ* alpha for cloning, mutagenesis, and allele replacement in bacteria. Plasmid *35*, 1-13.

Miller, M.B., and Bassler, B.L. (2001). Quorum sensing in bacteria. Annu Rev Microbiol *55*, 165-199.

Mills, D. (1985). Transposon mutagenesis and its potential for studying virulence genes in plant-pathogens. Annu Rev Phytopathol *23*, 297-320.

Mills, E., Pultz, I.S., Kulasekara, H.D., and Miller, S.I. (2011). The bacterial second messenger c-di-GMP: mechanisms of signalling. Cellular Microbiology *13*, 1122-1129.

Miyagawa, H., and Takaya, S. (2000). Biological control of bacterial grain rot of rice by avirulent strain of *Burkholderia gladioli*. Bull Chugoku Nat Agr Expt Sta *21*, 1-21.

Moreno-Paz, M., Gomez, M.J., Arcas, A., and Parro, V. (2010). Environmental transcriptome analysis reveals physiological differences between biofilm and planktonic modes of life of the iron oxidizing bacteria *Leptospirillum* spp. in their natural microbial community. Bmc Genomics *11*.

Morgan, M.K., and Chatterjee, A.K. (1985). Isolation and characterization of Tn5 insertion mutants of *Pseudomonas syringae* pv *syringae* altered in the production of the peptide phytotoxin syringotoxin. J Bacteriol *164*, 14-18.

Morgenstein, R.M., Clemmer, K.M., and Rather, P.N. (2010). Loss of the WaaL O-antigen ligase prevents surface activation of the flagellar gene cascade in *Proteus mirabilis*. J Bacteriol *192*, 3213-3221.

Mutz, K.-O., Heilkenbrinker, A., Loenne, M., Walter, J.-G., and Stahl, F. (2013). Transcriptome analysis using next-generation sequencing. Current Opinion in Biotechnology *24*, 22-30.

Nagamatsu, T. (2002). Syntheses, transformation, and biological activities of 7-azapteridine antibiotics: Toxoflavin, fervenulin, reumycin and their analogues. Chem Inform *33*, 261.

Nahar, K., Kyndt, T., De Vleesschauwer, D., Hofte, M., and Gheysen, G. (2011). The jasmonate pathway is a key player in systemically induced defense against root knot nematodes in Rice. Plant Physiology *157*, 305-316.

Nandakumar, R., Shahjahan, A.K.M., Yuan, X.L., Dickstein, E.R., Groth, D.E., Clark, C.A., Cartwright, R.D., and Rush, M.C. (2009a). *Burkholderia glumae* and *B. gladioli* cause bacterial panicle blight in rice in the southern United States. Plant Disease *93*, 896-905.

Nandakumar, R., Shahjahan, A.K.M., Yuan, X.L., Dickstein, E.R., Groth, D.E., Clark, C.A., Cartwright, R.D., and Rush, M.C. (2009b). *Burkholderia glumae* and *B. gladioli* cause bacterial panicle blight in rice in the southern United States. Plant Dis *93*, 896-905.

Ng, W.L., and Bassler, B.L. (2009). Bacterial quorum-sensing network architectures. In Annu Rev Genet, pp. 197-222.

Nystrom, T., and Neidhardt, F.C. (1992). Cloning, mapping and nucleotide sequencing of a gene encoding a universal stress protein in *Escherichia coli*. Molecular microbiology *6*, 3187-3198.

Okubara, P.A., Schroeder, K.L., and Paulitz, T.C. (2005). Real-time polymerase chain reaction: applications to studies on soilborne pathogens. Canadian Journal of Plant Pathology-Revue Canadienne De Phytopathologie *27*, 300-313.

Ouyang, Y.D., Chen, J.J., Xie, W.B., Wang, L., and Zhang, Q.F. (2009). Comprehensive sequence and expression profile analysis of Hsp20 gene family in rice. Plant Molecular Biology *70*, 341-357.

Parke, J.L., and Gurian-Sherman, D. (2001). Diversity of the *Burkholderia cepacia* complex and implications for risk assessment of biological control strains. Annu Rev Phytopathol *39*, 225-258.

Parsek, M.R., Val, D.L., Hanzelka, B.L., Cronan, J.E., and Greenberg, E.P. (1999). Acyl homoserine-lactone quorum-sensing signal generation. Proc Natl Acad Sci U S A *96*, 4360-4365.

Penfold, R.J., and Pemberton, J.M. (1992). An improved suicide vector for construction of chromosomal insertion mutations in bacteria. Gene *118*, 145-146.

Post, D.M.B., Yu, L.P., Krasity, B.C., Choudhury, B., Mandel, M.J., Brennan, C.A., Ruby, E.G., McFall-Ngai, M.J., Gibson, B.W., and Apicella, M.A. (2012). O-antigen and core carbohydrate of Vibrio fischeri lipopolysaccharide-composition and analysis of their role in Euprymna scolopes light organ colonization. Journal of Biological Chemistry *287*, 8515-8530.

Quinones, B., Dulla, G., and Lindow, S.E. (2005). Quorum sensing regulates exopolysaccharide production, motility, and virulence in *Pseudomonas syringae*. Mol Plant-Microbe Interact *18*, 682-693.

Raetz, C.R.H., and Whitfield, C. (2002). Lipopolysaccharide endotoxins. Annual Review of Biochemistry *71*, 635-700.

Ramos, C.G., da Costa, P.J.P., Doring, G., and Leitao, J.H. (2012). The novel cis-encoded small RNA h2cR is a negative regulator of hfq2 in Burkholderia cenocepacia. PLoS One *7*.

Ramos, C.G., Grilo, A.M., da Costa, P.J.P., Feliciano, J.R., and Leitao, J.H. (2013). MtvR is a global small noncoding regulatory RNA in *Burkholderia cenocepacia*. J Bacteriol *195*, 3514-3523.

Rao, K.M., and Rao Manibhushan, K.M.R. (1996). Sheath rot disease of rice (Daya Publishing House).

Raymann, K., Bobay, L.M., Doak, T.G., Lynch, M., and Gribaldo, S. (2013). A genomic survey of Reb homologs suggests widespread occurrence of R-bodies in proteobacteria. G3-Genes Genomes Genetics *3*, 505-516.

Rott, P.C., Costet, L., Davis, M.J., Frutos, R., and Gabriel, D.W. (1996). At least two separate gene clusters are involved in albicidin production by *Xanthomonas albilineans*. J Bacteriol *178*, 4590-4596.

Ryan, R.P., McCarthy, Y., Kiely, P.A., O'Connor, R., Farah, C.S., Armitage, J.P., and Dow, J.M. (2012). Dynamic complex formation between HD-GYP, GGDEF and PilZ domain proteins regulates motility in *Xanthomonas campestris*. Molecular microbiology *86*, 557-567.

Sambrook, J. (2001). Molecular cloning: a laboratory manual, 3rd Ed (Cold Spring Harbor Press).

Schaad, N.W., Jones, J.B., and Chun, W. (2001). Laboratory guide for identification of plant pathogenic bacteria. 3rd Ed. (The American Society of Phytopathological Society Press).

Schmid, N., Pessi, G., Deng, Y., Aguilar, C., Carlier, A.L., Grunau, A., Omasits, U., Zhang, L.-H., Ahrens, C.H., and Eberl, L. (2012). The AHL- and BDSF-dependent quorum sensing systems control specific and overlapping sets of genes in *Burkholderia cenocepacia* H111. PLoS One *7*.

Schmidtke, C., Findeiss, S., Sharma, C.M., Kuhfuss, J., Hoffmann, S., Vogel, J., Stadler, P.F., and Bonas, U. (2012). Genome-wide transcriptome analysis of the plant pathogen *Xanthomonas* identifies sRNAs with putative virulence functions. Nucleic Acids Research *40*, 2020-2031.

Schuhegger, R., Ihring, A., Gantner, S., Bahnweg, G., Knappe, C., Vogg, G., Hutzler, P., Schmid, M., Van Breusegem, F., Eberl, L.*, et al.* (2006). Induction of systemic resistance in tomato by N-acyl-L-homoserine lactone-producing rhizosphere bacteria. Plant Cell and Environment *29*, 909-918.

Severin, A.J., Woody, J.L., Bolon, Y.-T., Joseph, B., Diers, B.W., Farmer, A.D., Muehlbauer, G.J., Nelson, R.T., Grant, D., Specht, J.E.*, et al.* (2010). RNA-seq atlas of glycine max: a guide to the soybean transcriptome. Bmc Plant Biology *10*.

Shahjahan, A.K.M., Rush, M.C., Groth, D., and Clark, C. (2000b). Panicle blight. Rice J *15*, 26-29.

Sharma, S.B., and Signer, E.R. (1990). Temporal and spatial regulation of the symbiotic genes of rhizobium-meliloti in planta revealed by transposon tn5-gusA. Genes Dev *4*, 344-356.

Shingu, Y., and Yoneyama, K. (2004). Essential regulator gene *tox*R for toxoflavin biosynthesis of *Burkholderia glumae*. Journal of General Plant Pathology *70*, 108-114.

Silva, A.J., Sultan, S.Z., Liang, W.L., and Benitez, J.A. (2008). Role of the histone-like nucleoid structuring protein in the regulation of *rpoS* and RpoS-dependent genes in *Vibrio cholerae*. J Bacteriol *190*, 7335-7345.

Simon, R., Priefer, U., and Puhler, A. (1983). A broad host range mobilization systemfor in vitro genetic engineering: transposition mutagenesis in Gram negative bacteria. Biotechnology *1*, 784-791.

Sjoblom, S., Harjunpaa, H., Brader, G., and Palva, E.T. (2008). A novel plant ferredoxin-like protein and the regulator hor are quorum-sensing targets in the plant pathogen *Erwinia carotovora*. Mol Plant-Microbe Interact *21*, 967-978.

Sokol, P.A., Sajjan, U., Visser, M.B., Gingues, S., Forstner, J., and Kooi, C. (2003). The CepIR quorum-sensing system contributes to the virulence of *Burkholderia cenocepacia* respiratory infections. Microbiology-(UK) *149*, 3649-3658.

Solis, R., Bertani, I., Degrassi, G., Devescovi, G., and Venturi, V. (2006). Involvement of quorum sensing and RpoS in rice seedling blight caused by *Burkholderia plantarii*. Fems Microbiology Letters *259*, 106-112.

Sondermann, H., Shikuma, N.J., and Yildiz, F.H. (2012). You've come a long way: c-di-GMP signaling. Current Opinion in Microbiology *15*, 140-146.

Song, Y., Xie, C., Ong, Y.M., Gan, Y.H., and Chua, K.L. (2005). The BpsIR quorum-sensing system of *Burkholderia pseudomallei*. J Bacteriol *187*, 785-790.

Sorek, R., and Cossart, P. (2010). Prokaryotic transcriptomics: a new view on regulation, physiology and pathogenicity. Nature Reviews Genetics *11*, 9-16.

Staudinger, W. (2007). Investigations on flagellar biogenesis, motility and signal transduction of *Halobacterium salinarum*. In Membrane Biochemistry (Max Planck Institute of Biochemistry).

Stone, J.K., Mayo, M., Grasso, S.A., Ginther, J.L., Warrington, S.D., Allender, C.J., Doyle, A., Georgia, S., Kaestli, M., Broomall, S.M.*, et al.* (2012). Detection of *Burkholderia pseudomallei* O-antigen serotypes in near-neighbor species. Bmc Microbiology *12*.

Stoyanova, M., Pavlina, I., Moncheva, P., and Bogatzevska, N. (2007). Biodiversity and incidence of *Burkholderia* species. Biotechnology & Biotechnological Equipment *21*, 306-310.

Suarez-Moreno, Z.R., Devescovi, G., Myers, M., Hallack, L., Mendonca-Previato, L., Caballero-Mellado, J., and Venturi, V. (2010). Commonalities and differences in regulation of N-Acyl Homoserine Lactone quorum sensing in the beneficial plant-associated *Burkholderia* species cluster. Appl Environ Microbiol *76*, 4302-4317.

Subramoni, S., and Venturi, V. (2009). LuxR-family 'solos': bachelor sensors/regulators of signalling molecules. Microbiology-(UK) *155*, 1377-1385.

Suzuki, F., Sawada, H., Azegami, K., and Tsuchiya, K. (2004a). Molecular characterization of the tox operon involved in toxoflavin biosynthesis of *Burkholderia glumae*. J Gen Plant Pathol *70*, 97-107.

Suzuki, F., Sawada, H.A., Zegami, K., and Tsuchiya, K. (2004b). Molecular characterization of the *tox* operon involved in toxoflavin biosynthesis of *Burkholderia glumae*. J Gen Plant Pathol *70*, 97-107.

Svenningsen, S.L., Waters, C.M., and Bassler, B.L. (2008). A negative feedback loop involving small RNAs accelerates *Vibrio cholerae* transition out of quorum-sensing mode. Genes Dev *22*, 226-238.

Takeuchi, T., Sawada, H., Suzuki, F., and Matsuda, I. (1997). Specific detection of *Burkholderia plantarii* and *B. glumae* by PCR using primers selected from the 16S-23S rDNA spacer regions. Annals of the Phytopathological Society of Japan *63*, 455-462.

Takle, G.W., Toth, I.K., and Brurberg, M.B. (2007). Evaluation of reference genes for real-time RT-PCR expression studies in the plant pathogen *Pectobacterium atrosepticum*. Bmc Plant Biology *7*.

Tamura, K., Peterson, D., Peterson, N., Stecher, G., Nei, M., and Kumar, S. (2011). MEGA5: Molecular evolutionary genetics analysis using maximum likelihood, evolutionary distance, and maximum parsimony methods. Molecular Biology and Evolution *28*, 2731-2739.

Thomashow, M.F., Karlinsey, J.E., Marks, J.R., and Hurlbert, R.E. (1987). Identification of a new virulence locus in *Agrobacterium tumefaciens* that affects polysaccharide composition and plant cell attachment. J Bacteriol *169*, 3209-3216.

Thomsen, L.E., Chadfield, M.S., Bispham, J., Wallis, T.S., Olsen, J.E., and Ingmer, H. (2003). Reduced amounts of LPS affect both stress tolerance and virulence of *Salmonella enterica* serovar Dublin. Fems Microbiology Letters *228*, 225-231.

Tjaden, B., Goodwin, S.S., Opdyke, J.A., Guillier, M., Fu, D.X., Gottesman, S., and Storz, G. (2006). Target prediction for small, noncoding RNAs in bacteria. Nucleic Acids Research *34*, 2791-2802.

Toguchi, A., Siano, M., Burkart, M., and Harshey, R.M. (2000). Genetics of swarming motility in *Salmonella enterica* serovar Typhimurium: critical role for lipopolysaccharide. J Bacteriol *182*, 6308-6321.

Trimble, M.J., and McCarter, L.L. (2011). Bis-(3 '-5 ')-cyclic dimeric GMP-linked quorum sensing controls swarming in *Vibrio parahaemolyticus*. Proc Natl Acad Sci U S A *108*, 18079-18084.

Venturi, V., Rampioni, G., Pongor, S., and Leoni, L. (2011). The virtue of temperance: built-in negative regulators of quorum sensing in *Pseudomonas*. Molecular microbiology *82*, 1060-1070.

von Bodman, S.B., Bauer, W.D., and Coplin, D.L. (2003). Quorum sensing in plant-pathogenic bacteria. Annu Rev Phytopathol *41*, 455-482.

von Bodman, S.B., Majerczak, D.R., and Coplin, D.L. (1998). A negative regulator mediates quorum-sensing control of exopolysaccharide production in *Pantoea stewartii* subsp. *stewartii*. Proc Natl Acad Sci U S A *95*, 7687-7692.

Wada, T., Morizane, T., Abo, T., Tominaga, A., Inoue-Tanaka, K., and Kutsukake, K. (2011). EAL domain protein YdiV acts as an anti-FlhD(4)C(2) factor responsible for nutritional control of the flagellar regulon in *Salmonella enterica* serovar Typhimurium. J Bacteriol *193*, 1600-1611.

Wagner, V.E., Gillis, R.J., and Iglewski, B.H. (2004). Transcriptome analysis of quorum-sensing regulation and virulence factor expression in *Pseudomonas aeruginosa*. Vaccine *22*, S15-S20.

Wang, D., Seeve, C., Pierson, L.S., III, and Pierson, E.A. (2013). Transcriptome profiling reveals links between ParS/ParR, MexEF-OprN, and quorum sensing in the regulation of adaptation and virulence in *Pseudomonas aeruginosa*. Bmc Genomics *14*.

Wang, H.X., Ayala, J.C., Silva, A.J., and Benitez, J.A. (2012). The histone-like nucleoid structuring protein (H-NS) is a repressor of *Vibrio cholerae* exopolysaccharide biosynthesis (*vps*) genes. Appl Environ Microbiol *78*, 2482-2488.

Wang, X.Y., and Quinn, P.J. (2010). Lipopolysaccharide: biosynthetic pathway and structure modification. Progress in Lipid Research *49*, 97-107.

Waters, C.M., and Bassler, B.L. (2005). Quorum sensing: Cell-to-cell communication in bacteria. In Annual Review of Cell and Developmental Biology, pp. 319-346.

Weller, S.A., Elphinstone, J.G., Smith, N.C., Boonham, N., and Stead, D.E. (2000). Detection of *Ralstonia solanacearum* strains with a quantitative, multiplex, real-time, fluorogenic PCR (TaqMan) assay. Appl Environ Microbiol *66*, 2853-2858.

Winzer, K., Hardie, K.R., Burgess, N., Doherty, N., Kirke, D., Holden, M.T.G., Linforth, R., Cornell, K.A., Taylor, A.J., Hill, P.J.*, et al.* (2002). LuxS: its role in central metabolism and the *in vitro* synthesis of 4-hydroxy-5-methyl-3(2H)-furanone. Microbiology-(UK) *148*, 909-922.

Wosten, M., van Dijk, L., Veenendaal, A.K.J., de Zoete, M.R., Bleumink-Pluijm, N.M.C., and van Putten, J.P.M. (2010). Temperature-dependent FlgM/FliA complex formation regulates Campylobacter jejuni flagella length. Molecular microbiology *75*, 1577-1591.

Yabuuchi, E., Kosako, Y., Oyaizu, H., Yano, I., Hotta, H., Hashimoto, Y., Ezaki, T., and Arakawa, M. (1992). Proposal of *Burkholderia* gen. nov. and transter of 7 species of the genus *Pseudomonas* homology group-II to the new genus, with the type species *Burkholderia cepacia* (Palleroni and Holmes 1981) comb. nov. Microbiol Immunol *36*, 1251-1275.

Yamanaka, K., Zheng, W.D., Crooke, E., Wang, Y.H., and Inouye, M. (2001). CspD, a novel DNA replication inhibitor induced during the stationary phase in *Escherichia coli*. Molecular microbiology *39*, 1572-1584.

Yoder-Himes, D.R., Chain, P.S.G., Zhu, Y., Wurtzel, O., Rubin, E.M., Tiedje, J.M., and Sorek, R. (2009). Mapping the *Burkholderia cenocepacia* niche response via high-throughput sequencing. Proc Natl Acad Sci U S A *106*, 3976-3981.

Yoshida, H., Bogaki, M., Nakamura, M., and Nakamura, S. (1990). Quinolone resistance-determining region in the DNA gyrase gyrA gene of *Escherichia coli*. Antimicrobial Agents and Chemotherapy *34*, 1271-1272.

Yuan, X. (2004). Identification of bacterial pathogens causing panicle blight of rice in Louisiana. In Plant Pathology and Crop Physiology (Baton Rouge: Louisiana State University).

Zheng, A.P., Lin, R.M., Zhang, D.H., Qin, P.G., Xu, L.Z., Ai, P., Ding, L., Wang, Y.R., Chen, Y., Liu, Y.*, et al.* (2013). The evolution and pathogenic mechanisms of the rice sheath blight pathogen. Nature Communications *4*.

Zhou, H., Yao, F., Roberts, D.P., and Lessie, T.G. (2003). AHL-deficient mutants of *Burkholderia ambifaria* BC-F have decreased antifungal activity. Current Microbiology *47*, 174-179.

APPENDIX 1. GENES DIFFERENTLY EXPRESSED IN 336GR-1 AND LSUPB134 WITH Q VALUE LESS THAN 0.01.

Transcription Start	Translation Start	Translation Stop	Transcription Stop	Synonym	Product	E-value in WT	E-value LSUPB134	Str-and	5' UTR
184647	184722	185018	185047	bglu_1g01760	histone-like nucleoid-structuring protein H-NS	1298	198	+	75
209168	209213	210631	210639	bglu_1g01990	S-adenosyl-L-homocysteine hydrolase	1613	438	+	45
432078	431939	431736	431713	bglu_1g04140	Cold shock-like protein CspD	138	1733	-	139
	568804	569814		bglu_1g05390	allantoicase	1	28	+	
591328	591349	592242	592294	bglu_1g05590	glutamate/aspartate ABC transporter periplasmic glutamate/aspartate-binding protein	336	1433	+	21
	832318	830927		bglu_1g07680	coproporphyrinogen III oxidase	9	44	-	
902203	902316	902519	902533	bglu_1g08360	Cold-shock DNA-binding domain-containing protein	4413	580	+	113
902581	902637	903782	903782	bglu_1g08370	Exonuclease, DNA polymerase III, epsilon subunit family/GIY-YIG catalytic domain-containing protein	316	66	+	56
	908241	910517		bglu_1g08430	5-methyltetrahydropteroyltriglutamate--homocysteine S-methyltransferase	433	8	+	
1486607	1486631	1486903	1486972	bglu_1g13530	dna-binding protein hu-beta	28	495	+	24
1756218	1756228	1757418	1757428	bglu_1g16040	2-nitropropane dioxygenase family oxidoreductase	56	386	+	10
1757469	1757484	1758125	1758164	bglu_1g16050	OmpW family protein	175	1356	+	15
	1828440	1829153		bglu_1g16610	LuxR family autoinducer-binding transcriptional regulator	20	0	+	
	1831314	1832873		bglu_1g16630	AMP-dependent synthetase and ligase	67	0	+	
	1834945	1835280		bglu_1g16670	4Fe-4S ferredoxin iron-sulfur-binding domain-containing protein	100	0	+	
	1837176	1838441		bglu_1g16690	beta-ketoacyl synthase	20	0	+	

Table continued

Transcription Start	Translation Start	Translation Stop	Transcription Stop	Synonym	Product	E-value in WT	E-value LSUPB134	Str-and	5' UTR
	1839388	1840437		bglu_1g16710	alpha/beta hydrolase fold protein	17	0	+	
	1840444	1841160	1841160	bglu_1g16720	hypothetical protein	57	0	+	
	1841263	1842180		bglu_1g16730	hypothetical protein	31	0	+	
	1844183	1844629		bglu_1g16760	Thioesterase superfamily protein	35	0	+	
	1846225	1847226		bglu_1g16780	formyltetrahydrofolate deformylase	22	0	+	
	1847283	1848059		bglu_1g16790	ferredoxin--NADP reductase	19	0	+	
	1859777	1864318	1864318	bglu_1g16890	siderophore non-ribosomal peptide synthetase MbaF	126	9	+	
	1864326	1868825		bglu_1g16900	TubF protein	126	11	+	
	1868818	1872780		bglu_1g16910	TubD protein	107	9	+	
	1878621	1881047		bglu_1g16940	metallo-beta-lactamase family protein	142	25	+	
	1885418	1884495		bglu_1g16980	CmaB protein	494	57	-	
1983107	1983076	1982285	1982285	bglu_1g18030	ABC transporter-like protein	12	84	-	31
1983854	1983854	1983108	1983108	bglu_1g18040	Polar amino acid ABC transporter inner membrane subunit	7	76	-	
1984657	1984598	1983873	1983855	bglu_1g18050	amino acid ABC transporter inner membrane subunit	9	76	-	59
1985607	1985547	1984699	1984681	bglu_1g18060	amino acid ABC transporter periplasmic ligand binding protein	35	536	-	60
2005946	2005944	2005753	2005753	bglu_1g18330	hypothetical protein	3	113	-	2
2345762	2345761	2345120	2345120	bglu_1g21560	3-oxoadipate CoA-succinyl transferase subunit beta	2778	356	-	1
2346509	2346467	2345763	2345763	bglu_1g21570	3-oxoacid CoA-transferase subunit A	1371	291	-	42
	2513309	2512188		bglu_1g22970	diguanylate cyclase	15	0	-	
	2534389	2533643	2533643	bglu_1g23050	pyrroloquinoline quinone (coenzyme pqq) biosynthesis protein c	484	0	-	
	2536823	2537848	2537848	bglu_1g23070	Cysteine synthase	141	0	+	
	2538521	2539483		bglu_1g23090	Amidohydrolase family protein	169	0	+	
	2541200	2540808	2540808	bglu_1g23110	translation initiation inhibitor	151	0	-	
2544543	2544543	2543410	2543410	bglu_1g23140	ThiJ/PfpI family protein	583	21	-	0
	3570682	3572331		bglu_1g31420	2-isopropylmalate synthase	6	33	+	

Table continued

Transcription Start	Translation Start	Translation Stop	Transcription Stop	Synonym	Product	E-value in WT	E-value LSUPB134	Str-and	5' UTR
3575269	3575277	3575549		bglu_1g31460	hypothetical protein	20	237	+	8
	3575536	3577110	3577110	bglu_1g31470	cytochrome bd ubiquinol oxidase subunit I	15	186	+	
410194			410148	predicted RNA	antisense: bglu_1g03950	0	210	-	
749382			749306	predicted RNA	-	273	0	-	
910720			910843	predicted RNA	antisense: bglu_1g08440	310	0	+	
1825398			1825292	predicted RNA	-	233	0	-	
1854774			1854726	predicted RNA	-	574	0	-	
2553411			2553307	predicted RNA	-	394	0	-	
2547245			2547201	predicted RNA	-	643	0	-	
2514652			2514607	predicted RNA	-	542	0	-	
1111047			1111152	predicted RNA	-	364	3100	+	
2536744			2536822	predicted RNA	-	215	0	+	
2543409			2543339	predicted RNA	-	226	0	-	
2552217			2552128	predicted RNA	-	169	0	-	
3447223			3447187	predicted RNA	antisense: bglu_1g30330	0	211	-	
2534756			2534818	predicted RNA	-	234	0	+	
697028			696960	predicted RNA	-	22	299	-	
749206			749161	predicted RNA	-	299	0	-	
3206420			3206483	predicted RNA	antisense: bglu_1g28260	43	406	+	
3165627			3165676	predicted RNA	antisense: bglu_1g27930	48	417	+	
2094630			2094576	predicted RNA	-	270	2	-	
57300	57281	56532	56520	bglu_2g00530	Crp/Fnr family transcriptional regulator	54	258	-	19
	84899	83454		bglu_2g00820	aldehyde dehydrogenase	0	16	-	
	106495	107634		bglu_2g01020	ornithine cyclodeaminase	7	42	+	
	107708	108130		bglu_2g01030	endoribonuclease L-PSP	7	55	+	
144794	144816	145547		bglu_2g01310	GntR family transcriptional regulator	6	62	+	22
	145544	146707		bglu_2g01320	FMN-dependent alpha-hydroxy acid dehydrogenase	10	48	+	
	325267	325659		bglu_2g02780	Pectin degradation protein kdgF	35	0	+	
	395031	396233		bglu_2g03350	beta-ketoadipyl CoA thiolase	319	55	+	
	590925	588640		bglu_2g04930	5-methyltetrahydropteroyltriglutamate/homocysteine S-methyltransferase	15	0	-	
599439	599439	599741		bglu_2g05000	sarcosine oxidase subunit delta	61	0	+	

Table continued

Transcription Start	Translation Start	Translation Stop	Transcription Stop	Synonym	Product	E-value in WT	E-value LSUPB134	Str-and	5' UTR
	634645	634220		bglu_2g05270	hypothetical protein	50	0	-	
	677621	676152		bglu_2g05630	betaine aldehyde dehydrogenase	7	39	-	
	681572	683230		bglu_2g05670	EmrB/QacA subfamily drug resistance transporter	45	0	+	
	690946	691824		bglu_2g05740	putative Branched-chain amino acid aminotransferase	240	0	+	
692555	692555	693442		bglu_2g05760	phenazine biosynthesis PhzC/PhzF protein	139	0	+	
	765814	762722		bglu_2g06360	putative RND efflux transporter	439	3	-	
766950	766950	765811		bglu_2g06370	putative RND efflux membrane-fusion protein	184	0	-	
	767565	766990		bglu_2g06380	hypothetical protein	93	0	-	
	769152	769889	769889	bglu_2g06400	putative ubiquinone/menaquinone biosynthesis methyltransferase	5143	2	+	
	769891	770649		bglu_2g06410	GTP cyclohydrolase II	4625	2	+	
	770646	772337	772337	bglu_2g06420	WD-repeat-containing protein	4650	2	+	
	772445	773425		bglu_2g06430	serine/threonine kinase	1341	5	+	
	773425	774579		bglu_2g06440	riboflavin biosynthesis protein RibD	1116	5	+	
816774	816774	816043		bglu_2g06890	TenA family transcriptional activator	96	0	-	
	817470	816787	816787	bglu_2g06900	hypothetical protein	64	0	-	
	817866	817474	817474	bglu_2g06910	S-adenosylmethionine decarboxylase	63	0	-	
	835033	833645		bglu_2g07060	polygalacturonase	18	0	-	
	918549	918028		bglu_2g07570	PPE-repeat-containing protein	24	0	-	
	1260114	1246021		bglu_2g09910	Non-ribosomal peptide synthetase/polyketide synthase	117	1	-	
	1848065	1847346		bglu_2g14470	quorum sensing LuxR family sensor regulator	288	0	-	
1848141	1848141	1848593		bglu_2g14480	hypothetical protein	58	0	+	
1848865	1848865	1849476		bglu_2g14490	quorum sensing autoinducer synthase	114	0	+	

Table continued

Transcription Start	Translation Start	Translation Stop	Transcription Stop	Synonym	Product	E-value in WT	E-value LSUPB134	Str-and	5' UTR
1913274	1913222	1912998	1912998	bglu_2g15070	hypothetical protein	0	62	-	52
	2095671	2095402		bglu_2g16700	RebB protein	205	0	-	
	2180750	2184547		bglu_2g17390	nitrate reductase subunit alpha	4	40	+	
	2199314	2200108	2200108	bglu_2g17550	cyclopropane-fatty-acyl-phospholipid synthase	62	0	+	
	2200146	2201312		bglu_2g17560	putative gamma-butyrobetaine,2-oxoglutarate dioxygenase	37	0	+	
2299255	2299255	2298842	2298842	bglu_2g18430	heat shock protein Hsp20	816	130	-	
	2305361	2306308		bglu_2g18490	sugar ABC transporter periplasmic protein	2	23	+	
	2322481	2322020		bglu_2g18630	Insertion element IS402	2122	39	-	
	2341585	2341055		bglu_2g18780	transferase	8173	13	-	
	2343215	2341593	2341593	bglu_2g18790	hypothetical protein	4507	7	-	
	2406217	2404595		bglu_2g19330	chaperonin GroEL	227	47	-	
	2589411	2589860		bglu_2g20920	general secretion pathway protein I	27	0	+	
2632491	2632443	2631055	2631052	bglu_2g21230	anthranilate 1,2-dioxygenase subunit alpha	89	313	-	48
148599			148634	predicted RNA	-	0	270	+	
318997			319053	predicted RNA	-	454	0	+	
696150			696225	predicted RNA	antisense: bglu_2g05790	247	0	+	
741577			741568	predicted RNA	-	146	0	-	
761069			761078	predicted RNA	antisense: bglu_2g06340	155	0	+	
772338			772444	predicted RNA	-	1194	0	+	
1239003			1238994	predicted RNA	-	146	0	-	
1268019			1267604	predicted RNA	-	627	0	-	
1848285			1848066	predicted RNA	antisense: bglu_2g14480	272	0	-	
1848660			1848337	predicted RNA	antisense: bglu_2g14480	233	0	-	
1849575			1849658	predicted RNA	antisense: bglu_2g14500	213	0	+	
2158802			2158841	predicted RNA	antisense: bglu_2g17200	0	207	+	
2341054			2339949	predicted RNA	antisense: bglu_2g18770	2050	0	-	
2343262			2343216	predicted RNA	-	2638	0	-	
2684927			2684884	predicted RNA	-	0	225	-	
2196108			2196062	predicted RNA	-	356	0	-	
2589223			2589287	predicted RNA	-	246	0	+	
2162072			2162047	predicted RNA	antisense: bglu_2g17230	4044	21538	-	
81918			81889	predicted RNA	-	0	231	-	
1304941			1304996	predicted RNA	-	60	486	+	

Table continued

Transcription Start	Translation Start	Translation Stop	Transcription Stop	Synonym	Product	E-value in WT	E-value LSUPB134	Str-and	5' UTR
1913549			1913404	predicted RNA	-	42	267	-	
1593116			1593009	predicted RNA	-	22	186	-	
2100124			2100094	predicted RNA	antisense: bglu_2g16740	0	207	-	
1305443			1305584	predicted RNA	-	40	241	+	
2193685			2193625	predicted RNA	antisense: bglu_2g17480	202	0	-	
917050			916075	predicted RNA	antisense: bglu_2g07560	338	105	-	
	38148	36934		bglu_1p0350	monooxygenase FAD-binding protein	25	0	-	
	38521	38787		bglu_1p0360	ferric uptake regulator family protein	80	0	+	
	39751	38900		bglu_1p0370	AraC family transcriptional regulator	108	0	-	
	46278	46036	46036	bglu_1p0460	hypothetical protein	138	0	-	
	46886	46566		bglu_1p0470	transcriptional modulator of MazE/toxin, MazF	70	0	-	
47128	47128	46880		bglu_1p0480	transcriptional regulator/antitoxin, MazE	101	0	-	
	63450	65174		bglu_1p0660	methyl-accepting chemotaxis sensory transducer	20	0	+	
82147	82147	83994	83994	bglu_1p0890	peptidase C11	66	0	+	
105168			105213	predicted RNA	-	18	451	+	
45875			45826	predicted RNA	-	289	0	-	
46345			46279	predicted RNA	-	189	0	-	
13286	13286	13963	13963	bglu_2p0150	hypothetical protein	49	0	+	
	14604	15332		bglu_2p0170	IS element transposase	18	0	+	
	17054	15702		bglu_2p0180	Fis family two component sigma54 specific transcriptional regulator	26	0	-	
	55838	55068		bglu_2p0520	transposase B	26	0	-	
	56888	58075	58075	bglu_2p0540	8-amino-7-oxononanoate synthase	99	0	+	
	58154	59320		bglu_2p0550	D-amino acid oxidase Aao_1	75	0	+	
59323	59323	60306	60306	bglu_2p0560	zinc-containing alcohol dehydrogenase superfamily protein	52	0	+	
60347	60347	61357	61357	bglu_2p0570	biotin synthetase	99	0	+	
	61394	63157		bglu_2p0580	carbamoyltransferase	85	0	+	
	71224	77619		bglu_2p0600	polyketide synthase	39	0	+	
	77619	84764		bglu_2p0610	beta-ketoacyl synthase	34	0	+	

Table continued

Transcription Start	Translation Start	Translation Stop	Transcription Stop	Synonym	Product	E-value in WT	E-value LSUPB134	Str-and	5' UTR
	84890	85351		bglu_2p0620	putative exported avidin family protein	639	0	+	
	85523	86782	86782	bglu_2p0630	major facilitator superfamily protein	38	0	+	
	86817	87365	87365	bglu_2p0640	methylmalonyl-CoA epimerase	44	0	+	
	87408	89612		bglu_2p0650	methylmalonyl-CoA mutase	24	0	+	
	94170	93118		bglu_2p0700	AraC family transcriptional regulator	34	0	-	
84808			84889	predicted RNA	-	315	0	+	
85352			85443	predicted RNA	-	245	0	+	
56763			56887	predicted RNA	-	235	0	+	
	77891	78619		bglu_3p0710	IS element transposase	25	0	+	
	130818	130141		bglu_3p1280	hypothetical protein	22	0	-	
11922			12043	predicted RNA	antisense: bglu_3p0090	11571	3845	+	
108838	108838	108587		bglu_4p0960	PAAR repeat-containing protein	141	0	-	
	109387	108851		bglu_4p0970	hypothetical protein	80	0	-	
109461			109402	predicted RNA	-	339	0	-	
15217			15336	predicted RNA	antisense: bglu_4p0120	2513	743	+	

APPENDIX 2. THE EXPRESSION CONDITION OF 344 GENES THAT WERE UP-REGULATED BY QS AS DISPLAYED BY HEAT MAPS.

The expression level changed more than 8-fold between 336gr-1 and LSUPB134. Heat Maps were generated by ArrayStar to indicate the level of expression by extension of the color. Each row represents an individual gene. The left column in the grid represents the expression condition of genes in 336gr-1. The right column represents the expression condition of genes in LSUPB134.

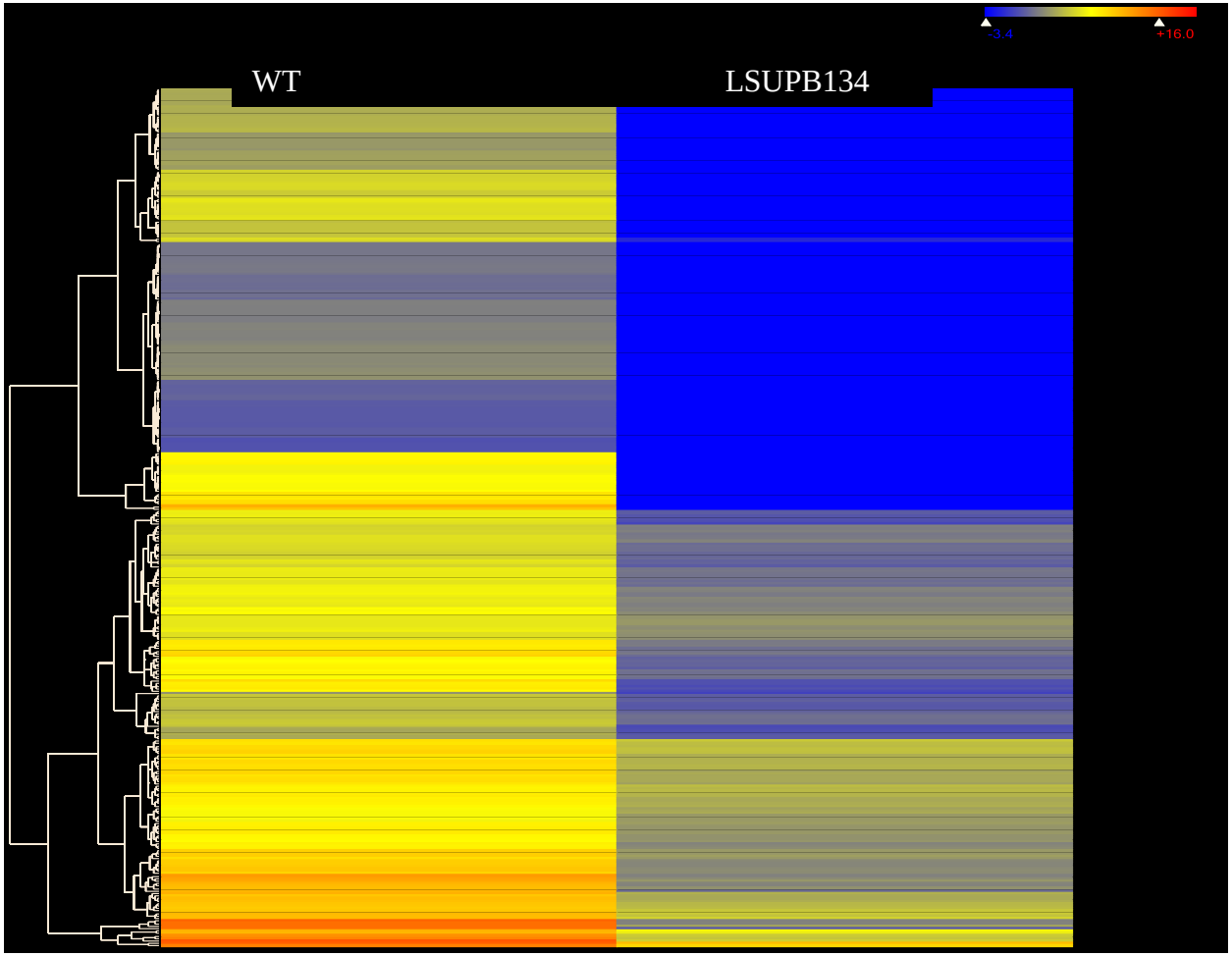

The following figures in Appendix 2 are close shot of different clusters

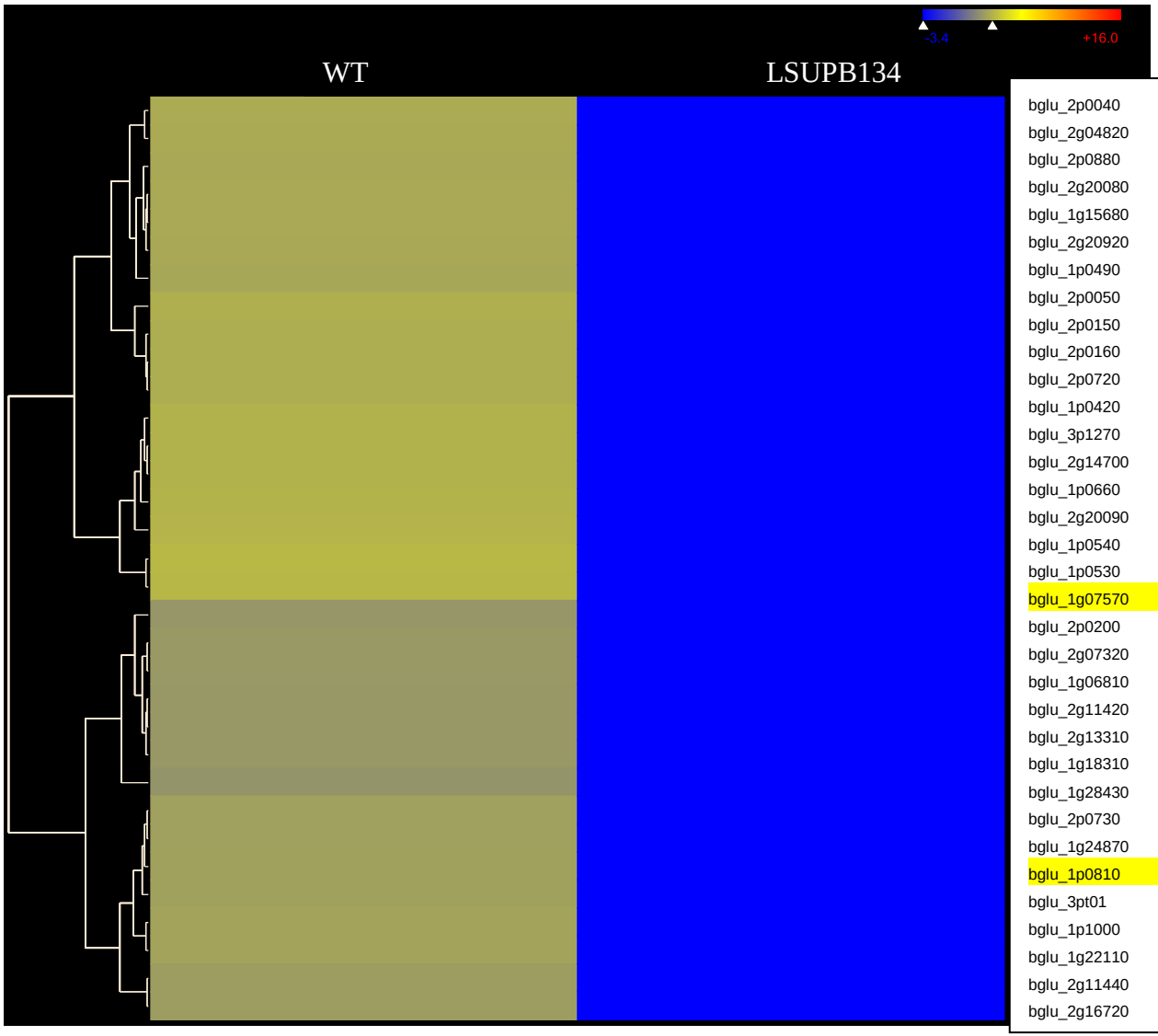

bglu_2p0040	hypothetical protein
bglu_2g04820	hypothetical protein
bglu_2p0880	hypothetical protein
bglu_2g20080	hypothetical protein
bglu_1g15680	bacteriophage protein
bglu_2g20920	general secretion pathway protein I
bglu_1p0490	integrase
bglu_2p0050	RES domain-containing protein
bglu_2p0150	hypothetical protein
bglu_2p0160	general secretion pathway protein I
bglu_2p0720	glucose-methanol-choline oxidoreductase
bglu_1p0420	transposase
bglu_3p1270	general secretion pathway protein I
bglu_2g14700	hypothetical protein
bglu_1p0660	methyl-accepting chemotaxis sensory transducer
bglu_2g20090	hypothetical protein
bglu_1p0540	sulfotransferase
bglu_1p0530	adenylylsulfate kinase
bglu_1g07570	urease subunit gamma
bglu_2p0200	Mn-containing catalase
bglu_2g07320	metallophosphoesterase
bglu_1g06810	hypothetical protein
bglu_2g11420	endoribonuclease L-PSP
bglu_2g13310	hypothetical protein
bglu_1g18310	hypothetical protein
bglu_1g28430	hypothetical protein
bglu_2p0730	alpha/beta hydrolase protein
bglu_1g24870	transmembrane efflux protein
bglu_1p0810	AraC family two component transcriptional regulator
bglu_3pt01	tRNA-Arg
bglu_1p1000	pyridoxamine 5'-phosphate oxidase family protein
bglu_1g22110	Xylono-1,4-lactonase
bglu_2g11440	anthranilate synthase component II
bglu_2g16720	hypothetical protein

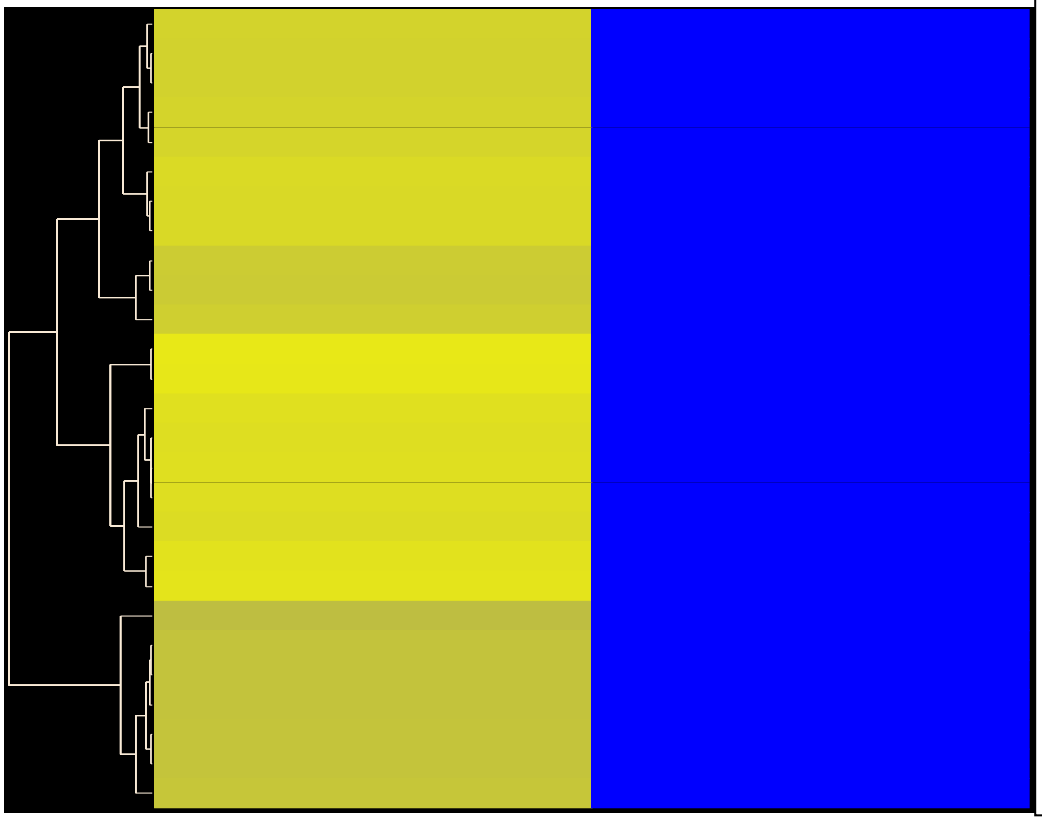

bglu_2p0180	Fis family two component sigma54 specific transcriptional regulator
bglu_2p0650	methylmalonyl-CoA mutase
bglu_4p0990	PAAR repeat-containing protein
bglu_1p0800	AraC family two component transcriptional regulator
bglu_1g16820	Branched-chain amino acid ABC-type transport system, permease
bglu_2p0610	beta-ketoacyl synthase
bglu_2p0700	AraC family transcriptional regulator
bglu_1p0350	monooxygenase FAD-binding protein
bglu_2p0520	transposase B
bglu_1g16690	beta-ketoacyl synthase
bglu_4p0200	hypothetical protein
bglu_2p0560	zinc-containing alcohol dehydrogenase superfamily protein
bglu_2p0590	short-chain dehydrogenase/reductase SDR
bglu_2p0600	polyketide synthase
bglu_2p0630	major facilitator superfamily protein
bglu_2p0640	methylmalonyl-CoA epimerase
bglu_1p0850	transposase
bglu_4p1080	hypothetical protein
bglu_1p0470	transcriptional modulator of MazE/toxin, MazF
bglu_1g16730	hypothetical protein
bglu_2p0240	methyl-accepting chemotaxis sensory transducer
bglu_3p0710	IS element transposase
bglu_1p0520	putative transposase
bglu_1p0790	ATPase-like protein
bglu_2g07060	polygalacturonase
bglu_1g04290	lipoprotein
bglu_4p1030	IS element transposase

bglu_2p0250	methyl-accepting chemotaxis sensory transducer
bglu_1p0650	methyl-accepting chemotaxis sensory transducer
bglu_3p0110	Thiol:disulfide interchange protein DsbD
bglu_2g19440	hypothetical protein
bglu_2g16040	hypothetical protein
bglu_2g20410	UDP-glucose 4-epimerase
bglu_4p0300	hypothetical protein
bglu_3p0510	ProQ activator of osmoprotectant transporter ProP
bglu_2g10310	d-isomer specific 2-hydroxyacid dehydrogenase
bglu_2g05430	hypothetical protein
bglu_2g20370	UspA domain-containing protein
bglu_2g16510	protein-tyrosine-phosphatase
bglu_2g20280	UspA domain-containing protein
bglu_2g00420	hypothetical protein
bglu_2g07990	N-acetyltransferase GCN5
bglu_1g14990	family 2 glycosyl transferase
bglu_2g07870	hypothetical protein
bglu_1g15890	hypothetical protein
bglu_1p0560	O-acetylhomoserine sulfhydrylase
bglu_2g09310	3-deoxy-7-phosphoheptulonate synthase
bglu_2g20520	NAD(P) transhydrogenase subunit alpha
bglu_2g22480	XRE family transcriptional regulator
bglu_2g07630	hypothetical protein

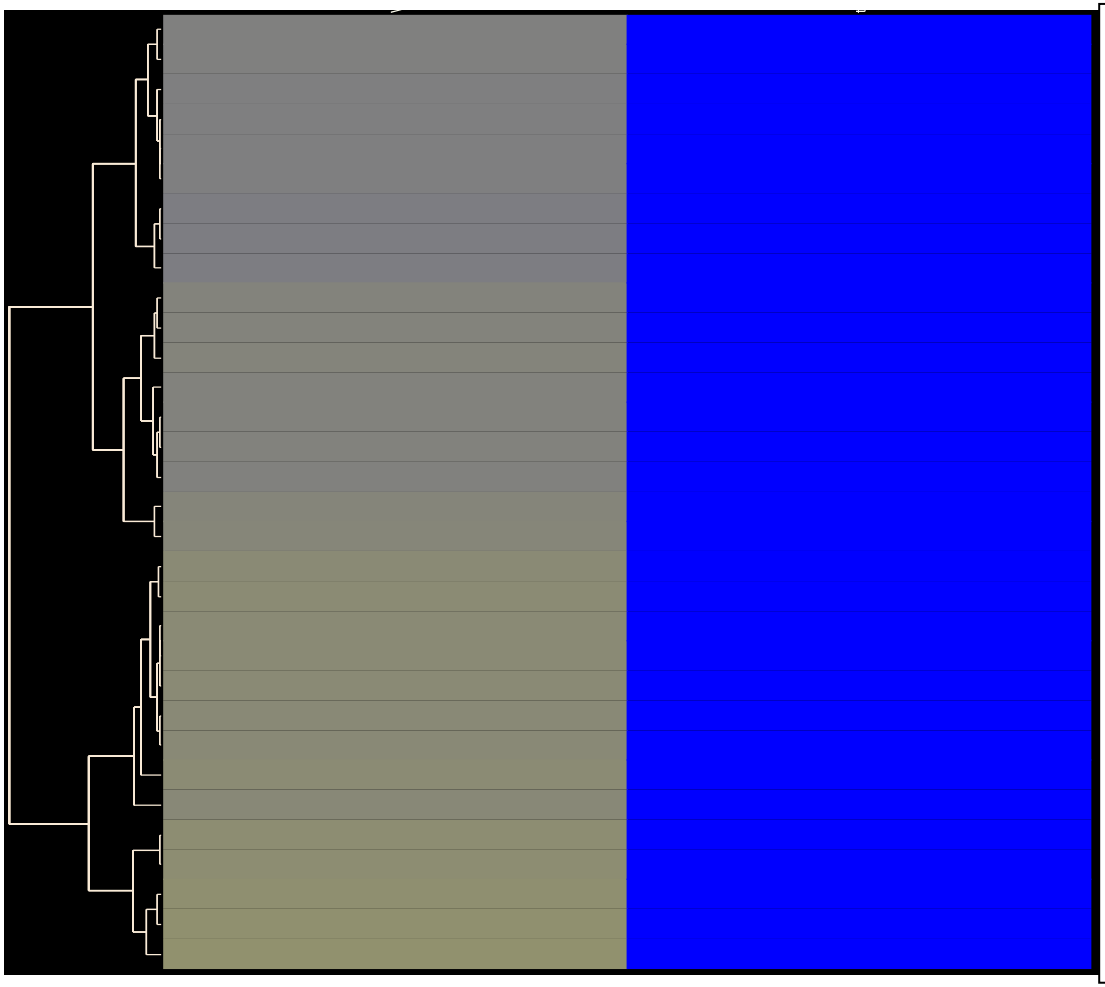

bglu_2p0490	IstB-like ATP-binding protein
bglu_1g22900	pili assembly chaperone
bglu_2g03790	putative proline racemase
bglu_2g21950	bacteriophage tail fiber protein
bglu_1g15630	bacteriophage protein
bglu_1g15830	phage transmembrane protein
bglu_2g19920	HEAT repeat containing protein
bglu_2g20180	cold-shock DNA-binding domain-containing protein
bglu_4p0150	hypothetical protein
bglu_3p0180	TraG-like protein
bglu_2g10680	hypothetical protein
bglu_2g20400	class I cytochrome c
bglu_3p1070	transposase
bglu_2g07410	pentapeptide repeat-containing protein
bglu_2g07910	hypothetical protein
bglu_1g18720	sulfate ABC transporter inner membrane subunit CysT
bglu_3p0610	DNA methylase N-4/N-6 domain-containing protein
bglu_2g11540	phenylacetate-CoA oxygenase subunit PaaA
bglu_2p0710	aldehyde dehydrogenase
bglu_1p0980	methyl-accepting chemotaxis sensory transducer
bglu_2g10410	AraC family transcriptional regulator
bglu_4p1070	hypothetical protein
bglu_1g22510	carbohydrate ABC transporter periplasmic sugar-binding protein
bglu_2g11550	putative acyl-CoA synthetase
bglu_2g21860	virion morphogenesis protein
bglu_2g20130	phospho-2-dehydro-3-deoxyheptonate aldolase
bglu_1g28460	hypothetical protein
bglu_3p0070	hypothetical protein
bglu_3p0650	hypothetical protein
bglu_3p0820	IstB-like ATP-binding protein
bglu_1p0070	IstA-like protein
bglu_1g15880	phage class 3 lipase

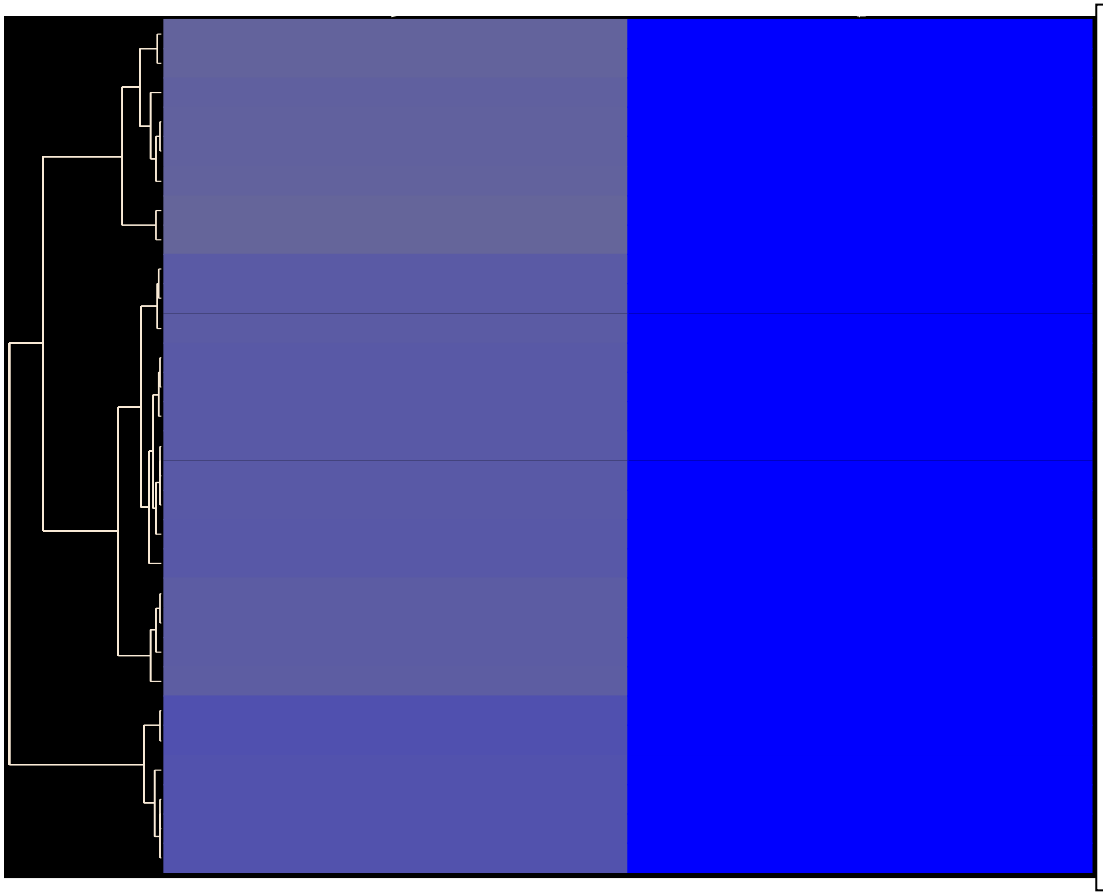

bglu_3p0120	hypothetical protein
bglu_2g14860	ABC-type amino acid transport
bglu_2g11110	type VI secretion system lysozyme-like protein
bglu_1p0380	hypothetical protein
bglu_4p0170	Zeta toxin family protein
bglu_4p0690	hypothetical protein
bglu_2g00970	Fis family transcriptional regulator
bglu_2g11520	phenylacetate-CoA oxygenase subunit PaaI
bglu_2g00400	hypothetical protein
bglu_4p0140	Thiol:disulfide interchange protein DsbD
bglu_2g20390	nitroreductase
bglu_2g00410	hypothetical protein
bglu_2g01580	type VI secretion system lysozyme-like protein
bglu_2g09330	Insertion element IS402
bglu_2g02450	type III secretion protein HrpB7
bglu_2g19770	4-hydroxyphenylacetate 3-monooxygenase reductase
bglu_1g22530	ABC transporter carbohydrate uptake transporter-2 family
bglu_2g11500	phenylacetate-CoA oxygenase/reductase subunit PaaK
bglu_1g22810	oxidoreductase
bglu_2g08040	putative PpiC-type peptidyl-prolyl cis-trans isomerase
bglu_1g14970	group 1 glycosyl transferase
bglu_2g10720	dihem cytochrome c
bglu_1g15090	zinc-binding dehydrogenase
bglu_2g01860	cytoplasmic chaperone TorD family protein
bglu_1g16570	phage SPO1 DNA polymerase-like protein
bglu_2g20470	polyhydroxyalkanoate depolymerase
bglu_2g22190	integrase
bglu_1p0060	integrase
bglu_4p0190	putative endonuclease

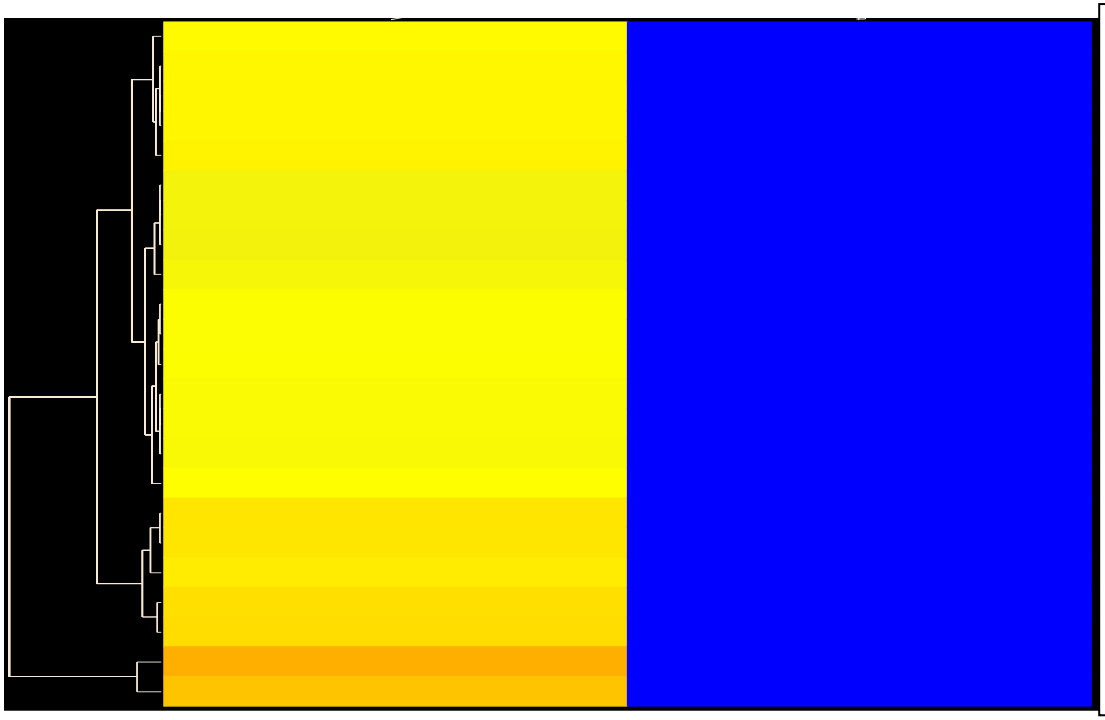

bglu_2p0540	8-amino-7-oxononanoate synthase
bglu_2p0570	biotin synthetase
bglu_1p0480	transcriptional regulator/antitoxin, MazE
bglu_4p0960	PAAR repeat-containing protein
bglu_1p0370	AraC family transcriptional regulator
bglu_2p0550	D-amino acid oxidase Aao_1
bglu_2g06910	S-adenosylmethionine decarboxylase
bglu_1g15710	hypothetical protein
bglu_1p0460	hypothetical protein
bglu_2p0580	carbamoyltransferase
bglu_1p0890	peptidase C11
bglu_2g05790	hypothetical protein
bglu_1p0360	ferric uptake regulator family protein
bglu_4p0970	hypothetical protein
bglu_1g16630	AMP-dependent synthetase and ligase
bglu_1g16670	4Fe-4S ferredoxin iron-sulfur-binding domain-containing protein
bglu_2g06370	putative RND efflux membrane-fusion protein
bglu_1g23090	Amidohydrolase family protein
bglu_2g14490	quorum sensing autoinducer synthase
bglu_2g06450	putative transposase
bglu_2g14480	hypothetical protein
bglu_2p0620	putative exported avidin family protein
bglu_1g23050	pyrroloquinoline quinone (coenzyme pqq) biosynthesis protein c

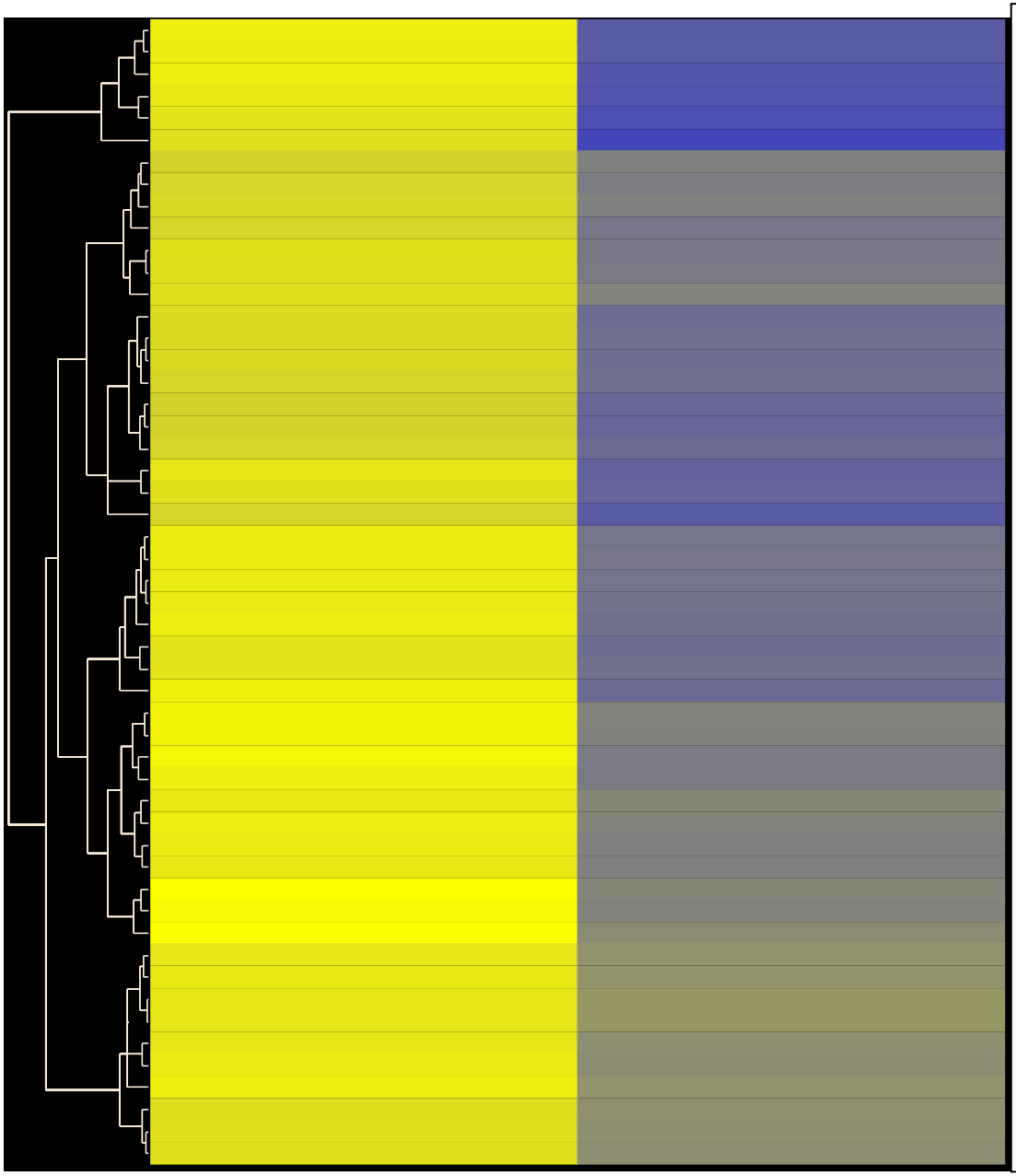

bglu_2p0150	hypothetical protein
bglu_2g09870	major facilitator superfamily protein
bglu_2g17550	cyclopropane-fatty-acyl-phospholipid synthase
bglu_2g02750	BarC
bglu_2g05680	Rhamnosyltransferase
bglu_2g16620	hypothetical protein
bglu_2p0940	putative signal peptide protein
bglu_2g19390	CAIB/BAIF family protein CoA transferase
bglu_1g16780	formyltetrahydrofolate deformylase
bglu_1g16580	glycogen synthase
bglu_2g02790	LysE family translocator protein
bglu_2g04980	L-serine ammonia-lyase
bglu_2g14500	N-acetyl-gamma-glutamyl-phosphate reductase
bglu_2g02580	hypothetical protein
bglu_2g02780	Pectin degradation protein kdgF
bglu_2g05250	methyl-accepting chemotaxis sensory transducer
bglu_2g05870	electron transfer flavoprotein subunit alpha
bglu_1g16700	beta-ketoacyl synthase
bglu_1g16770	(3R)-hydroxymyristoyl-ACP dehydratase
bglu_1g16760	Thioesterase superfamily protein
bglu_2g05670	EmrB/QacA subfamily drug resistance transporter
bglu_2g07570	PPE-repeat-containing protein
bglu_2g02810	nitrilotriacetate monooxygenase component A
bglu_3p1280	hypothetical protein
bglu_2g05780	putative MFS transporter
bglu_2g02770	4-hyroxy-2-oxovalerate/4-hydroxy-2-oxopentanoic acid aldolase
bglu_1g16720	hypothetical protein
bglu_1g16830	ABC transporter-like protein
bglu_2g05010	sarcosine oxidase subunit alpha
bglu_1g16660	peptidase C45
bglu_1g23060	hydrolase/decarboxylase
bglu_2g02760	acetaldehyde dehydrogenase
bglu_2g04990	sarcosine oxidase subunit beta
bglu_1g16650	GCN5-like N-acetyltransferase
bglu_1g16680	major facilitator superfamily protein
bglu_2g05270	hypothetical protein
bglu_2g06900	hypothetical protein
bglu_1p1010	AraC family transcriptional regulator
bglu_1g16790	ferredoxin--NADP reductase
bglu_2g09880	GNAT family acetyltransferase
bglu_1g14790	Secreted protein
bglu_1g16620	hypothetical protein
bglu_2g05000	sarcosine oxidase subunit delta
bglu_1g15700	bacteriophage protein
bglu_1g11550	hypothetical protein
bglu_1g14780	hypothetical protein
bglu_2g05860	Fe-S oxidoreductase
bglu_1g10710	peptidoglycan domain-containing protein
bglu_2g05660	glycosyl transferase family protein
bglu_2g05030	dihydroneopterin aldolase
bglu_2g16630	hypothetical protein
bglu_1g16960	transport/efflux protein

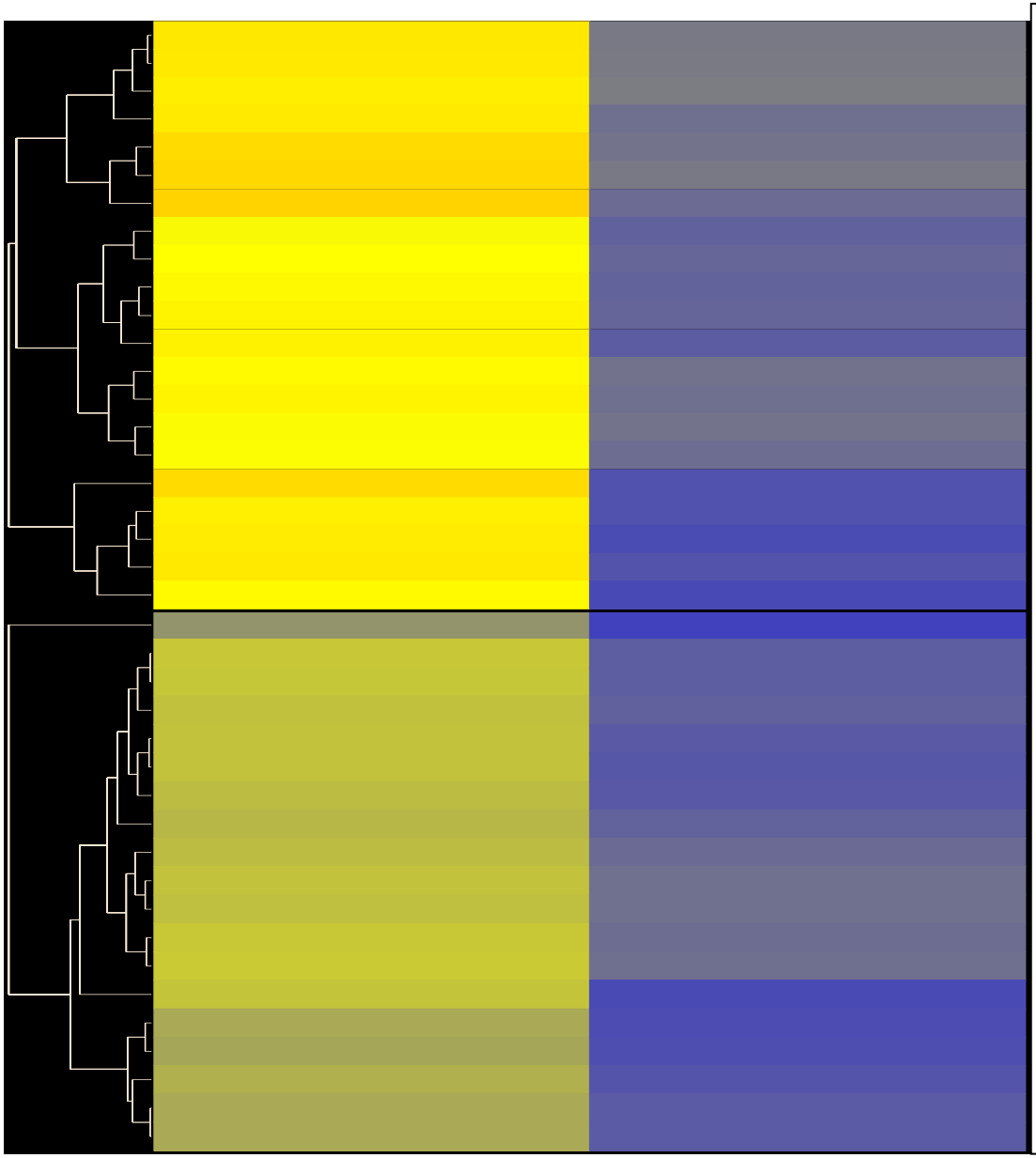

bglu_2g05720	MhpE-like protein
bglu_2g05770	ATP-dependent carboxylate-amine ligase domain-protein
bglu_1g23030	beta-ketoacyl synthase
bglu_1g23110	translation initiation inhibitor
bglu_2g05750	LmbE family protein
bglu_1g23040	Long-chain-fatty-acid--CoA ligase
bglu_2g09940	transcription factor jumonji
bglu_2g06380	hypothetical protein
bglu_1g23020	polyketide synthase
bglu_2g09920	Non-ribosomal peptide synthase
bglu_1g22650	Catalase
bglu_1g23080	acetyl-transferase
bglu_2g06890	TenA family transcriptional activator
bglu_2g09910	Non-ribosomal peptide synthetase/polyketide synthase
bglu_2g09890	beta-lactamase
bglu_1g23010	nonribosomal peptide synthase
bglu_2g05740	putative Branched-chain amino acid aminotransferase
bglu_2g05760	phenazine biosynthesis PhzC/PhzF protein
bglu_1g23070	Cysteine synthase
bglu_2g09860	beta-hydroxylase, aspartyl/asparaginyl family
bglu_2g06880	putative transferase
bglu_2g02440	type III secretion system ATPase
bglu_2g02800	Flavin reductase domain-containing protein
bglu_2g05020	sarcosine oxidase subunit gamma
bglu_2g04930	homocysteine S-methyltransferase
bglu_1g16610	LuxR family autoinducer-binding transcriptional regulator
bglu_1g16750	3-ketoacyl-CoA reductase PhaB
bglu_4p0950	IS element transposase
bglu_1g22970	diguanylate cyclase
bglu_2g03190	isoquinoline 1-oxidoreductase subunit alpha
bglu_2g19380	putative 3-oxacyl-ACP reductase
bglu_1g16740	acyl-CoA dehydrogenase-like protein
bglu_2g12840	carboxymuconolactone decarboxylase
bglu_1g10650	hypothetical protein
bglu_1g16710	alpha/beta hydrolase fold protein
bglu_2g04430	aldose 1-epimerase
bglu_2g04800	L-proline ABC transporter periplasmic glycine betaine
bglu_2g16610	AraC family transcriptional regulator
bglu_2g22530	TonB-like protein
bglu_1g11570	DJ-1/PfpI family protein

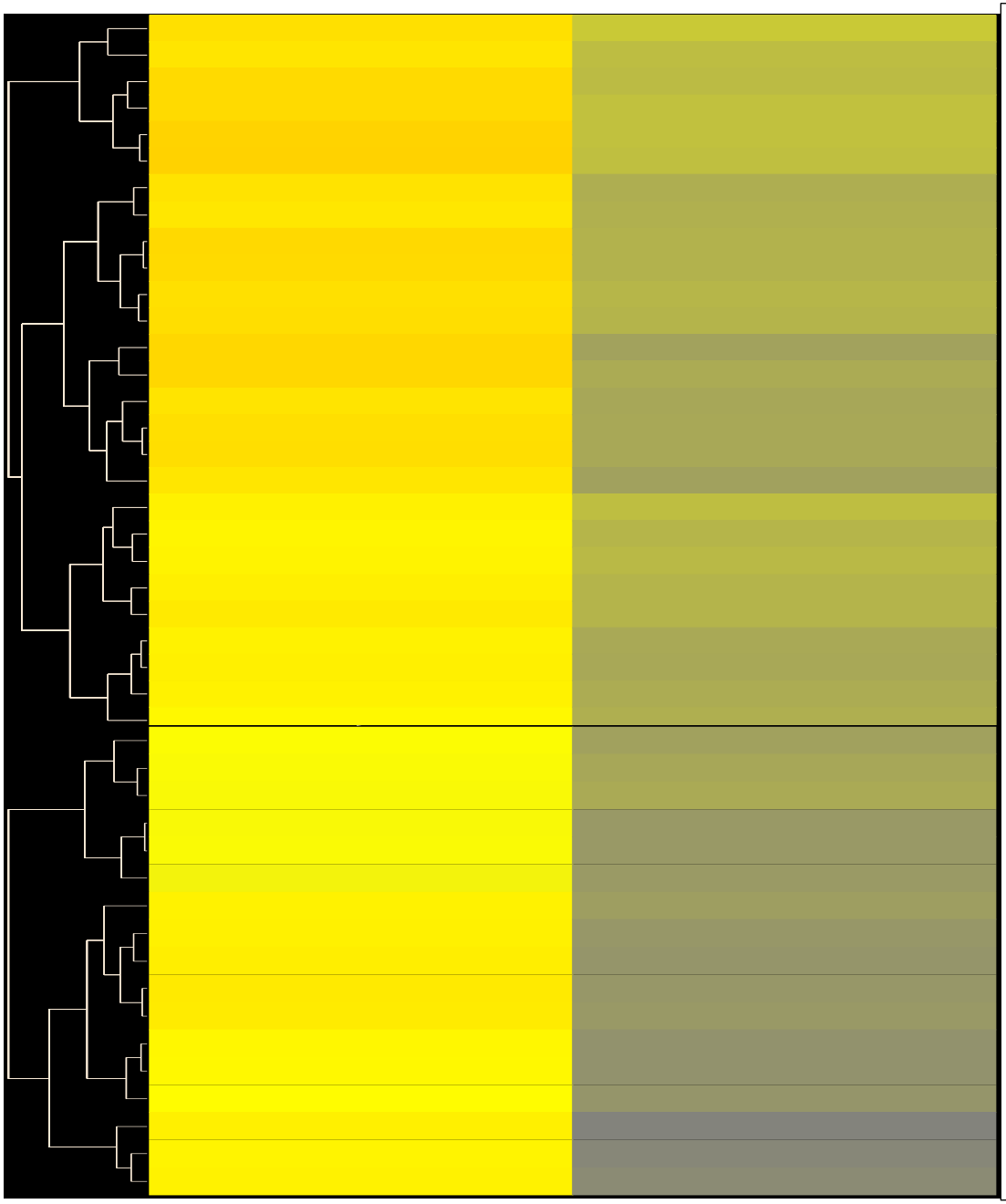

bglu_2g00620	3-oxoadipate CoA-transferase subunit A
bglu_1g17030	LuxR family autoinducer-binding transcriptional regulator
bglu_2g06870	flavin-nucleotide-binding protein
bglu_2g16660	RebB protein
bglu_2g16670	RebA protein
bglu_2g16710	RebB protein
bglu_2g05650	Rhamnosyltransferase 1 subunit A
bglu_1g16970	TauD/TfdA family dioxygenase
bglu_2g05800	Threonine dehydrogenase
bglu_2g16690	RebB protein
bglu_1g17020	alpha/beta hydrolase family protein
bglu_1g32670	Sodium/bile acid symporter family protein
bglu_2g14470	quorum sensing LuxR family sensor regulator
bglu_1g16990	phosphopantetheine-containing protein
bglu_2g16700	RebB protein
bglu_2g17500	phosphomethylpyrimidine kinase
bglu_1g23130	hypothetical protein
bglu_1g23120	hypothetical protein
bglu_2g05830	dipeptidase
bglu_1g16930	Thiotemplate mechanism natural product synthetase
bglu_1g26010	carbonate dehydratase
bglu_2g11820	glycoside hydrolase
bglu_1g26020	sulfate transporter
bglu_1g16890	siderophore non-ribosomal peptide synthetase MbaF
bglu_1g17000	peptide synthetase
bglu_1g16900	TubF protein
bglu_1g16910	TubD protein
bglu_2g01200	AMP-dependent synthetase and ligase
bglu_2g01210	hypothetical protein
bglu_2g05260	alpha/beta fold family hydrolase
bglu_2g05850	FAD/FMN-binding oxidoreductase
bglu_1g16920	non-ribosomal peptide synthase/polyketide synthase
bglu_1g22000	SIS domain-containing protein
bglu_2g02730	Demethylmenaquinone methyltransferase
bglu_2g02740	Branched-chain amino acid aminotransferase
bglu_2g09900	Thioester reductase
bglu_2g08910	hypothetical protein
bglu_2g18090	hypothetical protein
bglu_2g17490	putative thiaminase I
bglu_1g16840	Extracellular ligand-binding receptor
bglu_1g22990	Non-ribosomal peptide synthase
bglu_2g09930	hypothetical protein
bglu_2g16650	hypothetical protein
bglu_1g23100	di-heme cytochrome c peroxidase

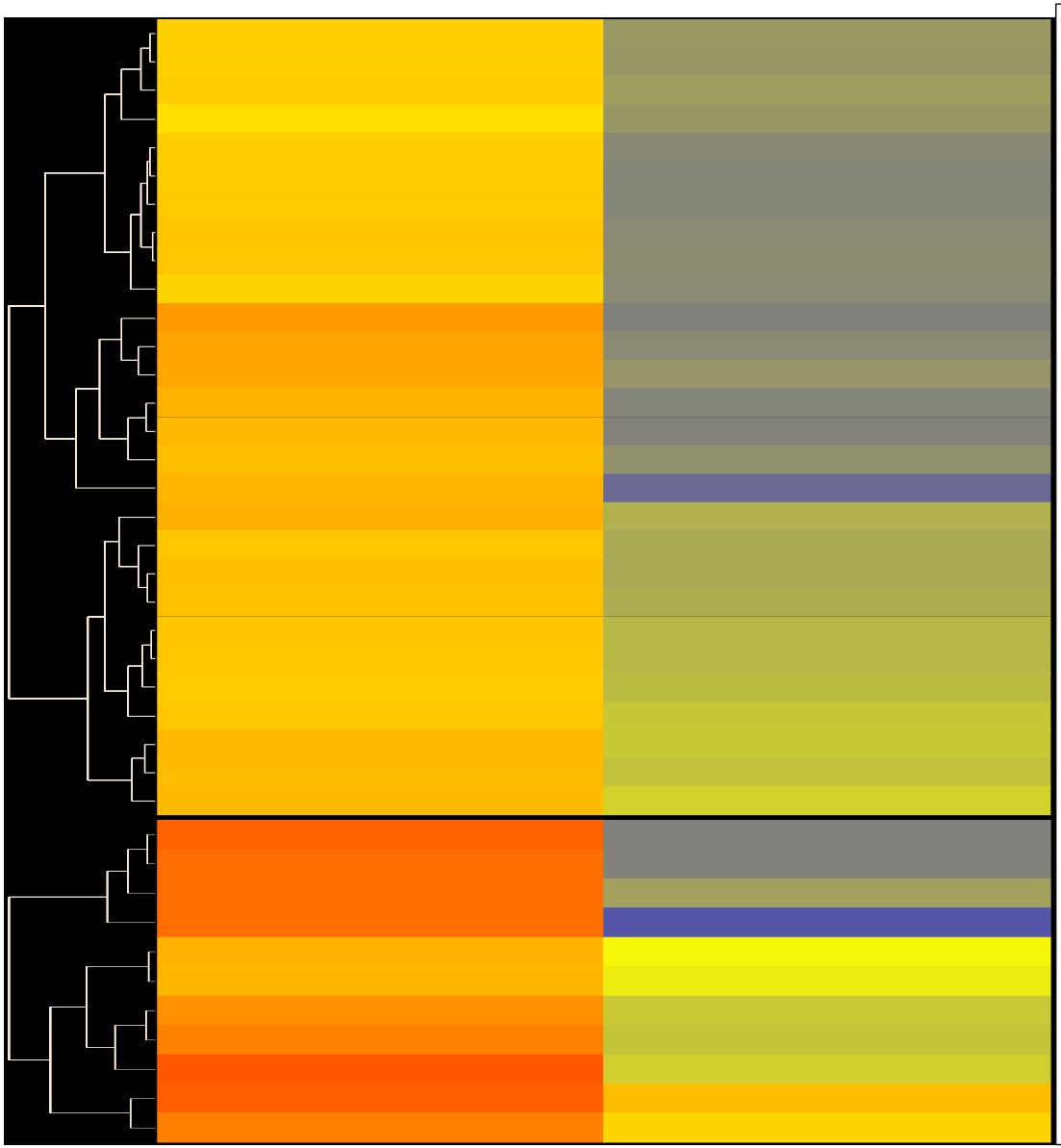

bglu_2g02700	peptide synthetase
bglu_1g16590	Serine metalloprotease
bglu_1g17010	transporter, CPA2 family
bglu_2g16680	RebB protein
bglu_2g02720	Non-ribosomal peptide synthesis thioesterase
bglu_2g06350	putative outer membrane protein OprM
bglu_2g09850	hypothetical protein
bglu_2g06360	putative RND efflux transporter
bglu_2g09950	metallo-beta-lactamase superfamily protein
bglu_2g17510	UbiE/COQ5 family methyltransferase
bglu_2g06430	serine/threonine kinase
bglu_2g06440	riboflavin biosynthesis protein RibD
bglu_1g23170	ABC transporter ATP-binding protein
bglu_2g09960	MbtH-like protein
bglu_1g23160	efflux ABC transporter permease
bglu_2g17540	MutT/nudix family protein
bglu_2g17530	putative nucleoside 2-deoxyribosyltransferase
bglu_2g02710	Non-ribosomal peptide synthase-like protein
bglu_2g17520	Thymidylate synthase
bglu_2g18640	non-ribosomal peptide synthase
bglu_1g08430	5-methyltetrahydropteroyltriglutamate--homocysteine S-methyltransferase
bglu_2g05730	putative coenzyme PQQ synthesis protein c
bglu_1g06960	LysR-family transcriptional regulator
bglu_1g23190	LuxR family transcriptional regulator
bglu_2g06340	putative transposase
bglu_1g22200	Crystal protein ET79
bglu_1g23140	ThiJ/PfpI family protein
bglu_1g23150	Auxin-binding protein
bglu_2g06400	putative ubiquinone/menaquinone biosynthesis methyltransferase
bglu_2g06420	WD-repeat-containing protein
bglu_2g18790	hypothetical protein
bglu_2g06410	GTP cyclohydrolase II
bglu_2g18430	heat shock protein Hsp20
bglu_1g16980	CmaB protein
bglu_2g18630	Insertion element IS402
bglu_2g18770	LysR family transcriptional regulator
bglu_2g18780	transferase
bglu_1g08360	Cold-shock DNA-binding domain-containing protein
bglu_1g21560	3-oxoadipate CoA-succinyl transferase subunit beta

APPENDIX 3. THE EXPRESSION CONDITION OF 43 GENES THAT WERE DOWN-REGULATED BY QS AS DISPLAYED BY HEAT MAPS.

The expression level changed more than 8-fold between 336gr-1 and LSUPB134. Heat Maps were generated by ArrayStar to indicate the level of expression by extension of the color. Each row represents an individual gene. The left column in the grid represents the exes in 336gr-1. The right column represents the expression condition of genes in LSUPB134.

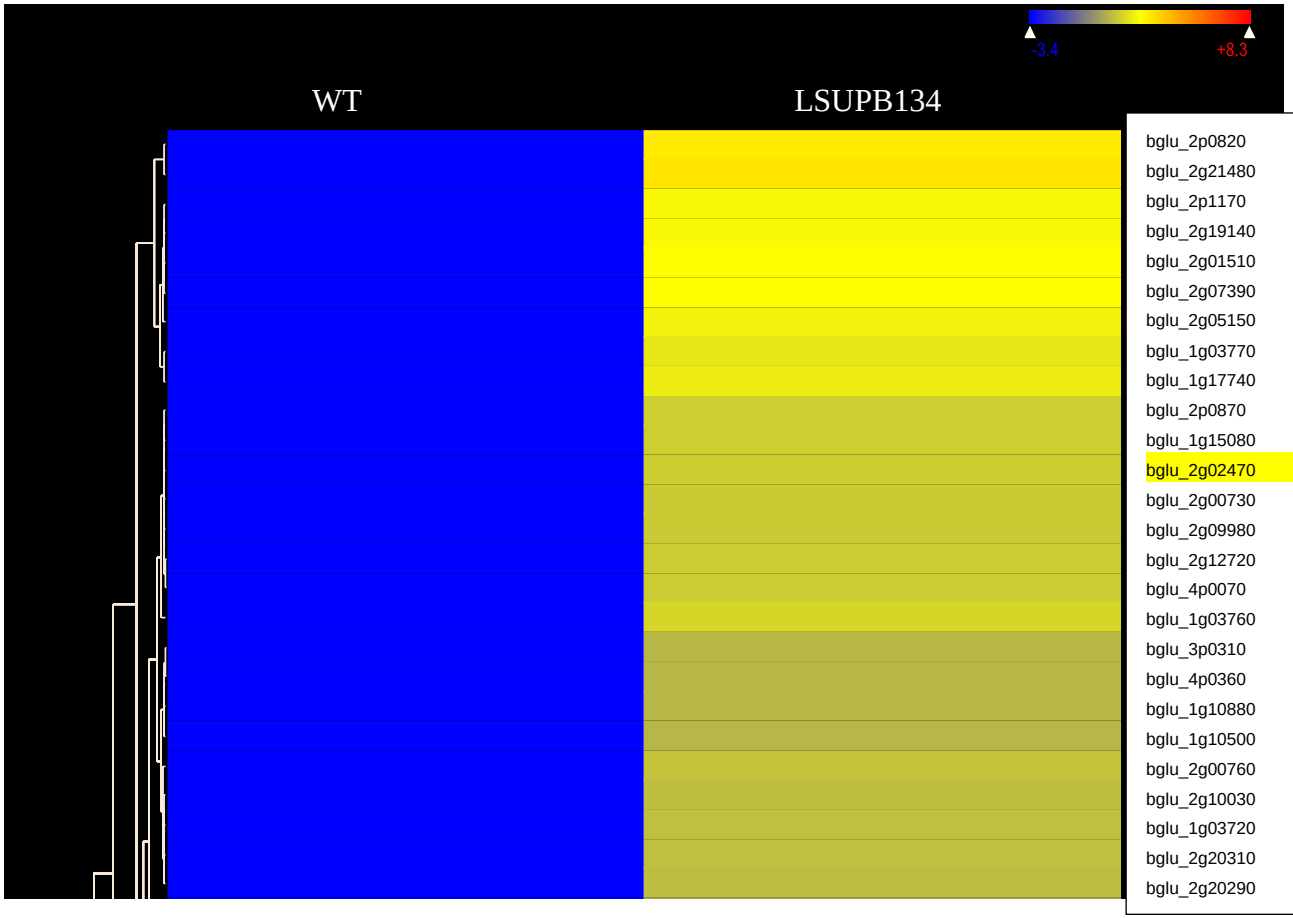

bglu_2p0820	DoxX family protein
bglu_2g21480	hypothetical protein
bglu_2p1170	hypothetical protein
bglu_2g19140	hypothetical protein
bglu_2g01510	Rhs family protein
bglu_2g07390	hypothetical protein
bglu_2g05150	Isochorismatase hydrolase
bglu_1g03770	hypothetical protein
bglu_1g17740	hypothetical protein
bglu_2p0870	DNA-directed RNA polymerase specialized sigma subunit, sigma24-like protein
bglu_1g15080	glutathione-independent formaldehyde dehydrogenase
bglu_2g02470	AraC family transcription regulator of pathogenicity genes
bglu_2g00730	hypothetical protein
bglu_2g09980	response regulator NasT
bglu_2g12720	hypothetical protein
bglu_4p0070	hypothetical protein
bglu_1g03760	phage transcriptional activator, Ogr/delta
bglu_3p0310	protein-disulfide isomerase
bglu_4p0360	protein-disulfide isomerase
bglu_1g10880	PRC-barrel domain-containing protein
bglu_1g10500	Binding-protein-dependent transport systems inner membrane component
bglu_2g00760	NIPSNAP family protein
bglu_2g10030	nitrite reductase (NAD(P)H) small subunit
bglu_1g03720	hypothetical protein
bglu_2g20310	hypothetical protein
bglu_2g20290	acetoacetyl-CoA reductase

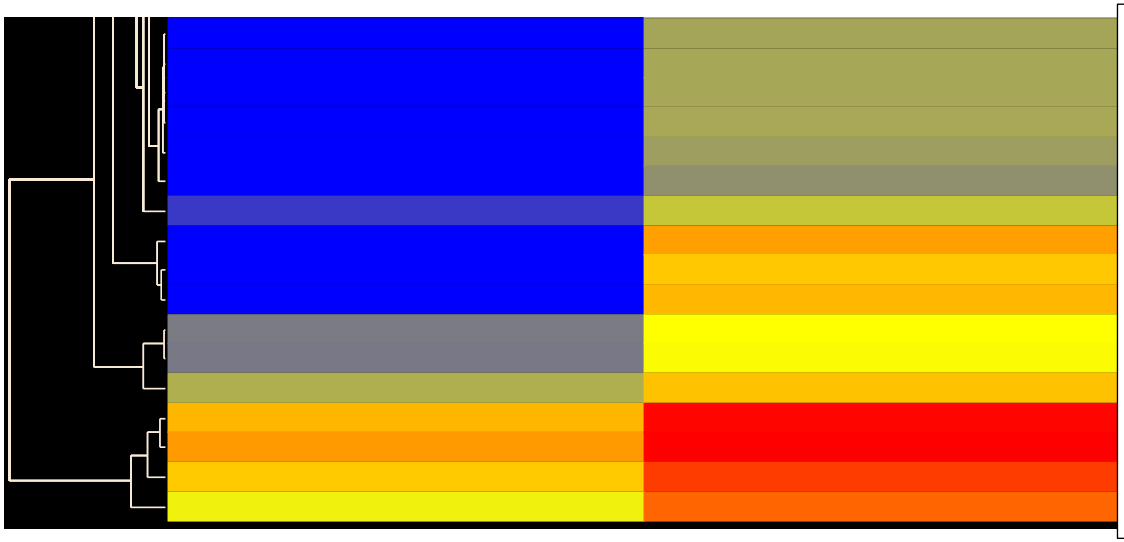

bglu_2g00960	hypothetical protein
bglu_2g20460	putative flavodoxin
bglu_1g10510	ABC transporter periplasmic substrate-binding protein
bglu_1g10520	transcriptional repressor, LacI family
bglu_1g15020	HAD-superfamily hydrolase
bglu_1g21230	phage P2 baseplate assembly protein gpV
bglu_3p0590	ParB-like nuclease
bglu_2g15070	hypothetical protein
bglu_1g19400	molybdenum-pterin binding protein
bglu_4p0910	hypothetical protein
bglu_2g01840	short-chain dehydrogenase
bglu_2g06530	major facilitator superfamily protein
bglu_2g04340	hypothetical protein
bglu_1g13530	dna-binding protein hu-beta
bglu_1g18060	amino acid ABC transporter periplasmic ligand binding protein
bglu_1g31470	cytochrome bd ubiquinol oxidase subunit I
bglu_1g18050	amino acid ABC transporter inner membrane subunit

APPENDIX 4. THE EXPRESSION CONDITION OF 241 GENES THAT CHANGED BETWEEN LSUPB145 SOLID AND LIQUID MEDIA AS DISPLAYED BY HEAT MAPS.

The expression level changed more than 8 folds. Heat Maps were generated by ArrayStar to indicate the level of expression by extension of the color. Each row represented individual gene. Each column in the grid represented the expression condition of genes. –S meant solid culture; -L meant liquid culture. Genes shown in chapter 5 discussion were highlighted.

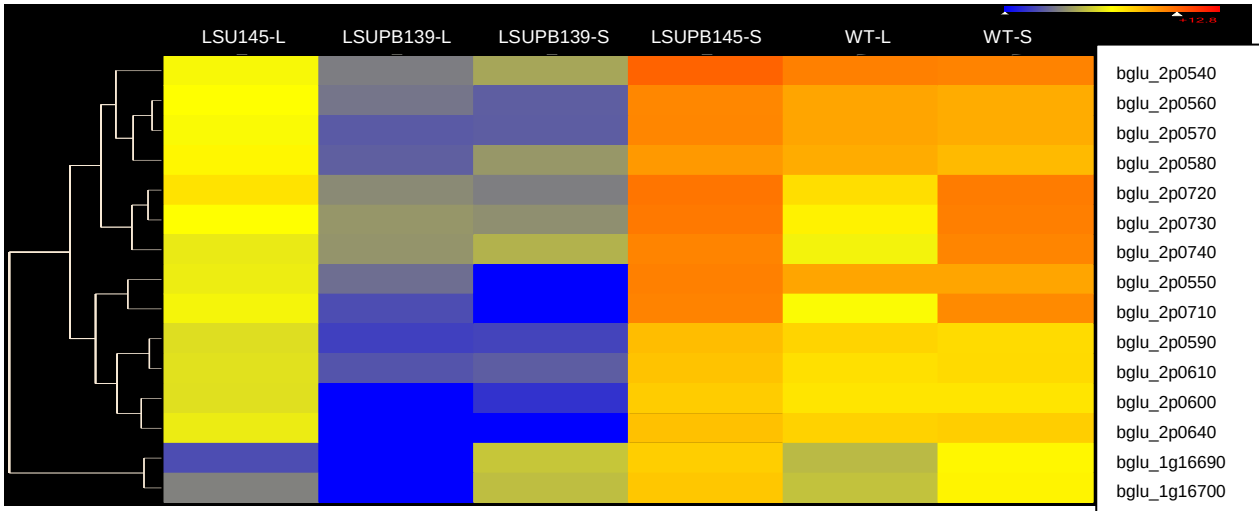

bglu_2p0540	8-amino-7-oxononanoate synthase
bglu_2p0560	zinc-containing alcohol dehydrogenase superfamily protein
bglu_2p0570	biotin synthetase
bglu_2p0580	carbamoyltransferase
bglu_2p0720	glucose-methanol-choline oxidoreductase
bglu_2p0730	alpha/beta hydrolase protein
bglu_2p0740	hypothetical protein
bglu_2p0550	D-amino acid oxidase Aao_1
bglu_2p0710	aldehyde dehydrogenase
bglu_2p0590	short-chain dehydrogenase/reductase SDR
bglu_2p0610	beta-ketoacyl synthase
bglu_2p0600	polyketide synthase
bglu_2p0640	methylmalonyl-CoA epimerase
bglu_1g16690	beta-ketoacyl synthase
bglu_1g16700	beta-ketoacyl synthase

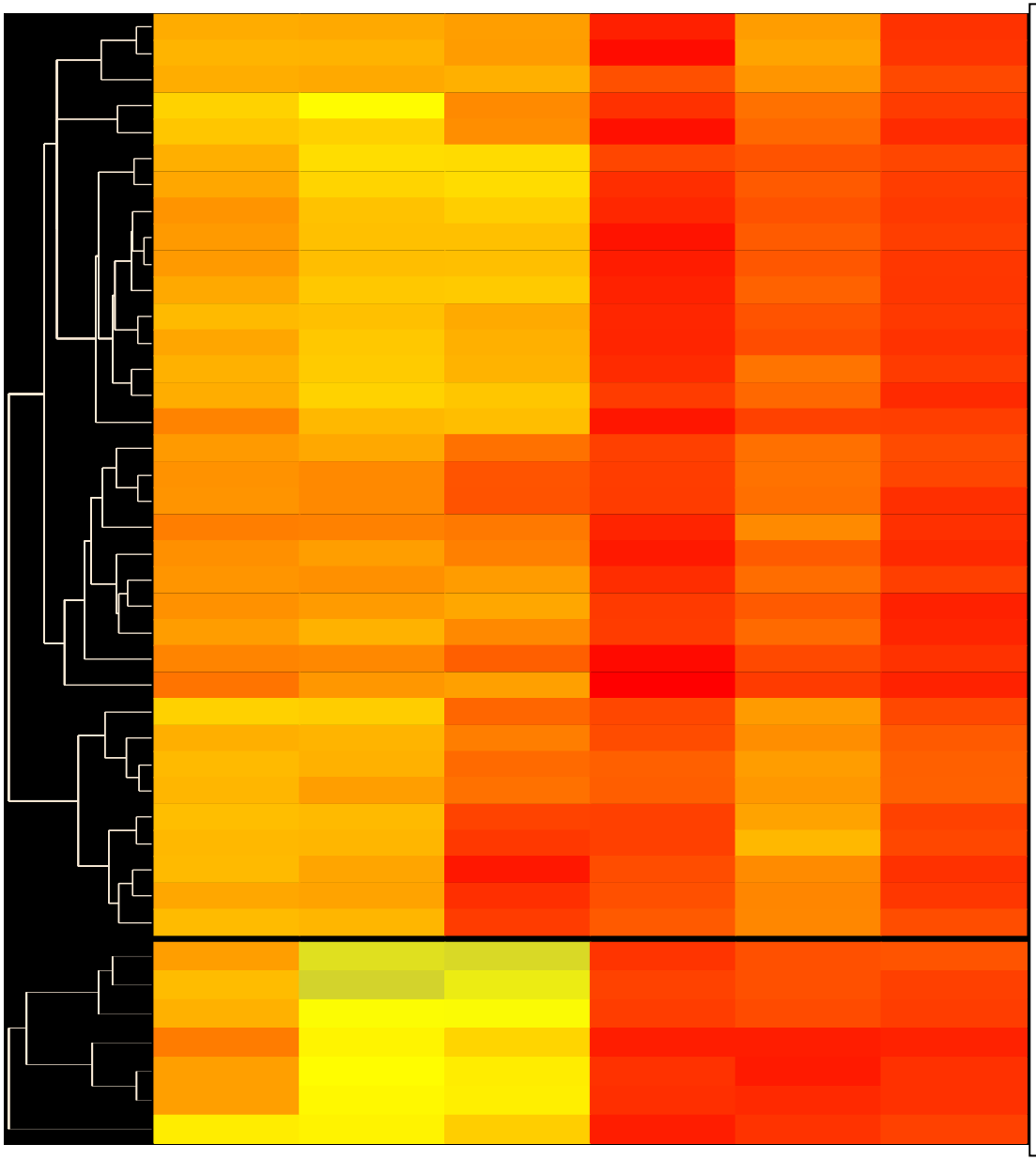

bglu_2p0620	putative exported avidin family protein
bglu_2g06430	serine/threonine kinase
bglu_2g06440	riboflavin biosynthesis protein RibD
bglu_2g06400	putative ubiquinone/menaquinone biosynthesis methyltransferase
bglu_2g06410	GTP cyclohydrolase II
bglu_2g06420	WD-repeat-containing protein
bglu_2g18790	hypothetical protein
bglu_2g01190	taurine catabolism dioxygenase tauD/tfdA
bglu_1g10700	glutathione S-transferase-like protein
bglu_1g22630	hypothetical protein
bglu_2g02710	Non-ribosomal peptide synthase-like protein
bglu_2g09850	hypothetical protein
bglu_2g06450	putative transposase
bglu_2g16650	hypothetical protein
bglu_2g16660	RebB protein
bglu_2g16670	RebA protein
bglu_2g17540	MutT/nudix family protein
bglu_2g18630	Insertion element IS402
bglu_1g10710	peptidoglycan domain-containing protein
bglu_1g16990	phosphopantetheine-containing protein
bglu_2g16700	RebB protein
bglu_2g02700	peptide synthetase
bglu_2g18880	hypothetical protein
bglu_1g13460	transport-associated protein
bglu_1g10590	MarR family transcriptional regulator
bglu_2g15435	Expressed protein GR10
bglu_2g17085	Expressed protein GR12
bglu_1g16980	CmaB protein
bglu_1g17030	LuxR family autoinducer-binding transcriptional regulator
bglu_1g22200	Crystal protein ET79
bglu_2g16710	RebB protein
bglu_2g05800	Threonine dehydrogenase
bglu_2g18090	hypothetical protein
bglu_2g18890	cyclopropane-fatty-acyl-phospholipid synthase
bglu_1g19670	TetR family transcriptional regulator
bglu_2g05830	dipeptidase
bglu_2g05910	proline/glycine betaine ABC transporter periplasmic protein
bglu_2g20990	heat shock protein Hsp20
bglu_1g21320	hypothetical protein
bglu_2g21000	heat shock protein Hsp20

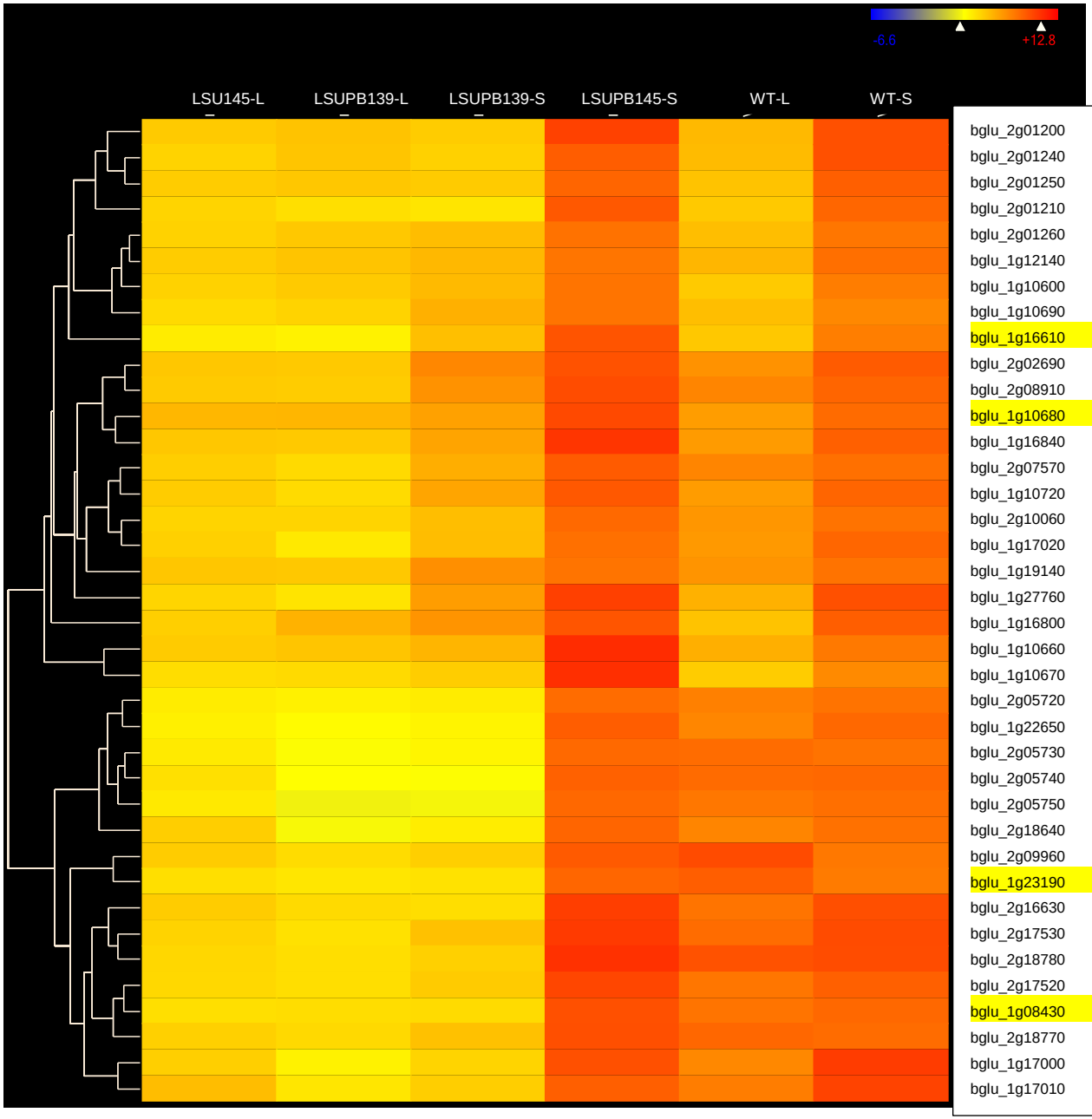

bglu_2g01200	AMP-dependent synthetase and ligase
bglu_2g01240	RND family efflux transporter MFP subunit
bglu_2g01250	Acriflavin resistance protein
bglu_2g01210	hypothetical protein
bglu_2g01260	multidrug efflux system outer membrane protein
bglu_1g12140	methlytransferase, UbiE/COQ5 family
bglu_1g10600	Inositol-phosphate phosphatase
bglu_1g10690	pyruvate dehydrogenase (lipoamide)
bglu_1g16610	LuxR family autoinducer-binding transcriptional regulator
bglu_2g02690	amino acid adenylation domain-containing protein
bglu_2g08910	hypothetical protein
bglu_1g10680	acylhomoserine lactone dependent transcriptional activator
bglu_1g16840	Extracellular ligand-binding receptor
bglu_2g07570	PPE-repeat-containing protein
bglu_1g10720	hypothetical protein
bglu_2g10060	poly (3-hydroxybutyrate) depolymerase
bglu_1g17020	alpha/beta hydrolase family protein
bglu_1g19140	class V aminotransferase
bglu_1g27760	hypothetical protein
bglu_1g16800	major facilitator superfamily protein
bglu_1g10660	Cupin 2 barrel domain-containing protein
bglu_1g10670	Rieske family iron-sulfur cluster-binding protein
bglu_2g05720	MhpE-like protein
bglu_1g22650	Catalase
bglu_2g05730	putative coenzyme PQQ synthesis protein c
bglu_2g05740	putative Branched-chain amino acid aminotransferase
bglu_2g05750	LmbE family protein
bglu_2g18640	non-ribosomal peptide synthase
bglu_2g09960	MbtH-like protein
bglu_1g23190	LuxR family transcriptional regulator
bglu_2g16630	hypothetical protein
bglu_2g17530	putative nucleoside 2-deoxyribosyltransferase
bglu_2g18780	transferase
bglu_2g17520	Thymidylate synthase
bglu_1g08430	5-methyltetrahydropteroyltriglutamate--homocysteine S-methyltransferase
bglu_2g18770	LysR family transcriptional regulator
bglu_1g17000	peptide synthetase
bglu_1g17010	transporter, CPA2 family

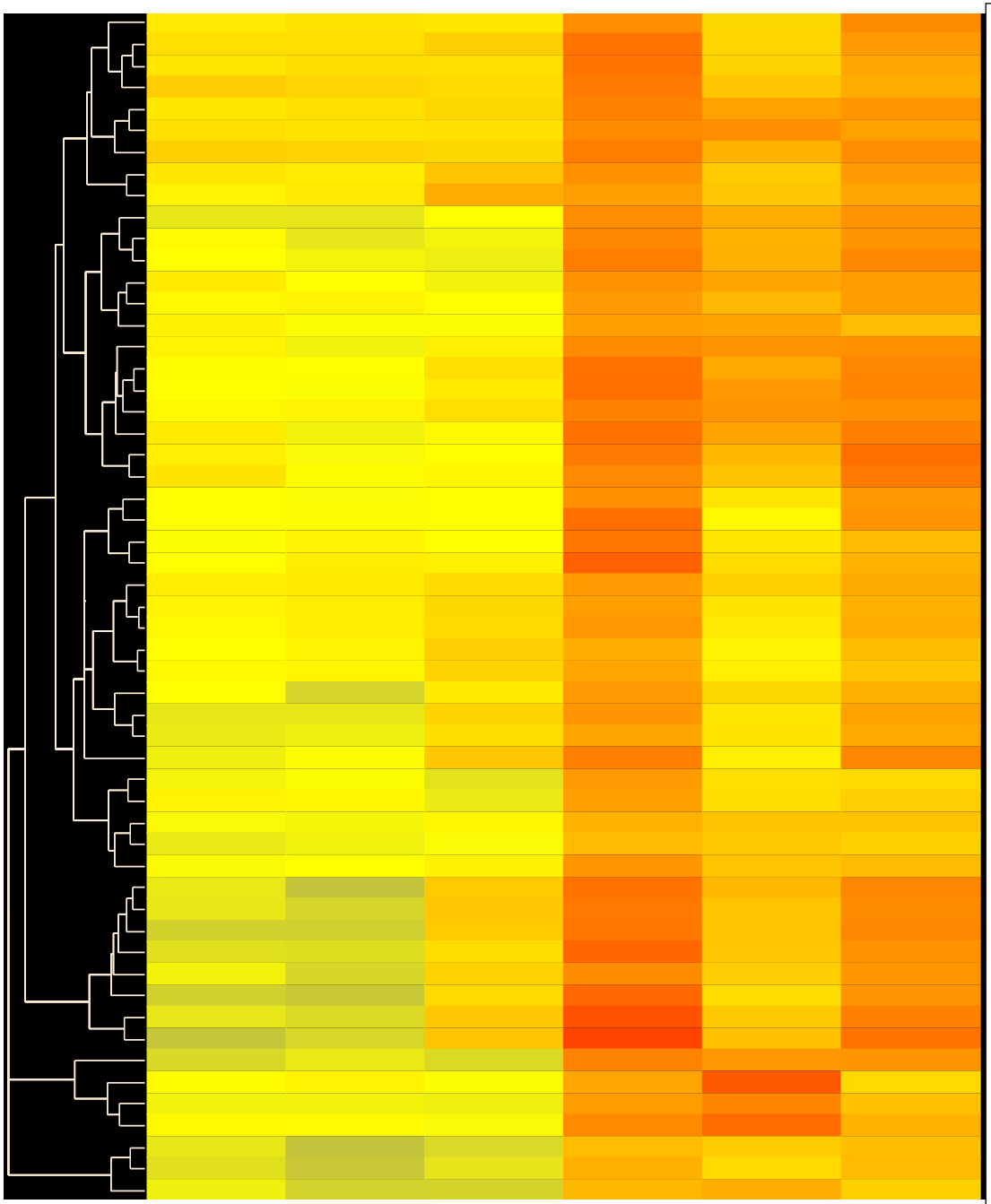

bglu_2g01220	Bcr/CflA subfamily drug resistance transporter
bglu_1g10610	Rieske (2Fe-2S) domain-containing protein
bglu_1g10620	hypothetical protein
bglu_1g10640	hypothetical protein
bglu_2g17490	putative thiaminase I
bglu_1g32670	Sodium/bile acid symporter family protein
bglu_1g21920	hypothetical protein
bglu_2g10055	Expressed protein SR2101
bglu_1g24870	transmembrane efflux protein
bglu_2g05760	phenazine biosynthesis PhzC/PhzF protein
bglu_2g16620	hypothetical protein
bglu_2g16720	hypothetical protein
bglu_2g05790	hypothetical protein
bglu_1g22640	Ankyrin repeat-containing protein
bglu_2g06910	S-adenosylmethionine decarboxylase
bglu_2g05770	ATP-dependent carboxylate-amine ligase domain-containing protein
bglu_2g17500	phosphomethylpyrimidine kinase
bglu_2g17510	UbiE/COQ5 family methyltransferase
bglu_1g16590	Serine metalloprotease
bglu_2g16640	hypothetical protein
bglu_1g16890	siderophore non-ribosomal peptide synthetase MbaF
bglu_1g16900	TubF protein
bglu_2g01230	DoxX family protein
bglu_1g10560	hypothetical protein
bglu_1g10630	dihydrodipicolinate synthetase family protein
bglu_1g10650	hypothetical protein
bglu_2g02760	acetaldehyde dehydrogenase
bglu_2g12830	GNAT family acetyltransferase
bglu_1g16780	formyltetrahydrofolate deformylase
bglu_2g07050	iron-containing alcohol dehydrogenase
bglu_2g15230	nitrilase/cyanide hydratase and apolipoprotein N-acyltransferase
bglu_2g02780	Pectin degradation protein kdgF
bglu_2g02790	LysE family translocator protein
bglu_2g02810	nitrilotriacetate monooxygenase component A
bglu_1g16790	ferredoxin--NADP reductase
bglu_2g04930	5-methyltetrahydropteroyltriglutamate/homocysteine S-methyltransferase
bglu_2g12690	VWA containing CoxE-like protein
bglu_2g05250	methyl-accepting chemotaxis sensory transducer
bglu_1g14790	Secreted protein
bglu_2g08940	LysR family transcriptional regulator
bglu_2g02720	Non-ribosomal peptide synthesis thioesterase
bglu_2g02740	Branched-chain amino acid aminotransferase
bglu_2g02730	Demethylmenaquinone methyltransferase
bglu_1g16670	4Fe-4S ferredoxin iron-sulfur-binding domain-containing protein
bglu_2g02770	4-hyroxy-2-oxovalerate/4-hydroxy-2-oxopentanoic acid aldolase
bglu_1g16630	AMP-dependent synthetase and ligase
bglu_1g16620	hypothetical protein
bglu_1g16640	hypothetical protein
bglu_2g17550	cyclopropane-fatty-acyl-phospholipid synthase
bglu_1g23050	pyrroloquinoline quinone (coenzyme pqq) biosynthesis protein c
bglu_1g23160	efflux ABC transporter permease
bglu_1g23170	ABC transporter ATP-binding protein
bglu_2g05780	putative MFS transporter
bglu_2g16610	AraC family transcriptional regulator
bglu_2g06880	putative transferase

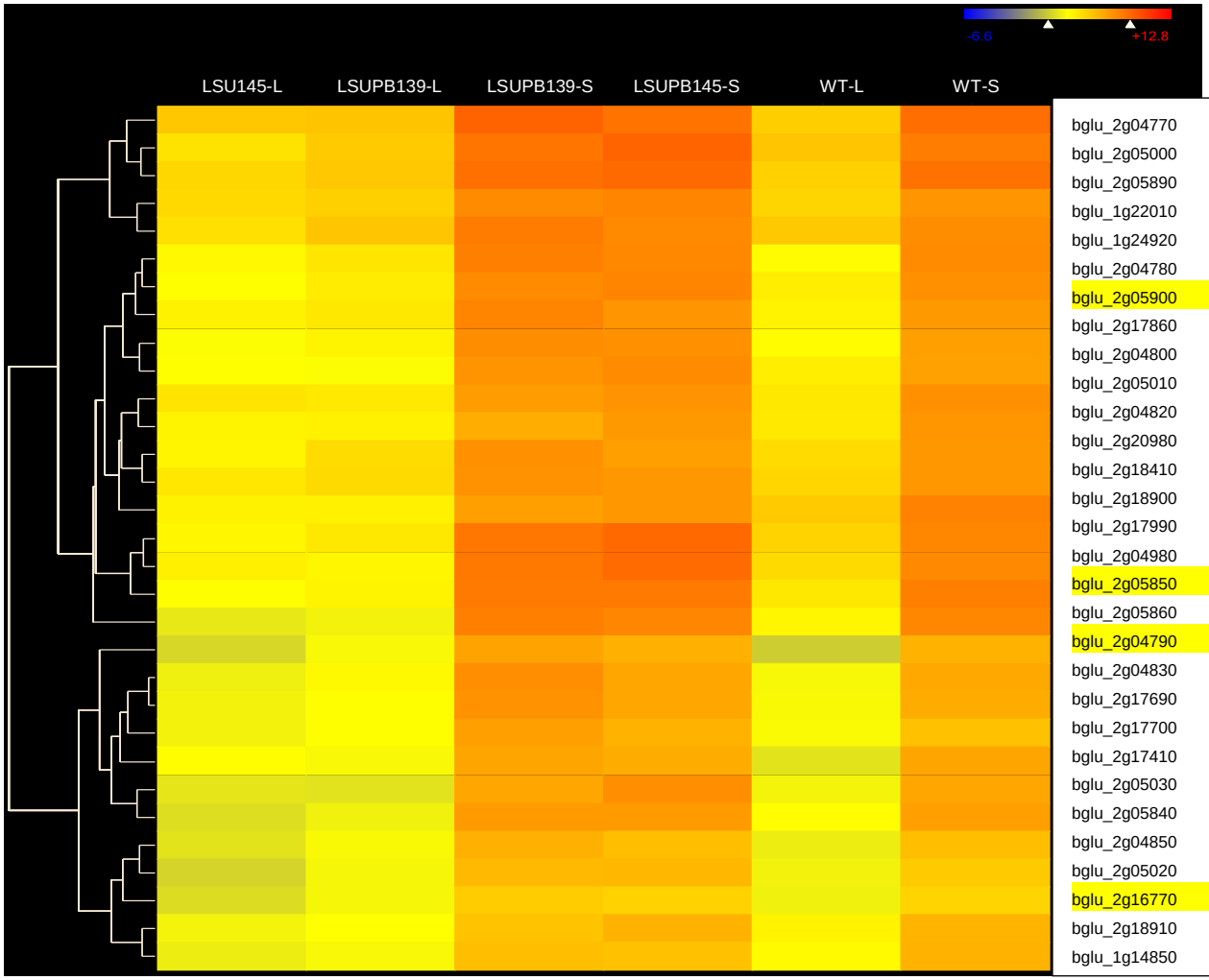

bglu_2g04770	glycine betaine/L-proline ABC transporter ATP-binding subunit
bglu_2g05000	sarcosine oxidase subunit delta
bglu_2g05890	Iron-sulfur cluster-binding protein
bglu_1g22010	sugar ABC transporter periplasmic sugar-binding protein
bglu_1g24920	transmembrane hydrogenase cytochrome b-type subunit
bglu_2g04780	choline ABC transporter membrane-spanning permease
bglu_2g05900	ferredoxin
bglu_2g17860	CsgG family protein
bglu_2g04800	glycine betaine/L-proline ABC transporter periplasmic glycine betaine
bglu_2g05010	sarcosine oxidase subunit alpha
bglu_2g04820	hypothetical protein
bglu_2g20980	secreted hydrolase-like protein
bglu_2g18410	malonate transporter subunit L
bglu_2g18900	lipocalin family protein
bglu_2g17990	hypothetical protein
bglu_2g04980	L-serine ammonia-lyase
bglu_2g05850	FAD/FMN-binding oxidoreductase
bglu_2g05860	Fe-S oxidoreductase
bglu_2g04790	AraC family transcriptional regulator
bglu_2g04830	hybrid cluster protein
bglu_2g17690	putative protease
bglu_2g17700	putative protease
bglu_2g17410	respiratory nitrate reductase chaperone NarJ
bglu_2g05030	dihydroneopterin aldolase
bglu_2g05840	4-vinyl reductase 4VR
bglu_2g04850	NAD-dependent epimerase/dehydratase
bglu_2g05020	sarcosine oxidase subunit gamma
bglu_2g16770	short chain dehydrogenase
bglu_2g18910	cyclopropane-fatty-acyl-phospholipid synthase
bglu_1g14850	sensor histidine kinase

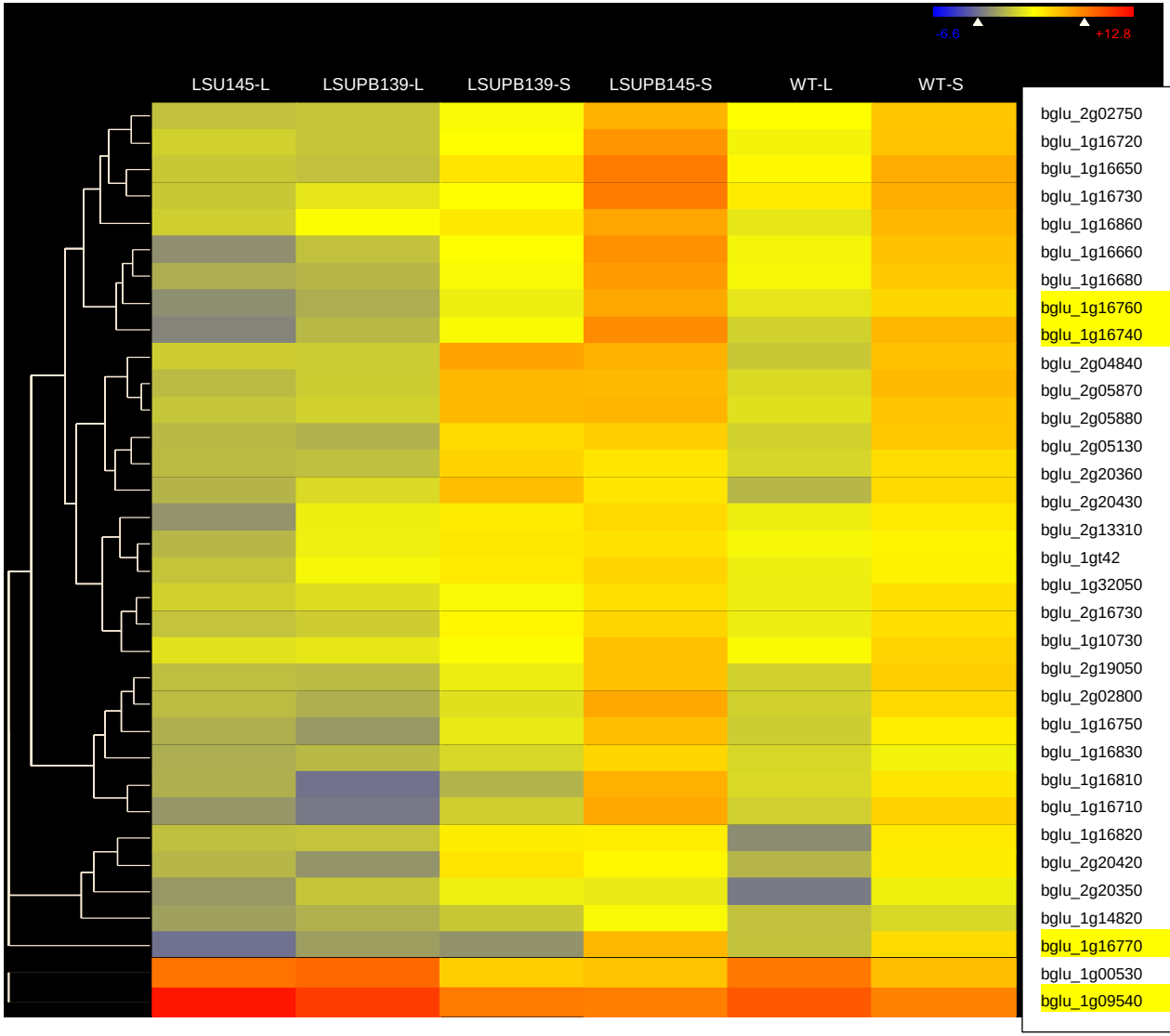

bglu_2g02750	BarC
bglu_1g16720	hypothetical protein
bglu_1g16650	GCN5-like N-acetyltransferase
bglu_1g16730	hypothetical protein
bglu_1g16860	alpha/beta hydrolase fold protein
bglu_1g16660	peptidase C45
bglu_1g16680	major facilitator superfamily protein
bglu_1g16760	Thioesterase superfamily protein
bglu_1g16740	acyl-CoA dehydrogenase-like protein
bglu_2g04840	oxidoreductase
bglu_2g05870	electron transfer flavoprotein subunit alpha
bglu_2g05880	electron transfer flavoprotein subunit beta
bglu_2g05130	winged helix family transcriptional regulator
bglu_2g20360	UspA domain-containing protein
bglu_2g20430	hypothetical protein
bglu_2g13310	hypothetical protein
bglu_1gt42	tRNA-Pro
bglu_1g32050	hypothetical protein
bglu_2g16730	Epoxide hydrolase-like protein
bglu_1g10730	hypothetical protein
bglu_2g19050	amidohydrolase
bglu_2g02800	Flavin reductase domain-containing protein
bglu_1g16750	3-ketoacyl-CoA reductase PhaB
bglu_1g16830	ABC transporter-like protein
bglu_1g16810	Inner-membrane translocator
bglu_1g16710	alpha/beta hydrolase fold protein
bglu_1g16820	Branched-chain amino acid ABC-type transport system, permease
bglu_2g20420	aminoglycoside phosphotransferase
bglu_2g20350	acetate kinase
bglu_1g14820	hypothetical protein
bglu_1g16770	(3R)-hydroxymyristoyl-ACP dehydratase
bglu_1g00530	phenylalanine 4-monooxygenase
bglu_1g09540	acyl carrier protein

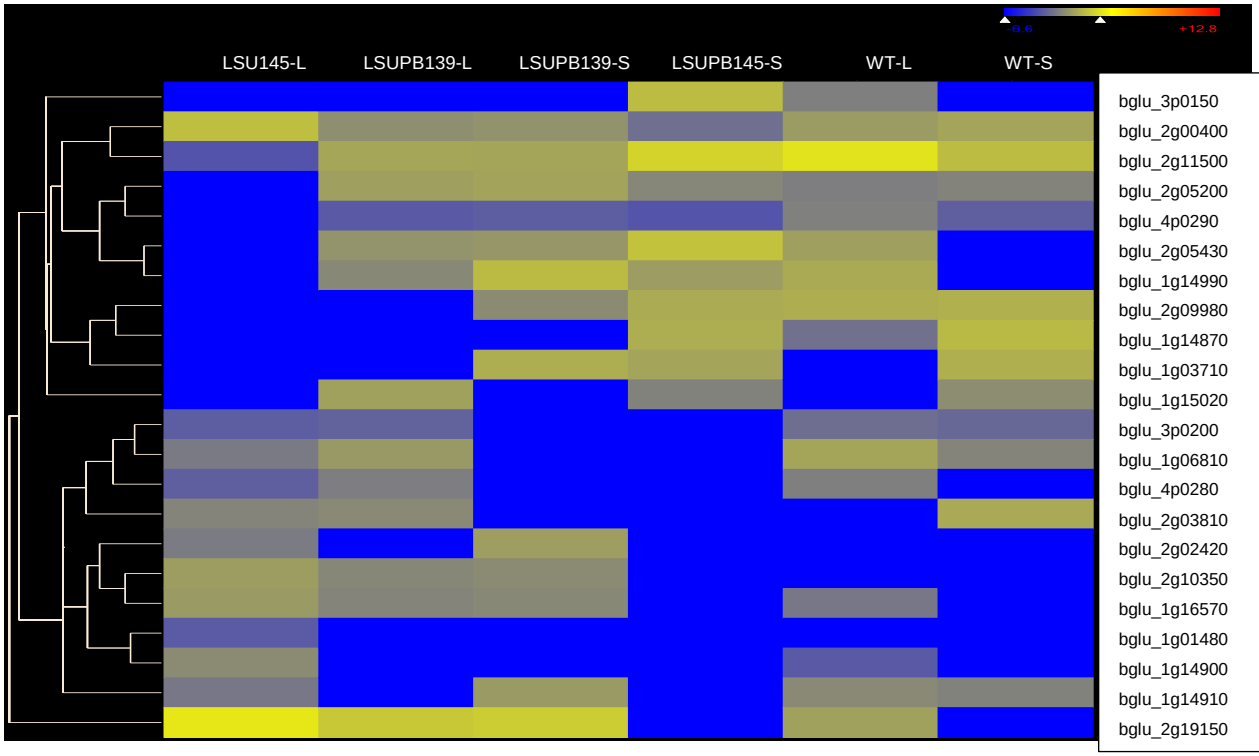

bglu_3p0150	hypothetical protein
bglu_2g00400	hypothetical protein
bglu_2g11500	phenylacetate-CoA oxygenase/reductase subunit PaaK
bglu_2g05200	putative permease
bglu_4p0290	conjugal DNA transfer protein TraU
bglu_2g05430	hypothetical protein
bglu_1g14990	family 2 glycosyl transferase
bglu_2g09980	response regulator NasT
bglu_1g14870	hypothetical protein
bglu_1g03710	hypothetical protein
bglu_1g15020	HAD-superfamily hydrolase
bglu_3p0200	TraF-like protein
bglu_1g06810	hypothetical protein
bglu_4p0280	type-F conjugative transfer system pilin assembly protein TrbC
bglu_2g03810	putative ferredoxin-containing oxidase
bglu_2g02420	type III secretion protein HrpB4
bglu_2g10350	hypothetical protein
bglu_1g16570	phage SPO1 DNA polymerase-like protein
bglu_1g01480	phage terminase, ATPase subunit
bglu_1g14900	family 2 glycosyl transferase
bglu_1g14910	LmbE family protein
bglu_2g19150	hypothetical protein

LETTER OF PERMISSION

Dear Dr. Chen,

It is not PLOS ONE policy to send out formal letters of permission as we apply the CC-BY License to all articles we publish. The full copyright of your article reads:"Copyright: © 2012 Chen et al. This is an open-access article distributed under the terms of the Creative Commons Attribution License, which permits unrestricted use, distribution, and reproduction in any medium, provided the original author and source are credited."

Under the CCAL, authors retain ownership of the copyright for their article, but authors allow anyone to download, reuse, reprint, modify, distribute, and/or copy articles in PLOS journals, so long as the original authors and source are cited. No permission is required from the authors or the publishers.You can find more information on this Creative Commons license here: http://creativecommons.org/licenses/by/2.5/

Please feel free to share this email with your graduate school in lieu of formally written permission statement.

Best Regards,
Will

PLOS I OPEN FOR DISCOVERY
Will Jackson I Publications Assistant, PLOS ONE
1160 Battery Street, Suite 100, San Francisco, CA 94111
plosone@plos.org I Main +1 415-624-1200
plos.org I Facebook I Twitter I Blog

---------- Original Message ----------
From: Ruoxi Chen [rchen5@tigers.lsu.edu]
Sent: 11/6/2013
To: one_production@plos.org
Subject: Re: Case: 02276322 "FW: put the publication in dissertation" ref:_00DU0Ifis._500U084PMf:ref

Hi Dear Jennafer,

Our graduate school asked me to obtain one formally written permission from Plos One to re-use my previously published article (doi:10.1371/journal.pone.0052150) as one chapter in my dissertation. My dissertation will be viewable on the web.

Can you send me one formal letter granting the permission to use this article? You letter will appear as an appendix in my dissertation.

Thank you very much

Ruoxi Chen

On Thu, Aug 15, 2013 at 4:35 PM, Jennafer Prongos <one_production@plos.org<mailto:one_production@plos.org>> wrote:

Dear Ruoxi,

The permission to re-use your article is already given upon publication. The full copyright of your article reads:
"Copyright: © 2012 Chen et al. This is an open-access article distributed under the terms of the Creative Commons Attribution License, which permits unrestricted use, distribution, and reproduction in any medium, provided the original author and source are credited."

You may include as much of your article in your dissertation as you need, provided you include a proper citation. It is that simple.

Please let us know if you have any additional questions.

Kind Regards,
Jennafer

THE VITA

Ruoxi Chen went to primary school and junior high from 1993-2000 in Heze city, China. She spent her high school in Shandong Heze No.1 Middle School from 2000 to 2004, and afterwards entered college in Taian city. In 2008, she attained her Bachelor of Science in Plant Protection, Shandong Agricultural University. In 2008 fall, she enrolled in the plant pathology and crop physiology department at Louisiana State University and attained her Master degree in 2011 fall.